The detection and clinical significance of *TP53* dysfunction in chronic lymphocytic leukaemia.

Ian Tracy, BSc.

Submitted in partial fulfilment of the requirements for a Doctorate of Philosophy awarded by Bournemouth University

Work undertaken at the Royal Bournemouth and Christchurch Hospital

Submitted September 2016

Abstract

Standard therapy for patients with chronic lymphocytic leukaemia involves the use of DNA damaging drugs. If the cellular DNA damage response has been compromised then these standard therapies will be ineffective at inducing apoptosis. Central to this response is the protein, p53. Loss of the chromosome containing the gene *TP53*, which encodes the protein p53 and/or mutation of the gene, occurs in approximately 5-10% of newly diagnosed CLL patients. This rises to over 30% in patients who relapse after therapy. In addition another important protein within the DNA damage response, the protein-kinase ATM, may be deleted and/or mutated in a further 20-30% of CLL cases. Loss of the chromosomal loci containing either *TP53* or *ATM* has been shown to predict a poor response to treatment and shorter overall survival. It is now known that detecting loss alone is insufficient as miss-sense or non-sense mutation of these genes alone can lead to an equally poor outcome. Screening these genes for mutations is not carried out routinely and can be technically challenging. In addition to this it is not fully understood to what degree other genes may be involved in dysfunction of the DNA damage response.

Functional assays provide an alternative method for testing the integrity of the p53-dependant DNA damage response without needing to focus upon specific genomic abnormalities. A flow-cytometry based assay, utilising etoposide/nutlin3a and developed in our laboratory, has already been shown to detect and discriminate between p53 and ATM abnormalities in a small series of patients. This project aims to assess the clinical value of the etoposide/nutlin3a functional assay for detecting abnormalities of the p53-dependant DNA damage response which would contra-indicate treatment with DNA damaging drugs in samples referred from around the UK.

A total of 472 samples from participating centres around the UK have been tested using the functional assay and also assessed for deletion of ATM and p53. The assay is largely unaffected by transport of whole blood samples across the UK if transit time is no greater than 48 hours and the sample is not stored above room temperature. Dysfunctional assay results have been shown to have a highly significant association with deletion of the genes for p53 and ATM. The use of nutlin3a has been shown to discriminate between dysfunctional cases with deletion of ATM or loss/mutation of p53. The assay has been shown to detect patients with mutation of the p53 gene who do not have concurrent deletion of the second allele. A novel dysfunctional response pattern involving p21 expression has been shown to associate with abnormalities of p53 rather than single nucleotide polymorphisms. The results also show that deletion of p53 and particularly ATM does not *per se* lead to a dysfunctional response as currently detected by the assay. This suggests that other mechanisms or genes are involved in resistance to DNA damage induced apoptosis.

Table of Contents

TABLE OF CONTENTS **4**

1 CHAPTER ONE: INTRODUCTION **16**

1.1 OVERVIEW 17
1.2 DEFINITIONS AND NOMENCLATURE 19
1.3 CHRONIC LYMPHOCYTIC LEUKAEMIA (CLL) 19
1.4 TREATMENT OF CHRONIC LYMPHOCYTIC LEUKAEMIA 25
1.5 GENOMIC ABNORMALITIES IN CLL 27
1.6 BIOLOGICAL AND MOLECULAR ASPECTS OF P53 33
1.6.1 Introduction to the DNA damage response *34*
1.6.2 The p53 dependant DNA damage response *35*
1.6.3 P53-DNA binding *37*
1.6.4 p53 protein modifications *37*
1.6.5 p53 isoforms *41*
1.6.6 p53 family members, p63 and p73 ..... *41*
1.7 MICRORNAS AND P53 43
1.7.1 P53 and miRNA transcription *45*
1.7.2 P53 and miRNA processing *45*
1.7.3 miRNAs in Chronic lymphocytic leukaemia *46*
1.8 PRINCIPALS OF MOLECULAR TECHNIQUES USED IN THIS WORK 47
1.8.1 Polymerase Chain Reaction *47*
1.8.2 DNA sequencing *50*
1.8.3 Pyrosequencing *51*
1.8.4 Restriction-fragment length polymorphism analysis *53*
1.8.5 Taqman™ hydrolysis probe technology *55*
1.9 FUNCTIONAL ASSAYS 57
1.9.1 Functional assessment of ATM/p53 in cancer *57*
1.9.2 Functional assays in CLL *59*
1.9.3 Nutlin3a in the functional assay of CLL cells *62*
1.9.4 The etoposide and nutlin functional assay in CLL *65*
1.10 PRIMARY HYPOTHESIS 67
1.11 AIMS AND OBJECTIVES 67

2 CHAPTER TWO: MATERIALS AND METHODS **69**

2.1 CLL PATIENT SAMPLES 70
2.2 STUDY DESIGN 70
2.3 SAMPLE PROCESSING 71
2.4 THAWING AND ENUMERATION OF VIABLE PBMC SAMPLES 72
2.5 DNA EXTRACTION 72
2.6 RNA EXTRACTION 73
2.7 POLYMERASE CHAIN REACTIONS (PCR) 74
2.8 CLONING 74
2.9 DNA SEQUENCING 75
2.10 PYROSEQUENCING 75
2.11 RESTRICTION FRAGMENT LENGTH POLYMORPHISM (RFLP) 76
2.11.1 Codon-31 of CDKN1A *76*
2.11.2 3'UTR of CDKN1A *76*
2.12 TAQMAN ASSAYS 76
2.12.1 Endpoint Genotyping *77*
2.12.2 Micro-RNA relative quantification *77*
2.13 FLUORESCENT IN-SITU HYBRIDISATION 78
2.14 ATM/P53 PATHWAY FUNCTIONAL ASSAY 80

3 CHAPTER THREE: FUNCTIONAL ASSAY PERFORMANCE **83**

3.1 HYPOTHESIS 84
3.2 CLASSIFYING THE FISH RESULTS 84
3.3 CLASSIFYING THE ASSAY RESULTS 85

3.3.1 Response to etoposide *85*
3.3.2 Response to etoposide plus nutlin3a *87*
3.4 ASSAY RESPONSES AND THE INCIDENCE OF CYTOGENETIC ABNORMALITIES DETECTED USING FISH 90
3.4.1 TP53 deletion is significantly associated with the non-responder and p21 failure categories *90*
3.4.2 ATM deletion is significantly associated with the nutlin-responder category *92*
3.4.3 The proportion of 17p-deleted cells influences the functional assay result *93*
3.4.4 The proportion of 11q-deleted cells does not influence functional status *94*
3.4.5 Summary *96*
3.5 THE ASSAY IDENTIFIES *TP53* MUTATIONS BUT NOT *ATM* MUTATIONS. 98
3.6 ANALYSIS OF THE P53 OVER-EXPRESSION CATEGORY 100
3.6.1 High baseline p53 is not required for the detection of dysfunctional responses. *102*
3.7 INVESTIGATING PREVIOUS THERAPIES IN THIS GROUP 104
3.8 SUMMARY 104

4 CHAPTER FOUR: INVESTIGATING THE P21-FAILURE ASSAY RESPONSE 106

4.1 OVERVIEW 107
4.2 HYPOTHESIS 108
4.3 THE P21-FAILURE RESPONSE DOES NOT ASSOCIATE WITH SINGLE NUCLEOTIDE POLYMORPHISMS OF THE *CDKN1A* GENE. 109
4.4 MIXING NORMAL AND P53 NULL CELLS *IN-VITRO* CAN REPLICATE A P21-FAILURE RESPONSE 111
4.5 *IN*-SILICO DILUTION OF P53-WILDTYPE WITH P53-MUTATED CLL CELLS 113
4.6 THE P21-FAILURE SAMPLES ARE ENRICHED FOR STRUCTURAL ABNORMALITIES OF *TP53*. 118
4.7 SUMMARY 119

5 CHAPTER FIVE: ANALYSIS OF HSA-MIR-34A CAN DETECT TP53 ABNORMALITIES BUT NOT ATM 120

5.1 OVERVIEW 121
5.2 HYPOTHESIS 121
5.3 SELECTION OF REFERENCE MICRO-RNA AND STANDARD RNA SOURCE 122
5.4 GENERATION OF EXTERNAL STANDARD CURVES FOR TARGET AND REFERENCE GENES. 126
5.5 CONCORDANCE OF MEASURED LEVELS OF MIR-34A DMSO STORED SAMPLES AND RNALATER STORED SAMPLES. 128
5.6 DESCRIPTION OF COHORT, MARKERS AND MIR-34A UNITS 130
5.7 MIR-34A EXPRESSION RESULTS 130
5.8 *HSA*-MIR-34A LEVELS IN SAMPLES WITH *ATM* ABNORMALITIES 132
5.9 *HSA*-MIR-34A LEVELS IN SAMPLES WITH *TP53* ABNORMALITIES 134
5.10 *HSA*-MIR-34A LEVELS IN SAMPLES WITH NO DETECTED ABNORMALITIES OF *ATM* OR *TP53*. 140
5.11 SUMMARY 142

6 CHAPTER SIX: VALIDATING ASSAY SAMPLES 144

6.1 OVERVIEW 145
6.2 HYPOTHESIS 145
6.3 PRELIMINARY INVESTIGATION ON AMBIENT EFFECTS 145
6.4 INVESTIGATING EFFECTS CAUSED BY DELAYS BETWEEN VENESECTION AND PROCESSING 147
6.4.1 Samples used in this section *147*
6.4.2 Comparison between two techniques for measuring cell viability *148*
6.4.3 Effects on cell death by drug treatments *149*
6.4.4 Spontaneous apoptosis is higher in samples which have spent a day or more between venesection and processing *151*
6.4.5 Spontaneous cell death is higher in samples with abnormalities of TP53 ..... *154*
6.4.6 Analysis of basal p53 and p21 protein levels *157*
6.4.7 Analysis of p53 and p21 protein responses in treated cultures *162*
6.4.8 Effect of transport upon functional categorisation of samples *163*
6.5 SAMPLES FROM DIFFERENT CENTRES DID NOT DIFFER IN FREQUENCY OF FISH RESULTS OR ASSAY RESULTS 166
6.6 EVOLUTION OF DYSFUNCTION OBSERVED IN PATIENT SAMPLES 167
6.7 SUMMARY 168

7 CHAPTER SEVEN: DISCUSSION AND CONCLUSION 170

7.1 INTRODUCTION 171
7.2 ASSAY DISCUSSION 171
7.3 CATEGORISATION 172
7.4 TP53 MUTATION, 17P DELETION AND NON-RESPONDERS: DISCUSSION 173
7.5 ATM MUTATION, 11Q DELETION AND NUTLIN RESPONDERS: DISCUSSION 174
7.6 INVESTIGATING P21-FAILURE: DISCUSSION 178
7.7 MIR-34A DISCUSSION 180
7.8 SAMPLE VALIDATION DISCUSSION 181
7.9 FUNCTIONAL ASSAY IN A CLINICAL VERSUS RESEARCH SETTING 184
7.10 FUTURE DIRECTION 186
7.11 CONCLUSION 187

8 PUBLISHED JOURNAL ARTICLES AND POSTERS 188

9 REFERENCES 190

10 APPENDICES 204

10.1 APPENDIX I: RESEARCH PARTICIPANT INFORMATION SHEET 204
10.2 APPENDIX II: PATIENT CONSENT FORM 208
10.3 APPENDIX III: ANTIBODIES 211
10.1 APPENDIX IV: REAGENTS AND MATERIALS LIST 212
10.2 APPENDIX V: PRIMERS 213
10.3 APPENDIX VI: POSTER FOR IWCLL. BARCELONA 2009. 214
10.4 APPENDIX VII: POSTER FOR IWCLL CONFERENCE, HOUSTON, TEXAS. 2011 215

Word Count: 49,840 over 216 pages

Document incl. references

List of Figures

Figure 1-1:*TP53* abnormalities and survival in patients treated with FCR**.** 25
Figure 1-2: The distribution of types of TP53 mutation and their relative incidence within the TP53 gene according to the IARC TP53 Mutation Database. (Brosh and Rotter, 2009) 30
Figure 1-3: The p53 nexus. 33
Figure 1-4: the p53 response pathway including the MDM2-p53 negative feedback loop and MDM4/Chk2 regulators 36
Figure 1-5: Model p53 response element (Wei *et al*, 2006). 37
Figure 1-6: Transcriptional targets of p53 within the intrinsic apoptosis pathway. 39
Figure 1-7: Transcriptional targets of p53 within the extrinsic apoptotic pathway. 40
Figure 1-8: Diagram illustrating the thermally controlled, targeted synthesis of complementary DNA during 1 cycle of a polymerase chain reaction 48
Figure 1-9: Temperature profile of a standard polymerase chain reaction 50
Figure 1-10: Example electropherogram showing a short DNA sequence 51
Figure 1-11: Diagram showing the basic chemistry of pyrosequencing. 52
Figure 1-12: An example pyrogram for a five nucleotide sequence: CGGAG. 53
Figure 1-13: Principal of Restriction fragment length polymorphism analysis .54
Figure 1-14: Principal of Taqman assay. 55
Figure 1-15: p53 induction using combination treatment of etoposide and nutlin 65
Figure 2-1: Chromosomal regions detected by Vysis FISH probes. (Abbot Molecular Inc 2011) 79
Figure 2-2: CLL DAPI-stained nuclei (Blue) with LSI TP53 (Red) and CEP17 (Green) probes 80
Figure 2-3: Flow chart showing strategy for assigning samples to functional groups 81
Figure 3-1: Showing the p53 and p21 responses to etoposide for 472 CLL cases. Markers indicating cut-off points for p53 and p21 are shown. Left panel shows all data. Right panel cropped to give greater detail of cases with dysfunctional responses. 86
Figure 3-2: Responses classified using etoposide treatment data only. n=472. 87
Figure 3-3: p53 and p21 responses to etoposide plus nutlin in 143 dysfunctional cases 88
Figure 3-4: Size of 17p-deleted clone as determined by FISH, displayed according to functional category. N=29. 93
Figure 3-5: Size of 11q-deleted clone as determined by FISH, displayed according to functional category. N=45 94
Figure 3-6: Boxplot showing p53 MFI induction in normal responders with (n=31) or without (n=277) deletion of 11q. 96
Figure 3-7. Bar chart showing the occurrences of all combinations of *ATM* and *TP53* abnormalities across the cohort, stratified by functional response to the etoposide/nutlin assay (n=123). 100
Figure 4-1: The CDKN1A gene structure. Image showing exons, introns and sites of codon-31 and 3′ UTR single nucleotide polymorphisms (SNPs) 107

Figure 4-2: Restriction digests to determine genotypes 109
Figure 4-3: LC480 output showing SNP genotypes at codon-31 and 3'UTR for 48 samples. 110
Figure 4-4: *In-silico* mixing experiments. 116
Figure 4-5: *In-silico* mixing experiments. 117
Figure 5-1: MiR-34a CP values for 13 cell lines and 2 samples arranged in ascending order. 124
Figure 5-2: RNU43 CP values for 13 cell lines and 2 samples arranged in ascending order. 124
Figure 5-3: MiR-30d CP values for 13 cell lines and 2 samples arranged in ascending order. 125
Figure 5-4: miR-34a external standard curve. Seven step, two-fold dilution series assayed in quadruplet. An error of 0.0266 and PCR efficiency of 1.797 was recorded for this curve. 126
Figure 5-5: miR-30d external standard curve. Seven step, two-fold dilution series assayed in quadruplet. An error of 0.00574 and PCR efficiency of 1.979 was recorded for this curve. 127
Figure 5-6: Showing the correlation of mir34a relative expression results for 9 matched samples stored in either RNAlater™ or cryopreserved at -70^{O}C. ...129
Figure 5-7: Results of mir-34a analysis showing the three main genotypic groups (n=114). 131
Figure 5-8: Boxplot showing mir-34a expression in the sub-categories of ATM abnormality (n=30) 132
Figure 5-9: Mir-34a results for samples with ATM abnormalities subdivided to show the effects of truncating and non-truncating mutations (n=30) 133
Figure 5-10: Mir-34a relative expression results for cases with *TP53* gene abnormalities, grouped according to genotypes (n=30). 136
Figure 5-11:Scatter plot showing the matched mir-34a and Del(17)p FISH clone size data for 20 cases with involvement of TP53. 137
Figure 5-12: Electropherograms of two cases with similar bi-allelic TP53 inactivation and differing levels of mir34a. 138
Figure 5-13: Pyramid diagram comparing the distribution of mir-34a relative expression results of p53 and ATM wildtype cases with p53 involved cases. 139
Figure 5-14: Receiver Operator Characteristics curve 139
Figure 5-15: All samples with no detected FISH loss or mutation of *ATM* or *TP53* (n=54) 140
Figure 5-16: Case LRF145 displayed unusually high expression of mir34a (mir-34a=133.6). The case was functionally classed as a non-responder. 141
Figure 5-17: Mir-34a results for 44/54 (81%) of cases that had no detected abnormalities of ATM or TP53 by FISH stratified by functional assay result and showing interquartile range. 141
Figure 6-1: Mean percentage of viable cells after storage under different conditions 146
Figure 6-2: Scatter plot showing the matched Trypan-blue and live-gate data for 64 paired data points. The data display a linear, positive correlation between the two measurements (n=64, r=.676, p<.001) 149
Figure 6-3: Paired viability data for control, etoposide and etoposide + nutlin 24hr cultures (n=112). Showing the paired data for the three treatment

conditions and displayed in order of descending percentage of viable cells in the control culture. 150
Figure 6-4: Paired viability data (n=112) stratified by the number of days between venesection and processing. Panels show data for the three treatment conditions. Data is displayed in descending order of viability in the control culture. 151
Figure 6-5: Effects of culture conditions on percentage of live cells according to time since venesection. 153
Figure 6-6: Control culture viability data for sixty-four samples with abnormalities of ATM or TP53. 154
Figure 6-7: Differences in control culture viability for cases with *ATM* gene abnormalities. 155
Figure 6-8: Differences in control culture viability for cases with TP53 gene abnormalities. 155
Figure 6-9: Comparison of the percentage of live cells in the control culture across the different genotypic sub-groups. 158
Figure 6-10: Basal p53 and p21 MFI levels in cases with no abnormalities of *ATM/TP53* grouped by time in transit. (n=149) 159
Figure 6-11: Etoposide response p53 and p21 MFI levels in cases with no abnormalities of ATM/TP53 grouped by time in transit. (n=149) 160
Figure 6-12: Analysis of p53 and p21 protein responses to etoposide plus nutlin. 161
Figure 6-13: The 99% confidence intervals for protein expression increase. Zero days versus one or more. 164
Figure 6-14:The 99% confidence intervals for protein expression increase. Zero, one, two and three days. 165
Figure 6-15: The distribution of interval times for 48 CLL patients sampled and tested twice. 167
Figure 7-1: Histogram showing the number of exons with missing data across the 155 samples tested. 176

List of Tables

Table 1-1: Incidence rates of CLL by Race/Ethnicity:.....20
Table 1-2: The Binet CLL staging system. 21
Table 1-3: The RAI CLL staging system. 22
Table 1-4: The hierarchy of CLL related chromosomal abnormalities detected using fluorescent *in-situ* hybridisation and genes involved. (Dohner *et al*, 2000).....28
Table 1-5: Incidence of cancers in normal, Li-Fraumeni syndrome and Li-Fraumeni like syndrome individuals. Adapted from (Varley et al., 1997) 29
Table 1-6: Post-translational modifications of p53 protein. 38
Table 1-7: Results summary from Lin et al, 2012 62
Table 3-1: Characteristics of cohort used in this section n=472 85
Table 3-2: Responses classified using etoposide treatment data only. n=472. 86
Table 3-3: Categorisation of 143 dysfunctional cases after evaluating nutlin response 88
Table 3-4: Categorisation of whole dataset. N=472.....89
Table 3-5: Comparison of etoposide responses and etoposide plus nutlin responses. n=472. 89
Table 3-6: Cross-tabulation of FISH results and functional assay results (n=472). 91
Table 3-7: Incidences of large and small 11q-deleted clone sizes across functional categories, n=45 95
Table 3-8: Average increase in p53 MFI after etoposide treatment in samples with a normal assay response and no detected *17p* deletion (n=307). 96
Table 3-9: Comparing the relative distribution of results between the present study and Lin *et al* (2012).....97
Table 3-10: Cross tabulation of genetic abnormalities according to functional category, n=123. 98
Table 3-11: Cross tabulation of screening results and assay responses showing bi-allelic states. n=123 99
Table 3-12: Showing the distribution of genomic abnormalities between the treated and treatment naïve patients.....104
Table 3-13:Showing the distribution of functional responses between the treated and treatment naïve patients.....104
Table 4-1: Frequency of genotypes determined by Endpoint genotyping. N=180. 110
Table 4-2: Results from two experiments mixing normal and non-responder CLL cells 112
Table 4-3: Samples selected for in-silico mixing experiments 114
Table 4-4: Incidence of genetic abnormalities involving *TP53* in 180 selected CLL cases.....118
Table 5-1: Crossing point values (CP) for thirteen cell lines and two patient samples showing the p53 status. 123
Table 5-2: Showing the CP values for miR-34a standard curve. The mean CP value of the four replicates and the standard deviation are also shown.....126
Table 5-3: Showing the CP values for miR-30d standard curve. The mean CP value of the four replicates and the standard deviation are also shown.....127
Table 5-4: Showing mir34a relative expression results for nine cases stored in either RNAlater™ or frozen at -70^{o}C.....128

Table 5-5: Summary of mir-34a relative expression results (n=114). 131
Table 5-6: Descriptive mir-34a relative expression data for 30 cases with abnormalities of TP53 135
Table 5-7: Details of two cases with similar bi-allelic TP53 inactivation and differing levels of mir34a. 138
Table 6-1: Functional assay results for sample storage study. 147
Table 6-2: Descriptive data for basal p53 and p21 protein levels in samples. 157
Table 6-3: Descriptive statistics for p53 and p21 protein responses to etoposide and etoposide plus nutlin treated culture conditions. 162
Table 6-4: Summary of FISH results grouped by contributing centre. (n=472) 166
Table 6-5: Summary of functional assay results grouped by contributing centre. (n=472).....166
Table 6-6: Details of five CLL cases which appeared to acquire dysfunction between two sampling points. 168
Table 6-7: Details of CLL cases which appeared to change dysfunctional category between two sampling points (n=5). 168

List of abbreviations

Alk	Alkylating agents
ANOVA	Analysis of variance
ASCII	American Standard Code for Information Exchange
ATM	Ataxia telangiectasia mutated
BCR	B-cell receptor
BTK	Bruton's tyrosine Kinase
CD	Cluster of differentiation
cDNA	Complimentary DNA
CEP	Chromosome centromere control probe
CI	Confidence interval
CLL	Chronic lymphocytic leukaemia
CNV	Copy number variants
CR	Complete response
dATPαS	deoxyadenosine alpha-thio triphosphate
DBD	DNA binding domain
DMSO	Dimethyl sulfoxide
DNA	Deoxyribonucleic acid
FACS	Flow assisted cell sorting
FASAY	Functional assessment of separated alleles in Yeast
FCS	Foetal calf serum
FISH	Fluorescent *in-situ* hybridisation
FITC	Fluorescein isothiocyanate
IGHV	Immunoglobulin Heavy-chain variable region
IR	Ionising radiation
HCL	Hairy-cell leukaemia
HRM	High-resolution melting
Kb	kilobases
kDa	Kilo-Daltons
LCP	Live cell percentage
LFL	Li-Fraumeni like syndrome
LFS	Li-Fraumeni syndrome
LRF	Leukaemia research foundation

LSI	Locus-specific identifier
MFI	Mean fluorescent intensity
miRNA	Micro-RNA
mRNA	Messenger RNA
NHL	Non-Hodgkin Lymphoma
OS	Overall survival
OR(R)	Overall response (rate)
PA	Purine analogues
PBMC	Peripheral-blood mononuclear cells
PBS	Phosphate buffered saline solution
PCR	Polymerase chain reaction
PE	Phycoerythrin
PFS	Progression-free survival
PR	Partial response
Q-RT-PCR	Quantitative reverse transcription PCR
RE	Response elements
RFLP	Restriction fragment length polymorphism
RNA	Ribonucleic acid
RTP	Room temperature and pressure
RT-PCR	Realtime PCR
SD	Standard deviation
SDS	Sodium-dodecyl-sulphate
SEER	Surveillance, epidemiology, and end results program
sIg	Surface Immunoglobulin
SMZL	Splenic marginal zone lymphoma
SNP	Single nucleotide polymorphism
TTFT	Time-to-first-treatment
UTR	untranslated region
UV	Ultraviolet
ZAP-70	Zeta-chain associated protein, 70kDa

Acknowledgments

I would like to thank the many people who have helped educate, train and mentor me throughout the years preceding and during the writing of this thesis.

Firstly, I give the deepest thanks to the staff and scientists of the Molecular Biology Department at the Royal Bournemouth and Christchurch hospital whose support made this project possible. In particular Professor David Oscier, Dr Giles Best, Dr Rachel Ibbotson, Dr Anne Gardiner, Dr Anton Parker and Dr Zadie Davis all provided advice, expertise and encouragement on a nearly daily basis. Also at the same department, I would like to thank Karen Kimpton, whose practical support made all the work possible; Ben Gregory who was able to provide technical skills whenever mine were found wanting and finally the cytogeneticists, Dr Sarah Mould and Dr Hazel Robinson.

From Bournemouth University, I would like to thank my supervisory team, Professor Ahmed Khattab and Dr Wei-jun Liang, for their patience and support in helping me get this thesis to submission. I must also thank the research administrators at Bournemouth for their continued patience, reminders, and kind words at times of stress (Louise Bryant, Karen Ward and Eva Papadopoulou).

The author would also like to express thanks to the Bournemouth Leukaemia Research Foundation for the funding of reagents used for this project and also many thanks to all the CLL patients who selflessly donate their blood today so that we may further our understanding of CLL and aid patients with this disease tomorrow.

Lastly, I must give thanks to my family, for providing the love, support and encouragement that got me to this point in my life. I am only sorry I took too long about getting here.

Declaration

I hereby declare that this thesis is my own work and that, to the best of my knowledge and belief, it contains no material which has been previously published or produced by another party in fulfilment, partial or otherwise, of any degree or diploma at another University or Institute of higher learning.

Chapter One:

Introduction & Literature Review

1.1 **Overview**

Non-surgical treatment of cancer historically relied on using radiation or DNA damaging drugs to induce apoptosis. When there is a clinical indication for treatment, most patients with chronic lymphocytic leukaemia (CLL) respond well to DNA damaging chemotherapeutics such as alkylating agents (alk) and purine analogues (PA). This response is improved by addition of the anti-CD20 antibody, Rituximab (Hallek et al., 2008). Tumour cell apoptosis induced using DNA damaging agents is reliant upon an intact p53-dependant DNA damage response pathway. Fluorescent *in*-situ hybridisation (FISH) is the currently employed method for detecting abnormalities of this pathway. This is achieved by identifying the loss of genetic material on chromosomes 17 and 11 which encompass the genes *TP53* and *ATM* respectively. These abnormalities are associated with a poorer response when treated with alkylating agents and purine analogues. Deletion of the short arm of chromosome-17 (17p) results in loss of *TP53*, the gene coding for p53 protein. This occurs in 5-10% of treatment naïve patients, increasing to over 30% in patients who have become refractory to standard DNA damaging therapy (Zenz et al., 2009). Deletion of a region on the long arm of chromosome-11 (11q22.3), which encompasses the *ATM* gene, is detected in 10% of CLL patients with early stage disease. This increases to 25% of untreated patients with advanced disease (Hallek, 2013b). Mutation screening of either gene is not yet routinely performed, yet it is known that mutations of p53 and ATM can occur alone and can have a similar impact upon outcome as deletion detected by FISH (Zenz et al., 2008b). A mutation of p53 in the absence of a deletion of 17p13.1 detected using FISH occurs in a further 5-10% of untreated CLL patients and in up to 50% of patients who are refractory to first line therapy administering alkylating agents and purine analogues (Zenz et al. 2012). Some patients who fail to respond to standard treatment have no detectable abnormalities of p53 or ATM. Curiously, a minority subset of patients with early stage CLL have abnormalities of p53 yet follow a benign clinical course, a phenomenon also observed in some patients with splenic marginal zone lymphoma (SMZL) (Best et al., 2008a, Tam et al., 2009). Determining what factors may be responsible for this benign course in the

presence of high-risk abnormalities could have clinical and therapeutic applications.

In this project a functional assay designed to detect defects within the ATM/p53-dependant DNA damage response will be performed for CLL patients prior to initial or subsequent treatments. The functional study results will be compared to FISH and mutation screening data for p53 and ATM and then correlated with clinical information where available. The primary aim is to determine whether the assay described herein is able to detect mutations and/or deletions of the *TP53* and *ATM* genes. The secondary aim is to determine whether the assay can differentiate between dysfunctional responses of the p53-dependant DNA damage response caused by either of the aforementioned genes. The tertiary aim is to assess the clinical relevance of the assay for predicting the response to treatment with DNA damaging chemotherapeutics.

1.2 Definitions and nomenclature

It would at this point be worth clarifying the nomenclature of the genes/proteins that are going to be frequently mentioned throughout this thesis.

The HUGO Gene Nomenclature Committee is the organisation responsible for providing guidelines on the naming of human genes and for the approval of new gene names and genes symbols. They define a gene as "a DNA segment that contributes to phenotype/function. In the absence of demonstrated function a gene may be characterised by sequence, transcription or homology". As well as a name, a gene is assigned a gene symbol, an often abbreviated form of the name in which all letters are capitalised and presented in italics. For example one gene of interest is *ATM*. This is the gene symbol for the gene named, Ataxia telangiectasia mutated. In this case the gene name is taken from the congenital disorder which prompted the research which led to its discovery. The gene symbol of the other gene of interest in this work is *TP53.* Its gene name, tumour protein p53 differs from ATM in that it is not named for a disease. Both *ATM* and *TP53* are protein coding genes and so the protein product also has a name. For most cases it is simply the same as the gene symbol except without the italics eg, ATM is the protein encoded by the *ATM* gene. This, however, is not the case for the protein product of the *TP53* gene. This is known as p53.

This understanding of the different names for the genes and proteins mentioned herein is important to avoid confusion eg, when discussing the relationships between mutations of the gene and the effect this has upon the protein.

1.3 Chronic Lymphocytic Leukaemia (CLL)

Chronic lymphocytic leukaemia (CLL) is the most common form of adult leukaemia in the western world (Montserrat et al., 1991, Oscier et al., 2012). Data from the National Cancer Institute's SEER (Surveillance Epideimology and End Results) review from 2005-2009 found the median age at diagnosis for CLL was 72 years (Oscier et al. 2012). The overall 5-year survival for CLL patients, relative to the general population, is 78.8%. In the United Kingdom

the age-standardised rate of new CLL diagnoses is 5.7 cases per 100,000 of the population per year (Cancer Research UK 2015). The incidence of CLL is approximately twice as high in males as in females for unknown reasons. The incidence of CLL also appears to be affected by race/ethnicity, with Caucasians showing the highest incidence rate. Table 1-1 contains the data on CLL incidence by Race reported in Howlader *et al*, (2013).

Table 1-1: Incidence rates of CLL by Race/Ethnicity:

Race/Ethnicity	Male	Female
All Races	5.8 per 100,000	3.0 per 100,000
White	6.1 per 100,000	3.2 per 100,000
Black	4.3 per 100,000	2.0 per 100,000
Asian/Pacific Islander	1.3 per 100,000	0.7 per 100,000
American Indian / Alaskan Native	2.5 per 100,000	
Hispanic	2.4 per 100,000	1.5 per 100,000

The highest incidence of CLL occurs in Caucasian populations which may support the role of genetic factors in the ontology of CLL. Table reproduced from (Howlader et al. 2013).

Statistical evidence for some genetic influence in CLL was found during a study of Swedish population data available on diagnoses made between 1958-2005 (Landgren et al., 2008). The rate of lympho-proliferative disorders, including CLL, in 26,947 first degree relatives of 9,717 CLL patients was compared to the same rate between 38,159 matched controls and 107,223 of their first degree relatives. Although the overall risk of familial CLL was very low, first degree relatives of CLL patients had an increased risk of developing CLL (HR=8.5; 95% CI=6.1-11.7) compared to controls as well as the non-Hodgkin lymphomas Lymphoplasmacytic lymphoma / Waldenström's macroglobulinemia (HR=4; 95% CI=2.0-8.2) and Hairy cell leukaemia (HR=3.3; 95% CI=1-10.9) (Goldin et al., 2009, Landgren et al., 2008). Genome wide SNP analysis has identified several alleles associated with risk of developing CLL and which appeared to have a cumulative effect upon the odds ratio of developing CLL (Crowther-Swanepoel et al., 2010).

Diagnosis of CLL is based upon a persistent (> 3 months) B-cell lymphocytosis of greater than $5x10^9$/L as assessed by a full blood count and

identified as monoclonal using flow cytometry (Bene et al., 2011). A recommended flow cytometry scoring system of five markers is used to identify CLL: expression of weak surface immunoglobulin (slg), CD5, CD23, and low/ absent expression of FMC7 and CD79b (Moreau et al., 1997). Four or five of these markers correctly indicates ninety-two percent of CLL cases (Cro et al., 2010).

CLL is incurable using chemotherapy and heterogeneous in its progression with overall survival ranging from months to decades (Oscier *et al*, 2012). Patients may fall into three broad categories: early stage with a low tumour burden, early stage at diagnosis with progression over time or advanced stage disease at diagnosis.

The Binet and Rai scales are the accepted systems for staging CLL at diagnosis (Rai et al., 1975, Binet et al., 1981, Hallek et al., 2008). These systems are summarised in Table 1-2 and Table 1-3, and are sometimes combined into A(0), A(I), A(II); B(I), B(II); and C(III), C(IV) stages.

Table 1-2: The Binet CLL staging system.

Binet stage	Areas of lymphoid involvement	Anaemia and/or thrombocytopenia
A	Less than 3	No
B	3 or more	No
C	Any number	Yes

Table 1-3: The RAI CLL staging system.

RAI stage	Required observation	May or may not be present
O	Lymphocytosis only	n/a
I	Lymphocytosis and enlarged nodes	n/a
II	Lymphocytosis and organomegaly (Liver or Spleen)	Enlarged nodes
III	Lymphocytosis and anaemia	Organomegaly or enlarged nodes
IV	Lymphocytosis and thrombocytopenia	Organomegaly, enlarged nodes or anaemia

Lymphocytosis requires clonal B-cell lymphocyte count >$5x10^9$/L as obtained by routine whole blood analysis.

A number of biological markers have been discovered which inform on CLL patient prognosis. These associate with parameters such as time to first treatment (TTFT) and overall survival (OS) in CLL patients. They can be divided into intrinsic and extrinsic factors depending upon whether they affect the underlying genetics of the CLL cell, or influence the interactions between the CLL cell and its microenvironment, respectively (Dal-Bo et al., 2009).

Sequence analysis of the rearranged immunoglobulin heavy chain variable (IGHV) region of the B-cell receptor (BCR) of the patients B-CLL clone was found to accurately differentiate between patients with indolent or aggressive disease. An IGHV sequence that is unmutated or has greater than 98% similarity to the germline sequence is associated with an aggressive disease (Damle et al., 1999, Hamblin et al., 1999). In addition to the percentage mutation relative to the germline, the use of particular stereotyped BCR genes, such as V3-21, has also been shown to be an independent prognostic marker (Tobin et al., 2002).

IGHV analysis is generally considered to be the gold standard for determining prognosis but other molecular features of poor prognosis have been identified. In particular, methods which are suited to flow cytometry have been developed as this is a platform which is particularly suited to the analysis of

samples derived from blood. A number of prognostic markers have been identified for this purpose.

Zeta-chain-associated protein kinase 70kDa (Zap-70) is a tyrosine-protein kinase involved in T-cell signalling which is normally expressed in T-cells and natural killer cells (Chan et al., 1992). It was shown to be aberrantly expressed in a subset of CLL patients and was associated with unmutated IGHV genes, a poorer clinical outcome and increased BCR signalling (Wiestner et al., 2003) (Chen et al., 2002) which lead to it being suggested as a surrogate marker for IGHV status(Crespo et al., 2003). B-CLL cells circulating in the peripheral blood have lower levels of ZAP-70 compared to their counterparts within lymph nodes suggesting that factors within the node micro-environment which promote proliferation are responsible for increasing ZAP-70 levels (Boelens et al., 2007). The expression of ZAP-70 protein has been shown to be suppressed by methylation of the ZAP-70 gene at the intron1-exon2 boundary (Corcoran et al., 2005). Zap-70 remains a prognostic marker of limited value as there are still questions regarding its stability over time, reproducibility of results between different centres and the best methodology for detection.

The surface antigen CD38 (cyclic ADP ribose hydrolase) is a regular feature of the B-CLL phenotype and its expression was linked to prognosis at the same time as V-Genes (Damle et al., 1999) and then subsequently shown to be predictive of survival in CLL patients (Mainou-Fowler et al., 2004, Morabito et al., 2001). The role of CD38 is thought to be linked to cell signalling in the micro-environment of proliferation centres such as the lymph nodes. CD38 has been shown to ligate to CD31, aka PECAM-1 (platelet endothelial cell adhesion molecule-1), a surface marker expressed on endothelial cells, platelets, macrophages, lymphocytes and granulocytes. This binding increases growth and survival of the CLL cells brought about by changes in their gene expression profile affecting up to 85 separate cellular pathways. Of these 85 pathways, 30% were shown to be involved in lymphocyte adhesion, movement and/or signalling (Deaglio et al., 2010). It has been shown that the levels of CD38 may change throughout the course of the disease (Hamblin et al., 2002). CD38 analysis can be combined with ZAP-70 analysis for flow cytometric analysis (Hassanein et al., 2010).

More recently another cell surface marker, CD49d (Integrin Subunit Alpha 4), has been shown to have strong prognostic value in CLL. Following a large study of 2972 CLL cases CD49d is now considered to be one of the strongest predictors of overall survival that can be determined using flow cytometry (Bulian et al., 2014). The Bulian study found that cases showing CD49d expression on ≥30% of the tumour cells reliably identified subsets of patients who had poor outcomes in terms of overall survival and treatment free survival. The authors found that there was no further prognostic information added by the analysis of either CD38 or ZAP-70 (Bulian et al., 2014).

It could be argued that at the point of needing treatment, predictive rather than prognostic tests are required. These are focused on detecting the intrinsic, high-risk genetic abnormalities that are associated with treatment failure, an approach that will be used in this study.

1.4 Treatment of chronic lymphocytic leukaemia

Aside from a minority of patients with prolonged disease free survival following allogeneic bone marrow transplant, CLL remains incurable. Treatment is currently recommended for patients showing signs of progressive or active disease (Hallek et al., 2008, Hallek, 2013b).

Recommended standard first line therapy for physically fit patients combines the purine analogue fludarabine, the alkylating agent cyclophosphamide and the anti-CD20 antibody, rituximab (FCR). This combination has been shown to give the best overall response rates (OR), complete remission rates (CR) and progression free survival (PFS) (Hallek et al., 2008). For patients who are less fit the single alkylating agent chlorambucil is used in combination with anti-CD20 antibodies (Hallek, 2013a).

If a patient does not relapse for 2 years after therapy then the first line therapy may be repeated when relapse does occur. For those patients who do relapse within this time-frame the mustard based compound, bendamustine, is recommended, alone or in combination with antibody therapy (Hallek, 2013b)

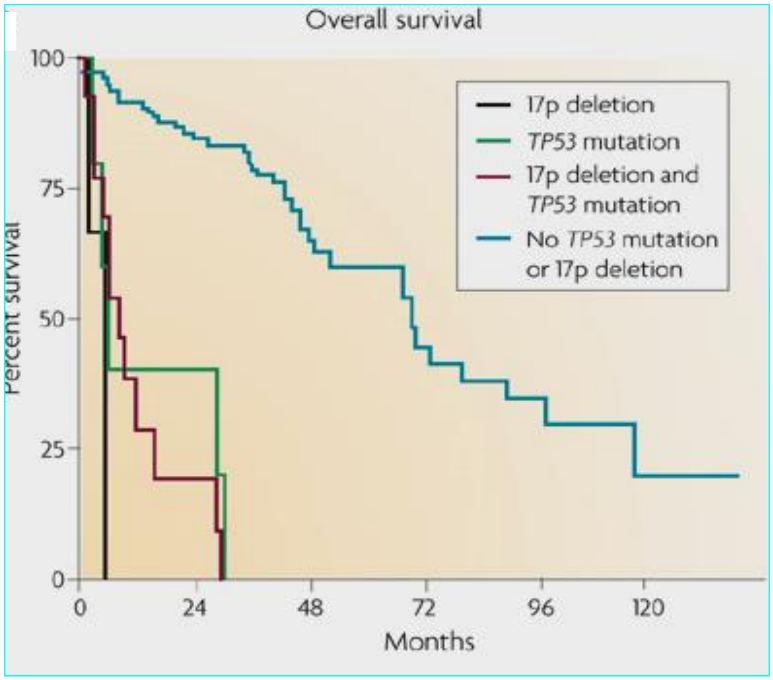

Figure 1-1:*TP53* abnormalities and survival in patients treated with FCR**.**

The overall survival of patients with any abnormalities of *TP53* is greatly reduced when compared to normal patients treated with fludarabine/cyclophosphamide and rituximab **(**FCR) (Zenz and Stilgenbauer, 2009, Zenz et al., 2010) .

Rituximab has additional benefit for patients with del11q and has been tested in combination with chlorambucil or bendamustine as a first line treatment (Zenz and Stilgenbauer, 2009). Fludarabine based therapy is ineffective for CLL with del17p and/or mutation of the *TP53* gene as is shown in Figure 1-1 which is reproduced from Zenz et al. (2010).

Fludarabine use in patients with del17p in less than 20% of the CLL clone has been shown to kill non-del17p CLL cells and enrich for del17p, fludarabine-resistant cells (Zenz et al., 2008a). The danger in these cases is that new mutations caused by DNA damaging agents could generate more aggressive sub-clones. Drugs that do not kill using DNA damage include immunotherapies such as the anti-CD20 antibody, Rituximab (Mabthera®) which may be used alone or in combination with other agents depending on patient fitness (Hallek et al., 2008). Other therapies showing activity in patients with del17p include the thalidomide derivative lenalinomide and the immunotherapy ofatumumab and these are currently being trialled (Coiffier et al., 2008, Ferrajoli et al., 2008).

New classes of drugs that target B-cell receptor mediated signalling are showing promise for CLL patients independently of del17p. The Brutons tyrosine kinase (BTK) inhibitor, ibrutinib (Imbruvica®), was licensed for the treatment of CLL in the UK in 2014 following impressive results in a phase III study in relapsed/refractory CLL patients (Byrd et al., 2014a).

A novel adaptation to the off-license, DNA damaging chemotherapeutic drug chlorambucil, has also been shown to have activity in cell lines which are normally resistant to chlorambucil (Fonseca et al. 2011). The use of a polypeptide bound to chlorambucil (mt-Chlor) actively targeted the alkylating agent to the mitochondria. In cell lines that were shown to be resistant to chlorambucil, mt-Chlor rescued the level of apoptosis induced to that seen in chlorambucil sensitive cell lines. In addition Fonseca *et al* also showed *in-vitro* that mt-Chlor had selective activity in primary CLL cells when compared to peripheral blood stem cells or erythrocytes and mononuclear cells from healthy donors (Fonseca et al., 2011).

1.5 **Genomic abnormalities in CLL**

Alterations of the genome are highly associated with cancer initiation and progression and there are several techniques for detecting them. This section will look at how the most recurrent abnormalities in CLL affect the disease.

Chromosome banding facilitates the visual identification of the entire human karyotype and is well suited to haemato-oncology (Sanchez et al., 1973, Yunis and Sanchez, 1975, Crowther-Swanepoel et al., 2010). Large gains, losses or translocations of genetic material that occur regularly in CLL are screened for using other techniques, in particular fluorescent *in-situ* hybridisation (FISH) is a robust methodology utilising fluorescent DNA probes to detect specific loci within the genome (Sandberg, 1981, Dohner et al., 1997a, Dohner et al., 1999, de Oliveira et al., 2010). New technologies for detecting copy number variants (CNVs) and loss of heterozygosity (LOH) with higher specificity, such as comparative genomic hybridisation to micro-arrays (array-CGH) (Pinkel et al., 1998, Tyybakinoja et al., 2007) and single nucleotide polymorphism (SNP) arrays (Ouillette et al., 2008, Sellick et al., 2005), may eventually supersede FISH and karyotyping. Cheaper options such as multiplex ligation-dependant probe amplification (MLPA) (Schouten et al., 2002) are also available.

Several loci, frequently altered in CLL, are regularly screened using FISH. Based upon previous studies (Dohner et al., 1999, Dohner et al., 1997a, Dohner et al., 1997b, Juliusson et al., 1990), Dohner *et al*, (2000) determined a hierarchy of common chromosomal abnormalities, stratified by median survival Table 1-4. With regards predicting response to chemotherapy the most relevant of these is loss/deletion of material on chromosomes 11q22-23 or 17p13.1 (del11q and del17p).

The poor prognosis, reduced overall survival (OS) and increased involvement of lymph nodes associated with del11q in CLL is thought to be due to loss of the *ATM* gene (Dohner et al., 1997b, Monni and Knuutila, 2001). The very poor prognosis of del17p is due to the loss of the gene for p53 (*TP53*), a central component of cell cycle and DNA repair pathways (Wei et al., 2006). Loss of one allele of *TP53* is advantageous for tumour cells allowing evasion of senescence and apoptosis pathways and resistance to DNA damaging

therapies. This is reflected in the recurrent detection of p53 abnormalities in all forms of cancer. Clinical trials have repeatedly shown that del17p is highly associated with a poor response to first line chemotherapy and shorter overall- and progression-free survival (OS/PFS) (Zenz et al. 2012).

Table 1-4: The hierarchy of CLL related chromosomal abnormalities detected using fluorescent *in-situ* hybridisation and genes involved. (Dohner *et al*, 2000)

Abnormality detected using FISH	Median survival (months)	Gene/s involved
Deletion 17p13.1	32	*TP53*
Deletion 11q22-23	79	*ATM, MRE11, H2AFX*
No abnormalities	111	n/a
Trisomy-12	114	Numerous candidates including *MDM2*
Deletion 13q14 only	133	miRNA's, *DLEU1* & *DLEU2*

In addition to deletion of chromosomes, the genes for *ATM* and *TP53* are also affected by mutations within the protein-coding DNA sequence. Non-sense mutations result in the production of truncated proteins or no protein at all. Miss-sense mutations may lead to the production of a full length protein with altered properties.

Dysfunction of the *ATM* gene through mutation is known to be the cause of the recessively inherited congenital condition, ataxia-telengiectasia (A-T) (Stankovic et al., 1998). In CLL cells ATM mutations result in defective DNA damage signalling and pro-apoptotic responses (Stankovic et al., 2004, Stankovic et al., 2002, Stankovic et al., 1999). Detecting mutations of *ATM* is complicated by the size and complexity of the gene (68 exons) (Stankovic et al., 1997). It was thought that mutation of the remaining copy of the *ATM* gene in CLL patients with del11q could be an important determinant of therapy resistance (Austen et al., 2007). An analysis on the impact of bi-allelic *ATM* gene abnormalities in 224 patient samples from the UKCLL4 trial, who received first line treatment with chlorambucil or fludarabine with and without cyclophosphamide, supports this hypothesis (Skowronska et al., 2012). This

retrospective study determined the status of both alleles for both the *ATM* and *TP53* genes, using FISH screening and mutational analysis, and then compared the median progression free survival (PFS) between groups. It found that cases with biallelic inactivation (mutation of one allele and deletion of the other) had a significantly shorter median progression-free survival than normal cases with no abnormalities (7.4 v 28.6 months). The effect was similar to that seen in patients with mono-allelic *TP53* alterations (6.7 v 28.6 months). In contrast there appeared to be little or no impact upon median PFS for *ATM* mutated cases which retained a second wildtype allele (30.8 v 28.6 months). With a median OFS of 17.1 months, cases with deletion of one allele without mutation of the second appeared to be intermediate between biallelic alteration (mutation and deletion) and wildtype cases. This suggests that 11q deletion may have a greater impact upon the disease than inactivation of the *ATM* gene via mutation, possibly through the loss of other genes located on chromosome 11.

Li-Fraumeni syndrome (LFS) and Li-Fraumeni-like syndrome (LFL) are congenital conditions usually involving a germline heterozygous mutation of *TP53* and a predisposition to cancer, the incidence rates are shown in Table 1-5 (Varley et al., 1997).

Table 1-5: Incidence of cancers in normal, Li-Fraumeni syndrome and Li-Fraumeni like syndrome individuals. Adapted from (Varley et al., 1997)

	Incidence of cancer	
	< 30 years old	**< 50 years old**
General population	2%	11%
Li-Fraumeni syndrome	56%	100%
Li-Fraumeni like syndrome	44%	78%

Somatic *TP53* mutations are predominantly single base, miss-sense transitions or transversions that cluster in exons 5-9 (Figure 1-2), which is the region which encodes the protein's DNA binding domain (DBD). Mutations within the DBD result in altered affinity for p53 response elements (REs). In addition, mutations within the DBD abrogate p53's transcription-independent, sequestering of pro-apoptotic proteins (Vaseva and Moll, 2009). Small

insertions and deletions occur less frequently and tend to occur outside of exons 5-9 (Cho et al., 1994, Soussi et al., 2006). Mutations may be classified as either contact or conformational mutants depending on whether the mutation affects amino acids that come into contact with DNA or alter the tertiary structure of the protein.

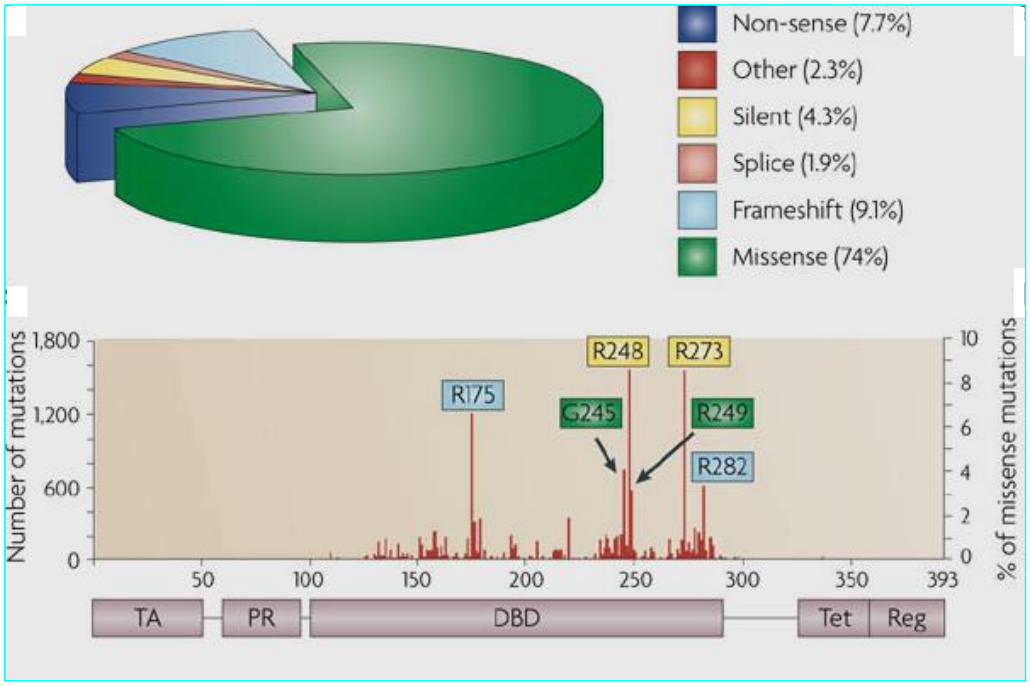

Figure 1-2: The distribution of types of TP53 mutation and their relative incidence within the TP53 gene according to the IARC TP53 Mutation Database. (Brosh and Rotter, 2009)

The effects of *TP53* gene mutation on p53 protein function can be described in three ways: (i) Loss of function is effectively a p53-null phenotype whereby p53 loses the ability to bind DNA; (ii) Gain of function involves p53 acquiring new properties, not seen in wildtype p53 (wtp53); and (iii) Dominant negative refers to mutant p53 interacting with the remaining wildtype p53 and inhibiting its normal action. These effects are not mutually exclusive and their occurrence may be influenced by cell type (Blagosklonny, 2000, Brosh and Rotter, 2009). While the first two of these effects refer to the transcriptional activity of the mutant p53 protein itself, the dominant negative effect may only occur in cells which have a heterozygous mutation with expression of both wildtype and mutant p53 protein within the cell. It has been shown *in-silico* that the presence of both results in the loss of transcription of familiar p53 transcriptional targets such as p21 and MDM2 (Junk et al. 2008). The authors

in Junk et al (2008) were able to show that the ability of wildtype p53 to bind the promoters of 324 targets genes was almost completely lost when mutant p53 was introduced.

An example of a gain of function is shown in a study of cell lines known to harbour common p53 mutations. Di Agostino et al (2006), found that in response to DNA damage mutant p53 protein interacted with the nuclear transcription factor complex, NF-Y. This in turn led to an increase in the expression of NF-Y targets genes such as cyclinA, cyclinB1, cdc25 and cdk1, ultimately leading to increased DNA synthesis. Under the same conditions wildtype p53 would normally co-localise with NF-Y to repress the expression of these genes. The authors of this study were able to show that this change in expression of cell cycle genes was due to the presence of the mutant p53 and not due to loss of the wildtype and therefore can be classified as a gain of function (Di Agostino et al., 2006).

In CLL, *TP53* mutation is commonly accompanied by del17p but between 6-23% of patients with mutations may have no detectable loss using FISH (Malcikova et al., 2009, Rossi et al., 2009). However, mono-allelic mutation cases have similar survival rates to bi-allelic cases (Zenz et al., 2008b) therefore mutation detection is an important analysis that should be used to complement FISH. Interestingly, a small subset of patients with these high risk genomic defects (del17p, *TP53* mutation) has been reported with clinically benign disease (Best et al., 2008a, Tam et al., 2009). It is thought that this may relate to the clinical heterogeneity of CLL as most of these benign patients have mutated IGHV sequences and may therefore lack proliferative capacity (Best et al., 2008a).

Detection of aberrant p53 protein stability in tumour cells is associated with *TP53* mutations (Chang et al., 2010, Chang et al., 2007). However evidence that p53 over-expression is context dependant suggests that its use alone may lead to error prone results (Colomer et al., 2003, Terzian et al., 2008, Zenz et al., 2008a).

Detecting mutations within *ATM* and particularly *TP53* is of importance due to the significant impact they have upon response to therapy. Detecting mutations by direct sequencing of genomic DNA has limited sensitivity as mutations in less than 20% of the sample become increasingly difficult to

detect. Time and labour are also factors that influence the use of sequencing, especially for large genes. To increase the sensitivity of mutation detection techniques have been developed to either enrich for mutated DNA in a sample or detect mutations with much higher sensitivity. Many of these screening techniques exploit the thermodynamic and conformational differences between wildtype and mutant DNA. High-resolution melting (HRM) analysis detects differences in melting temperature (T_m) between homoduplexes and heteroduplexes formed during PCR amplification of samples containing mutant DNA. Co-amplification at lower denaturing temperatures (COLD)-PCR preferentially amplifies mutant DNA during PCR and can be applied to increase the sensitivity of other PCR based technologies eg, Sanger-sequencing (Sanger et al., 1977) and pyrosequencing (Ronaghi et al., 1996).

A recent investigation of the UK CLL4 trial used capillary-electrophoresis single strand conformation (CE-SSCP) to detect *TP53* mutations (Gonzalez et al., 2011). This study analysed patient samples from 529 of the 777 trial participants. This study is particularly important as the CLL4 trial is now beyond the five year follow up point and all the participants were previously untreated. The study detected forty-three *TP53* mutations in forty (7.6%) patients. The three patients with two mutations detected were then analysed using FASAY and the mutations were confirmed as being located on separate alleles. As expected, this study found that the presence of a *TP53* abnormality was significantly associated with lower overall response rates (classified according to NCI criteria) and this was true whether for patients with del17p and a *TP53* mutation or those who had either del17p or *TP53* mutation alone. In addition, *TP53* mutations were significantly associated with shorter overall survival and shorter progression free survival. Importantly this study detected *TP53* mutations in the absence of del17p in about 3% of cases.

1.6 **Biological and Molecular aspects of p53**

In over thirty years since its discovery there have been paradigm shifts concerning the role of p53 in normal and cancerous cells (Bienz et al., 1984, Crawford et al., 1981, DeLeo et al., 1979, Gohler et al., 2002, Hinds et al., 1989, Liu et al., 1999, Pennica et al., 1984). It is an orchestrator of numerous cellular processes including apoptosis, and responds to a variety of intra- and extra-cellular stresses (Figure 1-3). Its main role is as a transcription factor (Calabretta et al., 1986, Mercer et al., 1984, Shohat et al., 1987). In 1994 it was named 'Molecule of the Year, 1993' (Beijnen, 1994).

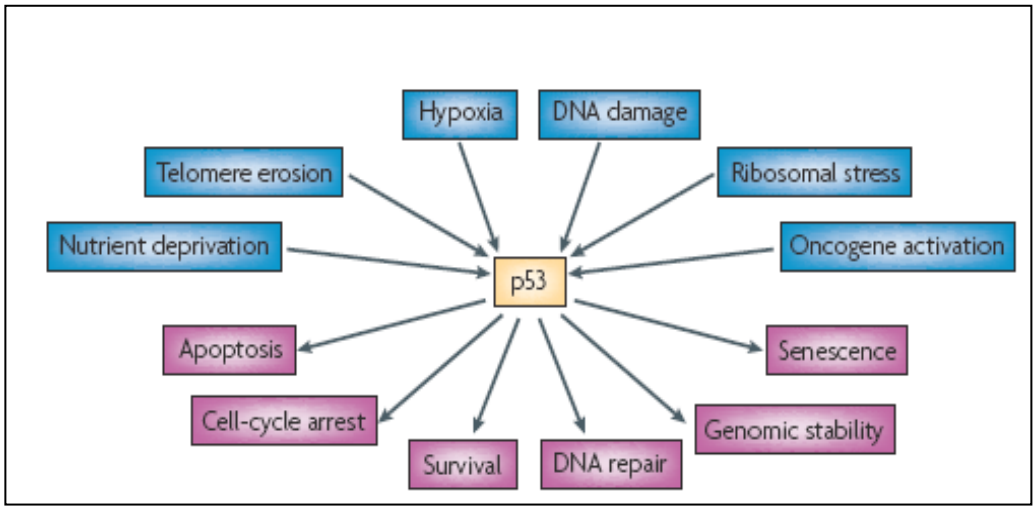

Figure 1-3: The p53 nexus.
The p53 protein responds to a wide variety of cellular stresses and through regulation of downstream gene expression is able to influence the cellular outcome of these stresses. (Vousdan and Lane, 2007)

In unstressed cells p53 is constitutively expressed but tightly regulated to prevent inappropriate activation of apoptotic or senescent genes. The activation of p53 occurs as a response to numerous forms of stress signalling. Oxidative stress, nutrient deprivation, hypoxia, DNA damage, loss of telomeres, miRNA processing and activation of oncogenes can all result in p53 activation. It is the role p53 has in control of the DNA damage response which is most relevant in terms of induction of apoptosis in tumours due to the DNA damaging nature of many chemotherapeutics.

1.6.1 **Introduction to the DNA damage response**

Before introducing the role of p53 specifically it is important to introduce the overall cellular response to different types to DNA damage. DNA damage occurs within cells daily and the sources of this damage are varied. It can occur as a result of environmental insults such as ultraviolet radiation or chemicals, including those produced in tobacco smoke. By-products of cellular metabolism such as reactive oxygen species can lead to DNA lesions. Also, DNA can also be damaged as a part of normal cellular processes such as breaks formed during DNA replication during the cell cycle. The type of damage that can occur to DNA is also varied, including base-pair mismatches and cross-linking of nucleotides, or single and double stranded breaks in the DNA.

In order to maintain the integrity of the genome cells have developed systems which sense damaged DNA, signal their presence and ensure their repair. Because there are differing types of DNA damage there are different mechanisms that are employed in their repair. Mismatches and insertion/deletions introduced during DNA replication are dealt with by the mismatch repair pathway (MMR) involving the creation of a single strand incision which is then acted upon by nuclease, polymerase and ligase enzymes. The base excision repair (BER) pathway detects and replaces damaged bases. Nucleotide excision repair (NER) is employed if adducts are detected which affect the structure of the helix, such as those caused by UV light. MMR, NER and BER are the pathways that deal with breaks affecting only a single strand of DNA. Double stranded DNA breaks can be repaired by either homologous recombination (HR) or by non-homologous end-joining (NHEJ). NHEJ is known to be error prone and results in the deletion of DNA bases but it can be employed at any stage in the cell cycle. It is also one of the mechanisms employed during V-D-J and class switch recombination as a part of normal B-cell maturation. Homologous recombination can repair double stranded breaks more accurately than NHEJ as this process uses the second allele as a template. Because of this reliance on the sister chromatid, HR can only be employed during the synthesis and G-2 stages of the cell cycle (Jackson & Bartek 2009).

1.6.2 **The p53 dependant DNA damage response**

The cellular response to DNA damage varies according to the type of damage itself. The ATM mediated response to oncogene activation or double stranded DNA damage is illustrated in Figure 1-4 (p36). In the response to double strand DNA breakages the initial sensor of DNA damage is the Mre11-Rad50-Nbs1 (MRN) complex, which displays a high affinity for the ends of double stranded DNA ensuring rapid association to the ends of broken DNA (Lisby et al., 2004, Petrini and Stracker, 2003). The MRN complex acts as a flexible tether, binding two ends of DNA and uncoiling them so that they are accessible to the kinase ATM (de Jager et al., 2001, Paull and Gellert, 1999). ATM perpetuates the DNA damage signal by phosphorylating the MRN complex, the histone H2Ax, and checkpoint-kinase-2 (Chk2) (Cai et al., 2009). ATM mediated phosphorylation of MDM2, MDM4 and p53 results in the interruption of p53 turnover and the rapid accumulation of p53 protein in the nucleus where it is then free to carry out its activities as a homo-tetrameric transcription factor (Dzikiewicz-Krawczyk, 2008, Hirao et al., 2000, Khosravi et al., 1999, Matheu et al., 2008). MDM2 is itself a target of p53 controlled transcription so if the DNA damage signal ceases MDM2-mediated degradation of p53 will resume, quickly restoring the cellular levels of p53 to a pre-stressed state. Interestingly, a SNP within the first intron of *MDM2* may adversely affect p53 function and is being evaluated for independent prognostic value in CLL (Asslaber et al., 2010, Merkel et al., 2010, Willander et al., 2010).

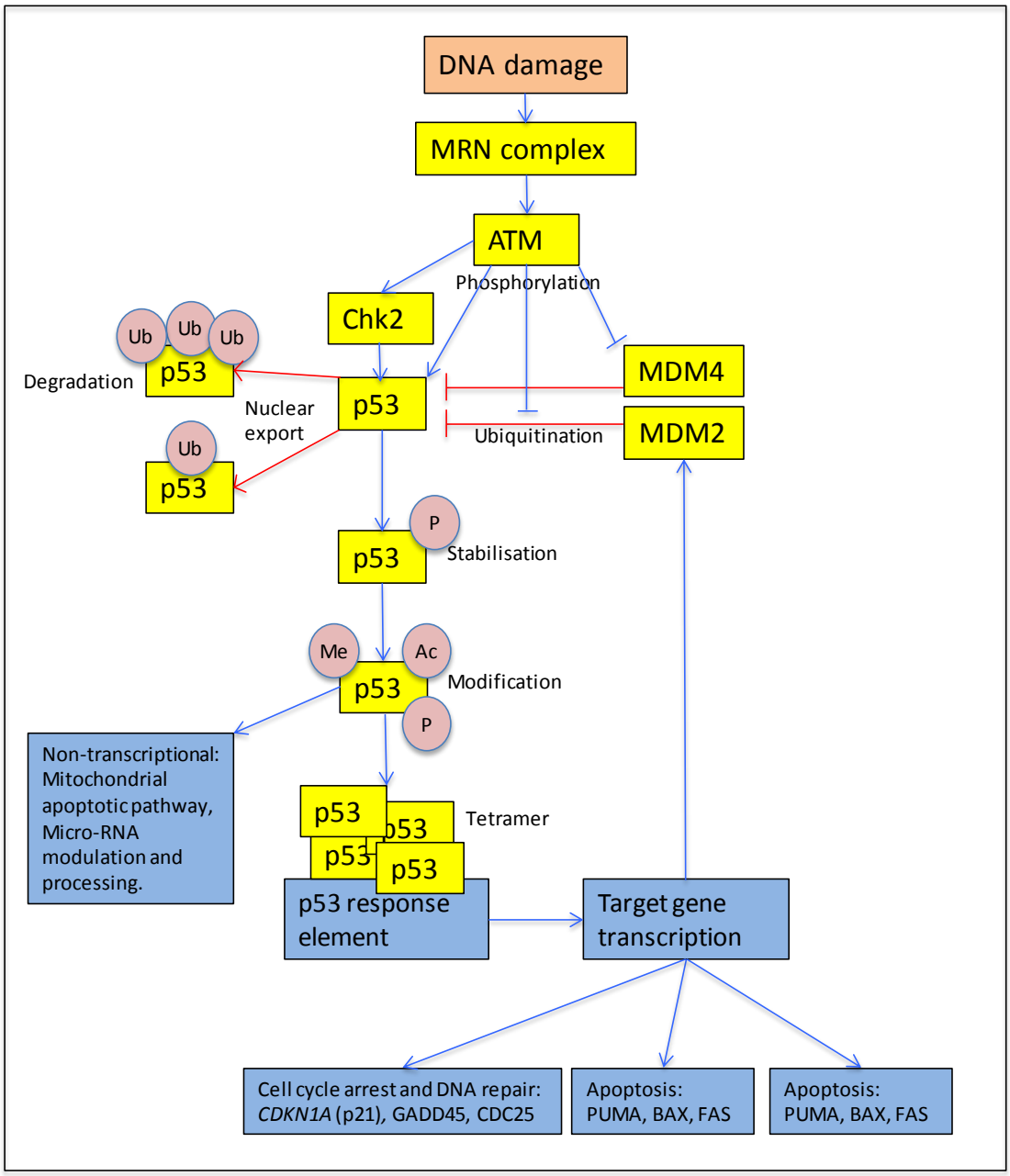

Figure 1-4: the p53 response pathway including the MDM2-p53 negative feedback loop and MDM4/Chk2 regulators

Activation of ATM results in phosphorylation of p53, Chk2, MDM4 and MDM2. Stabilised p53 protein is then subject to multiple modifications, mainly targeted to Lysine residues. Tetramers of p53 recognise response elements in DNA and activate transcription of target genes involved in diverse cellular processes. Among these is MDM2 which, if p53 activation signals are not continued, closes the negative loop by ubiquitinylating p53 and targeting it to the cytoplasm (mono-ubiquitinylation) for degradation by the proteosome (poly-ubiquitinylation). Ub = Ubiquitin; P = Phosphorylation; Me = Methylation; Ac = Acetylation

1.6.3 **P53-DNA binding**

The function of p53 as a transcription factor is intrinsically linked to its ability to recognise and bind to specific regions within the genome. The p53 DNA-binding domain (DBD) binds to degenerate DNA sequences known as response elements (REs) found within promoter regions or introns of hundreds of potential target genes (Cho et al., 1994, Gohler et al., 2002, Wei et al., 2006). Figure 1-5 below shows the model DNA binding motif determined experimentally by Wei et al, (2006). It shows the two, 10-nucleotide long, palindromic half-sites with the heights of the letters representing the relative occurrence of a given nucleotide at a given position in the sequence.

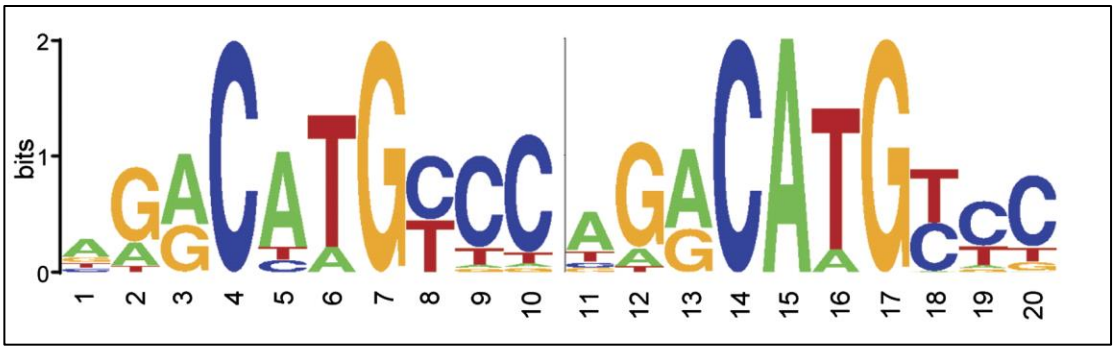

Figure 1-5: Model p53 response element (Wei *et al*, 2006).

The variable dissociation constant between the p53-DBD and different REs creates a sensitive, dose-dependent mechanism for controlling the sequence of genes targeted by p53. Notably the response elements of cell cycle arrest genes have a higher affinity for the p53-DBD than those of apoptosis related genes (Jordan et al., 2008, Weinberg et al., 2005).

1.6.4 **p53 protein modifications**

Further fine tuning of p53 activity is achieved via a variety of post-translational modifications. Table 1-6 shows a summary of these modifications and the proteins known to catalyse their addition and removal (Carter and Vousden, 2009).

Table 1-6: Post-translational modifications of p53 protein.

Protein modification	Modifier	Effect	Reference
Ubiquitination	MDM2	Negative feedback loop	Momand *et al* , 1992
	E4F1	Cell cycle arrest, not apoptosis	Cam et al, 2006
	CHIP	p53 degradation	Esser *et al,* 2005
	COP1	Negative feedback loop	Dorman *et al* , 2004
	Pirh2	Negative feedback loop	Leng *et al* , 2003
NEDDylation	FBX011	Inhibits p53 transcriptional activity	Abida et al, 2007
	MDM2	Inhibits p53 transcriptional activity	Xirodimas et al, 2004
Acetylation	Pcaf	Cell cycle arrest via p21	Liu et al, 1999
	CBP/p300	Apoptosis	
Methylation	Set8	Inhibits activation of highly responsive p53 targets	Shi et al, 2007
	Set7/9	p53 stabilisation	Chuikov et al, 2004
		Haplo-insufficiency causes loss of p21 and PUMA expression	Ivanov et al, 2007
	Smyd2	Mono- and di-methylation control of 53Bp1 binding to p53	Huang et al, 2006
SUMOylation	PIAS family proteins 1-4	Inhibits p53 transcriptional activity	Wu and Chiang, 2006
Phosphorylation	HIPK2	DNA damage response	Nardinocchi et al, 2009
		Upregulates tumour suppressor Pten	Meulmeester, 2008
	ATM	Serine-15 phosphorylation	Khanna et al, 1998
		Inhibition of p53-MDM2 interaction	Khosravi et al, 2009

A variety of modifications may be made to p53 which influence its stability and responsiveness to certain transcriptional targets. Some of these interactions are competitive such as E4F1 mediated ubiquitination competing with Pcaf mediated acetylation. The table above is not an exhaustive list of p53 modifications.

Of particular importance to the regulation of p53 protein is the E3-ubiquitin ligase, MDM2, which binds to p53, catalysing the addition of ubiquitin molecules. Mono-ubiquitylation exports p53 from the nucleus to the cytoplasm (Marchenko et al., 2007) where it has cytoplasmic, non-transcriptional roles (Erster et al., 2004, Kojima et al., 2006, Steele et al., 2008). Poly-ubiquitylation causes exportation from the nucleus and subsequent degradation in the proteasome. MDM4, a structural homologue of MDM2, inhibits p53 controlled transcription by binding to p53 but it does not have E3-ubiquitin ligase activity (Shvarts et al., 1996).

Acetylation of lysine residues has been shown to be indispensable for activation of p53 transcriptional programs. Acetylation of residues in the carboxy terminus of p53 by the acteyltransferase p300/CBP has been shown to enhance the sequence specific binding of p53. P300/CBP has also been shown to acetylate a residue within the DNA binding domain. Regulation of p300 acetylase activity is therefore an ancillary way of regulating p53 activity. P300 protein expression has been shown to be repressed by the chromatin remodelling protein in response to UV induced DNA damage, SMAR1 (Sinha et al., 2012). SMAR1 was also shown to interrupt p53-p300 interaction.

The protein p53 is known to control expression of genes involved in both the intrinsic and extrinsic apoptosis pathways and these are summarised in Figure

1-6 and Figure 1-7, respectively. The intrinsic pathway is activated by the use of DNA damaging therapies. The increased p53-dependant expression of pro-apoptotic Bcl-2 family proteins results in the sequestering of anti-apoptotic proteins of the same family (Vaseva and Moll, 2009). This allows the oligomerisation of BAX and BAK, also p53-targets, in the mitochondrial membrane, forming lipid pores that result in mitochondrial outer membrane permeabilisation (MOMP). MOMP is the apoptotic 'point of no return' (Dewson and Kluck, 2009). MOMP initiates the proteolytic caspase-cascade, breaking down the components of the cell in what was once termed 'death by a thousand tiny cuts' (Berg *et al*, 2002. p521).

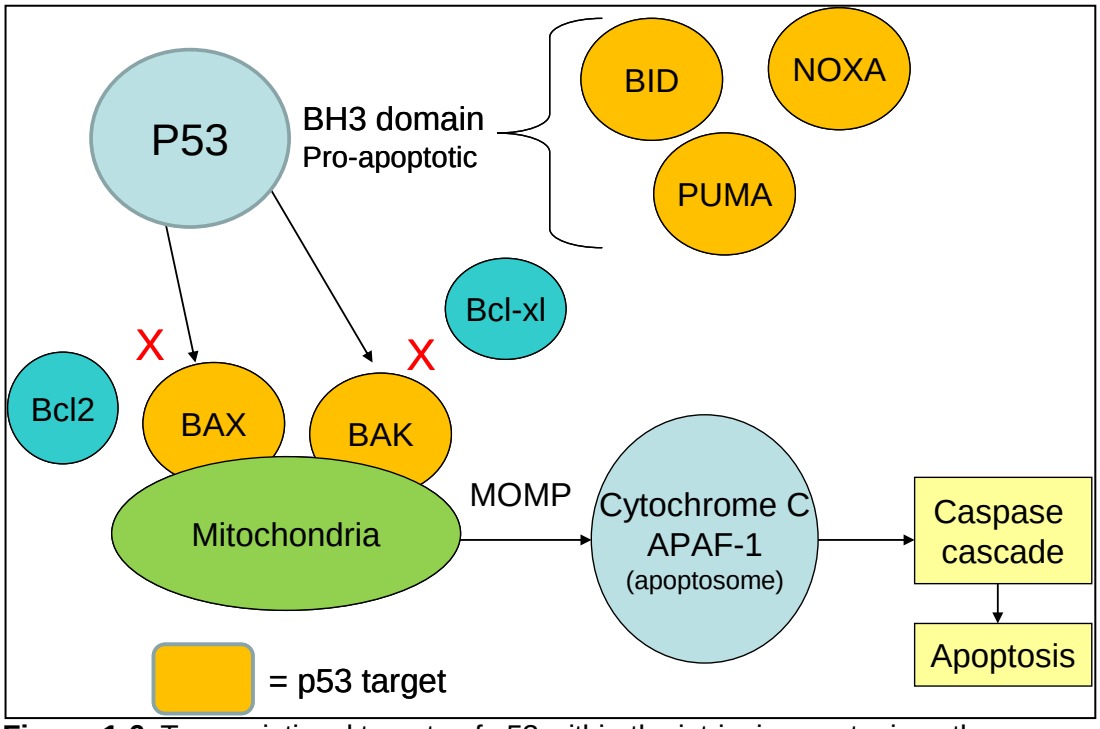

Figure 1-6: Transcriptional targets of p53 within the intrinsic apoptosis pathway.

In addition to its transcriptional effects, p53 also has non-transcriptional pro-apoptotic functions in the cytosol. In particular it has been shown that p53 protein can directly interact with the protein BAX leading to mitochondrial outer membrane permeabilisation, release of cytochrome-c and activation of the caspase cascade (Chipuk et al. 2004).

Micro-RNA transcription has been shown to be under the influence of p53 (He et al., 2007). miR-34a and miR-29c are significantly down-regulated in p53 abnormal CLL patients compared to normal CLL patients. This association

suggests that the analysis of certain micro-RNAs may be useful as a marker of p53 function (Asslaber et al., 2010, Merkel et al., 2010, Mraz et al., 2009, Zenz et al., 2009). Numerous non-transcriptional roles involving the mitochondria have been discovered for p53. In response to irradiation or etoposide p53 has a direct and rapid apoptotic role at the surface of mitochondria (Erster et al., 2004, Kojima et al., 2006, Steele et al., 2008). The p53-DBD binds anti-apoptotic Bcl-2, enabling Bax and Bak oligomerisation in the mitochondrial outer membrane (Vaseva and Moll, 2009) and there is evidence that p53 is imported into the mitochondria where it is involved in DNA repair during oxidative stress (Wong et al., 2009). p53 is also involved in microRNA processing(Suzuki et al., 2009).

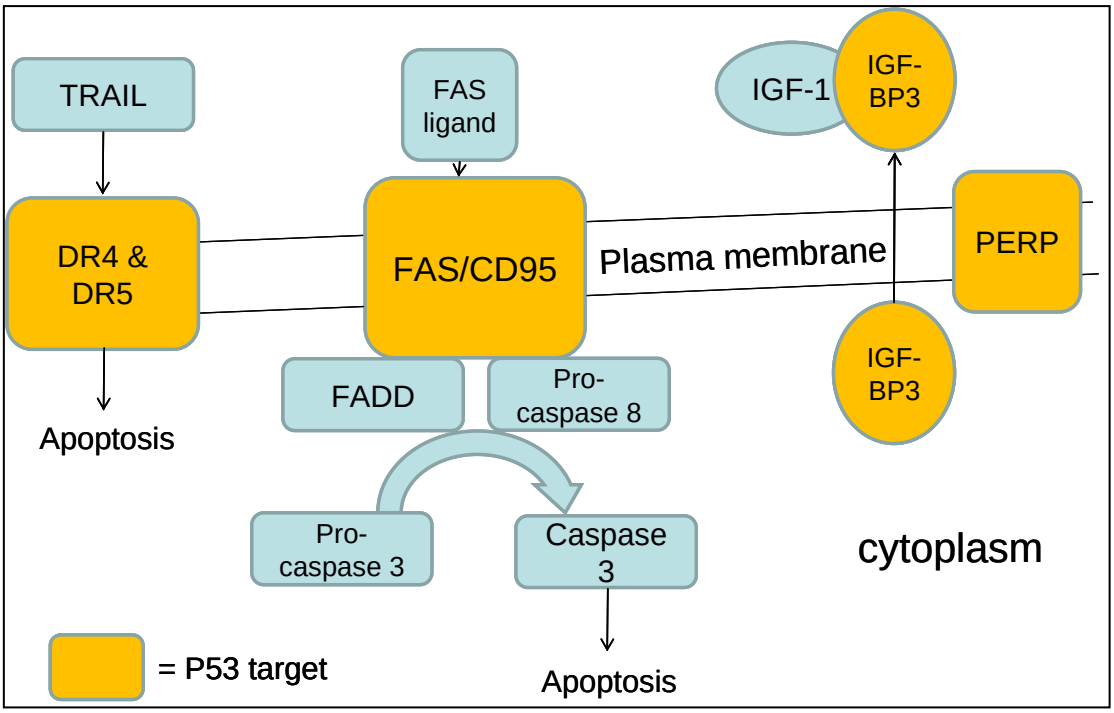

Figure 1-7: Transcriptional targets of p53 within the extrinsic apoptotic pathway.

The varied roles of p53 and the functional mutability of its DNA binding domain means the effects of deletion and miss-sense mutation are likely distinct from one another and may act synergistically when they co-occur. The protein-kinase ATM is integral to a normal DNA damage response but questions remain concerning the effects of haplo-insufficiency versus

mutation of ATM in CLL. It can also be seen that there are many other proteins involved in the cellular response to DNA damage that could, through dysfunction, inhibit or abrogate the apoptotic outcome. This is important as roughly half of CLL patients who are refractory to first line therapy have no detectable abnormalities of p53 or ATM.

1.6.5 **p53 isoforms**

The understanding of mechanisms that influence the behaviour of p53 has recently become more complex with the discovery that the *TP53* gene can be expressed in numerous different isoforms due to the presence of two different promoters, an internal START motif in intron 2, and a differential splicing site in intron 9 (Bourdon et al. 2005; Anensen et al. 2006). These result in the presence of four different amino acid termini eg full length p53 containing the entire transactivation domain (TAp53), ∆40p53, Δ133p53 and Δ160p53. In addition the alternative splicing of intron 9 leads to 3 different Carboxy termini eg full length p53 containing the entire oligomerisation domain (p53α), p53β and p53γ. It has been shown that these different isoforms can affect p53 transcriptional activity and that the α and β isoforms are expressed differently in CLL cells when compared to healthy B-cells (Sellmann et al. 2012; Bourdon et al. 2005). There is an inherent difficulty in taking isoforms in to account when using flow cytometry for measuring protein expression as it is not possible to differentiate between proteins of different lengths, something which can be achieved with some success using western blotting for example. In addition there are no commercially available anti-bodies that can discriminate between different isoforms.

1.6.6 **p53 family members, p63 and p73**

The protein p53 is one member of a family of transcription factors which share a similar structure and homology. These other family members are called p63 and p73. The roles that these different proteins have within the cell have a certain amount of overlap but p63 and p73 have been found to have other functions distinct from the functions of p53. The full length proteins of this family all have an N-termini TA domain, responsible for the transcriptional

activity of these proteins. They all have a core DNA-binding domain and an oligomerisation domain. In addition to these regions, p63 and p73 have an additional domain at the C-terminus called a Sterile Alpha Motif (SAM) which has protein-protein interaction functions. Similarly to p53, both p63 and p73 can be expressed as a variety of alternatively spliced isoforms. Importantly both can be expressed as ΔN variants lacking the N-termini transactivation domain (TAD) and so therefore lose the ability to trans-activate target promoters (Allocati et al. 2012). These ΔN variant isoforms are known to exert a dominant negative effect on the full length, transcriptionally active p53 family members and therefore have important roles in the negative regulation of p53 activity. Depending on the expressed isoform the outcome of DNA damage induced phosphorylation can have opposing effects. For example, it is known that c-Abl mediated phosphorylation of TAp63 in mammalian oocytes leads to the formation of active tetramers of the protein resulting in active transcription of target genes (Deutsch et al. 2011). Alternatively, it has been shown that in head and neck squamous cell carcinoma that phosphorylation of ΔNp63 by ATM leads to its degradation, resulting in the activation of TAp63 and the induction of apoptosis (Huang et al. 2008). Similarly to p63, TAp73 is also activated by protein modifiers such as p300, c-Abl, Chk1 and Chk2 and that the cell requires ΔNp73 to be degraded in order for apoptosis to proceed. Indeed high levels of ΔNp73 have been correlated with resistance to chemotherapy (Nicolai et al. 2015). Whilst the roles of p63 and p73 in promoting apoptosis have often been considered as an overlap with the role of p53 due to shared homology, it has also been shown that the combined loss of both p63 and p73 leads to a failure to undergo apoptosis in response to DNA damage, even in cells with fully functional p53 (Flores et al. 2002). There are other mechanisms of apoptosis which both p63 and p73 are involved in. TAp63/p73 can induce apoptosis via the mitochondria by upregulating the expression of BAX and PUMA, via the endoplasmic reticulum by increasing the expression of SCOTIN. It is also known that p73 regulates the extrinsic apoptosis pathway via upregulating the expression of CD95 whilst p63 can upregulated TRAIL-R1 and –R2 as well as TNF-R1. TAp63 and TAp73 also have roles in regulating the cell cycle via the upregulation of p21 and p57/KIP2 (Allocati et al. 2012).

In CLL there is little evidence to suggest a role of p63 in pathogenesis or chemo-refractoriness. However there is some evidence of a role for wildtype p73. For example it has been shown that in cells which are p53 dysfunctional, treatment with platinum based compounds can still induce cell cycle arrest and apoptosis as TAp73 leads to upregulation of p21 and BID (Tonino et al. 2015). Tonino *et al* (2015) also made the observation that the increased activity of TAp73 after treatment was due to post-transcriptional changes as the mRNA expression of p73 did not change.

1.7 **MicroRNAs and p53**

MicroRNAs are endogenously expressed RNA molecules that once fully processed are between 18-25 nucleotides in length. They are involved in the regulation of gene expression by targeting complementary sequences in the 3′UTR of one or more mRNAs. The end effect of this regulation depends on the level of complementarity between the miRNA and target sequence in the mRNA. Partial complementarity leads to repression of target mRNA translation whereas exact matches between the miRNA sequence and target mRNA leads to cleavage of the target. In mammals the primary mode of action appears to be translational repression through partially matching sequences (Bartel, 2004, Bartel, 2009).

Initially, miRNA is expressed as a primary miRNA transcript (pri-miRNA) which forms a 70-100 nucleotide hairpin structure. This is then processed in the nucleus by the ribonuclease, Drosha, to form a precursor miRNA (pre-miRNA) (Lee et al., 2003). Pre-miRNAs are then exported from the nucleus into the cytoplasm by the protein Exportin (Yi et al., 2003) where the ribonuclease, Dicer, processes the pre-miRNA into its shorter mature form (21-25 nucelotides) (Hutvagner et al., 2001). The mature miRNA then binds to the RNA-induced silencing complex (RISC) which then binds to the target mRNA facilitating either degradation, or more commonly in mammals, repression.

Micro-RNA regulation of mRNA translation was discovered in 1993. The gene, lin-4, was found in the nematode worm (*C.elegans*) to not code for a protein but instead its products were short RNA transcripts. These transcripts were found to cause the translational repression of the nuclear protein Lin-14,

leading to regulation of larval development. The authors speculated that this was due to the anti-sense complementarity between the RNA transcript sequence and the 3′-untranslated region (UTR) of the lin-14 mRNA (Lee et al., 1993). The next discovery of a miRNA, let-7, was not for several years but was also involved in the regulation of developmental timing in *C.elegans (*Reinhart *et al., 2000)*.

To date there have been hundreds of miRNAs characterised. The Sanger Institute maintains miRBase, an online database that catalogues each discovery and which is publicly available. Some individuals miRNAs have been shown to repress over a hundred target mRNAs and it is thought that approximately half of all cellular mRNA may be regulated by miRNAs (Cullen, 2011).

The roles that these miRNAs have in post-transcriptional regulation of gene expression is now understood to be involved in many cellular processes including cell cycle control, the DNA damage response and apoptosis.

Networks of microRNAs have been implicated in the direction of neuronal development and in maintaining plasticity of synapses later in life. Some microRNAs having also been linked to various behaviours in rodents with the miR-34 family implicated in learning and memory, exploration behaviour and anxiety (Olde Loohuis et al., 2012). Other non-coding RNAs (ncRNAs), including both long-noncoding RNAs and microRNAs, are being found to be important in understanding neurological conditions including drug addiction (Sartor et al., 2012) as well as regulation of the mu opioid receptor (MOR) by the micro-RNA, Let-7 (He & Wang 2012).

Viral MicroRNAs discovered in 2004 have been shown to be involved in certain viral infections, both in terms of the virus deregulating the endogenous expression of miRNAs as well as introducing exogenous viral microRNAs in to the cell (Cullen, 2011). In mice, miR-34a has been found to increase expression in later life. This increase was detected in the brain as well as plasma and peripheral blood mono-nuclear cells (PBMC) of mice (Li et al., 2011). These studies plus many others have shown that research into miRNAs is relevant to all areas of cell biology research.

1.7.1 **P53 and miRNA transcription**

The relationship between p53 and miRNAs has been shown to be transcriptional and non-transcriptional. Certain miRNAs are under the direct transcriptional control of p53 and are expressed in response to stresses that activate p53 such as DNA damage (Feng et al. 2011). The first miRNAs to be identified as under the direct transcriptional control of p53 were the hsa-mir34 family and these were shown to be involved in the apoptotic response (Chang et al. 2007). miR-34a, the product of a single transcript on chromosome 1p36, is expressed in most tissues. miR-34b and miR-34c are both transcribed from a single transcript on chromosome 11q and are primarily expressed in lung tissue.

1.7.2 **P53 and miRNA processing**

P53 has also been shown to be involved as a chaperone to the post-transcriptional maturation of certain miRNAs. For example in response to doxorubicin, p53 has been shown to promote the Drosha mediated processing of some miRNAs with growth suppressive functions. These included miR-143 which targets K-Ras and miR-16-1 and miR-145 which both target CDK6. K-Ras and CDK6 are both regulators of cell cycle and proliferation. This interaction of p53 with Drosha also required the presence of the DEAD box RNA helicases, p68 and p72. The same study also showed that two *TP53* mutants, R175H and R273H, reduced the processing of pri-miRNAs by Drosha and resulted in lower levels of mature miRNAs, including miR-16-1, miR-143 and miR-145 (Suzuki et al., 2009). This suggests that mutation of *TP53* can lead to deregulation of miRNA expression.

In addition to aiding the maturation of certain miRNAs, wildtype p53 also responds to disturbances in miRNA. Knockdown of Dicer to prevent the processing of pre-miRNAs into their mature forms has been shown to activate p53, causing a senescent phenotype in mouse embryonic fibroblasts. Deleting p53 rescued this effect allowing cells to continue to proliferate (Mudhasani et al., 2008). The miRNA, miR-504 has been shown to negatively regulate p53 protein expression by binding to two sites within the 3'UTR of *TP53* mRNA

(Hu et al. 2010). This provides a mechanism by which disruption of miRNA processing can lead to activation of p53.

These studies show that loss or mutation of p53 can lead to deregulation of cellular miRNA expression through several mechanisms and is not limited only to those microRNAs directly under p53s transcriptional control.

1.7.3 **miRNAs in Chronic lymphocytic leukaemia**

Due to its known relationship with p53 activation the microRNA, miR-34a, has been a subject of interest in the field of CLL research. It was shown a number of years ago in the p53 wildtype cell line, HCT116, that there is a positive feedback loop between p53 acetylation / activation, miR-34a expression, and *SIRT1* mRNA translation (Yamakuchi et al. 2008). SIRT1 (silent information regulator 1), is a deacetylase which targets and inactivates p53 protein, preventing p53-dependant activation of apoptosis related genes such as p21 and PUMA. It was shown that miR-34a targets the 3'UTR of *SIRT1* mRNA, blocking translation and consequently increasing p53 acetylation. Therefore a p53-dependant increase in miR-34a expression leads to further acetylation and activation of p53 protein via repression of *SIRT1* translation leading to activation of apoptosis genes including PUMA and p21 (Yamakuchi et al. 2008). It has also been established that absence of wildtype p53 leads to a reduction in the expression of miR-34a (Chang et al. 2007).

It has been previously shown that in CLL the expression of miR-34a is negatively affected by either deletion of 17p13.1 or by mutation of the *TP53* gene (Mraz et al. 2009; Dijkstra et al. 2008). It has been shown that CLL cells which are resistant to ionising radiation induce lower levels of miR-34a after DNA damage and this included cases with no detected abnormalities of p53 suggesting that miR-34a levels could be a more specific predictor of treatment resistance in CLL (Zenz et al. 2009). The authors of this study also found that the basal level of miR-34a was higher in wildtype CLL cells than *TP53* mutant CLL cells. This suggests that miR-34a is constantly expressed at low levels as a direct result of basal p53 activity. This is supported by the finding that variable basal of miR-34a in CLL cells is associated with a single nucleotide polymorphism of the *MDM2* gene, which is already known to affect p53-

protein regulation (Asslaber et al. 2010; Merkel et al. 2010). Taken together this suggests that miR-34a could be measured in unstimulated cells to predict treatment response. This could be advantageous for laboratories without a culturing facility.

1.8 Principals of molecular techniques used in this work

In order that the reader has an understanding of the common molecular biology techniques used in this study, the following section gives an introduction to the principals of the polymerase chain reaction (PCR), DNA sequencing using the Sanger method, pyrosequencing, restriction fragment length polymorphism analysis (RFLP) and finally Taqman™ probe based technologies.

1.8.1 Polymerase Chain Reaction

The polymerase chain reaction (PCR) is an *in-vitro* technique for generating millions of copies of DNA, spanning a selected region within the genome. It forms the basis of many molecular biology methodologies used in this study. The technique was developed in the 1980s and revolutionised molecular biology (Mullis et al. 1986). Polymerases are a class of enzyme which synthesise long chains of nucleotides along a template of DNA or RNA, utilising an oligonucleotide 'primer', bound to the template, as the initiation site for the strand to be synthesised. Complimentary copies of the template are created by sequentially incorporating deoxynucleoside triphosphates (dNTPs) in accordance with base-pair interactions with the template strand (Figure 1-8).

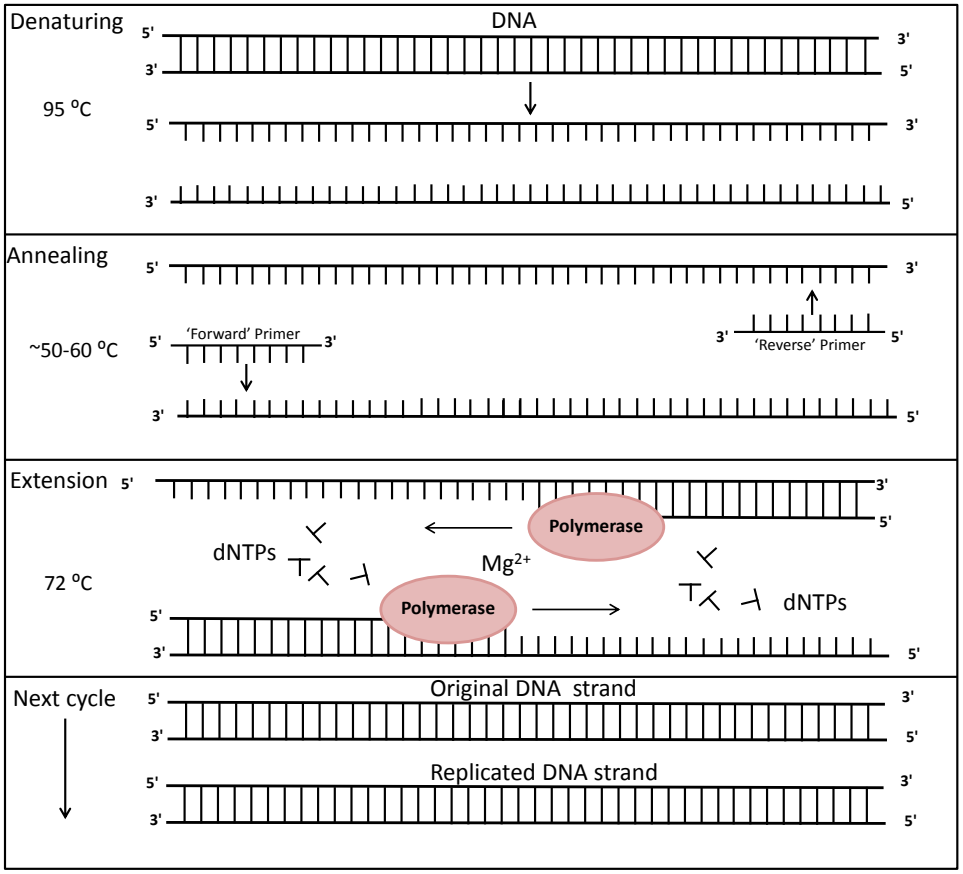

Figure 1-8: Diagram illustrating the thermally controlled, targeted synthesis of complementary DNA during 1 cycle of a polymerase chain reaction

Polymerases synthesise DNA in only one direction, requiring a 'primer' as a starting point for this synthesis. This is due to the enzyme binding the phosphate group found on the fifth sugar group carbon (5') of free dNTPs to the free hydroxyl group on the third sugar group carbon (3') of the previously incorporated nucleotide, eliminating a molecule of pyrophosphate (PPi) in the process. The primer is therefore essential as it provides the first free 3'-hydroxyl group from which the enzyme may begin synthesising a complementary strand. The direction of synthesis along the copied strand is described as being 5'→3', reflecting the orientation of the carbon atoms in the ribose sugar group of each nucleotide. The polymerase enzyme itself travels along the template strand 'reading' it in the 3'→5' direction. One of the most commonly used polymerase enzymes, *Taq*, was isolated from the thermophillic bacterium *Thermus aquaticus*, and becomes active at 72°C (Chien et al. 1976), allowing easier temperature control of polymerase *in-vitro*. Many improvements have been made to this and other polymerase enzymes

and four key characteristics are the focus of that work: Specificity, thermo-stability, fidelity and processivity.

At the beginning of a PCR reaction, before the initial denaturation stage, the polymerase can prematurely extend primers which have mis-primed as well as some primer-dimers therefore reducing the specificity of PCR amplification products. In order to improve specificity it is possible to manually add polymerase during the denaturation stage. This is described as a hot-start. A method to reversibly inactivate the polymerase enzyme so that it could be added to the reaction with the other reagents was developed in 1994. Researchers generated monoclonal antibodies which bound to and inhibited *Taq* at lower temperatures but which were denatured at 90^{o}C, therefore liberating the enzyme (Kellogg et al. 1994; Sharkey et al. 1994). Thermo-stability refers to the half-life of the enzyme at a given temperature. The half-life of *Taq* is sufficient for many applications but it may become a problem if prolonged high temperatures are required or the number of cycles will be very high. Alternative polymerases with higher thermo-stability have now been derived from hyperthermophilic bacteria, for example the enzyme *Pfu* is derived from the bacteria *Pyrococcus furiosus* (Lundberg et al. 1991). Fidelity refers to the error rate a particular enzyme displays and this is affected by the enzymes proofreading ability. Proofreading relies on the 3'→5' exonuclease activity of the enzyme in order to remove mis-matched nucleotides. Processivity describes the rate at which a polymerase incorporates nucleotides. There is a trade-off between fidelity and processivity as the exonuclease activity present in high fidelity polymerases reduces the processivity of the enzyme.

By designing and synthesising oligo-nucleotide primers in the laboratory in pairs that bind to opposite DNA strands at known locations and at temperatures approximately between 50-60^{o}C, it then becomes possible to use thermodynamics alone to denature DNA in a sample, control the annealing of primers to that DNA and then activate polymerases to begin extension of the primer across the sequence of interest. Figure 1-9 below illustrates a typical profile of the changes in temperature over time.

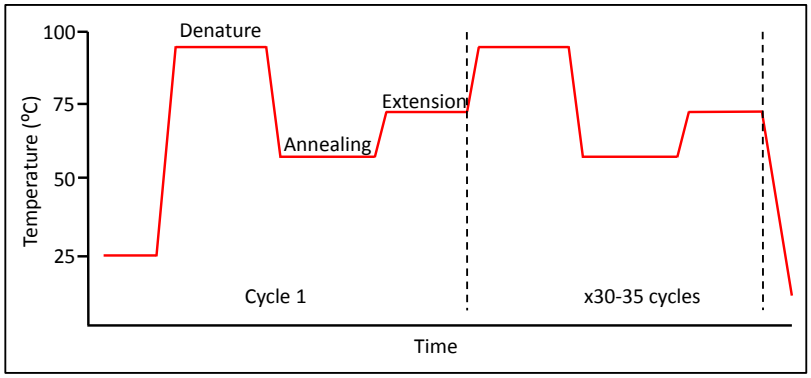

Figure 1-9: Temperature profile of a standard polymerase chain reaction

By ensuring that there is an excess of available dNTPs to synthesise the new DNA strands and free magnesium in the solution, this temperature controlled process can be continued for many repeating cycles potentially producing an exponentially increasing number of copied DNA products.

1.8.2 **DNA sequencing**

Sequencing of DNA is most often performed using the Sanger method (Sanger et al., 1977). The full title of the technique is the Sanger dideoxy chain termination method. This method requires a pool of template DNA containing the region of interest which is generated in a standard PCR reaction. The products of this PCR are then used in the Sanger chain termination reaction.

During PCR the incorporation of nucleotides into a newly synthesised strand of DNA by polymerase requires the free availability of the four possible deoxynucleoside triphosphates (dNTPs). For the Sanger sequencing reaction, dideoxynucleosides (ddNTPs) are added to the reaction alongside dNTPs and these are incorporated into the copied strands randomly during extension by polymerase. The difference between ddNTps and dNTPs is loss of the 3' hydroxyl group in the former. If a ddNTP is incorporated instead of a dNTP then the lack of a hydroxyl group at the 3' carbon of the extending strand abrogates the addition of any further dNTPs to that particular amplicon, it is for this reason that the method is referred to as ‘dideoxy chain termination’. The post-reaction solution contains millions of molecules of DNA which have been halted at random during extension. Therefore, across this population, every

nucleotide of the sequence is present as the terminal dideoxynucleotide of a replicated strand. Using electrophoresis it is then possible to resolve this population of amplicons by size and, therefore, by sequence. By labelling the ddNTPs in some way it is then possible to determine which ddNTPs have been incorporated and in which order, thus determining the sequence of a given region of DNA. This used to be achieved using a radio-isotope tag on ddNTPs for detection, and therefore required four separate reactions containing radio-labelled dideoxy-adenosine triphosphate, dideoxy-thymine triphosphate, dideoxy-cytosine triphosphate or dideoxy-guanine triphosphate. The electrophoresis of these reaction products would be performed in parallel and a radiogram would be prepared which could be read by eye.

Modern Sanger sequencing uses four, differently coloured, fluorescently labelled ddNTPs in the reaction solution. This allows the chain terminated products to be analysed concurrently using capillary electrophoresis to separate the amplicons by size and a laser-optics system to detect and discriminate fluorescence from the four differing ddNTPs. A software package then converts the signal data and generates an electropherogram showing the obtained sequence. Figure 1-10 below shows an example of an electropherogram obtained using the Sanger sequencing method for one of the cases used in this study.

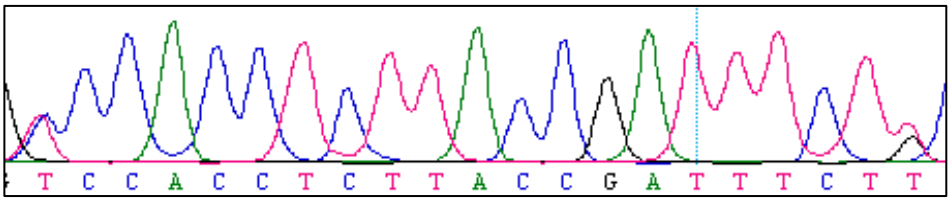

Figure 1-10: Example electropherogram showing a short DNA sequence

1.8.3 **Pyrosequencing**

Pyrosequencing differs from the Sanger method with respect to both chemistry and methodology. It is a chemiluminescent, enzymatic reaction requiring no electrophoresis. The sequence of a target region by determined by detecting the successful incorporation of deoxynucleoside triphosphate (dNTP) (Nyrén & Lundin 1985; Alderborn et al. 2000; Ronaghi et al. 1996). Figure 1-11 below gives a basic overview of the chemistry involved.

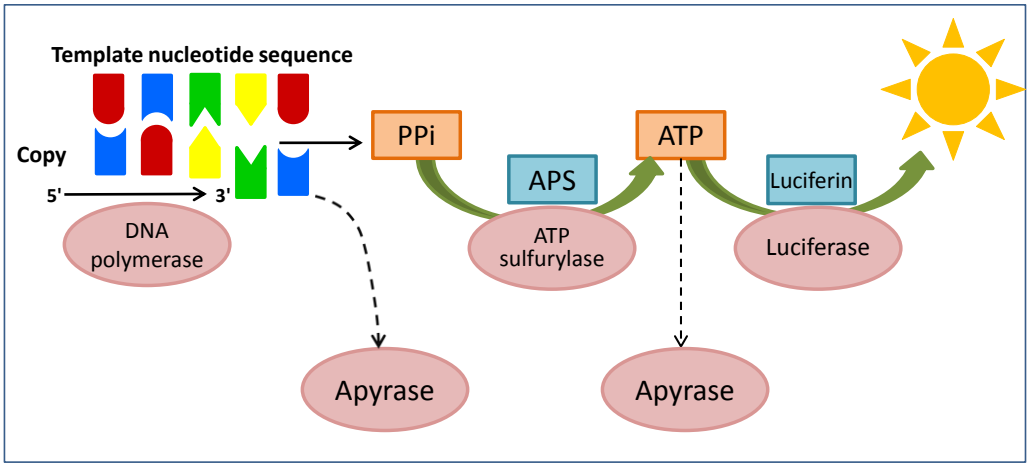

Figure 1-11: Diagram showing the basic chemistry of pyrosequencing.

Pyrosequencing requires template DNA produced by a standard PCR reaction. Only one strand will be pyrosequenced so one of the primers used during PCR is biotinylated, allowing that strand to be isolated through binding to streptavidin. A single primer, designed to bind 5' to the target to be sequenced, is hybridised to the template DNA. The extension of the primer over the target site is carried out in a repeating sequence of reactions, in which only one of the four possible dNTPs is made available to synthesise the new DNA strand. When the reaction solution containing the required dNTP is added, DNA polymerase catalyses its incorporation into the new strand and a molecule of pyrophosphate (PPi) is released for every molecule of dNTP added. The enzyme ATP sulfurylase then combines this PPi molecule with a molecule of adenosine'5 phosphosulphate (APS) to form one molecule of ATP. This molecule of ATP is then used by another enzyme, luciferase, to convert one luciferin molecule to oxyluciferin, a reaction which releases a detectable amount of light. This light is detected using a charge coupled device (CCD) camera and displayed as a peak on a pyrogram, an illustration of which is shown in Figure 1-12. Due to the equimolar relationship of this reaction, the peak height is directly proportional to the number of nucleotides incorporated therefore in the example in Figure 1-12 the sequence can be read as CGGAG.

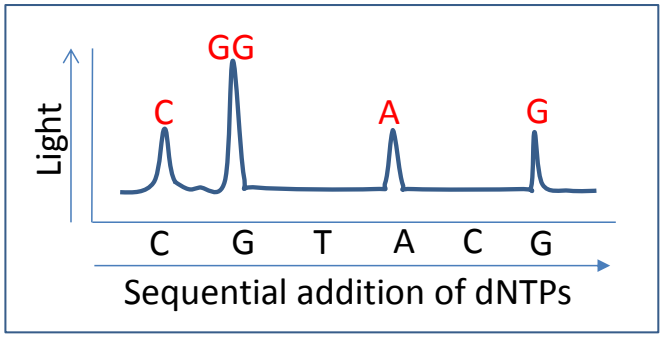

Figure 1-12: An example pyrogram for a five nucleotide sequence: CGGAG.

The nucleotide degrading enzyme, apyrase, constantly removes unused dNTPs allowing the sequential addition of the four dNTPs. An important note is that deoxyadenosine alpha-thio triphosphate (dATPαS) is used instead of deoxyadenosine triphosphate for incorporation into the copied strand during pyrosequencing. Whilst dATPαS is still efficiently used by DNA polymerase it cannot be used by luciferase.

1.8.4 **Restriction-fragment length polymorphism analysis**

Preliminary, low-cost analysis of single nucleotide polymorphisms (SNPs) was performed using restriction-fragment length polymorphism (RFLP) analysis on PCR amplified DNA. The use of restriction enzymes to detect polymorphisms was developed in the late seventies as a method for detecting a DNA polymorphism which is associated with sickle cell anaemia (Kan and Dozy, 1978). The technique can be adapted to detect other polymorphisms of interest. A summary diagram of RFLP is shown in Figure 1-13.

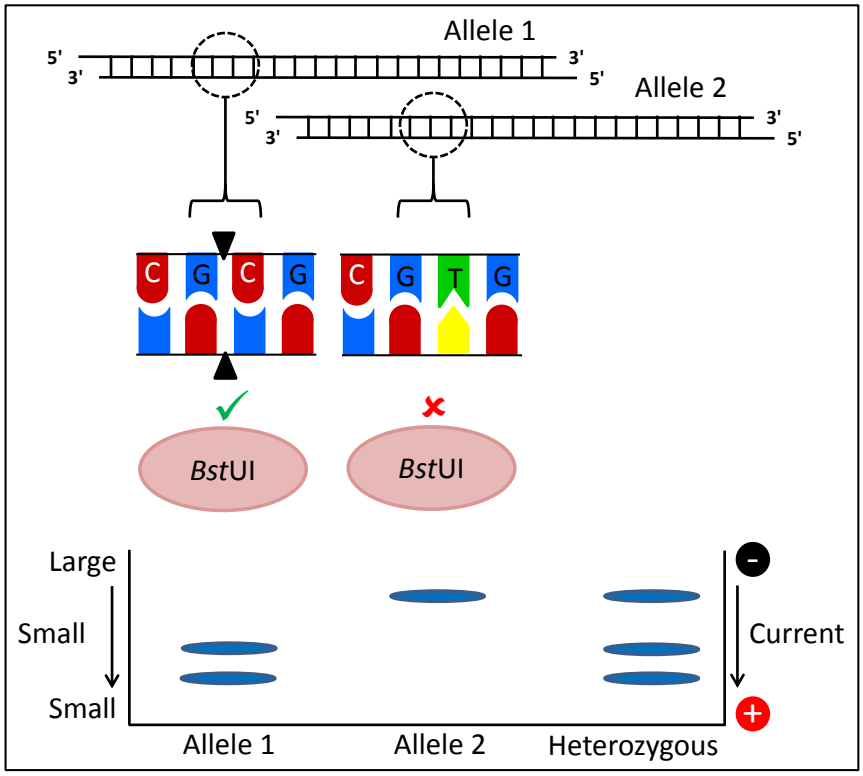

Figure 1-13: Principal of Restriction fragment length polymorphism analysis
In this example, the enzyme *Bst*UI recognises the nucleotide tetramer 5'-CGCG-3' within a sequence which it then cleaves between the central guanine-cytosine phosphodiester bond (allele 1). This restriction endonuclease can therefore be used to detect variant alleles if the presence of a single nucleotide polymorphism (allele 2) eliminates the binding motif.

Restriction endonucleases are a class of enzyme which recognise and cleave DNA at, or near to, sequence-specific regions of DNA called restriction sites. The cut is achieved by hydrolysing the phosphodiester bond between two nucleotides on each strand of DNA. A PCR reaction is performed, amplifying the loci containing the SNP of interest. The products of this reaction are subsequently incubated with the selected endonuclease. The digested and/or undigested products of this reaction are then separated by size in an agarose gel, using electrophoresis. The number and relative size of the bands can be used to determine either homozygosity or heterozygosity for the SNP of interest.

1.8.5 **Taqman™ hydrolysis probe technology**

Taqman™ hydrolysis probes were utilised in two methodologies during this study, Endpoint genotyping and relative quantification. Whilst the two methods differ slightly there is good cause to explain the chemistry of Taqman probes first. The underlying chemistry behind Taqman™ probe technology is based on the phenomenon of Förster resonance energy transfer (FRET), and on the 5'-3' exonuclease activity of *Taq* polymerase (Heid et al. 1996). Figure 1-14 below illustrates the principal of using a Taqman™ probe to detect the activity of polymerase during a PCR reaction.

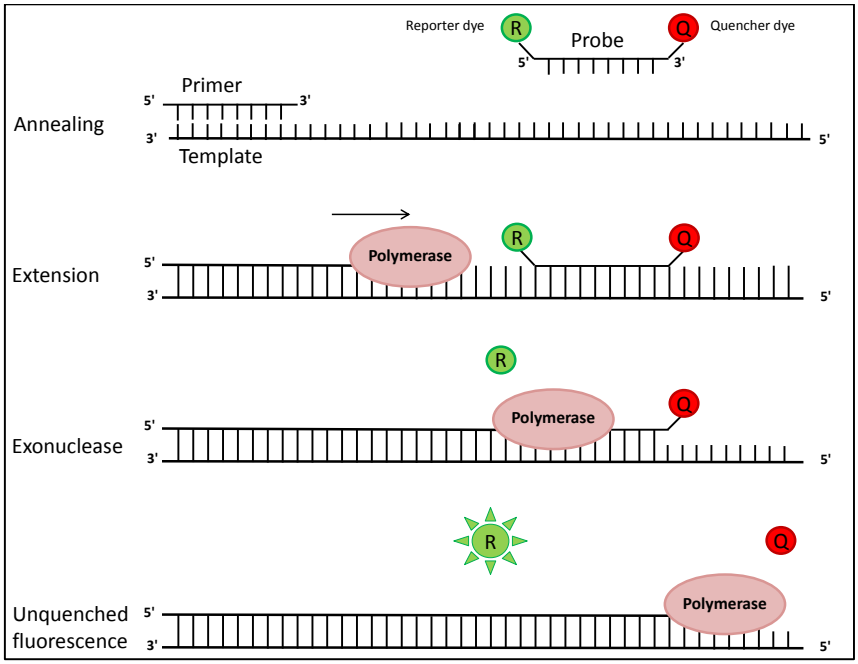

Figure 1-14: Principal of Taqman assay.

FRET describes a process of energy transfer between two light sensitive molecules in which one molecule described as the quencher, accepts the photons released by the second, described as the reporter. Whilst in close proximity to the reporter, the quencher effectively abrogates the light signal. This quenching effect is inversely proportional to the distance between the dyes. A Taqman™ probe is an oligonucleotide designed to bind within a given PCR amplicon. The probe has a reporter dye molecule bound to the 5' end and a quencher dye molecule bound to the 3' end. Whether in the reaction solution or bound to the target template, the oligo-bound quencher dye is close enough for FRET to prevent any light being released by the reporter

dye. During the annealing phase of amplification the probe binds to its target site within the amplicon being generated. During the extension phase, as polymerase reaches the bound probe, the 5'-3' exonuclease activity of the enzyme degrades the Taqman probe. This releases the reporter and then quencher dyes into solution. No longer held within proximity of the quencher dye, the reporter dye fluoresces and this light is measured. Therefore, a quantifiable light signal is released every cycle of PCR that is proportional to the number of copies of template that have been generated.

1.9 Functional assays

The term 'functional assay' is used within this work extensively in reference to the flow cytometric assay of intra-cellular p53 and/or p21 protein levels in primary CLL cells which have been treated *in-vivo* with DNA damage agents (Carter et al., 2004a, Best et al., 2008b). It should be remembered that in a broader sense functional assessment can take many forms and have many targets of interest, in many areas of cell biology research.

1.9.1 Functional assessment of ATM/p53 in cancer

Assessing the p53 pathway *in-vitro* using patients B-CLL cells may help to predict responses to DNA damage inducing therapies used to treat CLL. DNA damage responses may be elicited using ionising radiation or DNA damaging agents (Best et al., 2008b, Carter et al., 2004b, Pettitt et al., 2001). Activation of p53 may also be achieved by interrupting its steady-state turnover by MDM2. The small molecule, nutlin3a, directly inhibits the activity of MDM2, increasing the level of p53 and activating cell cycle and apoptosis genes in CLL cells (Secchiero et al., 2006). It does not appear to have this effect within cells in which p53 is mutated (Saddler et al., 2008, Terzian et al., 2008). The ability to induce a p53 response independently of the ATM mediated DNA damage signal is exploited for the functional assay used in this project (Best et al., 2008b). Interestingly, the inhibition of p53 by MDM4 cannot be disrupted by nutlin3a, although some putative dual-inhibitors of MDM2 and MDM4 have been identified (Barakat et al., 2010, Patton et al., 2006).

The fact that p53 is involved in the regulation of many proteins and in different pathways means there are many possible targets that could be measured to give an indication of abnormal p53 function either at the protein or mRNA level, including microRNAs (Asslaber et al., 2010, Merkel et al., 2010). The cell cycle arrest protein p21 is a well-documented and highly sensitive indicator of p53 activation that has been previously identified and used in work of a similar nature to this project (Carter et al., 2004a, Pettitt et al., 2001). Analyses of cases which do not respond to DNA damaging therapy have highlighted other proteins which could be used as predictors of response, such as polo-like kinase-2 (PLK2) (de Viron et al., 2009) and DNA protein

kinase (DNA-PK). DNA-PK expression shows a negative correlation with p53/ATM function, being higher in cells with the del11q or del17p abnormalities (Willmore et al., 2008) making it potentially of use as a surrogate marker of these high risk abnormalities.

One established technique for the functional assessment of *TP53* mutations on the transcriptional activity of p53 protein is the FASAY assay (functional assessment of separated alleles in yeast). This is an *in-vitro* assay in which *TP53* mRNA is reverse transcribed then amplified using PCR. The resulting PCR products, representing the expressed transcripts from within the cell, are then cloned in to a linear expression vector, pSS16, and introduced in to a yeast system. The yeast strain, yIG397, is a mutant exhibiting deficient adenine synthesis due to a mutation in the ADE2 gene. When grown on a medium containing reduced adenine the yeast produces metabolites giving the colonies a red colour. The yeast also contains a second copy of the ADE2 gene which is under the control of a p53 responsive promoter. Once the expression vector containing the copied *TP53* coding region is introduced in to the yeast system it will produce p53 protein. If the expressed p53 is wildtype or otherwise retains transcriptional activity then the ADE2 gene will be activated and the yeast will be able to metabolise adenine resulting in colonies appearing white. If the inserted *TP53* coding region contains a mutant that affects the transcriptional activity of p53 protein then the yeast will still be unable to metabolise adenine and the colonies will appear red. In addition, if the inserted gene retains only partial transcriptional activity then the colonies may appear pink. This is a fairly simple assay to perform and provides a robust method for determining the effect of a specific *TP53* mutation on the expressed proteins transactivation ability (Flaman et al. 1995; Ishioka et al. 1993).

Newer technologies allow the investigation of greater numbers of target genes than has been achievable with western blotting or flow cytometry. The use of real-time PCR based technology on microarray platforms enables the analysis of thousands of genes allowing the investigation to changes of the transcriptome in response to various stimuli. Drawbacks to the use of microarray technology include the obvious bias towards genes that have been selected for the array. Saturation means that an array may not always detect

significant differences in expression between genes. RNA sequencing (RNA-seq), an application of high throughput, deep sequencing technology, can analyse the entire transcriptome down to a single nucleotide resolution without being restricted to known genes in model organisms, or referring to reference genomes. It also detects a greater fold change in expression than micro arrays (Wang et al., 2009). An example of the potential use of RNA-seq in functional analysis of cellular responses is the analysis of changes to the transcriptome in HepG2 cells exposed to the carcinogen, benzo[a]pyrene (van Delft et al., 2012). There are currently a number of potential drawbacks to the use of RNA-seq. Firstly, RNA-seq tends to produce very large quantities of data. This data requires very powerful tools to analyse and typically users will need to use super-computers with high speed network connections and high volume data storage. Currently, software is not standardised and will often require bioinformatics specialists to work with the data prior to analysis. This may result in a lack of repeatability and inter-operator variability with results. In addition to this the matching of sample reads to reference genomes may be complicated by the presence of alternatively spliced isoforms or paralogous genes. Also, with cancer research, comparing data derived from a tumour cell to a normal counterpart can be difficult, especially if that normal counterpart / cell of origin is unknown. Cost is also one factor that is associated with almost all new technologies however this can be expected to drop over time.

This technology could be applied to functional assessment of the DNA damage response in CLL cells. Although use of RNA-Seq may be over-powered for regular use, it would be a powerful tool for the detection of novel alterations to the transcriptome after DNA damage.

1.9.2 **Functional assays in CLL**

The earliest use of functional assessment of the ATM/p53 DNA damage response pathway in CLL cells used ionising radiation to induce an ATM dependant damage response which was detected using western blotting to detect the presence of p53 and ATM proteins (Pettitt et al. 2001). The categorisation of dysfunctional samples in this paper was based upon two

observations of abnormal behaviour; either constitutive expression of p53 in control cells, which the authors termed as Type-A, and, failure to increase expression of p53 and p21 in response to DNA damage, coined Type-B. These two categories were found to be associated with genetic abnormalities of p53 and ATM respectively (Pettitt et al. 2001). In later work the same group showed that this form of assessment could be performed using a flow-cytometer instead of western blotting (Carter et al. 2004).

A third response pattern (Type-C), in which p53 but not p21 expression increases after IR treatment of cells, has also been reported (Johnson et al., 2009). To date, this failure of p21 to respond normally has been associated with polymorphisms of the *CDKN1A* (p21) gene (Johnson et al. 2009).

A fourth response category has also been observed in a small number of cases and is currently titled, Type-D. This pattern shows a failure of p53 measurements to increase beyond its accepted cut-off, yet p21 measurements increase above the accepted p21 cut-off (Johnson et al. 2009).

The ionising-radiation based functional assay has also been utilised to analyse 278 samples from the CLL4 trial (Lin et al., 2012). The published table showing associations between ATM-p53-p21 pathway defects and other biological variables is shown in Table 1-7, (p62). This cohort was not significantly different from the remainder of the CLL4 study (n=777) in terms of any of the clinical or biological parameters except that the number of samples with deletion of 11q was increased. This study detected Type A, B, C, and D dysfunction in 6 (2.2%), 146 (52.5%), 13 (4.7%) and 29 (10.4%) cases respectively. This left only 84 (30%) of the samples with a 'normal' functional response. An initial criticism of this therefore is the sheer number of dysfunctional samples found in a cohort of previously untreated patients; in particular the Type-B responders outnumber the normal responders. Also the Type-B group did not share the same poor outcomes as the Type-A and –C responders despite having similarly low levels of p21. To explain this discrepancy the authors suggest that ionising radiation may not recreate the effects of alkylating agents and purine analogues. This may be a drawback if an assay is attempting to predict the response to therapy in patients. In terms of detecting patients who have abnormalities of *TP53*, this study also failed to

accurately detect 15/21 (71.4%) of the *TP53* mutations and 13/18 (72.2%) of the 17p13.1 deletions. Unfortunately the authors were unable to analyse the Type-C cases for polymorphisms of the *CDKN1A* gene. This would have been a useful opportunity to increase the data available on this phenomenon.

A final concern is whether the functional assessment of cells that have been in storage for over five years is advisable, especially when the aim of these tests is to determine beforehand whether a patient B-CLL clone will respond to therapy. Unlike genetic analysis, functional analysis is almost certainly affected by extrinsic variables and the minimisation of these is of paramount importance.

Table 1-7: Results summary from Lin et al, 2012

Variables		Total	Normal	ATM-p53-p21 pathway defect n (%)				*P****
		n	n (%)	Type A	Type B	Type C	Type D	
Gender	Female	64	16 (19)	0 (0)	33 (23)	5 (38)	10 (34)	0.18
	Male	214	68 (81)	6 (100)	113 (77)	8 (62)	19 (66)	
Age group	<60	84	24 (29)	1 (17)	43 (29)	3 (23)	13 (45)	0.70
	60-	113	38 (45)	3 (50)	56 (38)	7 (54)	9 (31)	
	70+	81	22 (26)	2 (33)	47 (32)	3 (23)	7 (24)	
Binet stage	A*	72	27 (32)	1 (17)	30 (21)	5 (38)	9 (31)	0.33
	B	116	35 (42)	1 (17)	64 (44)	5 (38)	11 (38)	
	C	90	22 (26)	4 (67)	52 (36)	3 (23)	9 (31)	
TP53 gene	Wild type	235	76 (96)	0 (0)	122 (92)	10 (83)	27 (100)	<0.01
	Mutated	21	3 (4)	6 (100)	10 (8)	2 (17)	0 (0)	
IGHV mutation	<2%	156	43 (60)	5 ((83)	87 (66)	6 (55)	15 (60)	0.67
	>2%	89	29 (40)	1 (17)	44 (34)	5 (45)	10 (40)	
17p (TP53) deletion**	≤10%	238	73 (97)	1 (17)	126 (93)	12 (92)	26 (96)	<0.01
	>10%	18	2 (3)	5 (83)	9 (7)	1 (8)	1 (4)	
11q (ATM) deletion**	≤5%	189	59 (79)	6 (100)	95 (70)	10 (77)	19 (70)	0.44
	>5%	67	16 (21)	0 (0)	40 (30)	3 (23)	8 (30)	
6q deletion**	≤5%	184	63 (95)	5 (100)	85 (97)	10 (100)	21 (100)	>0.99
	>5%	6	3 (5)	0 (0)	3 (3)	0 (0)	0 (0)	
trisomy 12**	≤3%	230	64 (85)	6 (100)	125 (93)	11 (85)	24 (89)	0.38
	>3%	26	11 (15)	0 (0)	10 (7)	2 (15)	3 (11)	
13q deletion**	≤5%	159	42 (56)	6 (100)	86 (64)	9 (69)	16 (59)	0.26
	>5%	97	33 (44)	0 (0)	49 (36)	4 (31)	11 (41)	
Treatment allocation	Fluda+Cyclo	82	21 (25)	2 (33)	44 (30)	4 (31)	11 (38)	0.90
	Chlor	125	42 (50)	2 (33)	63 (43)	7 (54)	11 (38)	
	Fluda	71	21 (25)	2 (33)	39 (27)	2 (15)	7 (24)	

* Stage A progressive disease
** FISH data were sorted according to Dohner's hierarchical model[28,38]
*** *P* values were calculated using the Fisher-Freeman-Halton exact test

1.9.3 **Nutlin3a in the functional assay of CLL cells**

The use of nutlin in the functional assessment of CLL cell responses in order to detect clinically significant abnormalities has been investigated in a 2013 paper (Pozzo et al., 2013). In this study they adopted an RT-PCR approach that used only control versus nutlin treatment. In the methods the authors detail testing alternative assays including the combination therapy used in this study but the sample size was very small (n=10) including 3 cases with monoallelic mutation of *TP53* and 3 more with no detected deletion of 11q or 17p. The authors state that:

> "with the only exclusion of 2 out of 4 11q deleted cases, no relevant differences were detected in terms of type of response among experiments with the alternative treatments" (Pozzo et al., 2013).

This statement doesn't reflect the fact that half of the cases (2/4) with deletion of 11q22.3 did show value in the use of combination treatment which in itself represents 20% of a small, selected cohort. The details of the ten samples used, available in the supplementary data for the article, details that no *ATM* mutation screening had been performed on the four 11q deleted cases. In addition to this the clone size for one case which responded normally was just 10% of the cells observed and so could be reasonably interpreted as an issue of sensitivity. The author's study itself uses a training cohort of 100 and a validation cohort of 40 in order to test the single agent use of nutlin in detecting clinically relevant abnormalities of *TP53* (deletion and mutation) and ATM (deletion only). The training cohort contained 14 cases with a detectable deletion of 11q22.3, in the absence of *TP53* mutation / deletion. All of these cases gave a normal response when assessed by Western blot. If the authors had assessed the combination treatments on all of these cases they may have detected differences such as those seen in the original work by Best *et al* (2008). Furthermore, the validation cohort also demonstrated that the single agent assay cannot discriminate between cases with or without ATM and/or TP53 abnormalities. In the 42 cases listed in the supplementary data there were 6 cases with deletion of 11q22.3 of which 2 had concurrent involvement of TP53. The remaining four cases all tested normal using the single agent nutlin assay. One of the benefits of using Western blotting as opposed to flow cytometry to detect p53 protein, highlighted by the author, is the detection of frameshift mutations. These would be undistinguishable from full length p53 if using flow cytometry yet they can be easily discerned by relative size on a Western blot.

One study has investigated using a dual agent *in-vitro* functional assay in order to detect *ATM* mutations in CLL (Navrkalova et al. 2013). The authors exploit the different mode of action of the two chemotherapeutics, doxorubicin and fludarabine, in order to discriminate between cases with and without *ATM*

mutation. Both drugs lead to a p53-dependant increase in p21 expression however only doxorubicin does so in an ATM dependant manner. The authors used a custom resequencing micro-array platform to screen for *ATM* mutations in a cohort of 140 cases. Positive screens were then confirmed by direct sequencing. In total they identified 28 *ATM* mutations in 22 patient samples. The functional test they employed identified 16 cases as having *ATM* dysfunction, 4 cases gave normal responses and 2 cases were disregarded due to concomitant *TP53* abnormalities.

They also showed a definite functional difference between cases with sole deletion of 11q and sole *ATM* mutation. However they also found that in terms of time to first treatment both abnormalities had an equally detrimental effect compared to wildtype cases (Navrkalova et al. 2013).

1.9.4 **The etoposide and nutlin functional assay in CLL**

The flow-cytometry assay developed by Best *et al* (2008) and used in this project is modelled after the methodology of Carter *et al* (2004) with several key differences which are illustrated in Figure 1-15. DNA damage is induced using the topoisomerase II inhibitor, etoposide, rather than ionising radiation which avoids the need for specialist facilities. The small molecule nutlin3a is used to further stratify the Type-B dysfunctional response identified originally by Pettitt *et al* (2001). In most other respects the assays are the same, measuring the same targets (p53 and p21), and using the same antibody clones to detect them. The different systems of response classification are described below.

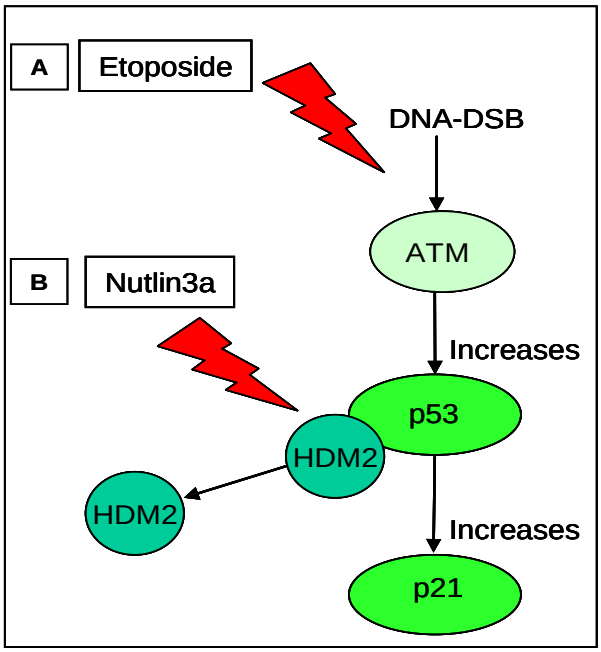

Figure 1-15: p53 induction using combination treatment of etoposide and nutlin

The assay uses two methods to induce p53/p21 responses, one of which is not reliant upon functional ATM. **A)** Etoposide induces DNA DSBs leading to an increase in p53 protein via the MRN complex and ATM signalling. **B)** Nutlin3a inhibits the interaction of MDM2 and p53 leading to accumulation of p53 by avoiding degradation by the proteosome (Best *et al*, 2008).

The increased stratification due to the use of nutlin3a requires different nomenclature than that used by Carter *et al* (2004). Figure 2-3 (p81) in the methods section shows the strategy for assigning samples to functional

categories. A normal response is characterised as an increase in expression of p53 and p21 in response to etoposide alone; the categorisation of dysfunction is then determined by the responses to etoposide plus nutlin. An MFI of greater than 8 for p53 in the control culture was classed as p53 over expression (p53oe) and is analogous to 'Type-A' dysfunction as defined by Carter *et al*, (2004). Cases which fail to increase expression of p53 and p21 in response to etoposide and etoposide plus nutlin3a were categorised as 'non-responders'. The nutlin-responder category identifies samples in which the use of nutlin3a recapitulates a normal response. Cases that fail to increase expression of p21 despite a normal p53 response to nutlin are referred to as p21-negative. This category is analogous to the Type-C response identified by Carter *et al* (2004) and Johnson *et al* (2009). The cut-offs used to define normal responses for p53 (≥30% increase in MFI) and p21 (≥15% increase in MFI) were previously derived by receiver operator characteristics (ROC) curve analysis (Best *et al*, 2008).

During the original development of this assay it was found that the non-responder and nutlin-responder dysfunctional responses occurred only in the presence of a mutation in the *TP53* or *ATM* genes respectively; loss of 17p13.1 or 11q22.3 alone did not confer a dysfunctional response (Austen et al., 2008, Best et al., 2008b).

The current explanation for approximately half of p21-negative/Type-C responders is interacting SNPs within *CDKN1A*, the gene encoding p21 (Johnson et al., 2009). In addition, the same group have now reported a fourth category of dysfunction, termed Type-D, in which p21 responds normally but p53 does not.

Compared to specific molecular tests, including FISH and DNA sequencing, functional assays represent a holistic, systems biology based approach that should be able to detect samples which may have multiple gene defects within the DNA damage response pathway.

1.10 Primary Hypothesis

The primary hypothesis to be dealt with in this thesis is as follows:
'The functional assay response categories associate with specific abnormalities of ATM and p53'.

The null hypothesis is therefore:
'The functional assay response categories do not associate with specific abnormalities of ATM and p53'.

Further questions will be addressed in subsequent result chapters; therefore a specific hypothesis statement will be made at the beginning of each.

1.11 Aims and Objectives

The aims of this project are as follows: (i) to determine the value of the etoposide/nutlin3a functional assay for detecting patients with abnormalities of the ATM-p53-dependant DNA damage response which would contra-indicate treatment with alkylating agents or purine analogues; (ii) to test the ability of the assay to discriminate between ATM and p53 abnormalities as these have differing prognostic impact in CLL. The objectives to be met for the completion of these aims are as follows:

1. Laboratory work

A cohort of patients, assembled as part of a Leukaemia Research Foundation (LRF) funded study, will be fully characterised using the etoposide/nutlin functional assay, FISH for 11q22-23 and 17p13.1 and mutation screening of *TP53* and *ATM* using HRM analysis. Additional, potentially relevant, markers of p53 DNA damage response dysfunction, including miR34a levels and functional single nucleotide polymorphisms, will be investigated using appropriate techniques.

2. Data analysis

The results of the functional analyses will be compared to other markers of DNA damage pathway dysfunction including FISH and mutation screening.

Associations between the assay result categories and other markers will be assessed using Fishers exact test.

Assay results will be correlated with clinical data (PFS and response to treatment) in order to determine whether the functional assay adds new predictive power over FISH and mutation screening.

A validation of the data will be performed by statistically testing for differences in the assay data between the samples that were sourced from the local clinic (Royal Bournemouth and Christchurch Hospital) and those samples which were sourced from referral centres and thus had extended amounts of time between venesection and processing/storage.

Chapter Two:

Materials & Methods

2.1 CLL patient samples

Samples of peripheral whole blood (20ml) were collected, with informed consent, in accordance with the Declaration of Helsinki, from Centres around the UK. A copy of the standard patient information sheet and standard consent form can be found in Appendix I (p204), and Appendix II (p208) respectively. All samples were anonymised, labelled, recorded and stored in accordance with the Human Tissue Act (2004). Work was ethically approved under the auspice of the Lym1 study, 'Identification and characterisation of prognostic factors in chronic B-cell lymphoproliferative disorders', MREC number 06/Q2202/30. All diagnoses were made by referring clinicians. Clonality of B-cell disorder was previously established at referring centres as a part of the routine diagnostics.

The anti-coagulant preservative, lithium-heparin, was used for all collected samples. Selected prognostic and predictive markers were analysed for all samples.

All antibodies, materials and reagents were purchased from recognised commercial suppliers. Details on antibodies can be found in appendix III, p211 and materials and reagents in appendix IV, p212.

2.2 Study design

The final design of this PhD would partly be dictated by the number of samples which could be successfully collected and fully analysed as testing the functional assay across a large cohort was the primary aim.

Samples were primarily taken from cases with active disease which ensured that the samples were relatively enriched for tumour cells. This also reflects the envisaged use of the etoposide/nutlin functional assay, namely to give additional information to clinicians when considering treatment.

All samples will be tested using the functional assay and their responses used to place them into predefined categories. All samples tested using the functional assay will also have sequence analysis of the *TP53* gene and mutation screening of the *ATM* gene performed. Results of FISH analysis of

chromosomal loci 11q22.3 and 17p13.1 of the same samples will be made available for the dataset.

Due to the relative rarity of CLL patients with *TP53* and *ATM* mutations and/or deletion of chromosomes 11q or 17p it was decided to not place restrictions on eligibility of cases such as clinical stage or IGHV status.

2.3 **Sample processing**

All open handling of patient blood was undertaken in a class-2 biological safety cabinet in the molecular pathology lab of the Royal United Bournemouth and Christchurch Hospital (RBCH). Personal protective equipment was used (Gloves, glasses and labcoat). Disposable glassware and plastic waste was collected and removed in accordance with local guidelines.

Upon receipt of whole blood samples, a 500 µl aliquot was removed kept aside for CD38 analysis and a 5 ml aliquot was kept for chromosome banding by Giemsa staining (Performed by AG, SM, SG). The remaining whole blood was separated by density gradient centrifugation using an equal volume of Ficoll Histopaque (Sigma Aldrich, UK). The lymphocyte / mononuclear cell fraction was collected from the interphase between the plasma and ficoll histopaque. The collected cells, further referred to as 'peripheral blood mono-nuclear cells' or PBMCs, were washed once in 3 ml phosphate buffered saline solution (PBS), enumerated and washed once more. The cells were then suspended in foetal calf serum containing 10% DMSO at a density of $2x10^7$ cells/ml.

Aliquots of cells (1ml) were placed in a Mr-Frosty™ tub (Nalgene, UK) containing 250ml iso-propanol and placed in a to -70^oC freezer in order to slow the cooling rate to -1^oC/minute. After 48 hours at this temperature the aliquots were transferred to liquid nitrogen (-175^oC) cooled containment for long term storage.

2.4 **Thawing and enumeration of viable PBMC samples**

When an aliquot of frozen PBMCs were required for use it was important to reduce the impact that the thawing process may have upon cell viability. Aliquots were retrieved from the liquid nitrogen storage and transported on dry-ice to the laboratory. The aliquots were thawed rapidly in a water bath (37^{o}C) till partly thawed. Using a sterile Pasteur pipette, the contents of the aliquot were then transferred to a 5 ml, round bottomed flow cytometry tube containing 3 ml of pre-warmed (37^{o}C) media or PBS, depending upon required usage. The sample was then pelleted in a centrifuge and the supernatant discarded. The pellet was resuspended in solution with 1 ml of media or PBS.

To determine how many viable cells had been recovered a 10 µl aliquot of the sample suspension was mixed 1:1 with the dye Trypan blue. Trypan blue selectively stains dead cells or cells which are lacking an intact cell membrane. The total numbers of viable and non-viable cells in a known volume were counted manually using a haemo-cytometer mounted on a light microscope. The data was then used to determine the total numbers of viable and dead cells in the sample suspension.

2.5 **DNA extraction**

In order to obtain nucleic acids for molecular analysis, DNA and RNA were extracted from PBMCs.

Genomic DNA was extracted from 5x10^{6} PBMCs using QIAmp DNeasy™ mini kits (Qiagen, UK) according to manufacturer's protocol for DNA extraction using spin-columns and a microcentrifuge. Briefly, cells were pelleted in the microcentrifuge at low speed (4000rpm). The supernatant was removed and the pellet was resuspended in a total volume of 200 µl of phosphate buffered saline solution (PBS). To this was added 20 µl of proteinase K and 4 µl of RNase A. This was mixed by vortexing and then left for 2 minutes at room temperature. To this was added 200 µl of the lysis buffer, then the sample was mixed thoroughly and incubated in a heat block at 56^{o}C for ten minutes. 200 µl of ethanol (96-100%) was added to the sample and mixed by vortexing.

A DNeasy spin column was placed in to a clean collection tube and then the sample solution was pipetted in to the column. This was centrifuged for 1 minute at 8000rpm. The flow through and collection tube were then discarded and the column placed in to a clean collection tube. 500 µl of the wash buffer (AW1) was added to the column and centrifuged for 1 minute at 8000rpm. The flow through and collection tube were discarded and the column placed in to a new collection tube. 500 µl of the second wash buffer (AW2) was added to the column before centrifuging at 14,000rpm for 3 minutes. Finally, place the column in to a clean 1.5 ml microcentrifuge tube and carefully pipette 100 µl of the elution buffer (AE) on to the membrane in the column. Allow the elution buffer to incubate on the membrane for 1 minute at room temperature and then spin for 1 minute at 8000rpm in order to elute the extracted DNA.
The eluted DNA was quantified using a Nanodrop-1000™ spectrophotometer. Extracted DNA samples were stored at -20^{o}C or used immediately as required.

2.6 **RNA extraction**

RNA required for the analysis of micro-RNAs was extracted from 1x10^{7} PBMCs using *Mir*Vana™ extraction kits (Life Technologies, UK). This product was used according to the manufacturer's protocol. Briefly, the cells were washed in cold PBS then pelleted in a microcentrifuge at low speed (4000 rpm). Cells were lysed by adding 600 µl of lysing solution. A 60µl volume of homogenising solution was added and the sample was left on ice for ten minutes. Working in a fume hood, 600 µl of phenol/chloroform solution was added and the solution was inverted by hand until it became milky in appearance. It was centrifuged at full speed (10,000rpm) for 5 minutes. From the clear, upper phase of the resulting solution 500 µl was removed by pipette in to a clean 1.5ml eppendorf. To this solution, 1.25 volumes of ethanol (625 µl) was added and the sample was then mixed. This solution was then pipetted into a *mir*Vana filter column in a clean collection tube. This was centrifuged at 10,000 rpm for 15 seconds. The flow through was discarded and the same step was repeated using the remaining sample. 700 µl of the supplied Wash solution-1 was added to the column and then the sample was

centrifuged at 10,000 rpm for 15 seconds discarding the flow through afterwards. This washing step was repeated a further two times using wash solution-2/3. After discarding the flow through the column was centrifuged for 1 minute to ensure all the solution was removed. The column was then transferred to a clean 1.5 ml collection tube and 100 µl of the elution buffer, pre-heated to 95^{o}C, was added. The sample was centrifuged at full speed (13,000 rpm) for 30 seconds and the collected solution could then be stored or used as required.

2.7 **Polymerase chain reactions (PCR)**

PCR was performed using Titanium™ *Taq* polymerase and buffer system (Clontech, USA). Oligonucleotide primers were designed using PSQ assay design software (Biotage, UK) and used at a final concentration of 400nM. Thermal cycling was performed on a Veriti® thermal cycler (Applied Biosytems, US). Oligonucleotide primer sequences used in this work are listed in appendix V, p213.

Successful PCR was confirmed by electrophoresis in 1.5% agarose gels containing GelRed (1:10,000). A 5 µl aliquot of the 50 µl PCR reaction was mixed with 1 µl of 6xTrackIt Cyan-Orange sample buffer and then loaded into wells. After electrophoresis, results were visualised using an ultra-violet light box. Images were captured using AlphaDigiDoc image capture software. Molecular weight ladder VIII (Roche Applied Science, UK) was used as a size standard unless otherwise indicated.

2.8 **Cloning**

Cloning of DNA fragments for sequencing was performed using the TOPO TA cloning kit, with One-shot™ TOP10 chemically competent *E.coli* cells purchased from Invitrogen, UK (Catalogues number: K457501. TOP10). PCR products generated using *Taq* polymerase were ligated in to the plasmid vector (pCR™4-TOPO®) according to manufacturer's instructions. Briefly, 1 µl of salt solution and 1 µl of the TOPO® vector were added to 4 µl of the PCR product. The 6 µl reaction was mixed gently and incubated for 5 minutes at

room temperature. The reaction was then placed on ice. *E.coli* cells were transformed according to manufacturer's instructions. Briefly, 1 vial of One-shot™ cells was thawed on ice. To these cells was added 4 µl of the TOPO® vector reaction. The sample was mixed gently then incubated on ice for 5 minutes. Transformed cells were then immediately spread on pre-warmed nutrient agar plates containing 50 µg/mL of ampicillin. The plates were then incubated overnight at 37^{o}C. A total of twenty individual colonies were picked from plates using sterile pipette tips. PCR amplification and sequencing of cloned products was performed using the TOPO TA vector primers which were supplied with the kit.

2.9 DNA sequencing

Sequencing of DNA fragments was performed using the Sanger method (Sanger et al., 1977). The Sanger chain-termination reaction carried out using BigDye™ Terminator 3.1 kits purchased from Applied Biosystems (Catalogue number: 4337455). The oligonucleotide primers used for PCR were also used for the Sanger dideoxy chain termination reaction. Chain termination reaction products were separated by capillary electrophoresis using an ABI310 Genetic analyser (Applied Biosystems, UK). Sequence data were analysed using DNAstar™ Seqman II software. *TP53* gene sequences were compared to wildtype reference sequence (*TP53* sequence GenBank accession number: X54156).

2.10 Pyrosequencing

The primers used for analysis of the codon-31 polymorphism in *CDKN1A* were a forward, biotinylated primer 5′-CTC TTC GGC CCA GTG GAC-3′, a reverse primer 5′-CTC ACG GGC CTC CTG GAT-3′ and a pyrosequencing primer 5′-AGC GCA TCA CAG TCG-3′ designed using PSQ assay design software (Biotage, UK). DNA amplification was carried out in Bournemouth by Ian Tracy. Pyrosequencing was performed by B. Gregory.

2.11 Restriction fragment length polymorphism (RFLP)

Preliminary, low-cost analysis of single nucleotide polymorphisms (SNPs) was performed using restriction-fragment length polymorphism (RFLP) analysis on PCR amplified DNA (Kan and Dozy, 1978).

2.11.1 Codon-31 of *CDKN1A*

Primers and PCR protocols used for the analysis of the *CDKN1A* codon-31 serine/arginine polymorphism were as described by (Johnson et al., 2009). The forward primer (5'-GTC AGA ACC GGC TGG GGA TG-3') and reverse primer (5'-CTC CTC CCA ACT CAT CCC GG-3') amplified a 273 basepair product. This was incubated with the restriction enzyme, *B1pI*, which recognises the restriction site 5'-GCTNAGC-3'. The serine allele retains the AGC of the restriction site, allowing cleavage by the enzyme. Alternatively, the arginine allele, AGA, eliminates the restriction site.

2.11.2 3'UTR of *CDKN1A*

Primers used to amplify target region and PCR protocols used for the analysis of the 3'UTR C>T single nucleotide polymorphism were as described by (Johnson et al., 2009). The forward primer (5'-AGT TCT TCC TGT TCT CAG CAG-3') and reverse primer (5'-CCA GGG TAT GTA CAT GAG GAG-3') amplified a 327 basepair product. This was incubated with the restriction enzyme, *PstI*, which recognises the restriction site 5'-CTGCAG-3'. The C allele retains the restriction site, allowing cleavage by the enzyme. Alternatively, the T allele eliminates the restriction site.

2.12 Taqman assays

Taqman hydrolysis probes were utilised in two methodologies during this study, Endpoint genotyping and relative quantification. Whilst the two methods differ slightly there is good cause to explain the chemistry of Taqman probes first.

2.12.1 Endpoint Genotyping

Endpoint genotyping is a robust real-time PCR methodology for determining the genotypes of previously characterised SNPs using fluorescent hydrolysis probes (Livak, 1999).

A real-time PCR reaction is performed to amplify the region of DNA containing the SNP of interest. In addition to PCR primers the reaction solution contains an excess of two fluorescently labelled hydrolysis probes which are specific to either of the two SNP variants. During the annealing stage of the reaction the probes bind to their targets. During the subsequent extension phase the probes are degraded and a fluorescent signal is measured.

Endpoint genotyping was performed on a 96-well Roche Lightcycler 480®. A total of 20ng of genomic DNA was genotyped according to manufacturer's instructions using kits supplied by Applied Biosystems, directed to each SNP (Codon 31: Catalogue number C_14977_20; 3'UTR: Catalogue number C_7514111_10). The dyes used were HEX and FAM.

2.12.2 Micro-RNA relative quantification

The relative quantification of micro RNA was achieved by quantitative real-time polymerase chain reaction (Q-RT-PCR), using Taqman™ hydrolysis probe technology. The experiments were performed using a 96-well Roche Lightcycler 480®. For each sample 20 ng of RNA was reverse transcribed using a high-capacity cDNA reverse transcription kit purchased from Applied Biosystems (Catalogue number: 4368814). Target specific reverse transcription primers were supplied with the taqman™ mircoRNA assays purchased from Applied Biosystems (Catalogue number: 4427975).

The Taqman™ microRNA assay was performed in triplicate for each sample. Each reaction contained 1.33 µl of the cDNA reaction product, miRNA specific Taqman™ probes, and Roche probe master-mix (Roche Catalogue number: 04707494001). Target and reference microRNAs for each sample were amplified in the same 96-well reaction plate in addition to negative controls and positive calibrators. A seven point, 2-fold serial dilution (100%-1.56%) standard curve was generated in quadruplet for both target and reference genes using total RNA extracted from the cell line, MCF-7, and then saved as an external standard for application to all subsequent experiments. In order to

calibrate the subsequent experimental runs, MCF-7 RNA was frozen at three concentrations of the serial dilution standard curve (50%, 12.5% and 3.125%). Batches of thirty-six patient samples plus the three calibrators and a negative control were reverse transcribed together. The calibrator cDNAs were then used in three subsequent taqman assays, each containing twelve patient cDNAs, the reverse-transcription negative control and a taqman reaction negative control. The normalised values from the experiments were then increased by a factor of 100. The final figures generated therefore describe the percentage of *hsa*-Mir-34a found in the test sample relative to MCF-7 cells, after correction for differences in the quantity of the reference gene (*hsa*-Mir-30d).

2.13 Fluorescent in-situ hybridisation

Fluorescent *in-situ* hybridisation was performed using Vysis CLL FISH probe kit, purchased from Abbot molecular, UK (Ref 4N02-020). FISH analysis was performed by A. Gardiner, S. Mould and S. Glide (specialist cytogeneticists) according to manufacturer's guidelines. The technique allows for the visualisation of specific regions of DNA within a cell. Specifically, a single stranded, fluorescently labelled DNA probe, called a locus-specific identifier (LSI), anneals to its complementary target within the genetic material of a cell. This region can then be visualised directly using fluorescent microscopy. Figure 2-1 (next page) shows the regions of chromosomes 11 and 17 which are targeted by the Vysis probes LSI ATM and LSI TP53, respectively (Abbot Molecular Inc 2011). All single locus probes were co-hybridised with a control probe specific to the centromere of the targeted chromosome, either CEP11 or CEP17.

Briefly, the procedure involves attaching peripheral blood mononuclear cells, derived from CLL patients, to microscope slides. The cellular DNA is then chemically denatured using a sodium citrate salt solution and the fluorescently labelled probes are allowed to hybridise to their target loci. Any unbound probe is removed by a series of washes and then the nuclei are counter-stained with the DNA specific dye, DAPI, which fluoresces blue. The probes

can then be viewed and counted using a fluorescence microscope with the required excitation and emission filters (Abbot Molecular Inc, 2011).

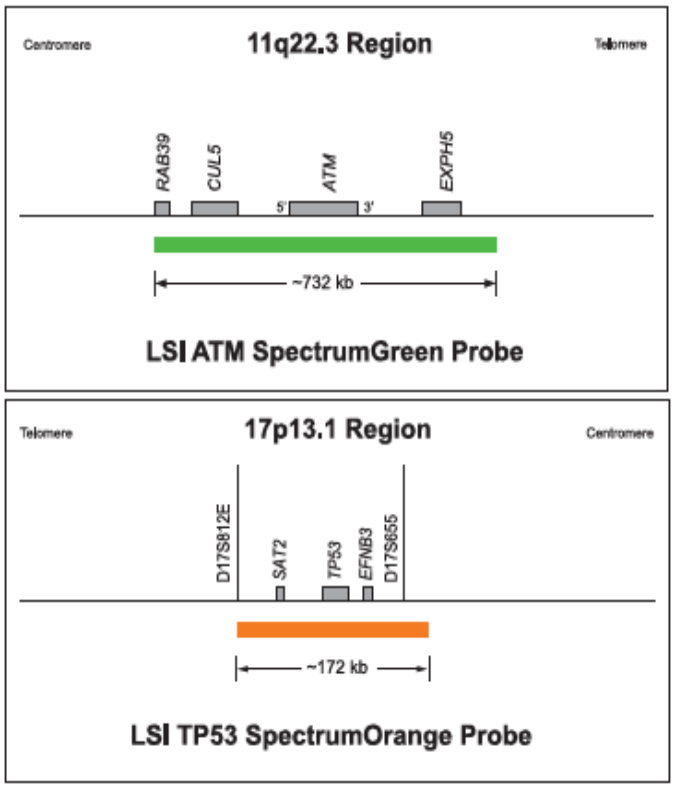

Figure 2-1: Chromosomal regions detected by Vysis FISH probes. (Abbot Molecular Inc 2011)

Figure 2-2 below shows five CLL nuclei stained using the LSI TP53 probe (orange/red) and the CEP17, chromosome-17 centromere-specific control probe (green). The proportion of cells missing one or both LSI TP53 signals can then be enumerated by counting a minimum of 200 cells.

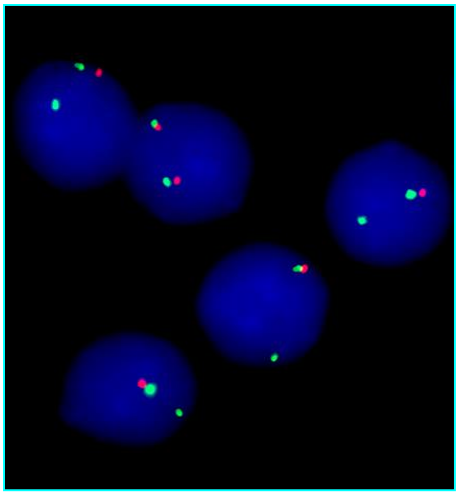

Figure 2-2: CLL DAPI-stained nuclei (Blue) with LSI TP53 (Red) and CEP17 (Green) probes

2.14 ATM/p53 pathway functional assay

To test the integrity of the p53-dependant DNA damage response pathway a functional assay was used that measures the change in levels of p53 and p21 proteins in response to DNA damage and MDM2 inhibition.

The functional assay used in this work was developed by Best *et al* (2008). Briefly, $2x10^7$ frozen peripheral blood mononuclear cells (PBMCs), were thawed and washed once in RPMIc (RPMI-1640 media containing 10% foetal calf serum and 2mM L-glutamine). PBMCs were split equally into 3 wells of a 24-well plate to a final volume of 1ml RPMIc per well containing either 1) no treatment control, 2) 50 µM final concentration etoposide or, 3) 5 µM nutlin3a and 50 µM etoposide. The cultures were incubated in a 5% CO_2 atmosphere at 37^oC for 24 hours. After harvesting cells were fixed in 2% paraformaldehyde solution for 30 minutes at 4^oC followed by permeabilisation in ice cold ethanol for 2 hours at -20^oC. Primary mouse-monoclonal antibodies, purchased from Dako UK, specific to human p53 (Clone DO-1), p21 (Clone EA-10) and an isotype matched control antibody (IgG2a) were incubated for 15 minutes. Samples were washed in phosphate buffered saline solution (PBS) and then a goat anti-mouse secondary antibody, conjugated to fluoro-isothiocyanate (FITC) was used to detect the primary antibody and amplify the signal. Antibody to CD2, conjugated to R-phycoerythrin (PE), was used to discriminate B-cells from T-cells. Data were gathered using a Becton

Dickinson FACScalibur™ flow-cytometer. The gating strategy used follows. Firstly light scatter properties were used to isolate the live lymphocytes. Within this gate CD2 negative cells (non T-cell) were selected for analysis. IgG2a antibody control was used to adjust laser voltages so the mean fluorescence intensity (MFI) in the FITC channel was set at 3.0. Further compensation of the PE channel was disregarded as the PE data was used qualitatively not quantitatively. Unless otherwise stated, 10,000 events were collected for each data acquisition. Data were analysed using CellQuest™ software.

The MFI of target proteins in the control culture was recorded and the percentage increase over the control was determined for the etoposide and etoposide-plus-nutlin3a treated cultures. An MFI of greater than, or equal to, 8 in the control culture was used to define abnormal over-expression of p53. Cut-off values for determining a normal increase of MFI, in relation to the control culture, for p53 and p21 were previously defined as 30% and 15% respectively (Best et al., 2008b). A flow chart showing the strategy for categorising samples is shown in Figure 2-3.

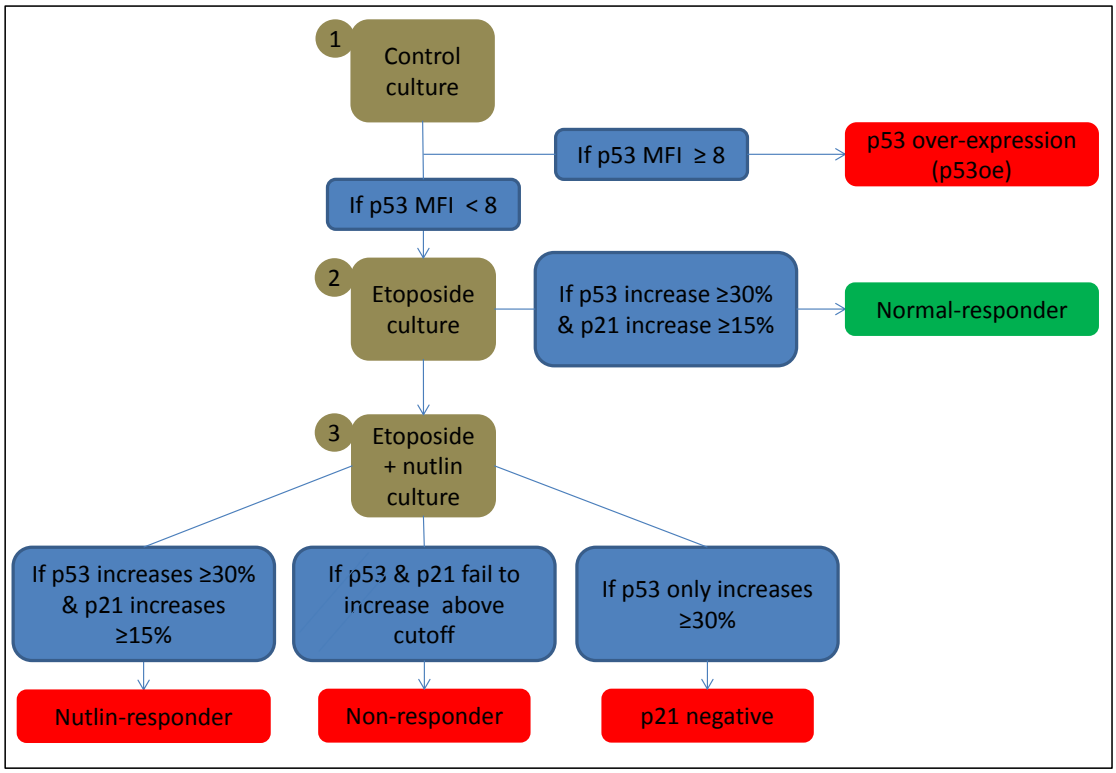

Figure 2-3: Flow chart showing strategy for assigning samples to functional groups

Categories based upon the changes to mean fluorescence intensity observed after treating cells with and without etoposide or etoposide plus nutlin3a.

Those samples which displayed abnormal over-expression of p53 in the control culture were classed as ‘p53 over-expressers’ (p53oe). Samples which exceeded these cut-off values in response to etoposide alone and did not show abnormally expressed p53 in the control were categorised as ‘Normal-responders’ on that basis alone (Best *et al*, 2008). All samples which failed to reach the cut-off for either p53 or p21 in the etoposide culture were considered as dysfunctional and the response to the etoposide plus nutlin3a culture was then used to assign these samples to specific dysfunctional categories. Samples which still failed to increase p53 and p21 expression were classed as ‘non-responders’. Any dysfunctional sample which increased p53 and p21 normally with the addition of nutlin was classed as a ‘nutlin-responder’. Samples for which only p53 responded normally were classed as ‘p21 negative’ or ‘p21-failure’.

Chapter Three:

Results

Functional Assay Performance

3.1 **Hypothesis**

The primary hypothesis for this section is as follows:
The functional assay response categories associate with specific abnormalities of ATM and p53.

The null hypothesis is therefore:
The functional assay response categories do not associate with specific abnormalities of ATM and p53.

3.2 **Classifying the FISH results**

Four hundred and seventy-two cases were selected for the following analysis. All cases had a confirmed diagnosis of CLL. No changes to diagnosis were reported at any time. Samples from the local clinic were selected on a consecutive basis and represented patients at all stages of disease. Patients recruited as part of the LRF study were selected if they had progressive disease and were at the point of requiring therapy, or, if they had relapsed after therapy. This was in order to increase the chances of obtaining as many cases with involvement of *TP53* or *ATM*.
All cases had FISH data on chromosomal loci 11q22.3 and 17p13.1 in addition to functional assay results. Deletion, detected using FISH, was determined by the proportion of examined cells with an abnormal number of fluorescent signals. The following, previously established, cut off values were used (Best et al. 2008). Cases with only one signal for 11q detectable in ≥5% of examined cells were classed as 11q-deleted. A cut-off of ≥10% was used for the detection of 17p deletion (*TP53*) as cases in the LRF CLL 4 trial with 5-10% loss of *TP53* were shown to be similar in terms of outcomes to those below 5% (Oscier et al., 2010). The main characteristics of the cohort used in this section are summarised in Table 3-1 below. Due to the use of samples from different centres, data was not complete for all cases.

Table 3-1: Characteristics of cohort used in this section n=472

Cohort characteristics				
Sex:		Male		Female
	n=469	320		149
Age at diagnosis:		Median		Range
	n=297	63		24-91
IGHV:		Mutated		Unmutated
	n=211	130		81
Binet stage at diagnosis:		A	B	C
	n=327	248	38	41
CD38 positivity:		≥30%		<30%
	n=234	62		172
CD49d positivity:		≥30%		<30%
	n=320	84		236
Previous therapy:		Treated		Untreated
	n=147	63		84

In addition to FISH analysis a subset of the cases had mutation screening and/or sequencing of the *ATM* and *TP53* genes. Unfortunately, due to cost constraints it was not possible to screen every sample which had FISH data available. Due to this, the analysis of mutations in addition to FISH data will be considered in results section 3.5 in a much smaller cohort.

3.3 **Classifying the assay results**

The median fluorescent intensity (MFI) measurements corresponding to p53 and p21 protein levels were recorded. Percentage increases over the control MFI were calculated for the etoposide and the etoposide plus nutlin3a cultures. These percentages were then used to assign a functional category according to the strategy laid out in Figure 2-3 (p81,) using previously defined cut-off values to define normal and dysfunctional p53 and p21 responses (Best et al., 2008b).

3.3.1 **Response to etoposide**

The increase in median fluorescent intensity (MFI) of p53 and p21 in the etoposide treated culture was calculated as a percentage over the control culture measurements. The data is shown in Figure 3-1.

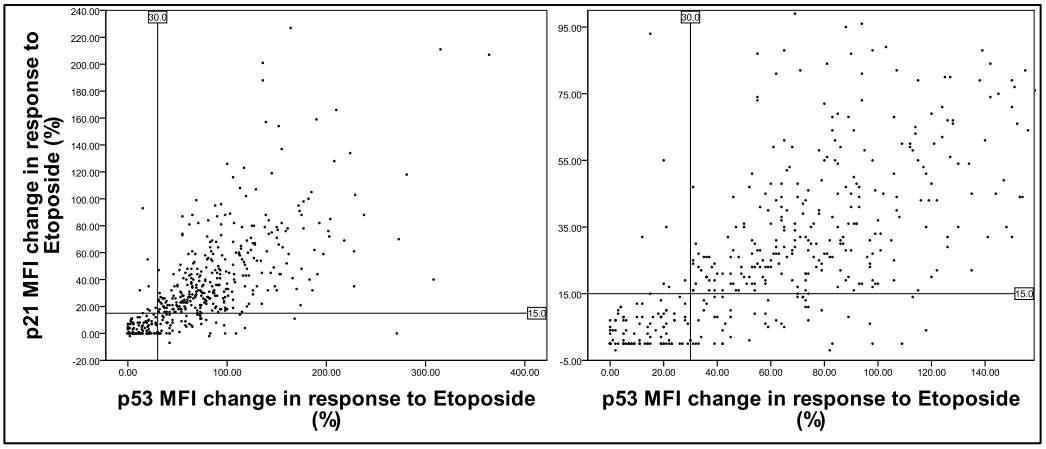

Figure 3-1: Showing the p53 and p21 responses to etoposide for 472 CLL cases. Markers indicating cut-off points for p53 and p21 are shown. Left panel shows all data. Right panel cropped to give greater detail of cases with dysfunctional responses.

The p53 and p21 responses to etoposide were then categorised according to the responses described for ionising radiation based assays (Carter et al. 2004). These results are shown in Table 3-2 and in Figure 3-2. A total of 321/472 (68.9%) samples responded normally to etoposide as a single agent therefore the overall incidence of dysfunctional responses to etoposide was 31.1%.

Table 3-2: Responses classified using etoposide treatment data only. n=472.

(Lin et al. 2012)	Response phenotype	Frequency	Percent
Normal	Normal	321	68
Type-A	p53oe	8	1.7
Type-B	No response	88	18.6
Type-C	p21 failure	47	10
Type-D	p53-p21+	8	1.7
Total	-	472	100

Basal over-expression of p53 in the control culture (p53oe) was observed in 8 cases (1.7%). These are analogous to Carter's Type-A cases. The Type-B response, failure to increase both p53 and p21, was the most frequently observed form of dysfunction, being recorded for 18.6% of cases (88/472). This represents 61.5% of the dysfunctional results (88/143). The p21-failure

response was detected in 47 (10%) cases. Finally, 8 cases (1.7%) failed to increase p53 above its 30% cut-off value despite increasing p21 sufficiently to reach its 15% cut-off. These responses were classified as Type-D due to a similar response having been previously described (Lin et al. 2012).

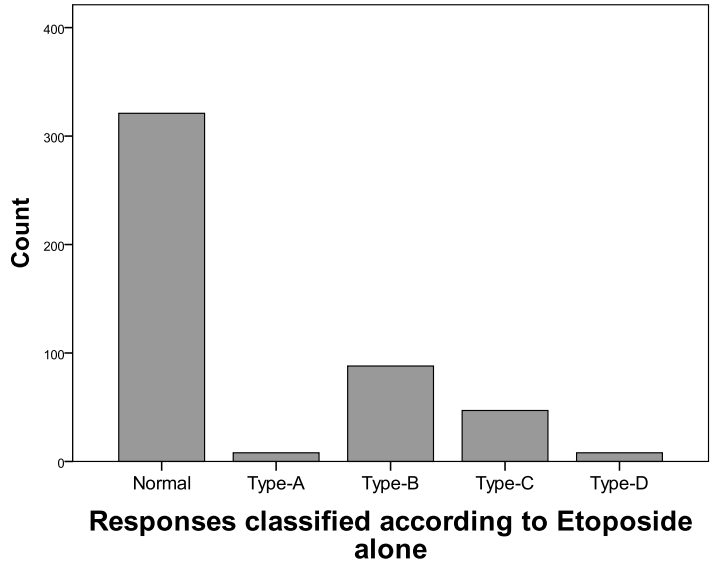

Figure 3-2: Responses classified using etoposide treatment data only. n=472.
Categories are titled according to Carter *et al*, 2004. Type-A = p53 over -expression; Type-B=No response; Type-C=p21 failure; Type-D =p53failed/p21responded.

These results, summarising the responses to the etoposide culture, are analogous to the types of results achieved using other single-agent functional tests of the ATM-p53-p21 DNA damage response pathway. As per the method laid out in 2.14, the normal-responding and p53 over-expressing cases were considered fully analysed. The remaining 143 dysfunctional cases were further categorised dependant on their p53 and p21 responses to the nutlin supplemented culture.

3.3.2 **Response to etoposide plus nutlin3a**

The 143 samples which did not sufficiently increase either p53 or p21 proteins in response to etoposide were re-evaluated using the p53 and p21 responses

in the etoposide-plus-nutlin treated cultures. The data are shown in Figure 3-3 and summarised in Table 3-3.

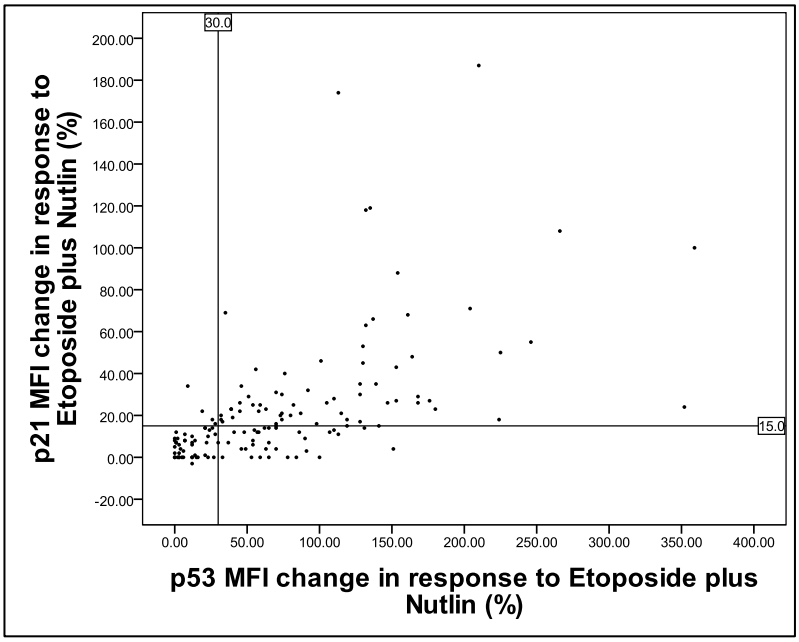

Figure 3-3: p53 and p21 responses to etoposide plus nutlin in 143 dysfunctional cases

The addition of nutlin induced a normal p53 and p21 response in 65 (45.5%) of the 143 dysfunctional samples, classifying them as nutlin-responders. Thirty-nine samples were classified as non-responders, maintaining a p53 and p21 incompetent response despite the addition of nutlin (39/143; 27.3%).

Table 3-3: Categorisation of 143 dysfunctional cases after evaluating nutlin response

Category	Frequency	Percent
Non-responder	39	27.3
Nutlin responder	65	45.5
p21 failure	35	24.5
Category-4	4	2.8
Total	143	100

Thirty-five samples failed to sufficiently increase p21 despite a rescued p53 response (p21-failures) and a further four did not raise p53 MFI above the cut-off despite doing so for p21. These four cases were grouped together under the label Category-4; a similar outcome has been previously reported using a

functional test on a CLL patient cohort (Lin et al. 2012). Lin *et al* referred to this result as Type-D but to avoid confusion it has been termed Category-4 in this study. The overall distribution of all 472 samples across all categories is shown in Table 3-4.

Table 3-4: Categorisation of whole dataset. N=472

Category	Frequency	Percent
Normal	321	68
p53oe	8	1.7
Non-responder	39	8.3
Nutlin responder	65	13.8
p21 failure	35	7.4
Category-4	4	0.8
Total	472	100

In order to make a comparison that demonstrates the effect of nutlin on these results the etoposide and etoposide plus nutlin frequencies are cross-tabulated in Table 3-5 below.

Table 3-5: Comparison of etoposide responses and etoposide plus nutlin responses. n=472.

		Nutlin response classification						
		Normal	Non-responder	Nutlin responder	p21 failure	p53oe	Category 4	Total
Etoposide response classification	Normal	321						321
	Type A					8		8
	Type B		39	36	11		2	88
	Type C			23	24			47
	Type D			6			2	8
	Total	321	39	65	35	8	4	472

In order to test the usefulness of the assay as a tool for detecting and differentiating between abnormalities involving loss of the chromosomal regions containing the genes for *ATM* and *TP53*, their distribution amongst the functional categories was analysed.

3.4 Assay responses and the incidence of cytogenetic abnormalities detected using FISH

The association between cytogenetic abnormalities of 11q and 17p detected by FISH and functional assay results was assessed. It was hypothesised that nutlin responders would be associated with *ATM*/11q abnormalities and non-responders would be associated with *TP53*/17p abnormalities.

The distribution of FISH results by functional category is shown in Table 3-6 (p91). Abnormal FISH results for the loci containing *ATM* and *TP53* were found in a total of 113 cases; their relative incidence in cases with or without dysfunction was analysed using Fisher's exact test. A significant association was found between dysfunctional assay responses and the presence of FISH abnormalities which were detected in 44/321 (13.7%) of the normally functioning samples and in 69/151 (45.7%) of the dysfunctional samples (13.7% v 45.7%, $p< .0001$). The distribution of abnormalities within the different functional categories led to the following observations.

3.4.1 *TP53* deletion is significantly associated with the non-responder and p21 failure categories

Comparing the incidence of FISH results within the normal responders to their incidence in the separate dysfunctional categories found heterozygous loss of *TP53* to be significantly associated with non-responders (3.1% v 35.9%, $p< .0001$), p53 over-expression (3.1% v 50%, $p=.0001$) and p21-failure (3.1% v 20%, $p=.0005$). Loss of *TP53* was detected in two nutlin-responders but this was not different to the incidence of *TP53* deletion in the normal functioning cases (3.1% v 3.1%, $p=1$). One case with Category-4 dysfunction was found to have Del(17)p but this was not significant, probably due to the very low number of Category-4 cases, n=4 (3.1% v 25%, $p=.129$).

Table 3-6: Cross-tabulation of FISH results and functional assay results (n=472).

	Normal		Non-responder			Nutlin-responder			p21-failure			Unclassified			p53 over-expression			
FISH Result	N	%	N	%	*p*	N	%	*p*	N	%	*p*	N	%	*p*	N	%	*p*	Total
no loss	277	86.3	20	51.3		34	52.3		21	60		3	75		4	50		359
Del11q	31	9.7	3	7.7	*1*	28	43.1	***<.0001***	6	17.1	*0.236*							68
Del17p	10	3.1	14	35.9	***<.0001***	2	3.1	*1*	7	20	***0.0005***	1	25	0.129	4	50	***0.0001***	38
Three p53 signals	1	0.3																1
Tetraploidy	1	0.3																1
Del11q and Del17p	1	0.3	2	5.1	***0.014***	1	1.5	*0.308*	1	2.9	*0.187*							5
Total	321		39			65			35			4			8			472

The incidences of 11q22.3 and 17p13.1 deletions, detected using FISH, in the dysfunctional categories were compared to their respective incidence in the normal responder group. *P* values were calculated using Fishers exact test.

3.4.2 *ATM* deletion is significantly associated with the nutlin-responder category

Heterozygous 11q deletion was detected in a total of 68 cases, 31 of which (45.6%) responded normally to etoposide alone making it the most common FISH abnormality found in the Normal functional category (31/321; 9.7%). Deletion of 11q did not occur in the p53 over-expression or unclassified cases. 11q deletion was detected in, but not significantly associated with, the non-responder (9.7% v 7.7%, p=1) and p21-failure (9.7% v 17.1%, p=.236) categories. The nutlin-responder category was however significantly associated with 11q deletion (9.7% v 43.1%, p <.0001). One sample with tetraploidy, confirmed by the Cytogenetics department of Royal Bournemouth Hospital, was found to give a normal functional response, as did another sample which was found to have three copies of *TP53*. Of five cases with loss of both FISH probes, 4/5 (80%) gave a dysfunctional result.

One explanation for the incidence of FISH abnormalities in the normal functional category could be that those cases have smaller deleted clone sizes, i.e. the proportion of cells examined with a missing/deleted FISH signal. A lower proportion of non-responding cells may be masked by a dominant, normally responding clone. Data on clone size was available for 29/38 cases with Del(17)p and 45/68 cases with Del(11)q and so this was investigated.

3.4.3 **The proportion of 17p-deleted cells influences the functional assay result**

It was hypothesised that normal functioning samples with Del(17)p would have smaller deleted clone sizes than those which had the same FISH result and gave a dysfunctional assay response. To clarify, the terms 'clone' and 'clone size' in this section refer to the proportion of examined cells which display only one FISH signal rather than the normal two. A deleted clone size of 100% refers to a sample in which all examined cells have only one allele.

Figure 3-4 shows the clone sizes of 29 of the 38/472 cases that had heterozygous deletion of 17p; information on the clone size was not available for 9 cases. A non-parametric Kruskal-Wallis test showed a significant difference in the deleted clone sizes across the functional categories (χ^2=10.339, df=3, *p*= .016).

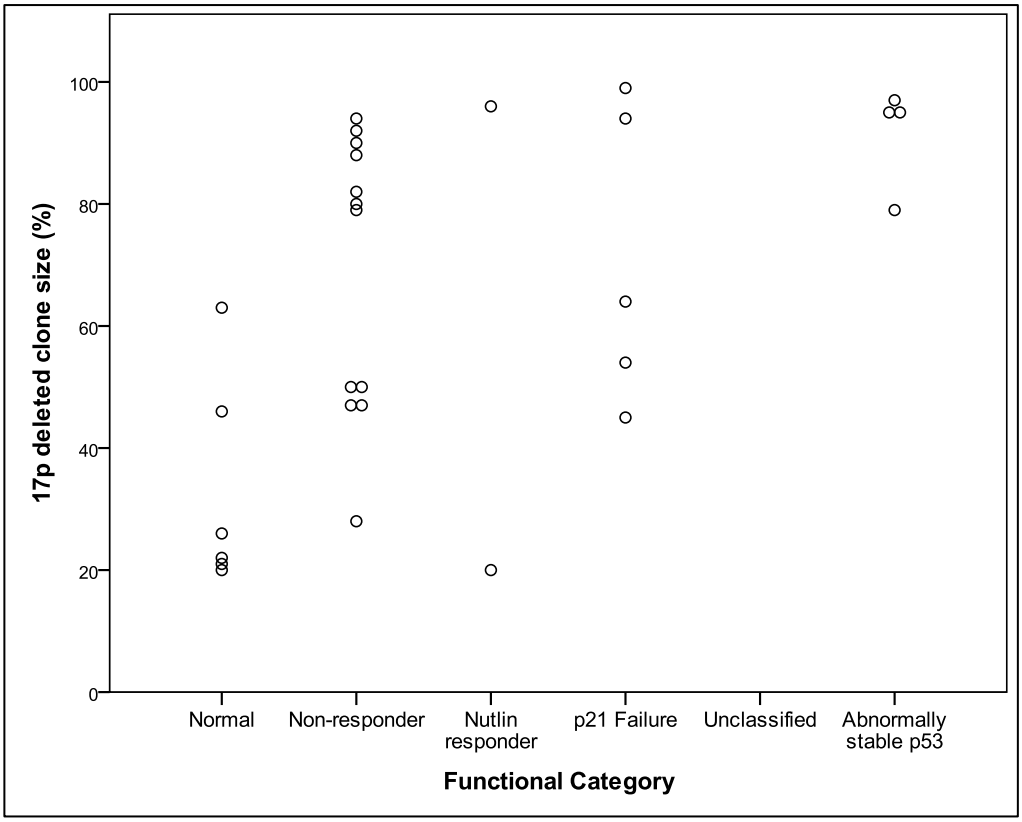

Figure 3-4: Size of 17p-deleted clone as determined by FISH, displayed according to functional category. N=29.

A two-tailed Mann-Whitney test was used to compare the 17p deleted clone sizes of the normal responders to the individual dysfunctional groups. The

clone sizes of the normal responder group was significantly different to the non-responder (*U*=6, *z*=-3.1, *p*= .002) and p21-failure groups (*U*=1, *z*=-2.345, *p*= .019). There is still overlap in the range of clone sizes between the normal and dysfunctional categories which may result from the influence of other abnormalities such as *TP53* mutation.

3.4.4 The proportion of 11q-deleted cells does not influence functional status

Figure 3-5, below, shows the range of clone sizes reported for all cases with 11q deletion as a sole abnormality and for which data on the proportion of deleted cells was available (n=45). A non-parametric Kruskal-Wallis test showed no significant difference in the deleted clone sizes across the functional categories (χ^2=2.886, df=3, *p*= .410). However, it can be seen that there is an apparent bi-modal distribution, with cases showing a large or small clone size and an absence of intermediate cases.

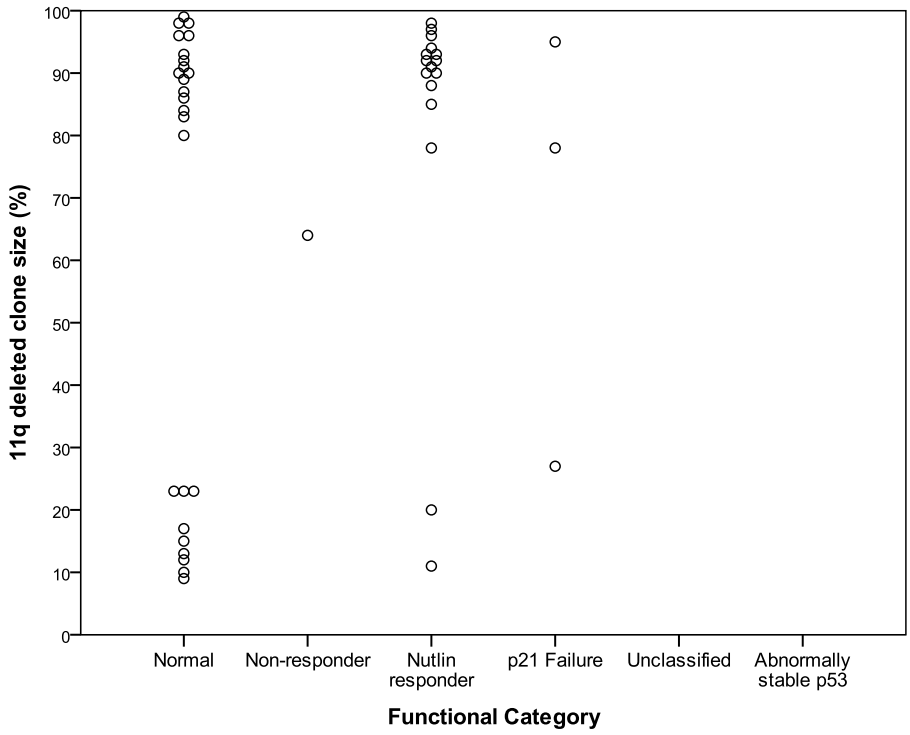

Figure 3-5: Size of 11q-deleted clone as determined by FISH, displayed according to functional category. N=45

Broadly grouping the clone sizes as either Large (>50%) or Small (<50%) suggested that the lower clone sizes may occur more frequently in the normal response category (Table 3-7). However, comparing the relative frequency of large versus small clone size between the normal and nutlin responders using Fisher's Exact test, did not find a significant difference, *p*=.1519.

Table 3-7: Incidences of large and small 11q-deleted clone sizes across functional categories, n=45

	Normal	Non-responder	Nutlin-responder	p21-failure	Total
Clone size >50%	16	1	14	2	33
Clone size <50%	9	0	2	1	12
Total	25	1	16	3	45

It was therefore decided to examine, in normal responder cases only, the etoposide induced increase of p53 between cases with no detected deletions (11q or 17p), and cases with 11q deletion. The aim was to determine whether the 11q deleted/normal responders still experienced a discernible impact on their p53 response to DNA damage or whether 11q deletion had no effect in those cases.

Selecting cases from the main cohort, there were a total of 308 normal responders with no detectable 17p deletion. Of these, 31 had a detected 11q deletion. Figure 3-6 below shows a box plot of the data for these groups.

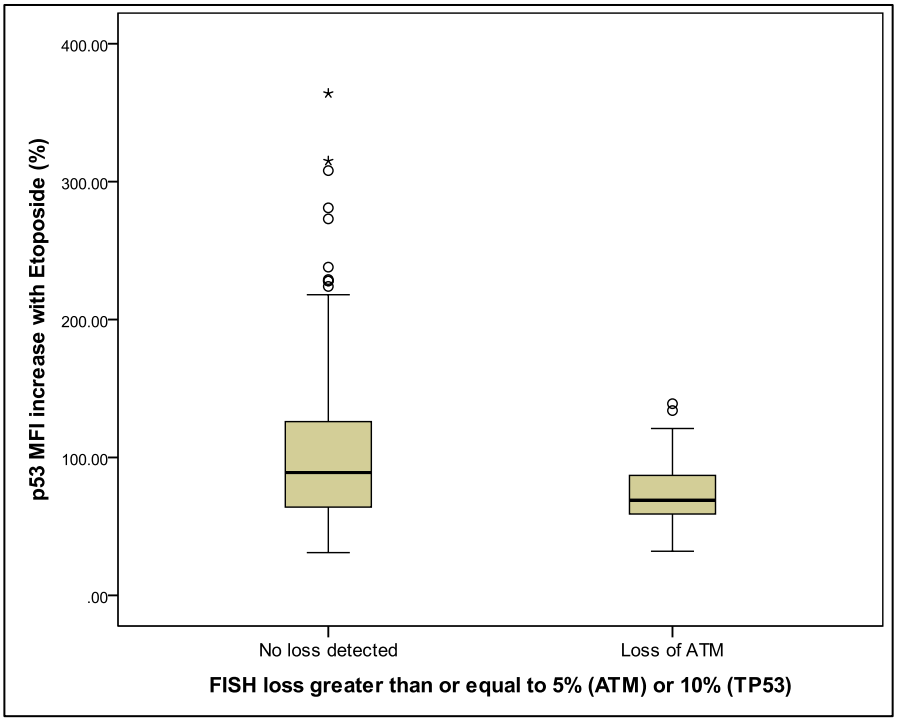

Figure 3-6: Boxplot showing p53 MFI induction in normal responders with (n=31) or without (n=277) deletion of 11q.

The descriptive data on the average increase in p53 MFI after etoposide treatment for these two groups is shown in Table 3-8. A t-test for the equality of the means found that there was a significant difference in average p53 MFI increase between cases with 11q deletion (M=75.3, SD=27.4) and those without (M=101.8, SD=53.6, t(60)=4.5, p<.001).

Table 3-8: Average increase in p53 MFI after etoposide treatment in samples with a normal assay response and no detected *17p* deletion (n=307).

Group	N	Mean %	Std. Dev	Median %	Min-max
No deletion	277	101.8	53.6	89	31-364
11q deletion	31	75.3	27.4	69	32-139

This data suggests that deletion of 11q attenuates the DNA damage response even in cases which were not classified as dysfunctional in response to etoposide.

3.4.5 **Summary**

It has been found that in terms of FISH results the assay detected a significant proportion of cases with deletion of either 11q22.3 or 17p13.1 and is able to discriminate between them by using nutlin to reactivate p53 in the

absence of functional ATM mediated signalling. Deletion of 17p13.1 was significantly associated with both the non-responder and p21-failure categories and deletion of 11q22.3 was significantly associated with the nutlin-responder category. These findings provide evidence of p21 failure being, in some cases, associated with abnormalities of *TP53.*

Despite these associations however, 127 of the 472 analysed cases (26.9%) had functional assay results that were unexpected, given the actual FISH results; 14% (45/321) of the normal responder samples were found to have FISH abnormalities whilst 54% (82/151) of the dysfunctional samples had no detectable abnormalities. The size of the deleted clone was investigated and shown to have an effect on the functional assay results in cases with deletion of 17p13.1 potentially raising questions about the sensitivity of the assay. In contrast, the size of the 11q22.3 deleted clone did not associate with dysfunction but did display a bimodal distribution of clone sizes; an effect that was not seen in cases with deletion of *TP53*.

The presence or absence of dysfunction in cases with loss of 11q22.3 detected by FISH could also be influenced by the mutational status of the remaining allele suggesting that heterozygous loss of *ATM* in and of itself is not sufficient to cause a dysfunctional response to etoposide treatment and the presence of an *ATM* mutation may be a determining factor in nutlin-responder dysfunction.

Importantly, half of the eight p53 over-expression cases had no loss of 17p13.1 or 11q22.3 detected by FISH. Abnormally stabilised p53 is an accepted marker of p53 abnormalities and so the question of whether mutations of *TP53* are present in these samples was addressed.

Table 3-9: Comparing the relative distribution of results between the present study and Lin *et al* (2012)

	Normal	Type-A	Type-B	Type-C	Type-D
Etoposide results	68	1.7	18.6	10	1.7
(Lin et al. 2012)	30	2.2	52.5	4.7	10.4

3.5 The assay identifies *TP53* mutations but not *ATM* mutations.

For the reasons outlined above the mutational status of *TP53* and *ATM* was investigated. Of the 472 cases used in the FISH analysis a total of 123 had complete genetic sequence screening of both the *ATM* and *TP53* genes carried out.

For a preliminary analysis the FISH and mutation results were combined. Cases with no abnormality of either gene detected were classed as normal. Cases were classed as having either a TP53 or ATM abnormality if they were found to have mutation and / or loss of that gene only. One case was classed as having involvement of both genes.

The incidence of TP53 or ATM abnormalities in each dysfunctional category was compared to the normally functioning group using Fisher's exact test to determine the *p* value with results of $p<.05$ being considered significant. The distribution of these results across the different functional categories is shown in Table 3-10. The normal response category (n=85) contained 3 cases (3.6%) with a detected abnormality of *TP53* and 18 cases (21.2%) with an abnormality of *ATM*. The Non-responder group (n=11) was found to have 7 cases (63.7%) with an abnormality of *TP53* which was significantly different to the Normal function group (3.6%v63.7%, $p<.0001$).

Table 3-10: Cross tabulation of genetic abnormalities according to functional category, n=123.

Functional category	**Normal**		**Non-responder**			**Nutlin-responder**			**p21-failure**			**p53 oe**			**Total**
Full screening result	**N**	**%**	**N**	**%**	***p***	**N**	**%**	***p***	**N**	**%**	***p***	**N**	**%**	***p***	
Normal	64	75.3	3	27.3		6	42.9		3	33.3		0			76
TP53 abnormality	3	3.6	7	63.7	**<.001**	1	7.1	0.46	4	44.4	**0**	4	100	**<.001**	19
ATM abnormality	18	21.2	0			7	50	**0.04**	2	22.2	1	0			27
ATM & TP53 involved	0		1	9.1	0.12	0			0			0			1
Total	85	100	11			14			9			4			123

The nutlin-responder category contained 1 case with TP53 involvement, which was not significant compared to the normal responders (3.6%v7.1%, $p=.462$). *ATM* abnormalities were detected in 7/14 nutlin-responder cases which was significantly different to the Normal functioning group (50%v21.2%, $p=.041$).

There was no significant difference in the incidence of *ATM* abnormalities between the p21-failure group and normal responders (22.2%v21.2%, p=1.0) but *TP53* abnormalities were significantly differently distributed (3.6%v44.4%, p=.0013) and accounting for nearly half of the p21-failure cases. All four cases with p53 over-expression were found to contain TP53 abnormalities (3.6%v100%, p<.001).

To summarise the incidences of abnormality, there were 20 cases with detected abnormalities of *TP53* (including 1 with an additional mutation of *ATM*) and 85% of these (17/20) gave some form of dysfunctional response to the assay. Of the 27 cases with a detected abnormality of *ATM,* (excluding the aforementioned case with concurrent *TP53* abnormalities), only 9 (33%) gave a dysfunctional result with the remainder giving a normal response to the assay.

The mutation and FISH data are shown in greater detail in Table 3-11 and Figure 3-7 below.

Table 3-11: Cross tabulation of screening results and assay responses showing bi-allelic states. n=123

Functional category	Normal		Non-responder		Nutlin-responder		p21-failure		p53 over-expression		Total
Full screening result	**N**	**%**	**N**	**%**	**N**	**%**	**N**	**%**	**N**	**%**	
Normal	64	75.3	3	27.3	6	42.9	3	33.3	0		76
TP53 deleted	1	1.2	2	18.2	0		0		0		3
TP53 mutated	1	1.2	0		0		2	22.2	1	25	4
TP53 deleted/mutated	1	1.2	4	36.4	1	7.1	2	22.2	3	75	11
Biallelic TP53 mutation	0		1	9.1	0		0		0		1
ATM deleted	13	15.3	0		6	42.9	1	11.1	0		20
ATM mutated	5	5.9	0		1	7.1	0		0		6
ATM deleted/ mutated	0		0		0		1	11.1	0		1
TP53 deleted/ mutated + ATM mutated	0		1	9.1	0		0		0		1
Total	**85**	100	**11**		**14**		**9**		**4**		**123**

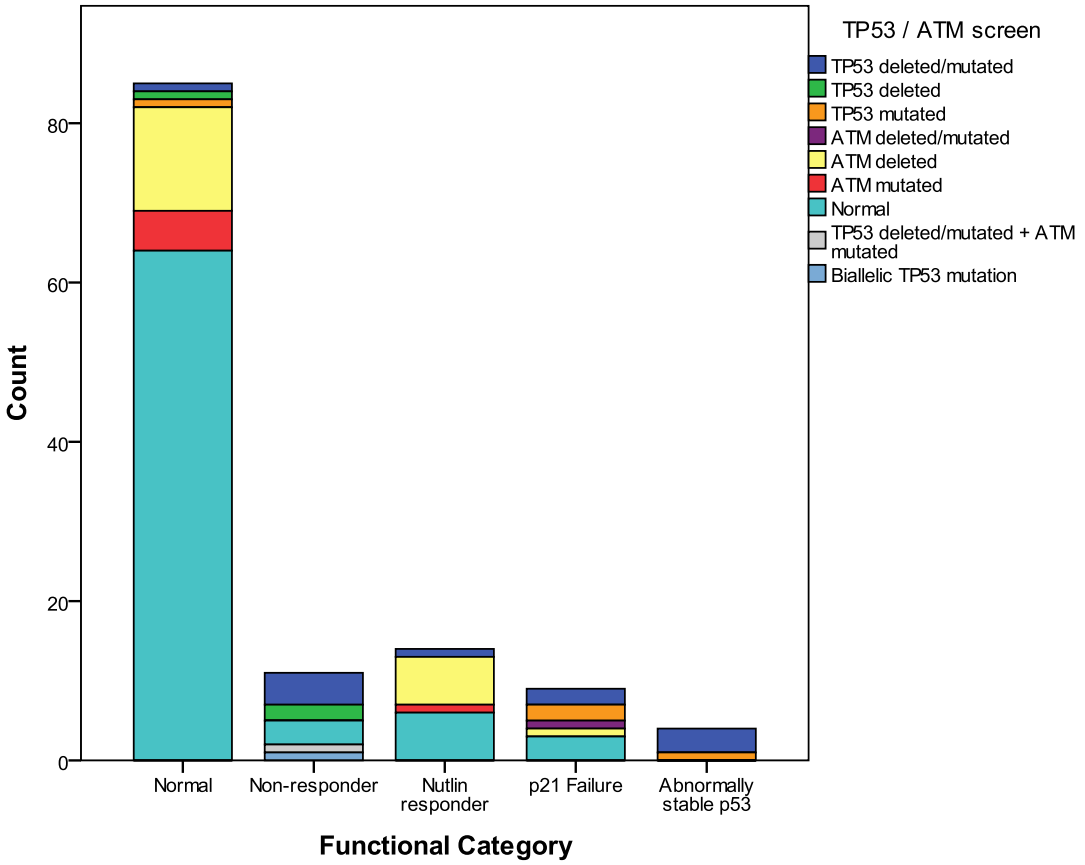

Figure 3-7. Bar chart showing the occurrences of all combinations of *ATM* and *TP53* abnormalities across the cohort, stratified by functional response to the etoposide/nutlin assay (n=123).

3.6 **Analysis of the p53 over-expression category.**

A commonly observed phenotype of *TP53*-mutated cells is the over-expression of p53. It is most often used as a marker of *TP53* mutation in cells that are assessed by histological examination or western blotting. The mechanism for this is thought to be loss of MDM2 transcription by p53 either through loss of function alone or coupled with a dominant negative effect as the mutated p53 inhibits the normal function of the wild-type protein. This then leads to absence of p53 proteolysis and cellular accumulation of the protein under unstressed conditions.

In previous FACS based, functional assays the over-expression of p53 in the control culture cells was the defining characteristic for assigning a functional response (Carter et al, 2006). In many of the results that have been published

however, this Type-1 group is often very small in comparison to other dysfunctional groups and demonstrably does not detect all TP53 abnormalities.

In the nutlin assay, high baseline expression was identified for samples which had a p53 control MFI of greater than eight. This is quite a high value which reflects the high specificity that can be achieved using this marker but at a heavy cost in terms of sensitivity, indeed it would not be possible to detect TP53 mutation and/or loss of 17p in the majority of cases using this metric alone. In the categorisation of samples using the etoposide plus nutlin assay it is the pattern of responses to treatment that are used. In order to determine whether the detection of high baseline p53 protein levels is a necessary metric, all samples which have been tested using the assay were screened for samples with this phenotype.

3.6.1 High baseline p53 is not required for the detection of dysfunctional responses.

From all the assay results that are available, regardless of any other genomic analysis or the disease diagnosis, there were 17 instances of a baseline p53-MFI higher than 8. FISH results for the *ATM* and *TP53* loci were available for 16 of these cases; 13/16 had TP53 mutation screening in addition. The one case without FISH results also did not have TP53 mutation results and was therefore removed. Of the remaining high baseline cases, 14/16 were diagnosed as CLL, in addition to one mantle cell lymphoma and a Burkitt's lymphoma.

All 16 cases displayed some form of structural abnormality of TP53 confirming the high level of specificity associated with this metric. Seven cases (43.75%) had loss of one FISH signal and a mutation of TP53, three (18.75%) had loss but no data on TP53 gene mutations and the remaining six (37.5%) had mutation of TP53 and no loss detected by FISH. Classifying the samples according to the p53 and p21 protein responses to drug treatments only, using the Best *et al (2008)* cut-offs, would have characterised 7/16 (43.75%) cases with p21-failure. The remaining nine cases all failed to upregulate both proteins above the cut-offs and would have been classified as Non-responder on that basis alone. In all 16 cases the etoposide plus nutlin culture did not activate the p53 pathway and so no cases would be categorised as nutlin-responder. This shows clearly that the detection of high-baseline p53 protein is dispensable for the detection of p53 dysfunction and that samples with this phenotype do not respond differently to nutlin than other cases with p53 abnormalities. So having established that these cases do not need to be identified on baseline p53 expression alone it was reasonable to question whether high baseline p53 is a stable marker.

Pettitt *et al* (2011), have reported that the Type-A group was associated with treatment failure and that this association was not discernible in their Type-B group. This may therefore mean that the detection of high baseline –p53 may have value but as their Type-B category contains patients with ATM as well as

TP53 abnormalities it is possible they were unable to detect the effect of low baseline, p53 involved cases.

3.7 **Investigating previous therapies in this group**

Within the fully characterised cohort, data on previous therapy was available for 121 samples. Fisher's exact test was used to detect a difference in the incidence of prior therapy between the genetic sub-groups or functional categories (Table 3-12 and Table 3-13).

Table 3-12: Showing the distribution of genomic abnormalities between the treated and treatment naïve patients

		TP53 or ATM abnormality										
		None	ATM mutation	ATM deletion	ATM biallelic	All ATM involved	TP53 mutation	TP53 deletion	TP53 biallelic	All TP53 involved	ATM & TP53	Total
Previously treated	No	44	4	6	0	10	1	1	3	5	0	59
	Yes	30	4	11	1	16	2	4	8	14	2	62
	p value		0.7125	0.1042	0.4133	0.0723	0.5669	0.1592	0.0566	**0.0188**	0.174	

Low numbers affected comparison of prior therapy within the different genotypic sub-groups. No groups achieved significance although a trend was observed in the bi-allelic *TP53* cases (p=0.0566). When combining the genotypic groups, excluding the 2 cases with both ATM and TP53 abnormalities, a significant association was seen for patients with any TP53 abnormalities (p=0.0188) but not for any ATM abnormalities (p=0.0723).

Table 3-13:Showing the distribution of functional responses between the treated and treatment naïve patients

		Functional category						
		Normal	Category-1	Category-2	Category-3	Category-4	All dysfunction	Total
Previously treated	No	48	4	3	1	3	11	59
	Yes	37	12	5	3	5	25	62
	p value		**0.0286**	0.4605	0.3225	0.4605	**0.0103**	

Similarly, the incidence of prior therapy in functionally normal cases versus all dysfunctional cases, regardless of category, showed a significant association (p=0.0103). However comparing the incidence of prior therapy in the individual categories of response found an association only for the Non-responder responders (p=0.0286).

3.8 **Summary**

This result section has shown that the use of etoposide and etoposide plus nutlin to perform a functional analysis of the ATM/p53 pathway in CLL cells can be used to successfully detect cases with abnormalities of the p53 gene

(either mutation and/or deletion of chromosome 17p) or deletion of chromosome 11q. The assay also successfully separates those cases with deletion of 11q from those with p53 abnormalities by using nutlin3a to activate p53 dependant signalling. The assay does not appear to be sensitive to the presence of mono-allelic *ATM* mutation and the cohort in general appears to lack cases with confirmed bi-allelic involvement of *ATM.* Deletion of 11q was the main type of abnormality detected in cases with normal function although the results show that these cases do have an attenuated response when compared to normal functioning cases without deletion.

This section has also shown that despite over expression of p53 in unstressed cells being highly specific for the detection of p53 mutation it is not very sensitive. If used alone to detect p53 mutations this phenotype gives a high rate of false negative results, as is the case for immunohistochemistry (Colomer et al. 2003). It has been shown that all 16 samples with p53 over-expression also displayed dysfunctional upregulation of p21. This took the form of either a non-responder or p21-failure categorisation.

In light of these results it is possible to reject the null hypothesis for this section and accept the hypothesis: 'The functional assay response categories associate with specific abnormalities of ATM and p53'.

Chapter Four:

Results

Investigating the p21-failure assay response

4.1 **Overview**

The categorisation of CLL samples based upon the response of p53 and p21 protein expression to the assay conditions aims to both detect and discriminate between genetic abnormalities of *ATM* and *TP53* that have adverse impacts upon patient care. In Chapter 3: Results, (pp83-104), it was found that the p21-failure response is significantly associated with p53 mutation and/or 17p-deletion, which is contrary to the currently published explanation (Johnson et al. 2009). This category requires further investigation to clarify its cause or causes.

The only published explanation for a similar response to *in-vitro* DNA damaging assays suggests that approximately half of these cases are accounted for by the presence of two, interacting polymorphisms within the p21 gene (*CDKN1A*) (Johnson *et al*, 2009). The first is a non-synonymous transversion in codon 31 resulting in a serine/arginine substitution (rs1801270). The second, rs1059234, is a C/T transition within the 3'UTR of the gene (Figure 4-1).

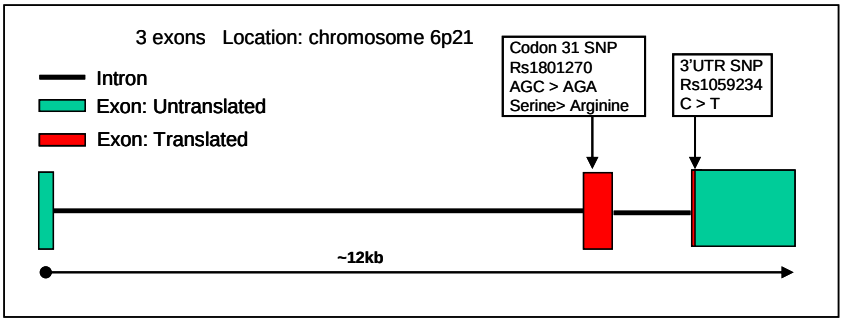

Figure 4-1: The CDKN1A gene structure. Image showing exons, introns and sites of codon-31 and 3′ UTR single nucleotide polymorphisms (SNPs)

The authors of that study found that heterozygosity for the rare allele at codon-31, combined with the presence of homozygosity for the common allele at the 3'UTR, was highly associated with the p21-failure response. The authors suggest that the arginine variant mRNA is unstable and as such is not translatable and that the presence of the variant allele in the 3′UTR stabilises the mRNA allowing translation. The 3′UTR variant could also affect the translation of the mRNA if the variant altered interactions with any known or unknown miRNAs.

It should be noted that although the assay is different, using ionising radiation alone to induce a DNA damage responses, it does describe similar responses. As this response pattern is observed when using the etoposide/nutlin assay it was decided to investigate the occurrence of *CDKN1A* polymorphisms in our p21-failure samples.

4.2 **Hypothesis**

The hypothesis for this chapter is as follows:

Hypothesis:

Cases displaying a p21-failure response to the assay associate with codon-31 and 3′UTR polymorphisms in the *CDKN1A* gene.

Null hypothesis:

Cases displaying a p21-failure response to the assay do not associate with codon-31 and 3′UTR polymorphisms in the *CDKN1A* gene.

4.3 The p21-failure response does not associate with single nucleotide polymorphisms of the *CDKN1A* gene.

In order to test for the effects of *CDKN1A* polymorphisms, which have previously been identified as associated with the p21-failure phenotype (Johnson et al. 2009), samples were selected from the cohort for which FISH results for del17p, *TP53* mutation (exons 5-9) and functional data was available.

Initially 23 p21-failure cases plus 20 abnormal (Non-responder or nutlin-responder) and 80 normal cases were analysed using PCR-RFLP as previously described (Johnson *et al*, 2009). Example results obtained using the PCR-RFLP method are shown in Figure 4-2.

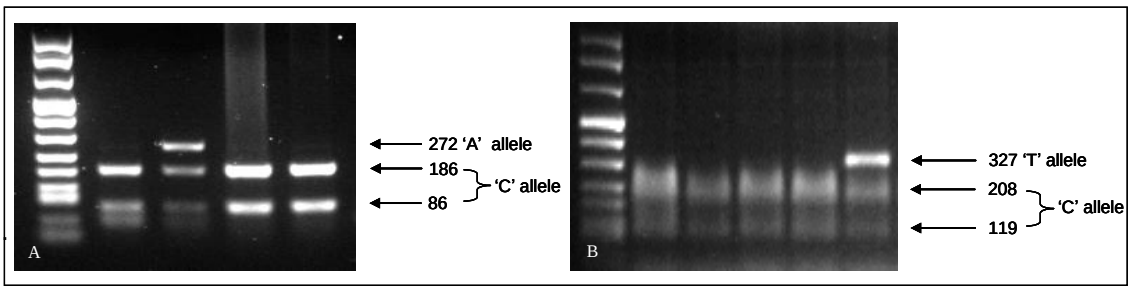

Figure 4-2: Restriction digests to determine genotypes
A) Codon 31 digestion. Enzyme *BlpI,* cuts the ancestral Serine 'C' allele and not the rare Arginine 'A' allele. B) 3′UTR digestion. Enzyme *PstI*, cuts the ancestral 'C' allele and not the rare 'T' allele.

Sequencing of the PCR products revealed that the primers for the 3'UTR SNP amplified non-specific products and re-optimisation of the PCR protocol failed to improve the results. High molecular weight DNA in some of the samples also may have led to the 3'UTR-RFLP results being unclear. The analysis of the two polymorphisms was therefore repeated in an expanded cohort using a more sensitive and specific technique.

A selected cohort of 180 cases, classified according to Best *et al* (2008) criteria, including 116 normal, 39 abnormal (non- or nutlin-responders) and 25 p21-failure cases were genotyped by endpoint genotyping on a Roche

LC480®. Figure 4-3 below, shows the output from one of the genotyping experiments, showing 48 cases.

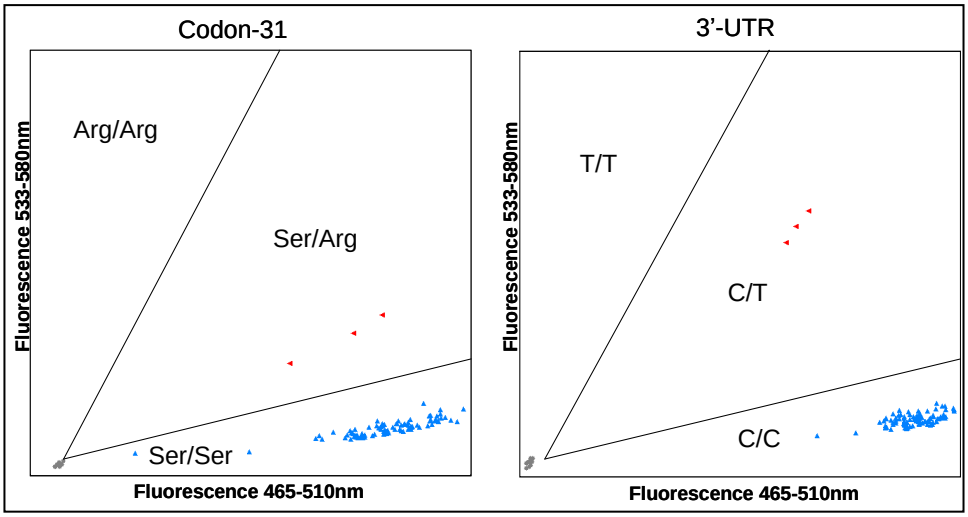

Figure 4-3: LC480 output showing SNP genotypes at codon-31 and 3'UTR for 48 samples.
The samples which were found to be heterozygous for one polymorphism were also heterozygous for the other, without exception.

In all cases tested, heterozygosity at the codon-31 polymorphism was accompanied by heterozygosity at the 3'UTR polymorphism. Likewise, homozygosity occurred at both SNPs. No cases were found to be homozygous for the rare allele nor were any cases found to be homozygous at one SNP and heterozygous at the other. This is a strong indicator that the two polymorphisms are linked, meaning the rare SNPs are present on the same allele and are co-inherited. This is supported by several previous studies in which these two SNPs were always linked (Facher et al. 1997; Konishi et al. 2000; Taghavi et al. 2010). For this reason the results have simply been classified as a single diplotype: either hetero- or homozygous, and shall be referred to as such, and are shown in Table 4-1.

Table 4-1: Frequency of genotypes determined by Endpoint genotyping. N=180.

Etoposide response	SNP diplotype		Total
	Homozygous	Heterozygous	
Normal	105	11	116
Abnormal	32	7	39
p21-failure	21	4	25
Total	158	22	180

Genotyping of 180 mixed function cases. The two SNPs in all 180 cases were found to occur as either a heterozygous or homozygous diplotype. No cases were found to be homozygous for the variant allele at either SNP.

The incidence of heterozygosity within the p21-failure response group was not found to be significantly different from its occurrence in the normal group (16% v 9.5%, *p*=.3063) or the abnormal group (16% v 18%, *p* =1.0). To confirm these results, 85 samples (including all p21-failure cases and all codon-31 heterozygotes) were reanalysed at codon-31 by pyrosequencing. Results confirmed the previous observations. This analysis shows that in our cohort polymorphic variants of *CDKN1A* do not associate with the p21-failure response.

4.4 Mixing normal and p53 null cells *in-vitro* can replicate a p21-failure response

We hypothesised that a p53–null sub-clone emerging from a previously p53-wildtype CLL would eventually result in a transition of category from a normal response to DNA damage, induced using etoposide, to a non-responder. During this transition, as the relative proportion of p53-null cells increases, it may be possible that a case could give a p21-failure response to DNA damage. This rationale was that the measured levels of p21 are lower than those for p53 in a typical normal responding CLL cell and that the recorded MFI values used to determine the percentage changes in protein are an average of several thousand measurements. As the background of null measurements increases the average p21 measurement would fall below its threshold of +15% before the p53 measurement falls below its threshold of 30%.

In order to test this, a non-responder CLL sample known to have loss of 17p detected in 68% of cells and a non-sense, 4 basepair insertion, within exon 5 of the remaining allele of *TP53*, was mixed with samples known to have normal functional status and no abnormalities of *TP53* or 17p. Normal cases were only selected if they were known to express lambda light-chains to allow discrimination from the non-responder sample, which was known to express kappa light chains.

The samples were cultured and prepared for FACS analysis separately according to the protocol in section 2.14 except for the addition of polyclonal, rabbit anti-human antibodies (Dako, Denamrk) specific to kappa (APC conjugated. Cat: C0222) or lambda (PE conjugated. Cat: R0437) light chains of the B-cell receptor. The PE conjugated antibody specific to the T-cell marker, CD2, was not used as kappa and lambda light chains are specific to B-cells. The samples were mixed in equal proportions immediately prior to data acquisition

A software gating strategy was used to select varying proportions of kappa/lambda (dysfunctional/functional) cells for analysis. It was possible to mimic a p21-failure result with varying proportions of non-responder cells and two examples of this are shown in Table 4-2.

Table 4-2: Results from two experiments mixing normal and non-responder CLL cells

	Percentage of non-responder cells added	Percentage increase in p53 protein	Percentage increase in p21protein	Functional category
Experiment 1	0	65	20	Normal
	3.7	49	9	p21-failure
	5	45	5	p21-failure
	10	31	2	p21-failure
	26	21	2	**Non-responder**
	30	17	0	**Non-responder**
Experiment 2	0	66	30	Normal
	14.5	39	19	Normal
	28	34	15	Normal
	27	43	7	p21-failure

Experiments were designed to investigate whether an emerging non-responder sub-clone can cause the p21-failure result. Non-responder cells were mixed with normal CLL cells which had no detectable abnormalities of *TP53*/17p

These preliminary experiments were not found to be always reproducible, even when selecting cells for repeat analyses from the same paired samples. It was decided that a less subjective analysis could be achieved by importing the raw data from a functional assay experiment into a spreadsheet where admixtures of cells from two datasets/samples could be created randomly, without bias and in any given proportions so that repeated random re-sampling could be performed.

4.5 *In*-silico dilution of p53-wildtype with p53-mutated CLL cells

CellQuest Pro™, reads and writes Flow Cytometry Standard (FCS) 2.0 binary data files which contain characters that cannot be read by programmes utilising the American Standard Code for Information Interchange (ASCII), including Excel. Conversion of FCS 2.0 files to an ASCII format was achieved using the downloadable third party software, FCSExtract Utility developed by Earl.F Glynn for the Stowers Institute of Medical research, USA (http://research.stowers-institute.org/efg/ScientificSoftware/Utility/FCSExtract/index.htm).

This technique allowed the selection of any previously analysed patient samples and did not require re-analysing samples using the functional assay or restriction of sample choice due to surface immunoglobulin light chain restriction.

FCS2.0 files were imported into FCSExtract utility and converted to ASCII format. This data was then exported to PASW™ statistics software package. The data corresponding to the forward and side light scatter results (P1 and P2 respectively) were plotted on a scatter-plot in order to generate an identical output to the forward / side scatter plot offered by the Cellquest software. This was used to determine the upper and lower values for P1 and P2 representing the 'live' cell fraction of the data for each patient sample used. The dataset for each patient was then cropped accordingly.

The paired P3 and P4 values from the remainder of the dataset, corresponding to FL1 (Fluorescein-isothiocyanate) and FL2 (Phycoerythrin), were then exported to Microsoft Excel™ software, these are the values corresponding to the labelled IgG2a control, anti-p53 or anti-p21 anti-bodies (FL1), and the CD2 antibody (FL2). CD2 Data was plotted as a histogram in order to determine the presence of CD2 positive cells (T-cells/NK-cells), which were then also excluded from the dataset.

In a representative *in-silico* mixing experiment one thousand data points were randomly selected from a p53 wildtype and a p53-dysfunctional dataset to produce a mixed dataset with 100, 75, 50, 25 and 0% dysfunctional cells. This

was replicated a total of ten times at each dilution. The mean of the ten replicates was then converted from channel values (0-1023) to linear 'MFI' values using the formula:

$$\text{Linear value} = 10^{(\text{Channel value}/256)}$$ (Cellquest Software Users Guide; p168)

This procedure was performed using the data from the control and etoposide treated culture conditions for both p53 and p21. The data was then used to generate a percentage change in linear value between the control and treated samples at each dilution point. The p53 and p21 results were then plotted on separate graphs using the percentage change in linear value on the Y-axis and the dilution along the X-axis. From these two graphs it was possible to determine the percentage of p53-null cells required to cross the cut-off values of 30% and 15% for p53 and p21 respectively.

Six samples were chosen for this analysis and four, separate, in-silico mixing experiments (a-d) were performed as described. The characteristics of the six cases (1-6) are shown in Table 4-3.

Table 4-3: Samples selected for in-silico mixing experiments

Sample	Etoposide induction of:		Function	17p13.1 FISH result	*TP53* mutation?
	p53	p21			
1	5%	3%	NR	94% Del 17p	2 basepair deletion
2	6%	0%	NR	68% Del 17p	4 basepair insertion
3	182%	100%	Norm	No loss	Wildtype
4	177%	78%	Norm	No loss	Wildtype
5	89%	36%	Norm	No loss	Wildtype
6	106%	25%	Norm	No loss	Wildtype

Two samples which failed to respond to etoposide treatment and were known to have bi-allelic inactivation of the *TP53* gene were selected. Four cases were selected which responded normally to etoposide treatment and had no detectable abnormalities of the *TP53* gene. NR= non-responder

Two samples which failed to respond to etoposide treatment and were known to have bi-allelic inactivation of the TP53 gene were selected. Four cases were selected which responded normally to etoposide treatment and had no detectable abnormalities of the TP53 gene. The results are shown in Figure 4-4 and Figure 4-5. It can be seen that a p21-failure response could result from

a p53 null clone emerging within a background of p53 wild type cells in experiments-a and -b (Figure 4-4). This contrasts with the other two examples shown in Figure 4 5. In experiment-c only a small p21-failure response range appeared before a Non-responder response was obtained. In experiment-d, no p21-failure response was seen and a normal response was maintained until approximately 85% of the data was from the p53 null sample. In this case the p53 wild type sample had particularly strong induction of both p53 and p21 protein. (Table 4-3. Sample 3). These experiments provide evidence to support the theory that the p21-failure response may be a transitional state between a normal functional response and a non-responder. This leads to the inference that p21-failure cases could be associated with the same acquired genetic abnormalities that are associated with non-responders.

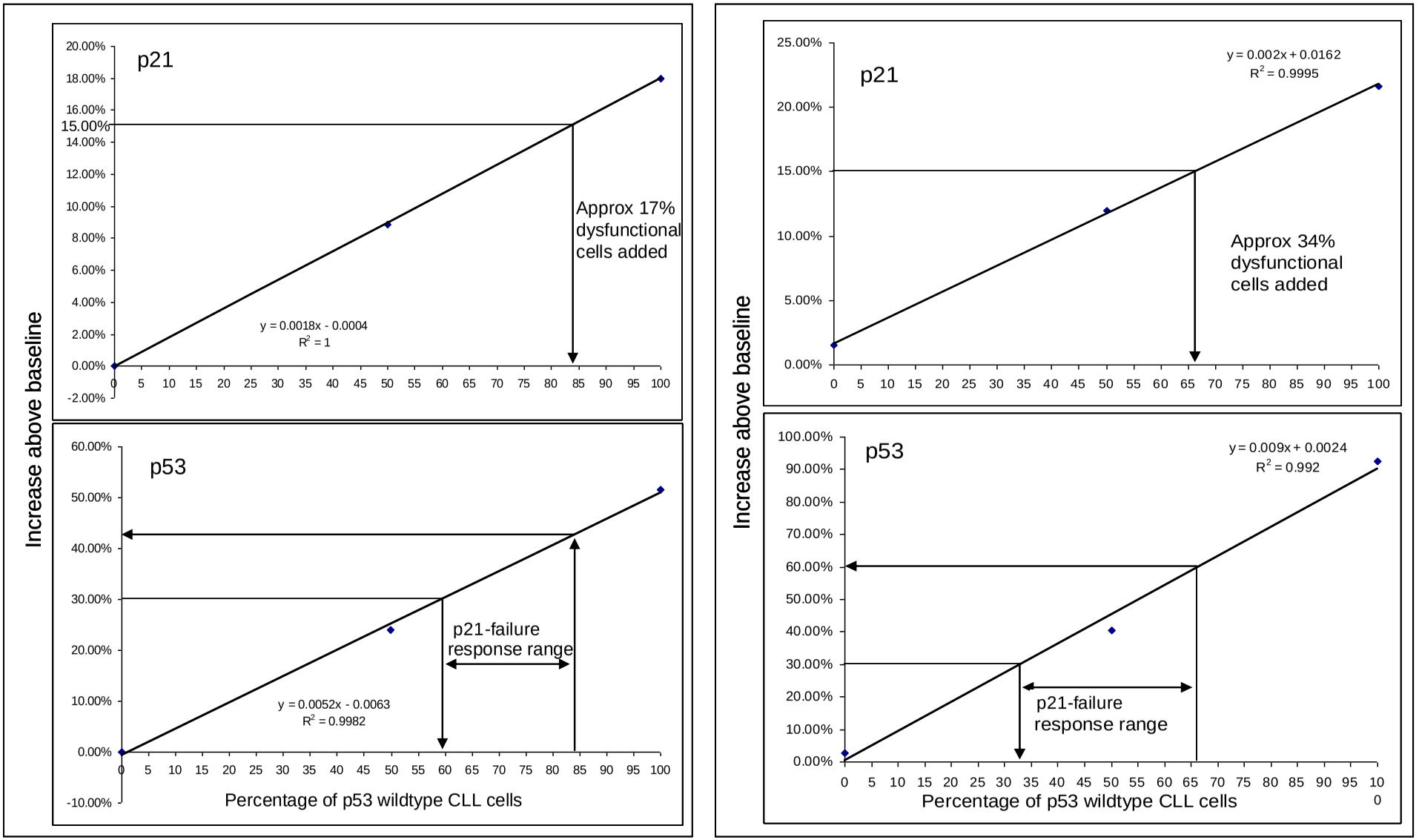

Figure 4-4: *In-silico* mixing experiments.

In these experiments the dilution of a normal functioning sample with data from a non-responder/p53-mutant case resulted in a clear p21-failure response. The percentage of non-responder cells required to reduce p21 below 15% is shown in the top panel. This result is then applied to the lower panel. The percentage of cells required to reduce p53 below 30% then delineates the range over which a p21-failure response would be observed. **Left:** Experiment-a using samples 2 & 4. **Right:** Experiment-b using samples 1 & 6

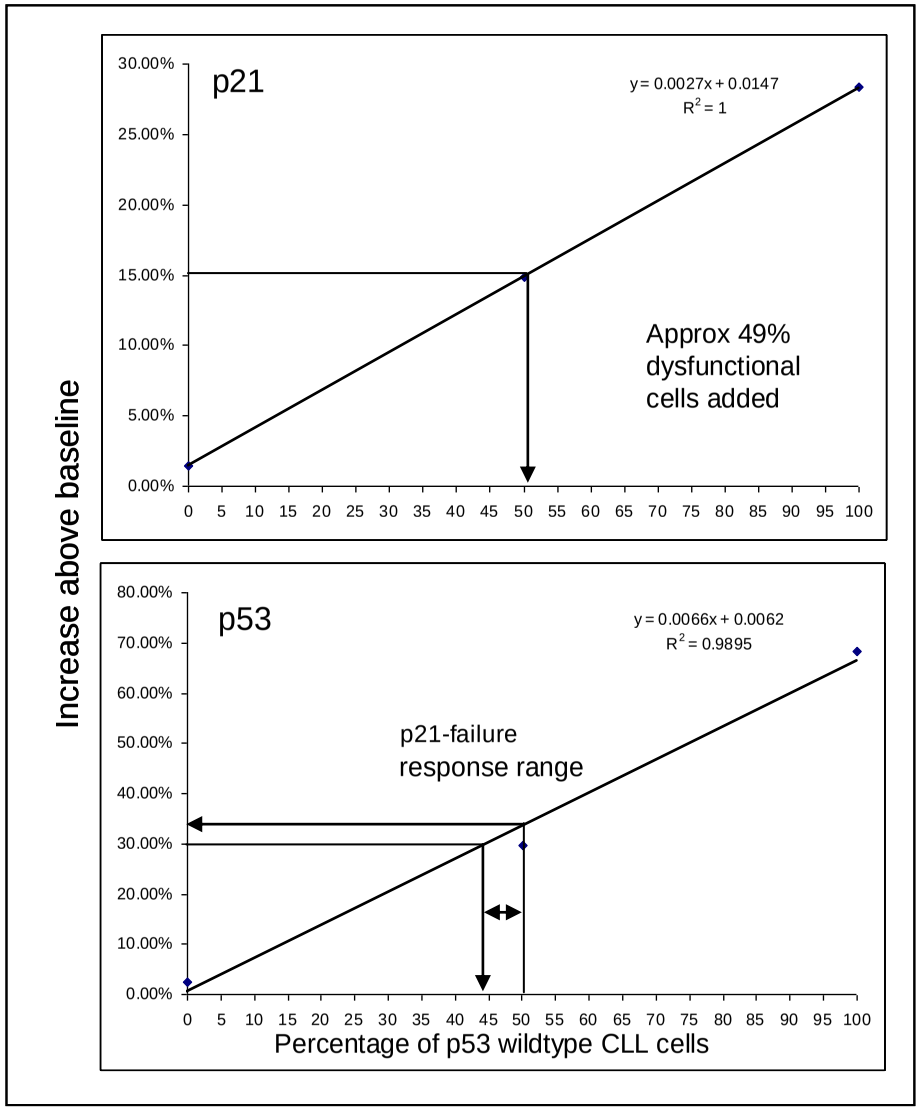

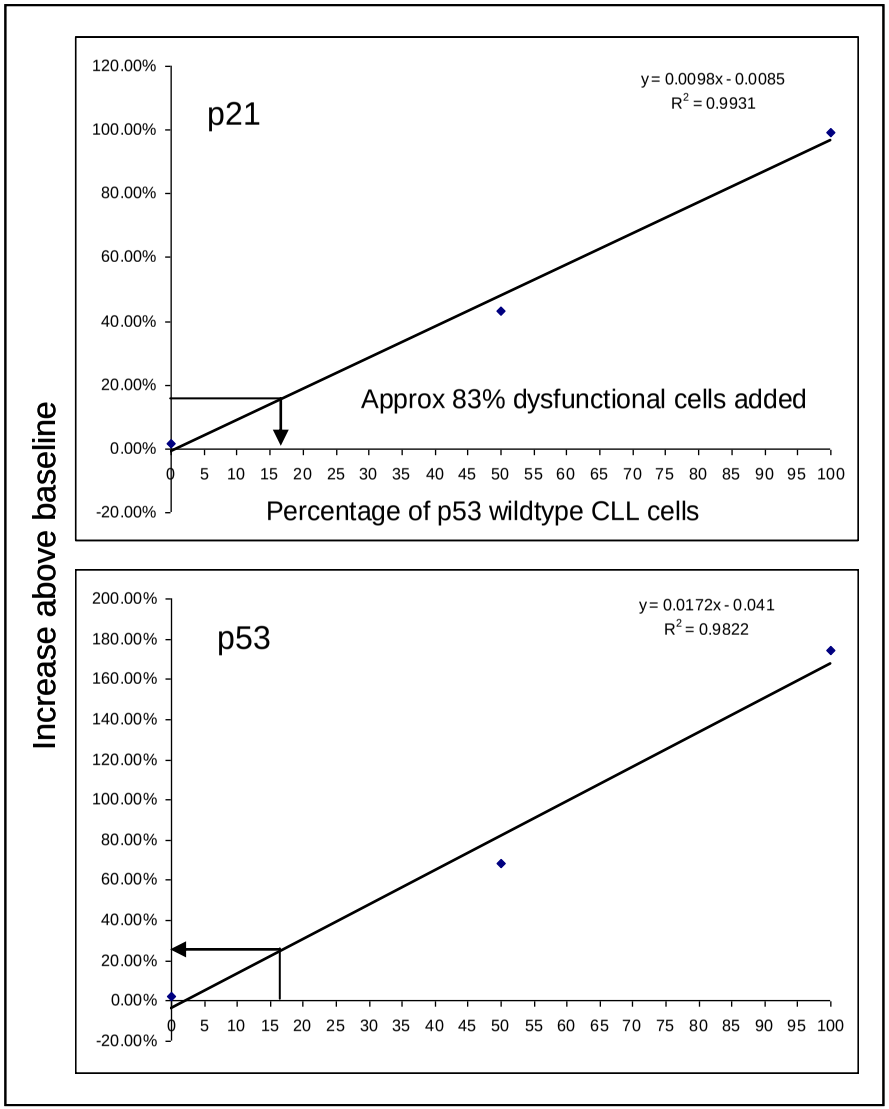

Figure 4-5: *In-silico* mixing experiments.

In these experiments the dilution of a normal functioning sample with data from a non-responder/p53-mutant case either resulted in **Left:** Experiment-c using samples 1 & 5. A small range over which a p21-failure phenotype would be observed or **Right:** Experiment-d using samples 1 & 3. No p21-failure response obtained.

4.6 The p21-failure samples are enriched for structural abnormalities of *TP53.*

Having shown that: (i) in this cohort the incidence of *CDKN1A* SNPs did not associate with p21-failure; and (ii) that an emerging p53-null clone could at least theoretically cause a p21-failure response; It was decided to test the incidence of both *TP53* mutation and deletion of 17p in the p21-failure group against their incidence within the normal responding group and within the other abnormal response cases using the same 180 samples which had been analysed for *CDKN1A* polymorphisms. The frequency of results is shown in Table 4-4. The incidence of *TP53* mutations in the p21-failure responders was significantly higher than in the normal responders (36% v 1.7%, $p < .0001$) but not the other abnormally responding cases (36% v 41%, $p = .7951$). Likewise, loss of the *TP53* gene locus was significantly enriched in the p21-failure cases when compared to the normal cases (52.2% v 6.9%, $p < .0001$) but not when compared to the remaining abnormally functioning cases (52.2% v 38.5%, $p = .4268$).

Table 4-4: Incidence of genetic abnormalities involving *TP53* in 180 selected CLL cases

Etoposide response	TP53 mutation n=180		Del 17p13.1 n=178	
	Yes	No	Yes	No
Normal	2	114	8	108
Abnormal	16	23	15	24
p21-failure	9	16	12	11
Total	27	153	35	143

Results of sequencing for mutations of *TP53* within exons 4-9 and fluorescent in-situ hybridisation analysis to detect loss of chromosomal locus 17p13.1.

This suggests that the p21-failure response is indeed associated with acquired genetic abnormalities rather than germline polymorphisms. Despite the significant involvement of *TP53* abnormalities, some individuals have no detectable loss of chromosome 17p or mutations of *TP53*. However, in light of the known adverse prognosis of *TP53* mutation and/ or deletion, a p21-failure

result should prompt investigation of *TP53* gene status. The existence of a subset of TP53 mutated CLL tumours which do not show high baseline p53 expression nor a completely abrogated p53 response indicates that p21 expression may be a more specific and sensitive readout of p53 function.

4.7 **Summary**

This section has shown that single nucleotide polymorphisms at codon-31 and in the 3'UTR of *CDKN1A,* previously found to be associated with a failure to express p21 in response to ionising radiation (Johnson et al., 2009), do not appear to be related to the analogous p21-failure response in this study. Therefore the null hypothesis for this section will be accepted: 'Cases displaying a p21-failure response to the assay do not associate with codon-31 and 3′UTR polymorphisms in the *CDKN1A* gene'.

Different methods were used to genotype cases. Firstly the same RFLP method employed by Johnson et al (2009) was used to determine the genotypes of both SNPs in 123 cases. This was followed by genotyping using Taqman™ technology, again for both SNPs of interest, in 180 cases. Pyrosequencing was used to further confirm the results of codon-31 polymorphism data. It was found that the two SNPs, codon-31 and 3'UTR, are linked, occurring together as a diplotype in all 180 cases tested. This was found to be in agreement with the majority of previously published studies involving these SNPs (Konishi et al. 2000; Mousses et al. 1995; Facher et al. 1997; Taghavi et al. 2010) and directly contradicted the findings of the Johnson paper (Johnson et al. 2009). A significant association between the p21-failure response and *TP53* abnormalities was observed and investigated. It was determined through experimental methods, and a novel computational method, that it is possible for an emerging non-responding / p53-null clone to cause the p21-failure response although this may vary from case to case. In addition this explanation does not account for all p21-failure cases within the cohort as *TP53* abnormalities were undetectable in a subset of cases.

Chapter Five:

Results

Analysis of *Hsa*-miR-34a expression can detect TP53 abnormalities but not *ATM*

5.1 **Overview**

The interest in mir34a analysis stems from its relationship with p53 and its role in the DNA damage response pathway (Zenz, Benner, et al. 2008). The finding that p53 mutation and deletion, either together or independently, affect the induction of this micro-RNA in response to DNA damage suggests that it could be an alternative indicator of p53 dysfunction in CLL (Zenz et al. 2009). Zenz *et al* also reported that a significant difference in baseline miR-34a expression could be detected in samples with or without *TP53* abnormalities. This marker could be of interest as it would reduce the time to perform the analysis as cell samples would not require culturing or treating with drugs or ionising radiation.

The micro-RNA, *hsa*-miR-34a, is under the direct transcriptional control of the p53 protein (Chang et al. 2007). It has been shown that the cellular concentration of this non-coding RNA is increased in response to cellular stresses including double stranded DNA damage. A constitutive level of *hsa*-miR-34a in a resting cell is also maintained through continuous transcription by p53 (Zenz *et al*, 2009). It therefore follows that, in response to double stranded DNA damage, the status of the ATM gene also has an effect on miR-34a expression due to its role in p53 signalling (Hermeking 2010). It is unknown at this time whether abnormalities of the *ATM* gene have any impact upon the basal level of miR-34a expression.

5.2 **Hypothesis**

The hypothesis for this chapter is as follows:

Hypothesis:

Basal miR-34a expression is an indicator of ATM and p53 function in CLL.

Null hypothesis:

Basal miR-34a expression is not an indicator of ATM and p53 function in CLL.

5.3 Selection of reference micro-RNA and standard RNA source

The relative quantification of expression requires standard curves to be generated for both the target and reference genes and both need to be derived from an RNA source (cell line) which ideally will express both target and reference genes at higher levels than the test samples. In addition the selected reference gene should be expressed at a similar level to the target gene in the test samples and the cell line to be used as a reference. Previous studies of *hsa*-miR-34a levels in CLL have used small nuclear RNA U6 as the reference gene for normalisation (Zenz *et al*, 2009). In a separate study, colleagues within our research group examined the uniformity of expression levels of a panel of micro-RNAs and small nuclear RNAs in CLL patient samples. The results of this work showed that within the candidates tested, the small nuclear RNA U6 did not have the most stable expression across the CLL samples tested. The results did highlight two potential candidate genes that were more stably expressed in CLL, *hsa*-miR-30d and RNU-43.

To select a source of RNA for generating the standard curves and to determine which of the previously identified stable reference genes was most appropriate, two CLL patient samples and 13 cancer cell lines were screened in single reactions using for each mircro-RNA of interest. The p53 status of cell lines was checked against the literature (Berglind et al. 2008). Amplifications of *hsa*-miR-34a, *hsa*-miR-30d and RNU-43 were performed on each of the 15 samples and the crossing points (CP) values were then used to compare the relative expression levels of target and reference genes across the samples and cell lines tested. The results are shown in Table 5-1 (p123).

Table 5-1: Crossing point values (CP) for thirteen cell lines and two patient samples showing the p53 status.

		miR-34a	miR-30d	RNU43
Patient	**p53 status**	**CP**	**CP**	**CP**
LRF 74	Mutant	33.2	26.32	27.15
LRF 81	Wildtype	31.1	27.61	27.16
Cell Line	**p53 status**	**CP**	**CP**	**CP**
HBL-2	Wildtype	36.82	30.82	28.9
HCT-116	Wildtype	27.99	27.63	28.38
JVM3	Wildtype	37.06	36.53	34.14
LS174T	Wildtype	26.85	26.6	27.72
Lovo	Wildtype	27.3	27.34	28.16
M901	Wildtype	37.36	28.19	28.81
MCF7	Wildtype	26.67	25.59	28.36
MDA-MB-231	Mutant	31.17	27.88	29.79
Raji	Mutant	35.78	27.24	27.13
T47D	Mutant	26.95	27.47	29.45
VLD-1	Wildtype	28.24	28.4	28.88
WiDR	Mutant	27.81	24.25	28.71
ZR-75-01	Wildtype	26.65	26.1	28.74

CP values are inversely related to the concentration of the sample. LRF 81 has no detected *TP53* abnormalities. LRF 74 has biallelic inactivation of *TP53*.

The two patient samples (LRF 74 and LRF 81) were selected to represent the expected high and low extremes of mir34a expression in the cohort to be analysed. Case LRF 81 had no detected abnormalities of *ATM* or *TP53* and was found to have a normal p53/p21 response to DNA damage induced by etoposide. In contrast, LRF 74 was found to have biallelic inactivation of *TP53,* confirmed by cloning and sequencing, and it was known to not upregulate p53 or p21 in response to DNA damage. Figure 5-1, Figure 5-2 and Figure 5-3 reproduce the results shown in Table 5-1 for each of the measured microRNAs. The cell lines and CLL samples are arranged, left to right, on the x-axis in order of increasing CP value, which can be interpreted as decreasing concentration.

Five of the thirteen cell lines gave miR-34a CP values higher than the lowest of the two CLL samples, indicating lower expression (Figure 5-1) and so would be unsuitable for generating a standard curve as the highest concentration possible would be lower than that expected of the CLL samples, these were: HBL-2, JVM-3, M901, MDA-MB-231 and Raji.

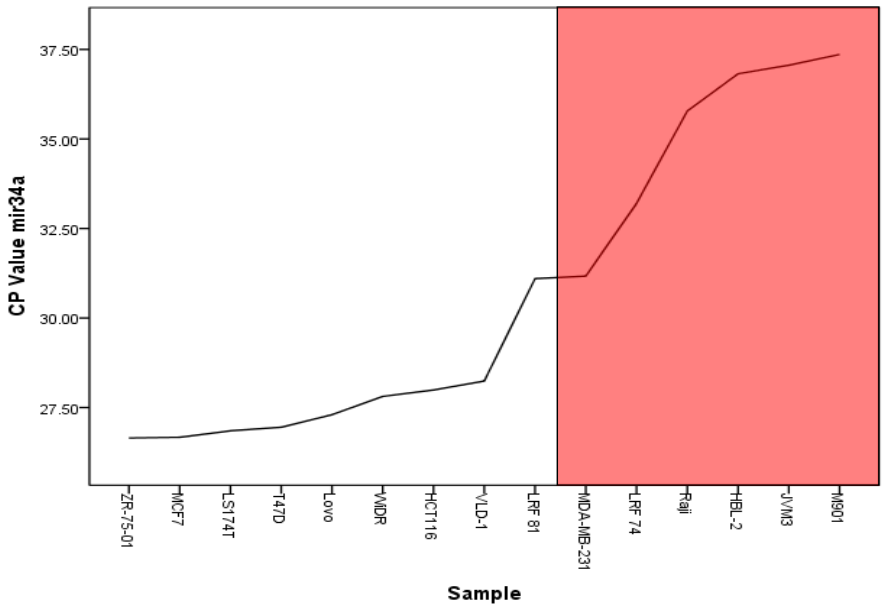

Figure 5-1: MiR-34a CP values for 13 cell lines and 2 samples arranged in ascending order.
Cell lines and CLL samples are arranged in order of ascending CP value (descending concentration). Five cell lines (HBL-2, JVM-3, M901, MDA-MB-231 and Raji) were rejected for having lower concentration of the target, mir34a, than the CLL samples.

Of the eight remaining cell lines, none had CP values for RNU-43 lower than the two CLL samples. It was decided that RNU-43 could therefore not be used for the reference gene standard curve, as the CLL samples would potentially have higher RNU-43 expression than the highest concentration possible available in any of these cell lines (Figure 5-2).

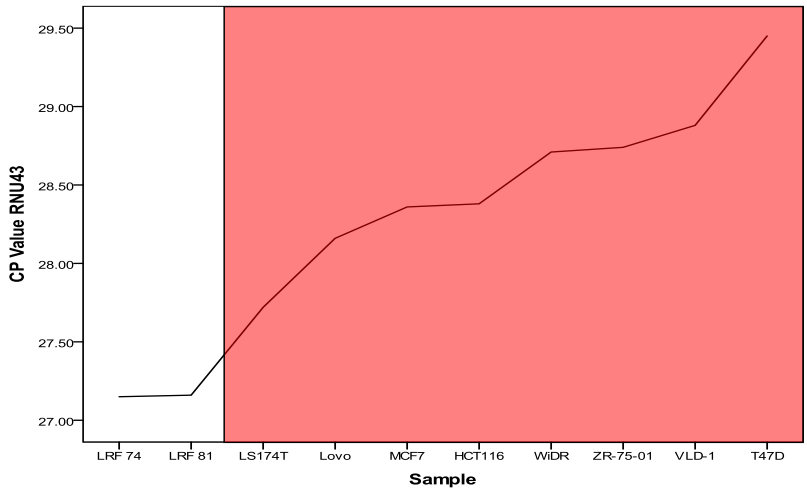

Figure 5-2: RNU43 CP values for 13 cell lines and 2 samples arranged in ascending order.
Cell lines and CLL samples are arranged in order of ascending CP value (descending concentration). RNU43 was not expressed at a sufficiently concentration in any cell line for it to be used for standard curve.

Three cell lines, ZR-75-01, MCF-7 and WiDR, had both lower miR-30d and miR-34a CP values, and therefore higher expression, than the CLL samples and so would be suitable for generating standard curves. The CP value for miR-30d in cell line, ZR-75-01, was only slightly lower than the lowest CLL sample, LRF-74, and was therefore removed in preference of either MCF-7 or WiDR (Figure 5-3),.

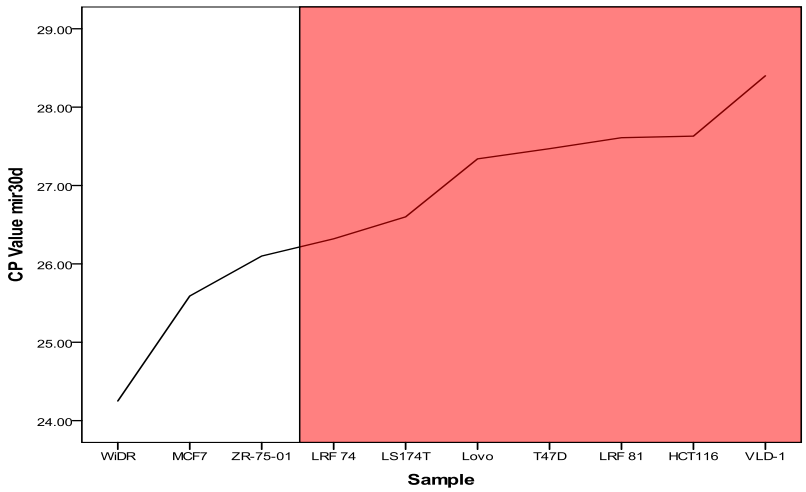

Figure 5-3: MiR-30d CP values for 13 cell lines and 2 samples arranged in ascending order.
Cell lines and CLL samples are arranged in order of ascending CP value (descending concentration). Three cell lines had higher concentration of mir-30d than both CLL samples (ZR-75-01, MCF-7, WiDR).

The decision to use MCF-7 cell line was made on the basis that the miR-34a and mir-30d CP values for MCF-7 were comparable to each other (less than a 2-fold difference), whereas for WiDR, there was a CP difference of 3.56 between the miR-34a and miR-30d results, suggesting that miR-30d has approximately 8-fold higher expression than miR-34a in that cell line.

5.4 Generation of external standard curves for target and reference genes.

To maximise the number of samples that could be run in triplicate on each 96-well plate and hence reduce cost, external standard curves were generated for application to subsequent experiments. A seven step, two-fold dilution series of MCF-7 RNA was used to generate standard curves for the target and reference genes, giving a 64-fold range of concentration. Each standard curve was generated in quadruplet reactions. The results for miR-34a are shown in Figure 5-4 and Table 5-2. The results for miR-30d are shown in Figure 5-5 (p127) and Table 5-3 (p127).

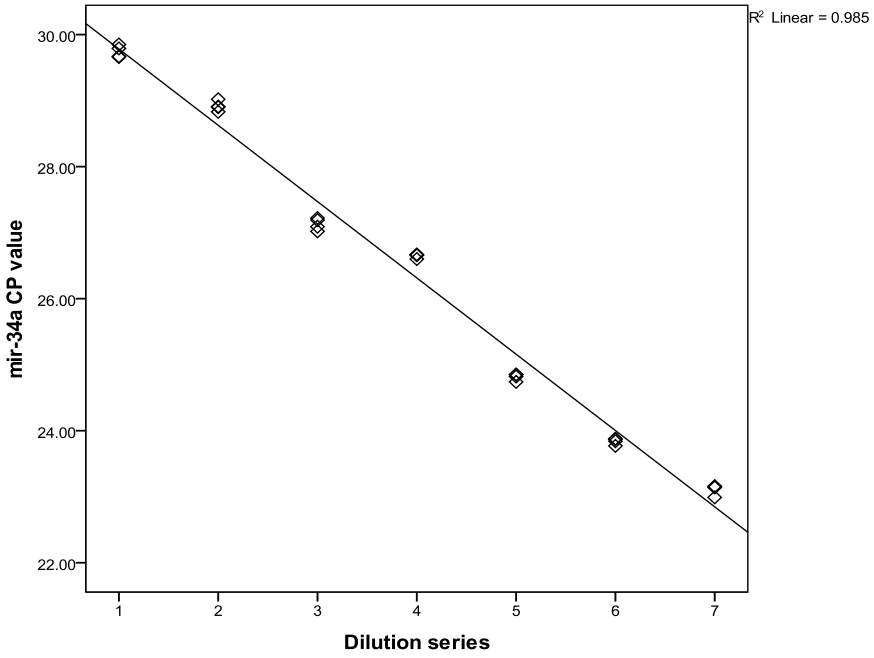

Figure 5-4: miR-34a external standard curve. Seven step, two-fold dilution series assayed in quadruplet. An error of 0.0266 and PCR efficiency of 1.797 was recorded for this curve.

Table 5-2: Showing the CP values for miR-34a standard curve. The mean CP value of the four replicates and the standard deviation are also shown.

mir34a	Replicate No					
Percentage	CP 1	CP 2	CP 3	CP 4	mean	Std.Dev
100	22.99	23.15	23.16	23.14	23.11	0.080
50	23.88	23.77	23.87	23.84	23.84	0.050
25	24.82	24.74	24.85	24.85	24.82	0.052
12.5	26.66	26.6	26.67	26.66	26.65	0.032
6.25	27.09	27.02	27.19	27.22	27.13	0.092
3.125	28.83	28.91	28.9	29.02	28.92	0.079
1.562	29.66	29.67	29.79	29.85	29.74	0.093

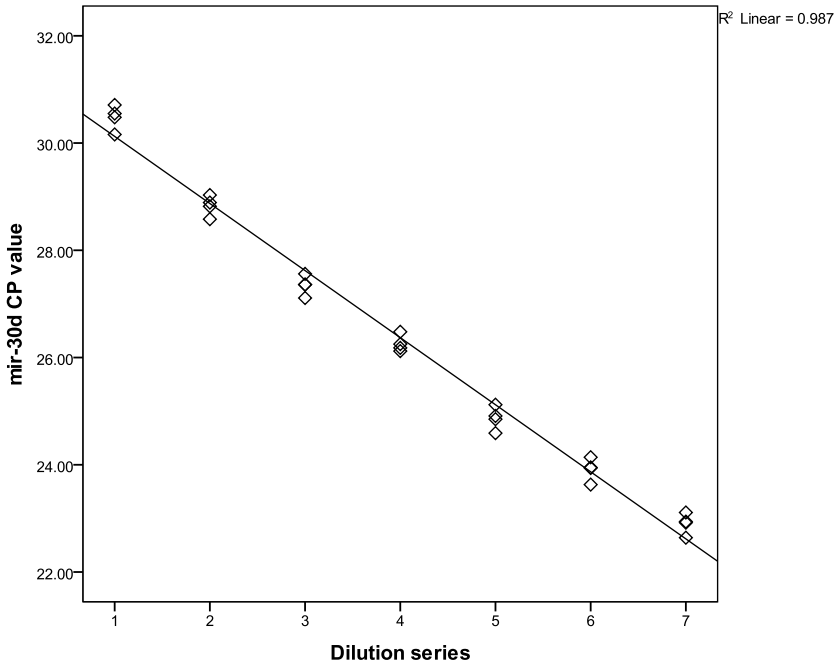

Figure 5-5: miR-30d external standard curve. Seven step, two-fold dilution series assayed in quadruplet. An error of 0.00574 and PCR efficiency of 1.979 was recorded for this curve.

Table 5-3: Showing the CP values for miR-30d standard curve. The mean CP value of the four replicates and the standard deviation are also shown.

mir30d						
Percentage	**CP 1**	**CP 2**	**CP 3**	**CP 4**	**mean**	**Std.Dev**
100	22.64	22.94	22.92	23.11	22.90	0.195
50	23.63	23.94	23.95	24.14	23.92	0.211
25	24.59	24.85	24.91	25.12	24.87	0.218
12.5	26.12	26.25	26.18	26.48	26.26	0.158
6.25	27.11	27.36	27.36	27.56	27.35	0.184
3.125	28.58	28.82	28.89	29.03	28.83	0.188
1.562	30.16	30.48	30.55	30.71	30.48	0.231

The standard deviation from the mean of the mir-34a replicates was less than 1% of the mean CP at each dilution. The standard deviation of the mir-30d replicates was higher than the miR-34a but was also less than 1% of the mean CP. Both of these results confirm that any variation between the replicates, for instance due to pipetting errors, was minimal. The efficiency computed for the miR-34a and mir-30d reactions were 1.797 and 1.979 respectively. Efficiencies of approximately 1.8 are considered acceptable for relative quantification and both results satisfy this requirement with the latter being quite close to the theoretical maximum of 2.0. The error associated with

the standard curves was 0.0266 and 0.00574 for mir-34a and mir-30d respectively, which are both lower than the value of 0.2 which is given as the maximum acceptable error in the Roche LC480 handbook. These results showed the standard curves that were generated were acceptable for use in the subsequent relative quantification experiments. Aliquots of MCF-7 RNA at the 50%, 12.5% and 3.125% concentrations were stored at -70^{o}C for use as calibrators in all test experiments. This methodology allows for mir-34a/mir-30d analysis of 12 test samples to be run in triplicate on each 96-well Taqman™ reaction.

5.5 Concordance of measured levels of miR-34a DMSO stored samples and RNAlater stored samples.

In order to determine whether PBMC samples only available as FCS/10%DMSO frozen (-70^{o}C) aliquots could be used, a selection of nine LRF samples were chosen to test for concordance of mir-34a results between matched cryopreserved cells and cells stored in RNAlater™. The samples were selected to represent different *TP53*/*ATM* genotypes and therefore expected to have a range of miR-34a expression, with sample aliquots in both storage conditions derived from the same whole blood specimen. After extraction of RNA from both storage media samples were assayed in parallel, with all reverse transcription reactions and amplifications carried out in the same run. The results are shown in Table 5-4.

Table 5-4: Showing mir34a relative expression results for nine cases stored in either RNAlater™ or frozen at -70^{o}C.

	mir34a		FISH		
Sample	RNAlater	Frozen (-70C)	11q clone (%)	17p clone (%)	p53 mutation
LRF 79	19.85	15.40	93	0	0
LRF 75	21.24	22.93	90	7	0
LRF 73	25.24	25.32	0	0	0
LRF 217	2.84	2.20	92	0	unk
LRF 142	43.18	60.55	0	0	0
LRF 130	0.13	0.14	0	96	0
LRF 127	13.59	10.16	0	25	1
LRF 116	4.74	1.46	97	0	0
LRF 112	4.48	3.27	0	0	0

FISH data is shown as percentage of cells examined showing loss of signal (clone size). Mutation data is shown as binary: 1=Mutated 0=No mutation.

The samples showed a significant correlation between RNAlater™ preserved cells and those stored in FCS/10%DMSO (-70^{o}C) (r= .973, p< .001, R^2= .947). These results, also shown in Figure 5-6, show that samples which are only available as FCS/10%DMSO (-70^{o}C) stored cells could be included in the series in order to better understand the effects of *ATM* and *TP53* gene abnormalities on basal miR-34a expression.

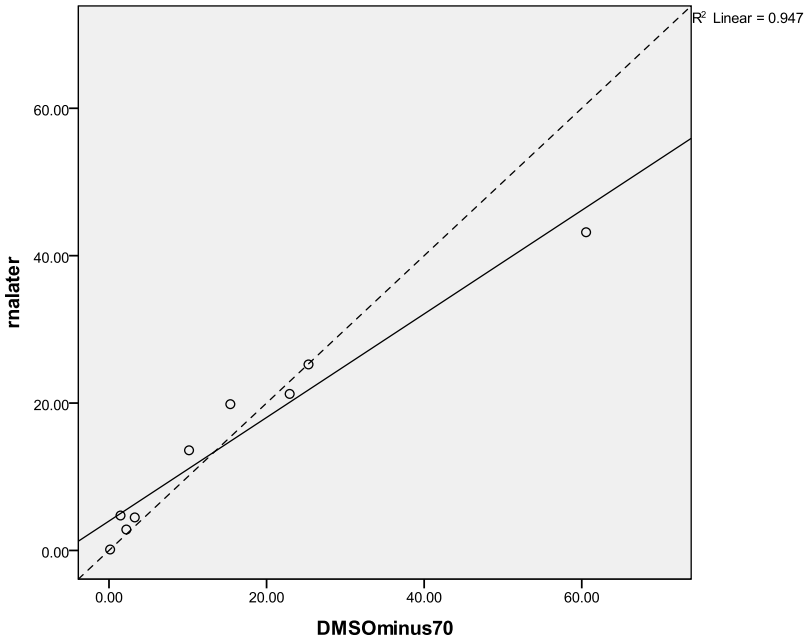

Figure 5-6: Showing the correlation of mir34a relative expression results for 9 matched samples stored in either RNAlater™ or cryopreserved at -70^{O}C.
Concordance of mir-34a expression in matched samples from the same case that were stored in both RNAlater and FCS/10%DMSO at -70^{o}C. These results show that DMSO frozen CLL samples could be used as surrogates in the absence of RNAlater stored samples.

On the basis of this result it was decided to enrich the cohort with samples from the CLLIV trial for which the FISH and mutation status of *ATM* and *TP53* were known. The reason was to increase the number of samples with known biallelic inactivation of *ATM* and *TP53* so that their relative effects upon basal mir-34a expression could be analysed. For further assurance that the CLLIV cell samples would give analogous results to the local and LRF samples the distribution of mir34a results in the ATM and TP53 wildtype genogroup (n-=80) was compared across the three sets of samples and was not found to be significantly different (K=1.277, p= .528). This was also the case for the samples with *ATM* gene involvement of any form (n=36, K=2.701, p= .259) or

TP53 gene involvement (n=51, *K*=5.471, *p*= .065). The mir34a results ranged widely with a 100,000-fold range (0.007-216) across the 166 samples tested. The 5% trimmed mean was 11.56 (SD=22.8) and the median was 9.02. The data were not normally distributed.

5.6 Description of cohort, markers and mir-34a units

Analysis of basal expression of mir-34a was performed on 166 samples representing 161 CLL patients, 5 of which had a subsequent sample from a later time-point tested. These samples were selected to represent as many sub-groups of interest as possible and they are not intended to represent a specific clinical cohort of CLL patients. The sample selection was enriched for cases with mono and bi-allelic abnormalities of *ATM* and *TP53*, samples which show dysfunction but do not have these poor prognosis markers, and samples with forms of dysfunction for which the mechanism responsible is in dispute (Type–C/p21failure).

The aims of using this group are to determine whether the measurement of basal mir-34a is a reliable indicator of *TP53* abnormalities, whether it can detect *ATM* abnormalities (both mono and bi-allelic) and also how it relates to the categorisation of samples using the etoposide/nutlin assay.

5.7 Mir-34a expression results

Of 161 individuals tested, 114 had FISH and mutation screening results for both *ATM* and *TP53*. Figure 5-7 (p131) shows the results of mir-34a analysis for these 114 cases split broadly into those with no involvement of either *ATM* or *TP53* (n=55), *ATM* gene involvement (n=28) or *TP53* involvement (n=31). The data for each of these groups was not normally distributed so they were analysed using non-parametric methods. The results, summarised in Table 5-5 (p131), show that despite differences in both the means and medians between the groups there is considerable overlap in the range of data. The comparison of median mir-34a results between each of the three groups (Figure 5-7 ,p131) suggests that abnormalities of *TP53* (median mir34a=1.30) sufficiently alter mir-34a levels to make them discernible from

cases with no abnormalities detected (median mir34a=14.80, *z*=-5.356, *p*< .001) and cases with abnormalities of the *ATM* gene (median mir34a=11.41, *z*=-4.516, *p*<.001).

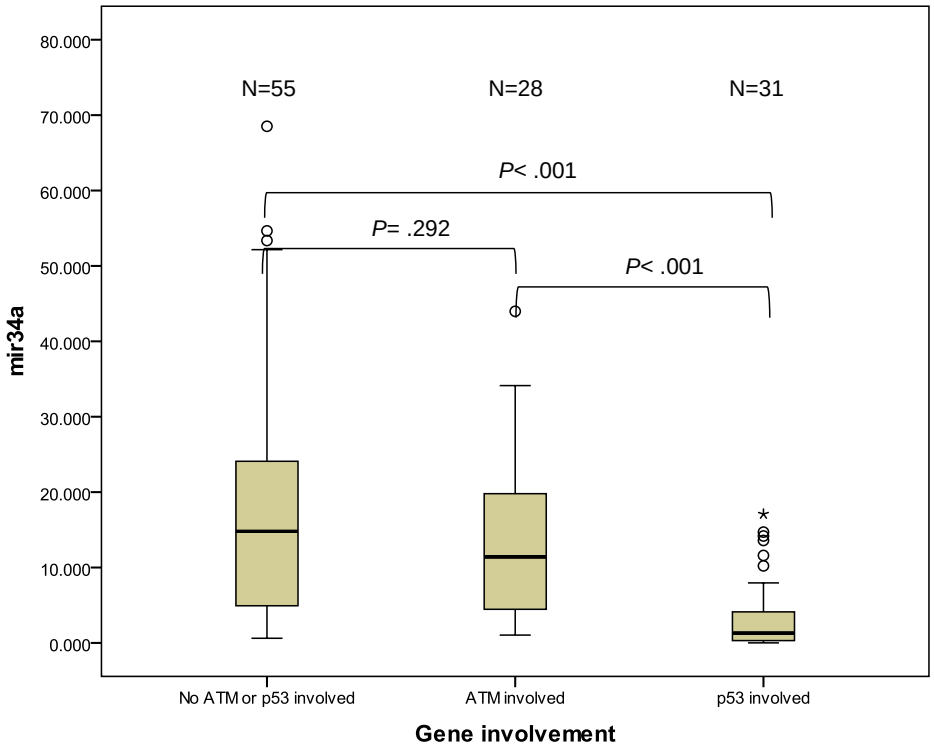

Figure 5-7: Results of mir-34a analysis showing the three main genotypic groups (n=114).
These results show that there is a significant difference in the mean mir-34a result for each of the three group comparisons. The median mir-34a result for the group with involvement of *TP53* was significantly different to the group with no detected abnormalities and the group with abnormalities of the *ATM* gene. The difference between the *ATM* involved group and those samples with no abnormalities was not found to be significant.

Table 5-5: Summary of mir-34a relative expression results (n=114).

	N	Mean	Median	Std. Deviation	Minimum	Maximum
ATM & p53 Wildtype	55	20.29	14.80	22.59	.616	133.200
ATM involved	28	13.22	11.41	10.46	1.040	43.980
p53 involved	31	3.81	1.30	5.21	.007	17.090

Mir-34a results for 114 cases with full FISH and mutation screening for *ATM* and *TP53*. Although the mean mir-34a results for each genotypic group were different between groups it can also be seen that there is considerable overlap between the groups. This suggests that a cut-off value for p53 related mir-34a under-expression may be difficult to determine.

With regards the lower average mir-34a result for *ATM* involved cases compared to those with no detected abnormalities, the lack of a significant

difference in median (z=-1.055, p= .296) suggests that the difference is not sufficient to reliably separate the two genotypes although it is of note that the mean and median for those cases is intermediate to the no abnormality and *TP53* involved groups. The *ATM* and *TP53* involved group were analysed in more detail in order to determine whether different combinations of poor risk markers affected mir-34a expression differently.

5.8 *Hsa*-Mir-34a levels in samples with *ATM* abnormalities

It has been shown in recent analysis of the UKCLL4 trial cohort that there is a difference in outcome between cases with mono or biallelic *ATM* abnormalities (Skowronska et al. 2012). Therefore the 30 cases with *ATM* gene defects were subdivided into those with mono-allelic deletion detected by FISH (n=11), mono-allelic mutation (n=6) and biallelic inactivation (n=13). The results are displayed in Figure 5-8.

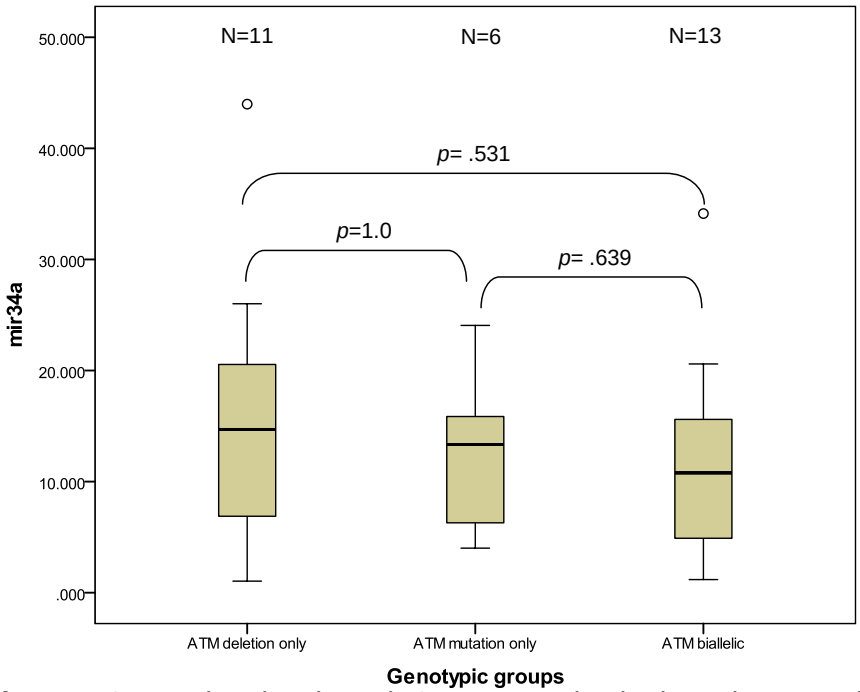

Figure 5-8: Boxplot showing mir-34a expression in the sub-categories of ATM abnormality (n=30)
The median value of mir-34a in samples with bi-allelic inactivation of *ATM* was not significantly different to those with either monoallelic deletion or mutation. There was also no difference detected between cases with either type of mono-allelic abnormality.

It can be seen that there was no significant difference in the expression of mir-34a regardless of the type of *ATM* abnormality. All of the cases with mono-allelic mutation had non-truncating mutations but the cases with bi-allelic inactivation could be split into those with deletion of *ATM* accompanied by non-truncating (n=9) and truncating (n=4) mutations. None of the differences between any of these genotypic groups was significant although very low numbers may be responsible for this (Figure 5-9).

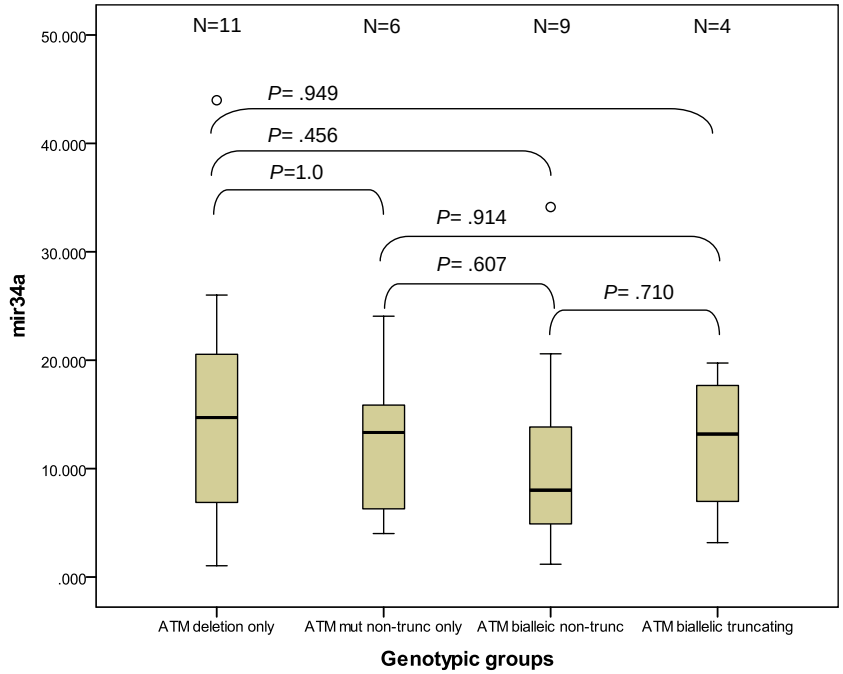

Figure 5-9: Mir-34a results for samples with ATM abnormalities subdivided to show the effects of truncating and non-truncating mutations (n=30)

Due to low numbers the lack of significance may not be due to an absence of effect but the figure would suggest that different combinations of *ATM* abnormality cannot be differentiated by the baseline level of mir-34 and therefore that *ATM* abnormalities do not affect the basal transcription of mir-34a.

The results of this section show that the mir-34a levels in cases with involvement of the *ATM* gene are not significantly lower than those cases with no involvement of *ATM* or *TP53* (detected by FISH or mutation screening) and the broad overlap of results means that they cannot be easily differentiated from one another. The analysis of median mir-34a levels in the different genotypic sub-groups of ATM abnormality suggests that the differing effects of truncating/ non-truncating mutations and mono-/ bi-allelic inactivation seen in the UKCLL4 cohort may relate specifically to the response to therapy and that

these abnormalities have little distinguishable effects on the basal expression of mir-34a. In contrast, *TP53* has previously been shown to impact upon the basal expression of mir-34a (Zenz et al. 2009) and so it was decided to confirm this previous finding within the cohort and test how the results of the functional assay relate to this.

5.9 *Hsa*-mir-34a levels in samples with *TP53* abnormalities

Of the 114 samples with full FISH and mutation screening of both *ATM* and *TP53*, thirty-three were found to harbour some abnormality of *TP53* and this was shown, in section 5.7 (p130), to associate with lower levels of mir-34a than those found in those cases with no abnormalities or with *ATM* abnormalities. Subdivision of these 30 samples according to the combinations of gene defects is shown in Figure 5-10 (p136). The majority of cases displayed biallelic inactivation of *TP53* (22/30; 72%) which in all except one case consisted of deletion of one allele detected by FISH and mutation of the second. The single exception to this was determined to have bi-allelic mutation of *TP53,* confirmed by cloning and sequencing of genomic DNA (one missense mutation on one allele and a 10bp deletion on the second allele). Mono-allelic deletion accounted for 18% of cases (5/30) and mono-allelic mutation 10% (3/30). No statistically significant difference was found between the three genotypes but this may be due to the lack of numbers in the different groups. The descriptive data for these sub-groups is shown in Table 5-6. Cases with mono-allelic deletion of *TP53* do not have the very low levels of mir-34a that appear to be evident in the cases involving a mutation of *TP53*. This suggests that one wildtype allele of *TP53* may be sufficient to maintain the basal level of mir-34a. Of the three cases with mono-allelic mutation of *TP53,* sequence data was available on two and this demonstrated that one case had loss of heterozygosity (LOH) resulting in no wildtype *TP53* being present whilst the other had equal proportions of mutant and wildtype DNA, indicating that the entire CLL clone was mutated.

Table 5-6: Descriptive mir-34a relative expression data for 30 cases with abnormalities of TP53

Genotypic group	N	Mean	Median	Minimum	Maximum
p53 deletion only	5	9.27	7.96	.007	19.880
p53 mutation only	3	1.43	0.54	.222	3.530
p53 biallelic	22	3.68	0.95	.126	17.090

Summary showing the mean, median and range of mir-34a results obtained for sub-groups with abnormalities of *TP53*. Despite the low numbers in the groups with mono-allelic abnormalities there is a suggestion that cases that do not involve a mutation of *TP53* have higher mir-34a expression.

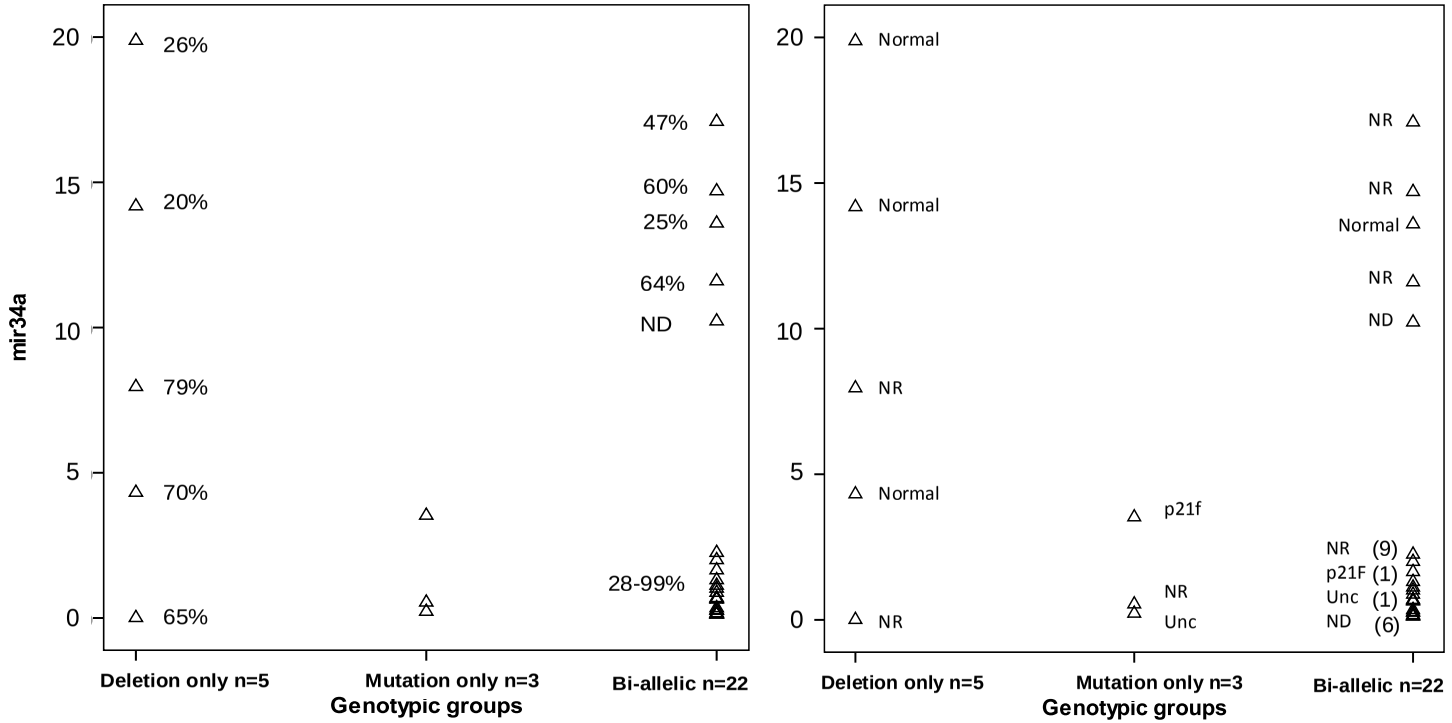

Figure 5-10: Mir-34a relative expression results for cases with *TP53* gene abnormalities, grouped according to genotypes (n=30).

Left: Labels show the percentage of cells with loss of *TP53* as detected using FISH. It can be seen that cases with lower deleted clones sizes have a higher expression of mir-34a and that even in those cases with no detected mutation of *TP53,* loss alone can reduce the expression to levels comparable to those with mutation. The majority of cases with bi-allelic abnormalities of *TP53* (17/22; 77%) had very low mir-34a expression. The remaining 23% (5/22) of cases with bi-allelic involvement showed mir-34a expression >10u despite large clone sizes. **Right**: Labels show the functional category of the samples. Functional analysis had been performed on 28/30 cases (the two cases without this data were from the UKCLL4 cohort and viable PBMCs were not available for analysis). Some form of dysfunction was detected in all except one of the cases with a known mutation of *TP53* 22/23 (96%). Of the five cases with deletion only, dysfunction was only detected in two cases (40%). ND=no data; NR= non-responder; p21f= p21 failure; Unc=Unclassified.

In order to detect any effect of dosage, the clone sizes of the 20/30 cases with loss of *TP53* detected by FISH for which the percentage of cells with loss was known were plotted against their matched mir-34a results (Figure 5-11).

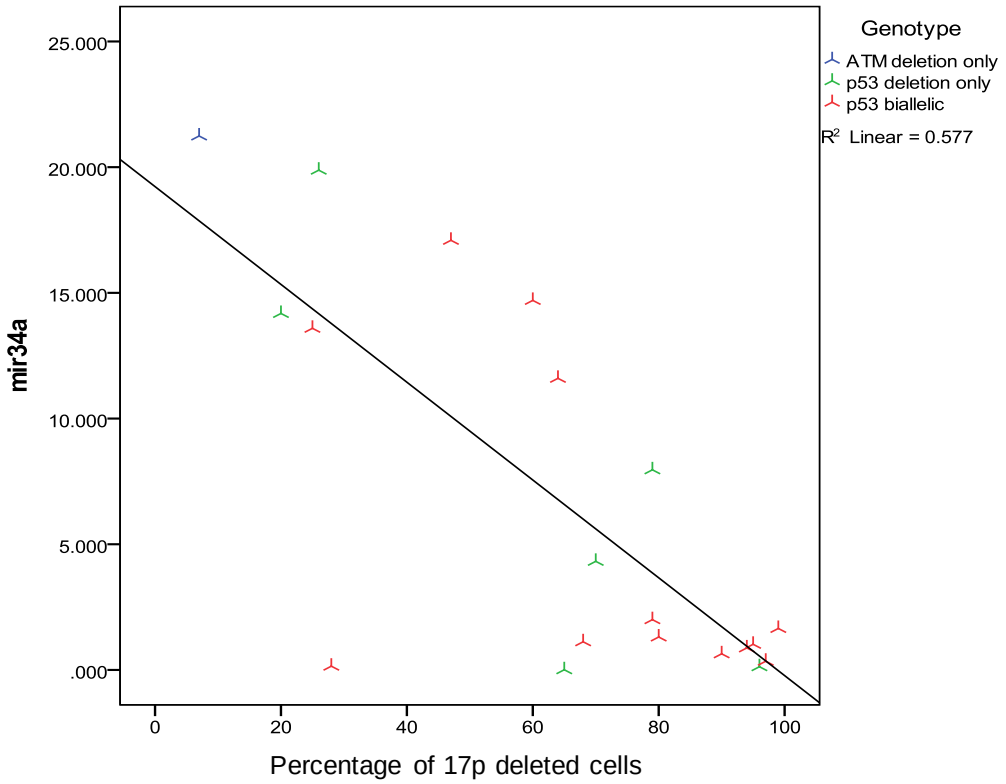

Figure 5-11:Scatter plot showing the matched mir-34a and Del(17)p FISH clone size data for 20 cases with involvement of TP53.
The case labelled as ATM deletion-only had 90% loss of the *ATM* locus determined by FISH but also had a very small clone (7%) which appeared to have deletion of the *TP53* locus. Pearson analysis found a significant negative correlation between the two variables (r[20]= -.760, p< .001).

The results show that there is a clear trend for the cases with highest proportion of 17p-deleted cells to have the lowest mir-34a levels. These two variables were found to significantly correlate with each other (r[20]= -.760, p< .001).

It can however be seen that some samples do not follow the trend. For example two bi-allelic cases are evident that have approximately equal FISH clone sizes (25 v 28%) but disparate mir-34a results (13.559 v 0.149). Relevant information on these two cases is shown in Table 5-7 and electropherogram images of the detected *TP53* mutations are shown in Figure 5-12.

Table 5-7: Details of two cases with similar bi-allelic TP53 inactivation and differing levels of mir34a.

				Promoter activity (% of W/T)*		Increase over baseline in response to Etoposide	
Case No	**Mir-34a**	**17p Clone**	**TP53 mut**	**MDM2**	**Waf1**	**p53**	**p21**
127	13.559	25%	S241Y	0	10.8	349	21
108	0.149	28%	M237I	11.5	0.7	0	0

It can be seen that there are differences in terms of the mutation identified, response to etoposide treatment, and published residual activity of the identified mutations towards both the *CDKN1A* (p21/Waf1) and *MDM2* promoters which was obtained from the IARC TP53 mutation database. This suggests that the nature and location of the mutation has an effect upon the differing levels of basal mir-34a transcription with some being similar to wildtype.

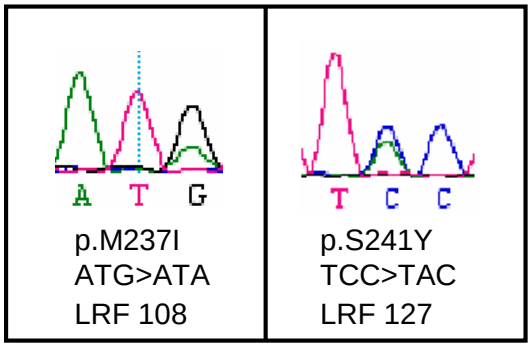

Figure 5-12: Electropherograms of two cases with similar bi-allelic TP53 inactivation and differing levels of mir34a.

The overlapping distribution of the results for both the 'wildtype' and *TP53* involved groups is shown in Figure 5-13 as a pyramid diagram, where it can be seen that setting a cut-off value for mir-34a expression to detect a majority of *TP53* abnormalities will likely include a substantial number of the 'wildtype' cases. This shows that in the majority of cases the basal expression of mir-34a is negatively affected. However, despite many of the cases with mono- or bi-allelic inactivation of *TP53* having very low mir-34a levels, nearly a quarter (7/30; 23%) had mir-34a levels in excess of 10 which would place them within the interquartile range of the samples with no detected abnormalities of *ATM* or *TP53*.

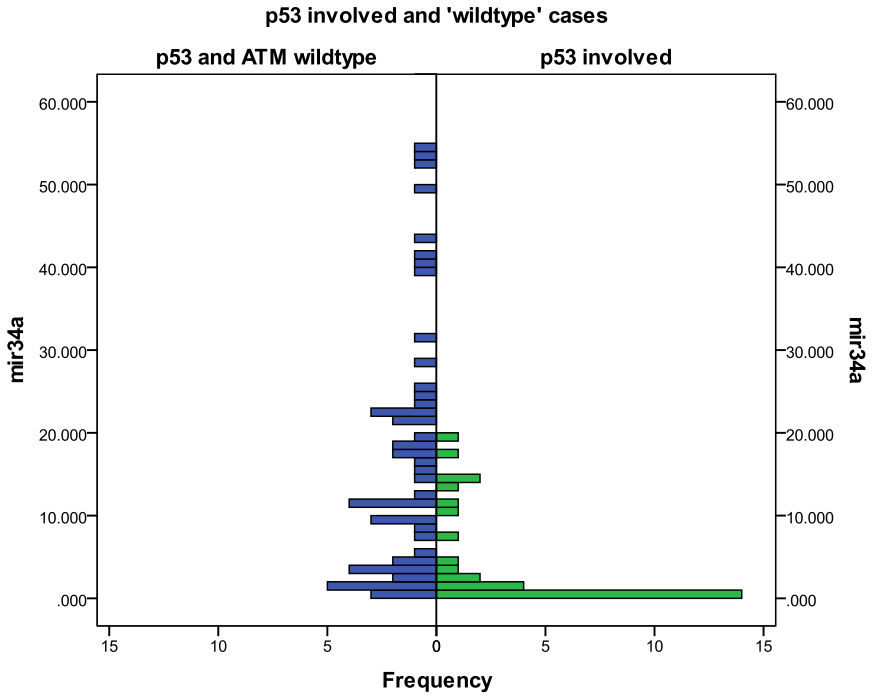

Figure 5-13: Pyramid diagram comparing the distribution of mir-34a relative expression results of p53 and ATM wildtype cases with p53 involved cases.

Receiver Operator Characteristics (ROC) were used to attempt to set a cut-off, using all 114 mir-34a relative expression results, to detect cases with any involvement of *TP53*. The ROC curve is shown in Figure 5-14. To maximise sensitivity and specificity a mir-34a cut-off of 2.30 would give 85.5% sensitivity and 66.7% specificity, correctly identifying 66% (20/30) of the cases with abnormalities of *TP53* and incorrectly identifying 14% (12/84) of the cases with no abnormalities of *TP53*.

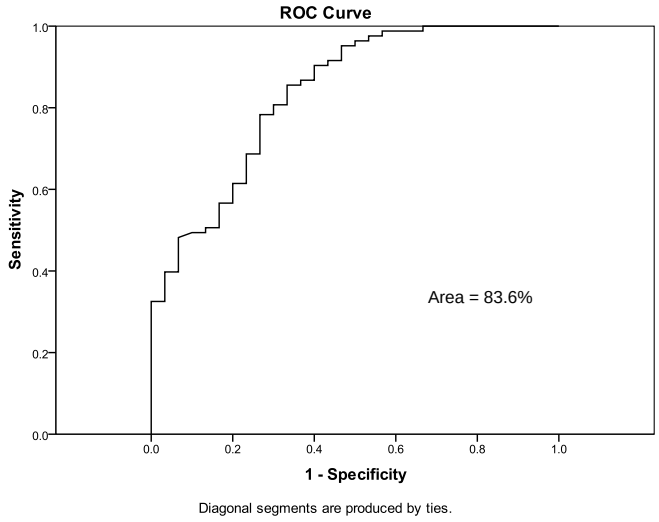

Figure 5-14: Receiver Operator Characteristics curve

5.10 *Hsa*-Mir-34a levels in samples with no detected abnormalities of *ATM* or *TP53*.

A total of 54 samples had no abnormalities of *ATM* or *TP53* detected by FISH and mutation screening/sequencing and they are displayed in Figure 5-15, in descending order of mir34a relative expression results with markers to show the median and interquartile range.

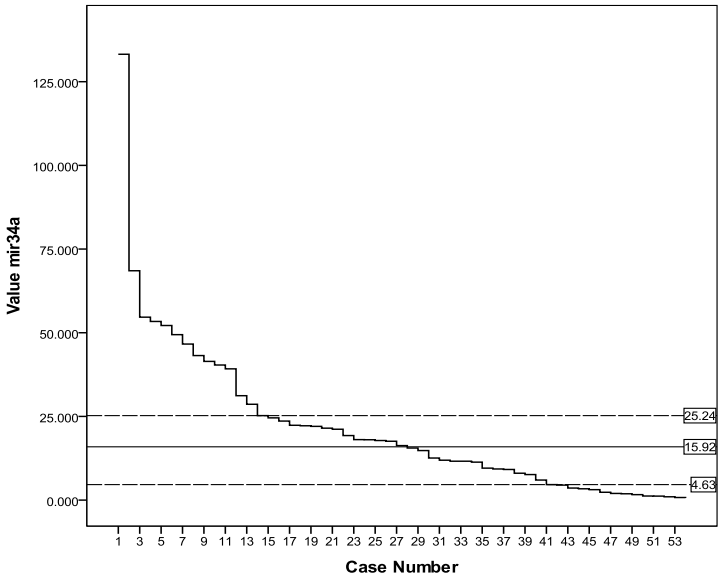

Figure 5-15: All samples with no detected FISH loss or mutation of *ATM* or *TP53* (n=54)
Samples are arranged in descending mir-34a value. The median (mir-34a=15.92), 25th (mir-34a=4.63) and 75th (mir-34a=25.24) percentiles are shown, delineating an interquartile range of 20.61.

The mean and median mir-34a results for this group were 21.16 and 15.92 respectively (SD=22.88). The comparison of the range (0.616-133.2) and interquartile range (4.63-25.24) shows that this sample group contained one outlier case with very high mir-34a and a substantial number of cases with very low mir-34a results and this was also previously observed in Figure 5-13 (p139). A timeline of clinical events for the case with very high mir-34a expression, LRF 145, is described in Figure 5-16. This patient was diagnosed at Binet/Rai stage B3 in December 2008, three months previous to donating the sample that was analysed. It can be seen that this patient did not respond to treatment with fludarabine and cyclophosphamide and *in-vitro* testing with the etoposide/ nutlin functional assay identified the sample as a non-

responder They were subsequently treated with the mono-clonal, antibody therapy, Alemtuzumab, to which they had a general partial response. At their last follow-up (24th August 2010), they had not required further treatment.

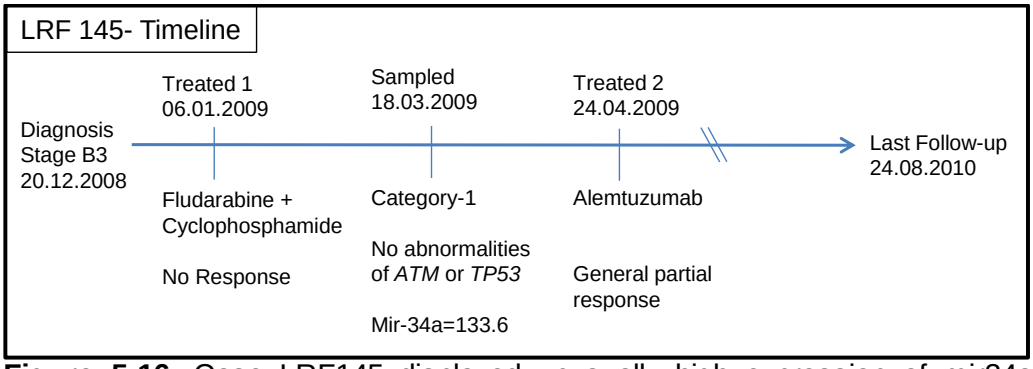

Figure 5-16: Case LRF145 displayed unusually high expression of mir34a (mir-34a=133.6). The case was functionally classed as a non-responder.

This suggests that exceptionally high levels of mir34a may also predict DNA damage response pathway failure in cases with no other high risk abnormalities.

Functional analysis results were available for 44/54 of the p53 and ATM wildtype samples. They are shown in Figure 5-17, grouped according to functional assay result and showing the interquartile range.

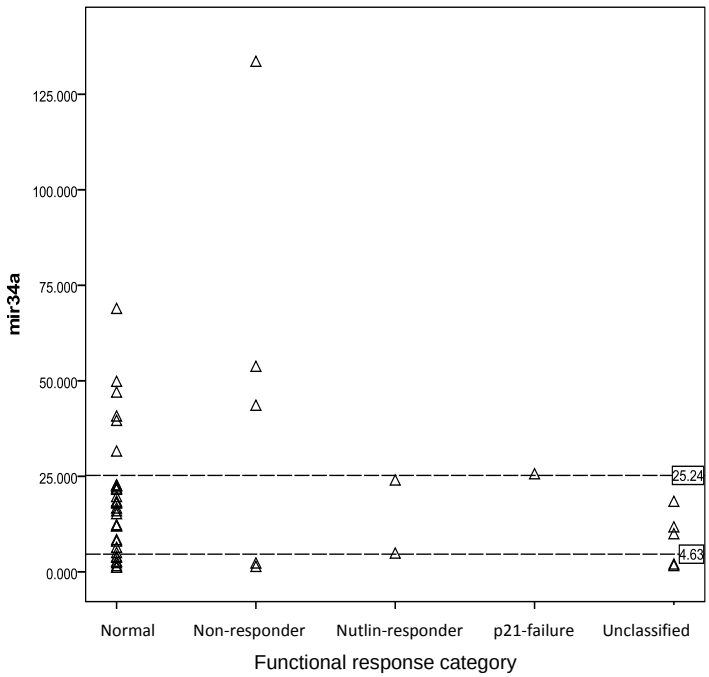

Figure 5-17: Mir-34a results for 44/54 (81%) of cases that had no detected abnormalities of ATM or TP53 by FISH stratified by functional assay result and showing interquartile range.

Dysfunction was detected in 13/44 (30%) cases and these were unequally distributed towards the lower (5/13, 38%) quartile as opposed to the upper quartile (3/13, 23%) and the interquartile range (5/28, 18%). This suggests that baseline mir-34a expression may be deregulated by mechanisms apart from *ATM* or *TP53* gene loss and/or mutation and that this results in the low basal expression seen in cases with *TP53* abnormalities. The cases which showed dysfunction despite no *TP53* or *ATM* gene defects being detected by FISH or mutation screening were further investigated using all data that was available of those cases.

Alternatively it could be hypothesised that the low level of mir34a in cases with no detected mutation of *TP53* or loss of 17p detected may be due to deregulation of the DNA damage response through a p53-independent mechanism. In total 16/55 samples with no detected abnormalities of either gene had mir-34a levels that measured within the 99% confidence interval for cases with detected involvement of p53 (1.42-6.97, n=33). These cases were examined further. Of those with data available it was known that 8/13 had been previously treated, of whom 7/8 were then subsequently treated after the date of the sample tested. One further case, not previously treated was treated after the date of the sample.

5.11 **Summary**

This section has shown that measuring the relative expression of the micro RNA *hsa*-miR-34a in unstressed CLL cells can identify cases with abnormalities of the *TP53* gene but not *ATM*. Therefore the null hypothesis for this section will be accepted: 'Basal miR-34a expression is not an indicator of ATM and p53 function in CLL'. There is however considerable overlap between groups with and without *TP53* involvement. An attempt to set a miR-34a cut-off value for detecting *TP53* abnormalities was made using receiver operator characteristics (ROC). A cut-off of 2.30 would give 85.5% sensitivity and 66.7% specificity, correctly identifying two thirds of the cases with abnormalities of *TP53* but incorrectly identifying 14% of the cases with no abnormalities of *TP53*.

Chapter Six:

Results

Validating assay samples

6.1 **Overview**

It was decided to investigate the effects of storage and transport upon peripheral blood mononuclear cells derived from whole blood specimens delivered from a number of centres around the UK. In the case of LRF study samples this involved the transport of venesectioned whole blood in vacutainers containing Lithium/heparin preservative. Samples sent from Leicester were cryo-preserved aliquots of peripheral blood mononuclear cells (PBMCs).

6.2 **Hypothesis**

The hypothesis for this chapter is as follows:

Hypothesis:

Assay results will be affected by prolonged time between venesection of blood sample and storage of PBMCs.

Null hypothesis:

Assay results will not be affected by prolonged time between venesection of blood sample and storage of PBMCs.

6.3 **Preliminary investigation on ambient effects**

Whole blood from local CLL patients (n=10) was collected and then aliquots were taken into 5 ml sterile plastic tubes and resealed. These aliquots were stored at different temperatures (room temperature, 37^{o}C and 4^{o}C) and for different time periods (24 and 48 hours) before separation of the PBMC fraction and cryo-preservation as described in section 2.3. The remainder of the whole blood sample was processed for PBMCs as normal. A portion of 2x10^7 cells were taken after centrifugal separation of blood. These were immediately placed into the functional assay culture conditions and are further described as ‘fresh’. Finally, an aliquot of fully processed PBMCs (2x10^7 cells.ml^{-1}) was frozen in an ultra-low temperature freezer (-80^{o}C) instead of a liquid nitrogen container (-175^{o}C). All assay conditions (excluding the ‘fresh’) from each separate whole blood sample were kept frozen for a minimum of

one week before being retrieved, thawed and tested concurrently using the functional assay as described in the methods section.

Cell viability was assessed on cells sampled before, and cells sampled after, overnight incubation in the functional assay control culture using the Trypan-Blue dye exclusion test as described in section 2.4. Viability is defined as the percentage of cells excluding the dye. The results of all replicates for six patients are shown in Figure 6-1. This preliminary data shows that storage at 37^{o}C is the most detrimental variable introduced. It can also be seen that there is a repeated negative impact on viability introduced by the process of overnight culture as per the functional assay methodology described in section 2.14. CLL cells do die spontaneously *in-vitro* however.

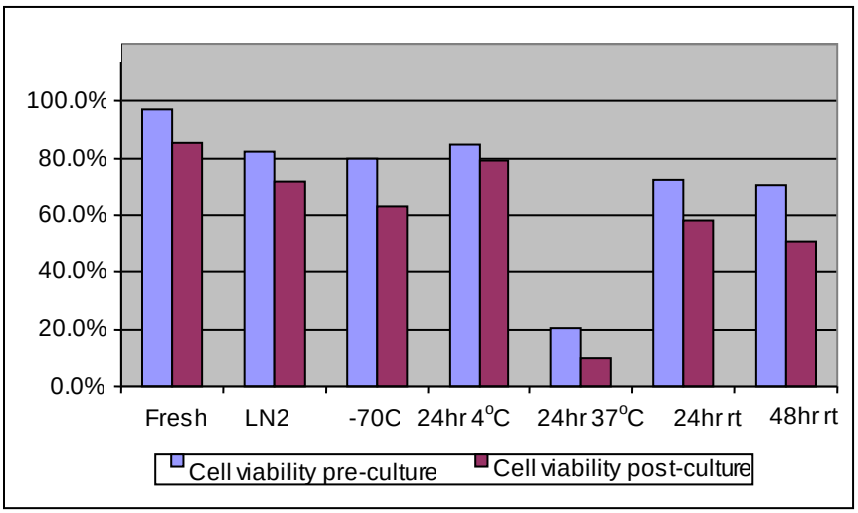

Figure 6-1: Mean percentage of viable cells after storage under different conditions
Results of viability testing using Trypan blue exclusion test. All replicates for 6 individuals are shown. LN2 = Liquid nitrogen storage.

Table 6-1 below shows the functional assay results of 10 whole blood samples, handled and stored as previously described. These include the individuals in Figure 6-1 plus four other individuals for whom the Trypan-Blue data had not been collected.

Table 6-1: Functional assay results for sample storage study.

Sample	Immediate assay	Immediate cryo-storage	Immediate storage -70°C	24hours at 4°C *	24hours at 37°C *	24hours at RTP *	48hours at RTP *
a	3	3	3	1	1	3	NT
b	2	2	2	2	2	2	2
c	N	N	N	N	1	N	N
d	2	2	2	2	2	2	2
e	N	N	N	N	N	N	N
f	N	N	N	N	N	N	N
g	N	N	N	N	N	N	N
h	N	1	N	N	1	N	N
i	N	N	NT	N	2	N	NT
j	N	1	1	1	1	1	1

Lymphocytes were separated from aliquots of whole blood immediately or after storage at different temperatures and for different time periods. Conditions returning an aberrant result are highlighted.
RTP: room temperature and pressure; * before cryo-storage in liquid nitrogen; NT not tested. 1 = Non-responder; 2 = Nutlin-responder; 3 = p21-failure; N = normal

Storage at 37^{o}C is again shown to be the most detrimental factor. The single discordant result for a sample stored for 24 hours at 4^{o}C came from patient (a) who has returned a p21-failure result on all other occasions of testing (n=3) and is known to have low level loss of 17p13.1 (~10%). Patient (h) is a normal functioning sample with no currently identified abnormality that has shown a normal result previously. Patient (j) has on all other occasions (n=3) returned either non-responder or p21-failure results and is known to have loss of 17p13.1. Notwithstanding the three samples from patients a, h and j highlighted in Table 6-1, it is clear that temperature is a more immediate critical factor than duration of storage. Although some testing is still required, the reduced sample viability after 48 hrs at room temperature and pressure (RTP) does not seem to affect reproducibility. Therefore samples which are up to two days old and that have not been stored in excessive heat may still be acceptable for the assay.

6.4 **Investigating effects caused by delays between venesection and processing**

6.4.1 **Samples used in this section**

The patient cohort used in this study was derived from samples that were obtained from the local CLL clinic, n=112, and also from referring participant clinics across the UK, n=134 (LRF group). Samples derived from the latter

were delivered to the Bournemouth laboratory as lithium/heparin preserved whole blood samples and would have spent a minimum of one day in transit. It was not assumed that the analysis of these samples would generate the same functional results as locally sourced samples. In order to control for any differences introduced by the transport of samples this section will look at whether viability of the samples and/or the expression of p53 and p21 from these two subsets differed. The measure of cell viability used in this section was derived from the light scattering properties of the cells. This data was recorded by the FACScalibur flow cytometer at the same time as measurements of p53 and p21 protein was made for the etoposide and nutlin functional assay.

6.4.2 **Comparison between two techniques for measuring cell viability**

In order to compare the two techniques available for measuring cell death, the percentage of cells determined as live using the Trypan Blue exclusion test was compared to the percentage of cells determined to be viable by their light scattering properties. Trypan blue data was collected for 64 cases and a correlation with the percentage of cells in the live gate was tested for. The matched results are shown below in Figure 6-2.

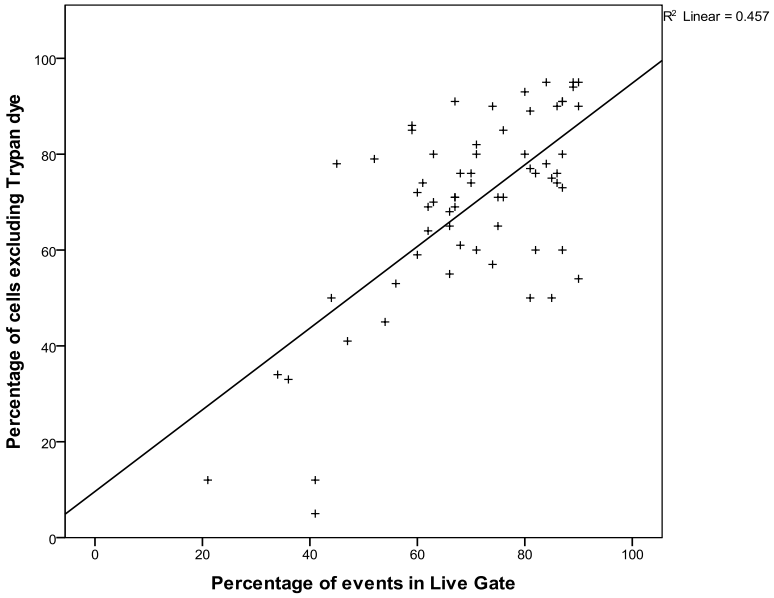

Figure 6-2: Scatter plot showing the matched Trypan-blue and live-gate data for 64 paired data points. The data display a linear, positive correlation between the two measurements (n=64, r=.676, *p*<.001)

The mean percentages of live cells determined by the Trypan-Blue exclusion test ($\bar{x}$=69%, SD=20.07) and the percentage of events in the FACS live gate ($\bar{x}$=70%, SD=15.92) were similar and the two variables were not found to differ significantly in terms of distribution (p=0.701). The average difference between each matched result was not significantly different to zero ($\bar{x}$=-0.72%, 95% CI=-4.46-3.02, *t*=-0.384, *p*=0.702). The percentage of cells considered to be alive based upon their light scattering properties will therefore be referred to as the viability for the remainder of this result section.

Establishing that the viability data correlates with assessment of cell viability determined using the Trypan Blue exclusion test meant it was possible to use this data to test for effects on cell viability which may have been introduced during the time between venesection and sample processing.

6.4.3 **Effects on cell death by drug treatments**

Analysis of cell death rates was performed on the 112 samples which had viability data calculated for the control, etoposide and etoposide plus nutlin cultures, and which also had no detected abnormalities of either the *ATM* or *TP53* genes as determined by FISH and mutation screening/ sequencing. The *Komorgorov-Smirnov* statistic was significant (*p*<.05) for both control and

etoposide plus nutlin treated culture data therefore they were treated as not normally distributed. The etoposide treated culture data was normally distributed (p=.2). It was assumed there would be some spontaneous apoptosis in the control culture and that additional cell death would be detected in the etoposide culture which would be further enhanced by the addition of nutlin. The paired data are shown in Figure 6-3, arranged, left to right, in descending order of calculated viability in the control culture.

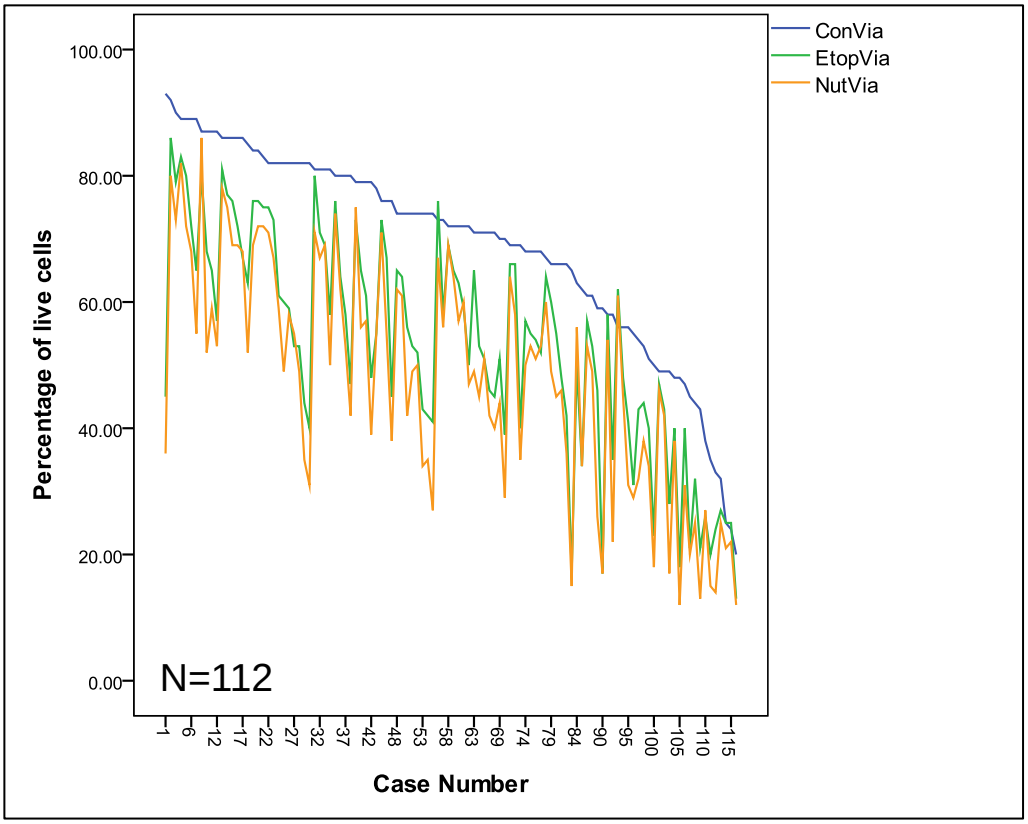

Figure 6-3: Paired viability data for control, etoposide and etoposide + nutlin 24hr cultures (n=112). Showing the paired data for the three treatment conditions and displayed in order of descending percentage of viable cells in the control culture.

As expected, the percentage of live cells in the control (Mean=69.3%; SD=16) was significantly higher than in the etoposide treated culture (Mean 53.4%; SD=17.3; p< .001) and the etoposide plus nutlin culture (Mean 48.4%;SD=18.1; p< .001). The figure also shows that there is considerable variation in the reduction of live cells caused by etoposide (Mean=-15.8%; SD=10.9%; Median=-13.5%; Range=-48-6). The additional reduction in live cells due to nutlin3a can also be observed and it appears closely related to the effect of etoposide (Mean=-5%; SD=4.5%; Median=-4%; Range=-20-6). Bivariate analysis of the 112 paired cases found the amount of cell death in

the control culture to be significantly correlated with the level of cell death in the both the etoposide (n=112, r= .787, p< .001) and etoposide plus nutlin (n=112, r = .742, p< .001) cultures. A much stronger correlation was seen between the drug treated cultures (n=112, r = .969, p< .001).

The paired data were then clustered according to the recorded time between sample venesection of the whole blood sample at the contributing centre and arrival in the laboratory (Figure 6-4). This was to determine whether the variation in effect of the drug treated cultures was introduced during this time.

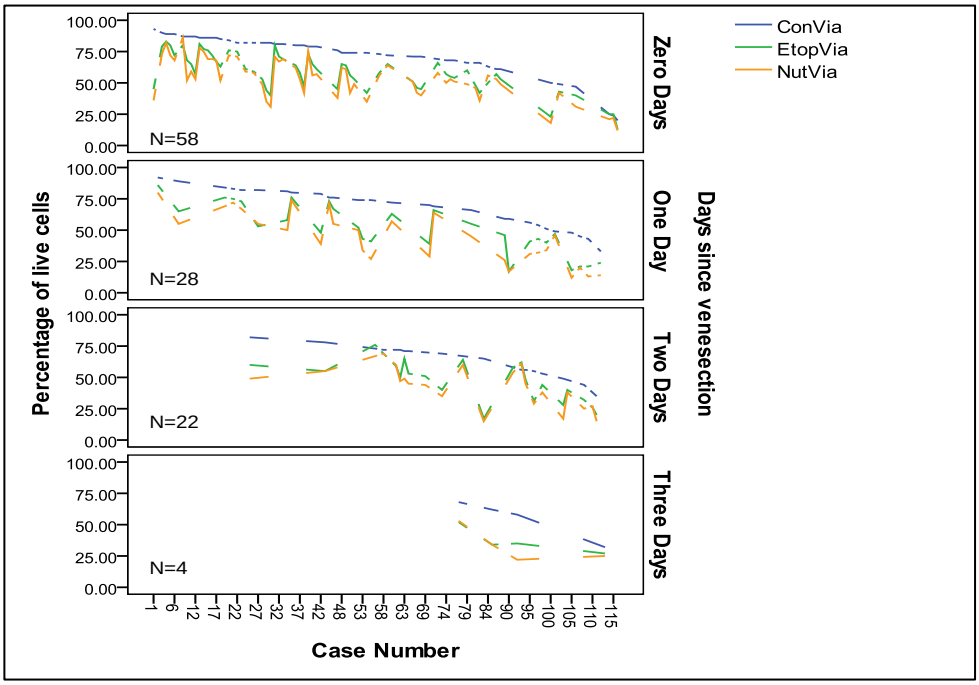

Figure 6-4: Paired viability data (n=112) stratified by the number of days between venesection and processing. Panels show data for the three treatment conditions. Data is displayed in descending order of viability in the control culture.

It can be observed that viability tended to drop with increasing time since venesection. It can be seen that the variation in effect on viability caused by etoposide is not attributable to time since venesection. This variation may probably be due to inherent differences between samples. This is of interest as approximately one-third of patients who relapse after therapy do not have any detectable abnormalities of *ATM* or *TP53*.

6.4.4 Spontaneous apoptosis is higher in samples which have spent a day or more between venesection and processing

One-way ANOVA was used to compare the level of cell death between the samples which were processed the same day as venesection (n=58) and the

samples which had an intervening period of one day or more (n=54). A boxplots of the results are shown in Figure 6-5, (panel A). This showed a significant reduction in live cells in the one day or more group for the control (73.6%v65%; *F*=9.279; *p*= .003), etoposide (58%v48.6%; *F*=8.744; *p*= .004) and etoposide plus nutlin (53.6%v42.9%; *F*=10.481; *p*= .002) culture conditions. A similar comparison of the samples which had a one-day interval between venesection (n=28) and those which had an interval of two-days or more (n=26) is shown in Figure 6-5 (Panel B). A significant reduction in the two days or more group was only found for the control culture (68.8%v60.5%; *F*=4.471; *p*= .039) although viability was still reduced in both the etoposide (51%v46%) and etoposide plus nutlin (44.2%v41.5%) conditions. These results suggest that the effect of time between venesection and processing on cell death may be cumulative but is most pronounced during the first 24hours. Having shown an effect upon the level of cell death caused by some mechanism related to the time between venesection and sample processing it was decided to test for the same effects in those cases which had detectable abnormalities of *ATM* and/or *TP53.* Defects of these genes, in particular *TP53*, and their respective protein products may modulate the cellular responses to stress insults during this time.

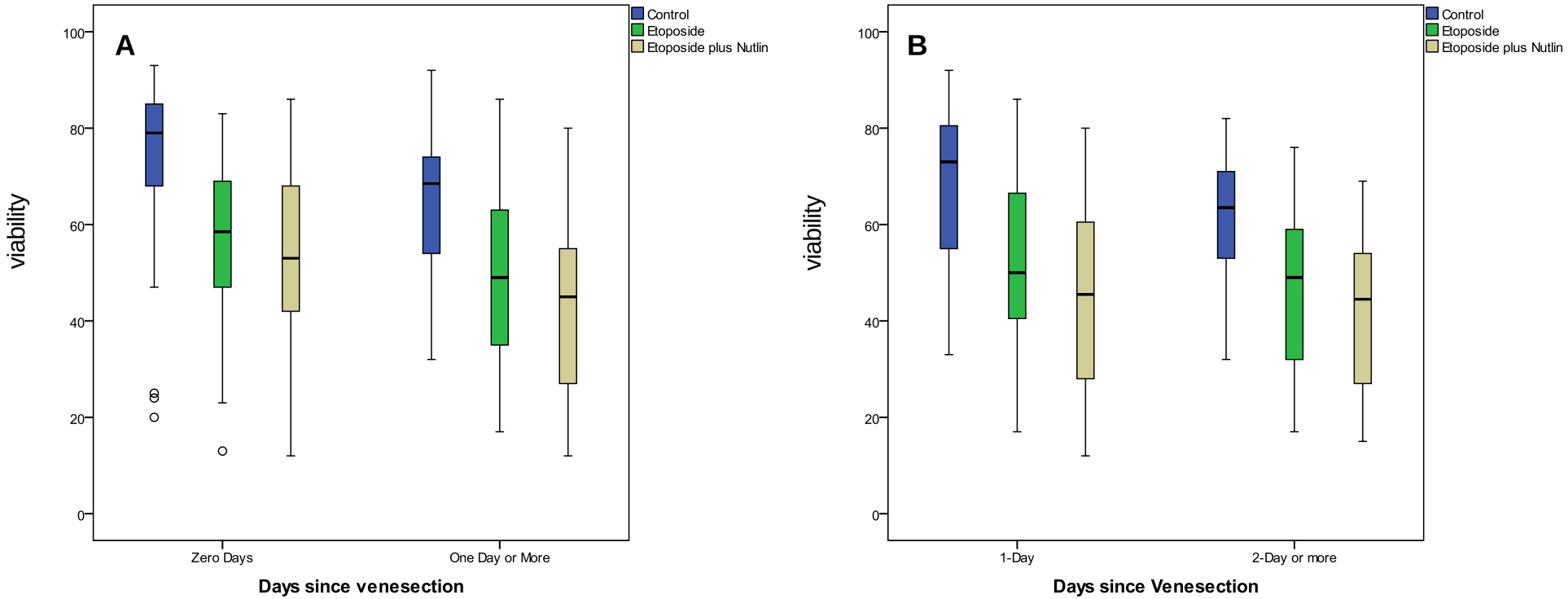

Figure 6-5: Effects of culture conditions on percentage of live cells according to time since venesection.

Panel **A)** The left hand plot shows the samples which were processed the same day as venesection (n=58) against the samples which had an intervening period of one day or more (n=54) and illustrates a significantly higher level of mean cell death in the latter for the control (73.6%v65%; *F*=9.279; *p*= .003), etoposide (58%v48.6%; *F*=8.744; *p*= .004) and etoposide plus nutlin (53.6%v42.9%; *F*=10.481; *p*= .002) culture conditions. **B)** Similar comparison of the samples which had a one-day interval between venesection (n=28) and those which had an interval of two-days or more (n=26) found a significant reduction in the latter for only the control culture (68.8%v60.5%; *F*=4.471; *p*= .039) although viability was still reduced in both the etoposide (51%v46%) and etoposide plus nutlin (44.2%v41.5%) conditions.

6.4.5 **Spontaneous cell death is higher in samples with abnormalities of *TP53***

The samples with abnormalities of *ATM* or *TP53* were analysed to determine whether these abnormalities had any impact upon the rate of cell death in samples which had been in transit for a day or more. Given the role of p53 protein in response to many diverse cellular stresses it seems reasonable to assume that genetic abnormalities involving *TP53* might affect the rate of cell death in transported samples. Control culture viability data was available for 64/97 samples which had detected abnormalities. Figure 6-6 shows that for the group with abnormalities (*ATM* and/or *TP53*) there is a lower median viability in the samples that have been transported (Median=63%, n=35) than those that had not (Median=72%, n=29). This difference was not significant (z= -1.363, p= .173).

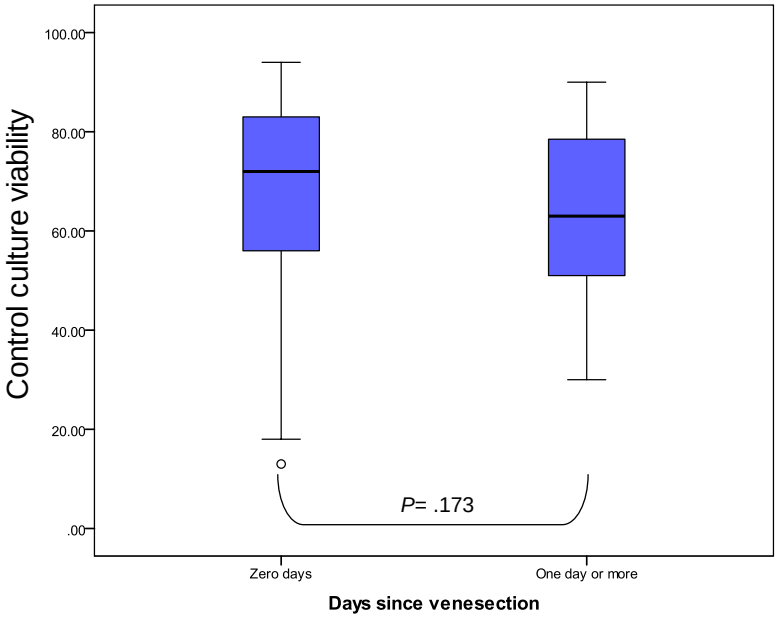

Figure 6-6: Control culture viability data for sixty-four samples with abnormalities of ATM or TP53.

Figure 4.6: For 29 samples which took less than a day, the median control viability was 72% (range 13-94%), compared to a median of 63% (range30-90%) for the 35 samples which took a day or more. Despite this reduction in median value the difference was not statistically significant (*z*= -1.363, *p*= .173).

In order to determine whether the lack of effect was due to differences between the *ATM* and *TP53* involved cases these two genotypic groups were tested individually. Data for cases with *ATM* involvement is shown in Figure 6-7, grouped according to time between venesection and processing in the

laboratory. It can be seen that samples which took one day or more (n=13, median=68%, range=30-87%) had lower viability than those cases which took less than one day (n=10, median=83.5%, range=18-94%) but the difference was not significant (*z*=-1.799, *p*= .077 [Exact Sig.]).

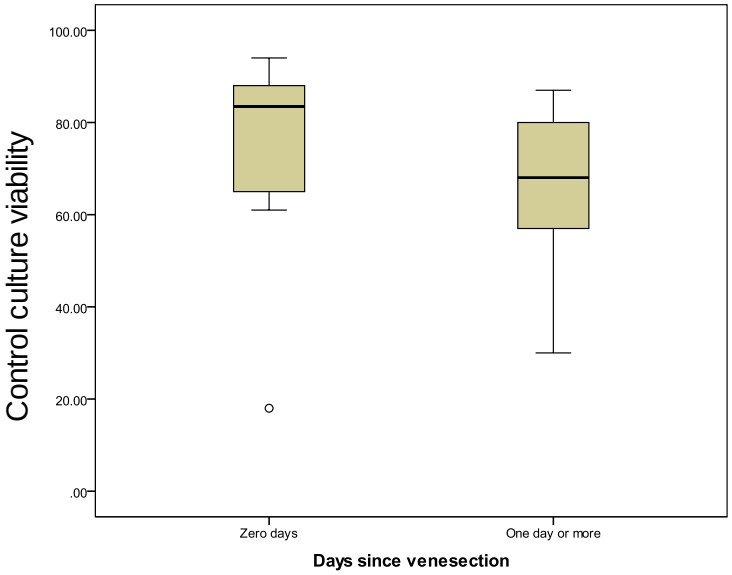

Figure 6-7: Differences in control culture viability for cases with *ATM* gene abnormalities.

The viability data for the control cultures in cases with known abnormalities of *TP53* is shown in Figure 6-8, grouped according to time between venesection of the sample and processing in the laboratory.

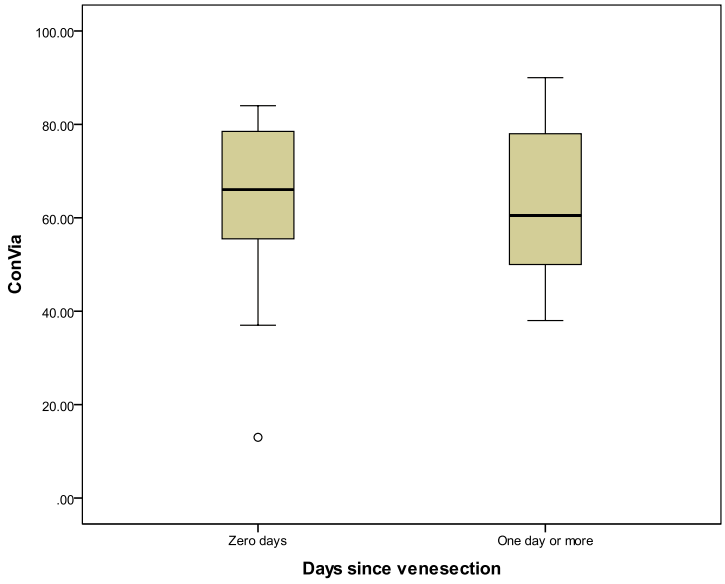

Figure 6-8: Differences in control culture viability for cases with TP53 gene abnormalities.

Samples with deletion and/or mutation of the *TP53* gene which took one day or more to be processed (n=22, median= 60.5%, range=38-90%) had only a slighter lower level of cell viability than those cases which took less than a day (n=19, median=66%, range=13-84%) and the difference was not significant (*z*=-0.549, *p*= .583).

Despite no statistically significant difference between the 0-Day and 1-Day or more groups for either genotype the difference between the two groups for the *ATM* involved cases was starkly different to those cases with *TP53* involvement.

In addition to the finding that cases with *TP53* defects may have different levels of spontaneous cell death than cases with *ATM* gene defects, comparison of the 0-day group with no abnormalities to the 0-day groups in each of these genotypes (Figure 6-9, p158) showed that the percentage of live cells in the cases with *ATM* abnormalities (n=10, median=83.5%, range=18-94%) was not significantly different to that observed in the cases with no detected abnormalities (n=60, median=79%, range=20-93%, *z*=-1.050, *p*= .294). In contrast the percentage of live cells in the *TP53* involved cases (n=19, median=66%, range=13-84%) was significantly lower than the cases with no abnormalities (*z*=-2.428, *p*= .015) and those with *ATM* involvement (*z*=-2.158, *p*= .031 Exact). This difference was lost when performing the same analysis on samples which had taken a day or more.

6.4.6 **Analysis of basal p53 and p21 protein levels**

Having shown a significant effect upon cell death between samples which had or had not been transported using the live cell percentage data, the median fluorescent intensity (MFI) data was similarly analysed to determine if the transport of samples also affected the expression of p53 and p21 proteins. This analysis was performed on the samples which had no detected abnormalities of *ATM* or *TP53* first (n=149). The results in Figure 6-10 (p159) and Table 6-2 shows that the level of p53 and p21 in the control culture was not significantly affected by transport suggesting that any possible activation of p53 controlled stress responses during transport and storage did not carry over into the culturing of cells.

Table 6-2: Descriptive data for basal p53 and p21 protein levels in samples.

Group statistics					t-test for Equality of Means	
MFI variable	**Days since venesection**	**N**	**Mean MFI**	**Std. Deviation**	***t*-score**	**Sig. (2-tailed)**
p53 Control	Zero Days	72	3.85	0.79	1.027	.306
	One Day or More	77	3.73	0.68		
p21 Control	Zero Days	72	3.23	0.51	1.156	.249
	One Day or More	77	3.14	0.38		

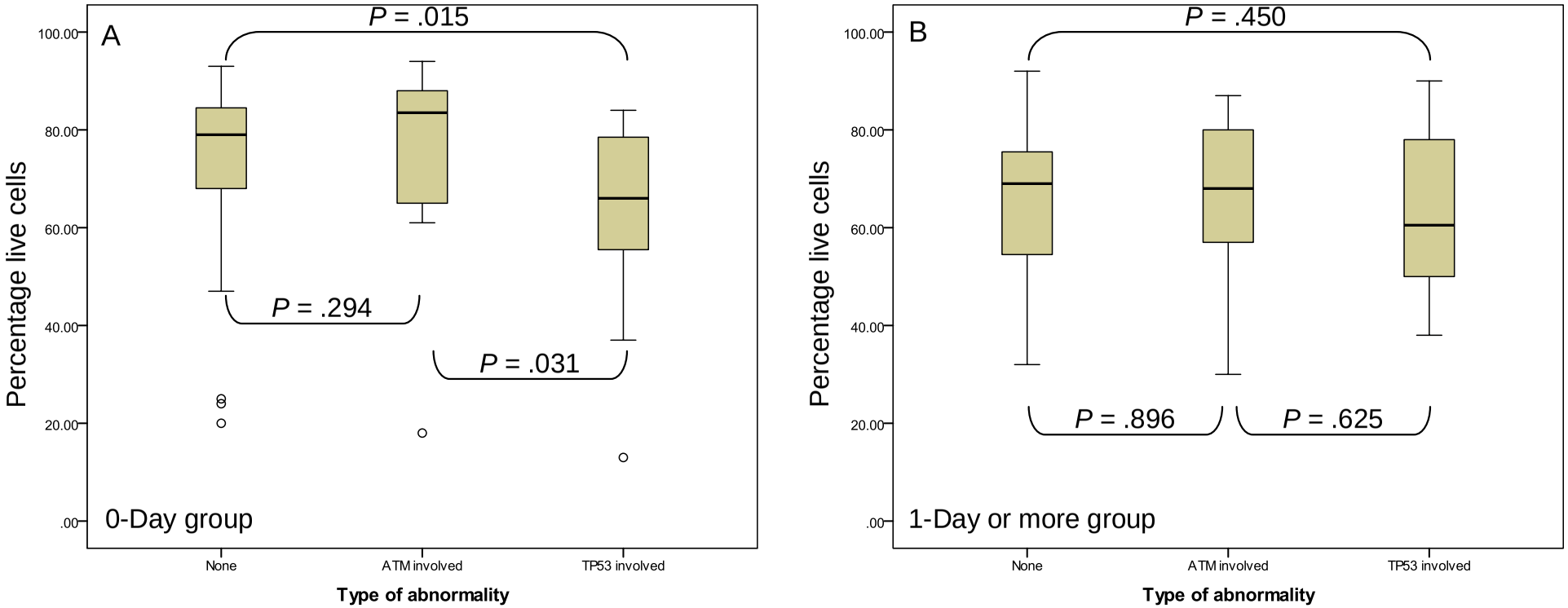

Figure 6-9: Comparison of the percentage of live cells in the control culture across the different genotypic sub-groups.

Panel A) In samples that took less than a day to arrive in the lab, 89 had data on control viability. The percentage of live cells in samples with no abnormalties detected (n=60, median=79%, range=20-93%) was not significantly different to those samples with *ATM* involvement (n=10, median=83.5%, range=18-94%, *z*=-1.050, *p*= .294), however, samples with *TP53* involvement (n=19, median=66%, range=13-84%) were significantly different to both the cases with *ATM* involvement (*z*=-2.158, *p*= .031 Exact) and those with no detected abnormalities (*z*=-2.428, *p*= .015). Panel **B)** In samples which took a day or more to arrive in the Bournemouth laboratory, 91 had data on control viability. The percentage of live cells in samples with no abnormalities detected (n=56, median=69%, range=32-92%) was not significantly different to the *ATM* involved cases (n=13, median=68%, range=30-87%, *z*=-0.130, *p*= .896) or the *TP53* involved cases (n=22, median=60.5%, range=38-90%, *z*=-0.755, *p*= .450). There was also no significant difference between the cases with *ATM* and *TP53* involvement (*z*= -0.495, *p*= .625

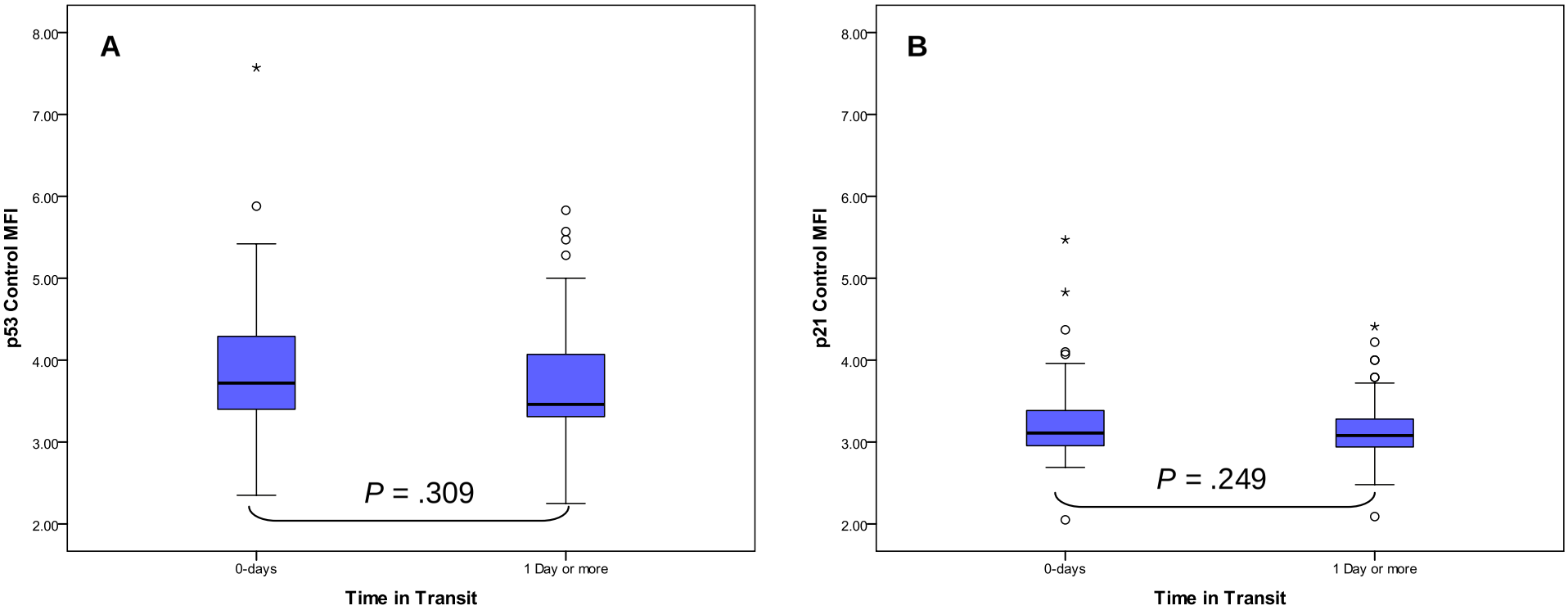

Figure 6-10: Basal p53 and p21 MFI levels in cases with no abnormalities of *ATM/TP53* grouped by time in transit. (n=149)

These figures show that there was no significant effect on the expression of either protein in the control cultures, suggesting that there was no inappropriate activation of *TP53*. **Panel A)** The level of p53 protein in samples that took less than a day to arrive in the laboratory (n=72, mean=3.85, SD=0.79) was not significantly different from those samples which took a day or more (n=77, mean=3.73, SD=0.68, *t*= 1.027, *p*= .306). **Panel B)** The level of p21 protein in samples that took less than a day to arrive in the laboratory (n=72, mean=3.23, SD=0.51) was also not significantly different to those that took a day or more (n=77, mean=3.14, SD=0.38, *t*=1.156, *p*= .249).

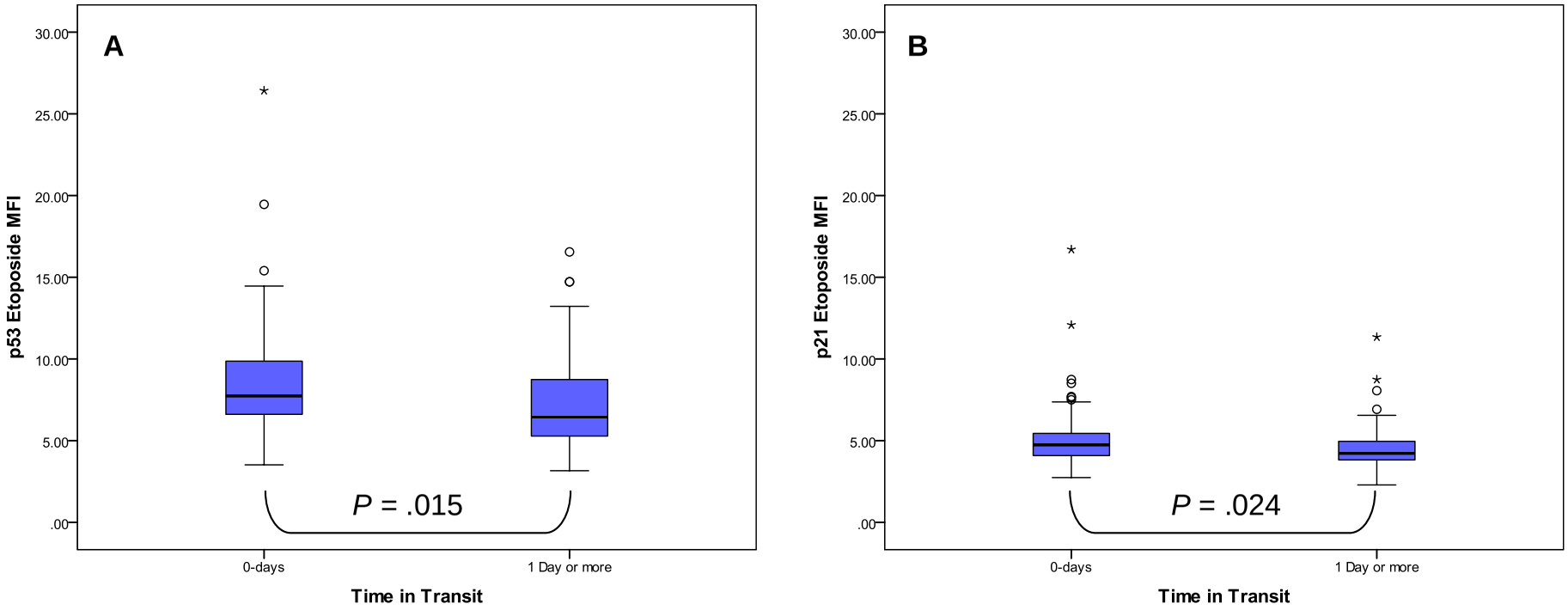

Figure 6-11: Etoposide response p53 and p21 MFI levels in cases with no abnormalities of ATM/TP53 grouped by time in transit. (n=149)

A) The expression of p53 protein in samples which took less than a day to arrive in the laboratory (n=72, mean= 8.63, SD=3.52) was significantly different to those samples which took a day or more (n=77, mean=7.35, SD=2.84, *t*= 2.455, *p*= .015). **B)** The expression of p21 protein in samples which took less than a day to arrive in the laboratory (n=72, mean=5.22, SD=2.04) was significantly higher than those samples which took a day or more (n=77, mean=4.58, SD=1.36, *t*= 2.279, *p*= .024).

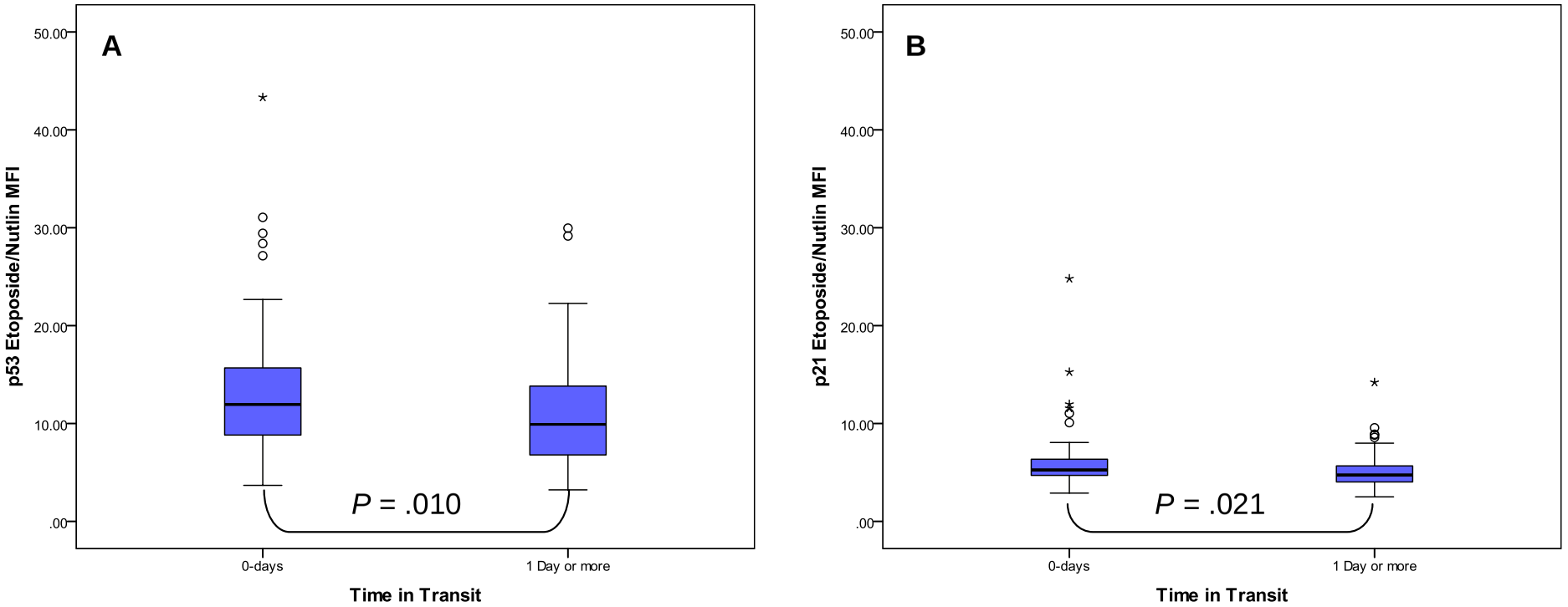

Figure 6-12: Analysis of p53 and p21 protein responses to etoposide plus nutlin.

Showing data for 149 samples with no detected abnormalities of *ATM* or *TP53*. **A)** The expression of p53 protein in samples which took less than a day to arrive in the laboratory (n=72, mean= 13.46, SD=6.87) was significantly different to those samples which took a day or more (n=77, mean=10.84, SD=5.28, *t*= 2.613, *p*= .010). **B)** The expression of p21 protein in samples which took less than a day to arrive in the laboratory (n=72, mean=6.10, SD=3.03) was significantly different to those samples which took a day or more (n=77, mean=5.16, SD=17.2, *t*= 2.339, *p*= .021).

6.4.7 Analysis of p53 and p21 protein responses in treated cultures

Having shown that the baseline expression of p53 and p21 in the control cultures was not significantly affected by transport Figure 6-10 (p159), the responses of these two proteins to the treated cultures was examined in the 149 cases with no detected abnormalities of *ATM* or *TP53.* This data is summarised in Table 6-3. The results in Figure 6-11 (p160) show that in response to etoposide a significant difference in p53 protein expression was observed between the samples which had taken more than a day to arrive in the laboratory (n=77, mean=7.35, SD=2.84) and those which had been processed the same day (n=72, mean= 8.63, SD=3.52, *t*= 2.455, *p*= .015). The same effect was observed for p21 protein expression (n=77, mean=4.58, SD=1.36 versus n=72, mean=5.22, SD=2.04, *t*= 2.279, *p*= .024). Figure 6-12 (p161) shows the data for protein expression in response to etoposide plus nutlin. The same significant difference was observed between the two groups for both p53 expression (n=77, mean=10.84, SD=5.28 versus n=72, mean= 13.46, SD=6.87 *t*= 2.613, *p*= .010) and p21 expression (n=77, mean=5.16, SD=17.2 versus n=72, mean=6.10, SD=3.03, *t*= 2.339, *p*= .021). What is not clear from this data is whether the effect is due to an actual difference in protein expression per cell between the two groups or if the increased cell death in the samples which took a day or more to arrive caused the mean to be lowered.

Table 6-3: Descriptive statistics for p53 and p21 protein responses to etoposide and etoposide plus nutlin treated culture conditions.

Group statistics					t-test for Equality of Means	
MFI variable	**Days since venesection**	**N**	**Mean MFI**	**Std. Deviation**	***t*-score**	**Sig. (2-tailed)**
p53 Etoposide	Zero Days	72	8.63	3.52	2.455	.015
	One Day or More	77	7.35	2.84		
p53 E+Nutlin	Zero Days	72	13.46	6.87	2.613	.010
	One Day or More	77	10.84	5.29		
p21 Etoposide	Zero Days	72	5.22	2.04	2.279	.024
	One Day or More	77	4.58	1.36		
p21 E+Nutlin	Zero Days	72	6.10	3.03	2.339	.021
	One Day or More	77	5.17	1.72		

6.4.8 **Effect of transport upon functional categorisation of samples**

In order to determine whether the reduced p53 and p21 protein responses might be sufficient to cause miss-categorisation of normal samples as dysfunctional, the MFI data for the treated cultures was converted into four variables representing the percentage increase above the respective control for p53 and p21, in both treatment cultures. These are the same metrics used for categorising sample responses according to Best et al. (2008b). Cut-offs of 30% and 15% increase above the control for p53 and p21 respectively were used to define a normal response. The 99% confidence interval for the 149 cases with no abnormalities was plotted. The results are shown in figures Figure 6-13 (p164) and Figure 6-14 (p165). When the data is displayed on a day-by-day basis, as shown in Figure 6-14, there appears to be a risk of three day old samples being capable of enough variation so as to be misclassified as dysfunctional. It should be noted however that the low numbers in the three-day group (n=6) may be responsible for the large confidence interval.

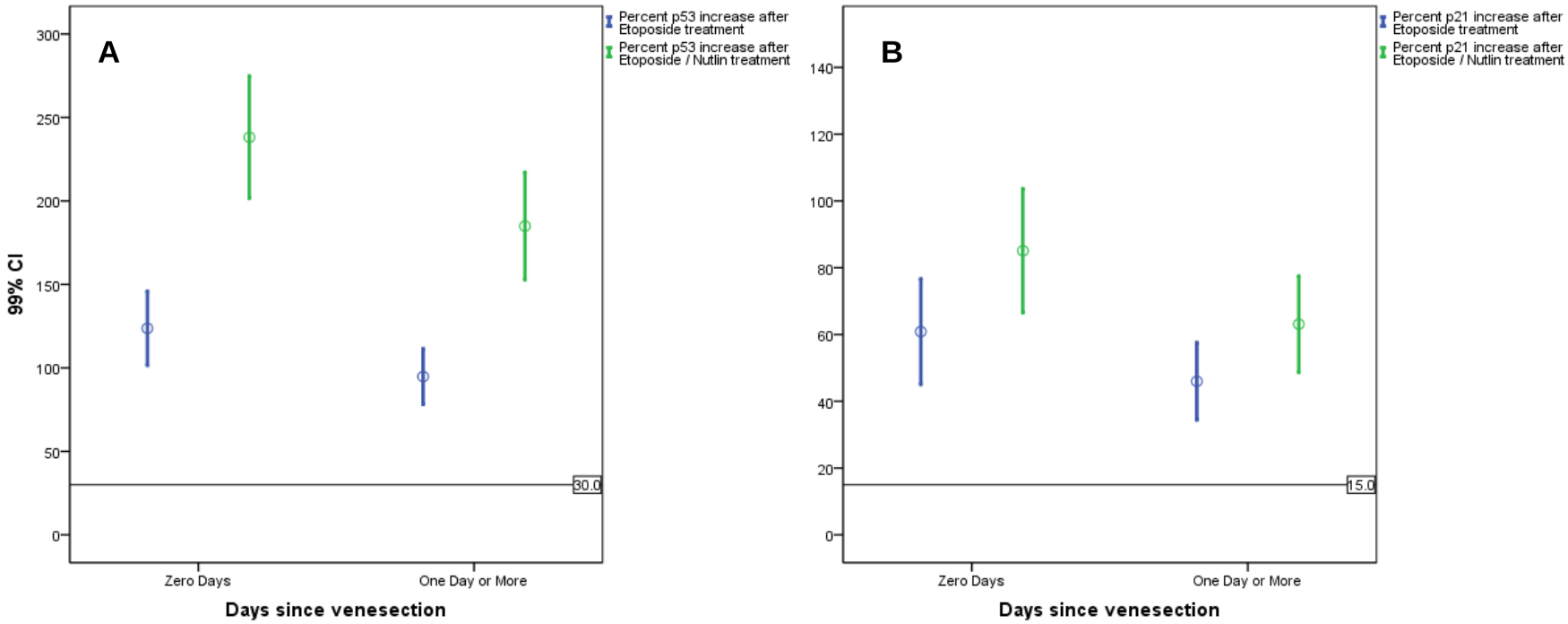

Figure 6-13: The 99% confidence intervals for protein expression increase. Zero days versus one or more.

Comparing the samples which took less than a day (n=72) and those which took a day or more to arrive in the lab (n=77) shows that despite the attenuated increase of both (A) p53 and (B) p21 proteins in response to both treatment conditions, there does not appear to be sufficient reduction to cause a misclassification of normal samples as abnormal. The respective cut-off values determined by Best et al (2008) are shown

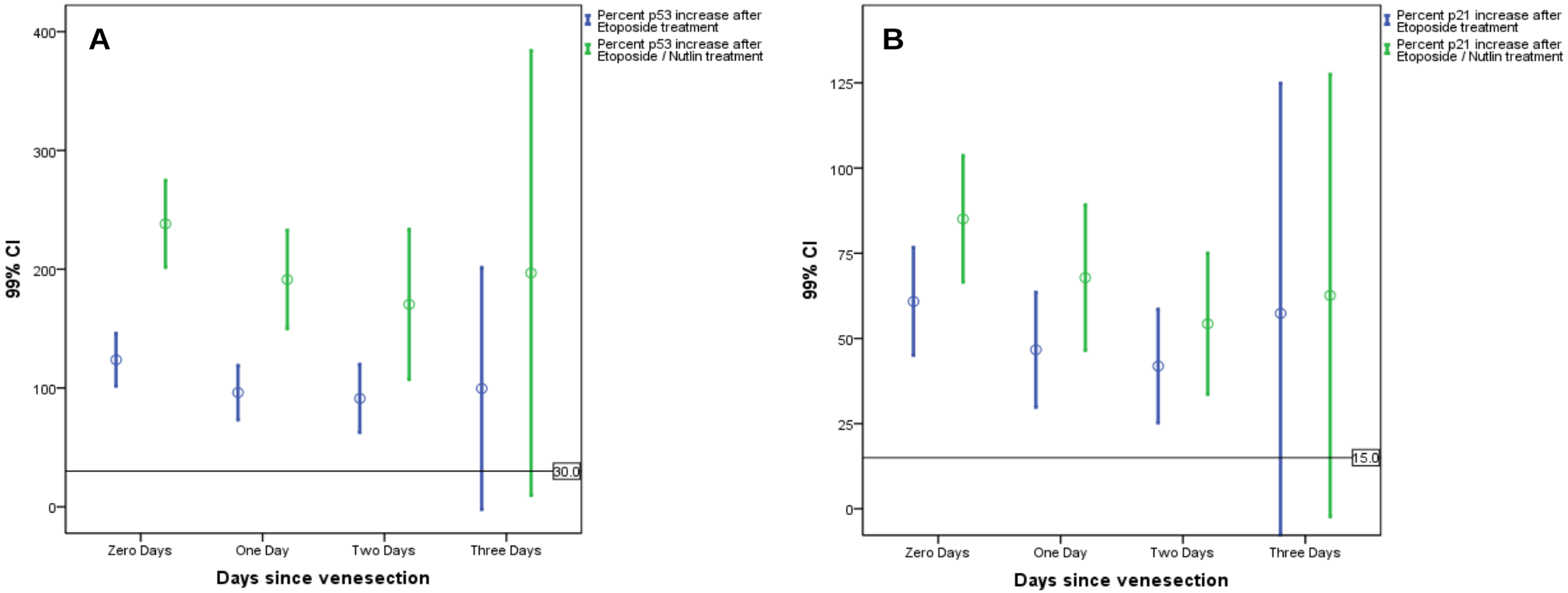

Figure 6-14:The 99% confidence intervals for protein expression increase. Zero, one, two and three days.

Comparing the samples which took less than a day (n=72) to those which took one (n=46), two (n=25) or three (n=6) days to arrive in the laboratory. The cut-off values determined by Best et al (2008) are shown

6.5 **Samples from different centres did not differ in frequency of FISH results or assay results**

It was decided to retrospectively examine the frequency of FISH results and functional assay results across the different groups of samples which were tested in the main assay results in section 3 (p83). The distribution of 11q and 17p FISH abnormalities across the three contributing centres is shown in Table 6-4. The proportion of normal vs abnormal FISH results did not differ significantly between the three centres (x^2=11.321, *df*=10, *p* =.333).

Table 6-4: Summary of FISH results grouped by contributing centre. (n=472)

	Contributing centre			
FISH results	Bournemouth	Leicester	LRF study	Total
No loss	82	148	129	359
Del(11)q	19	26	23	68
Del(17)p	10	10	18	38
x3 (17)p signals	1	0	0	1
Tetraploidy	1	0	0	1
Loss of both loci	1	3	1	5
	114	187	171	472

The distribution of functional assay results across the three sources of samples used is shown Table 6-5. The incidence of dysfunction was not found to differ significantly across the three centres (x^2=9.547, *df*=10, *p* =.481). This shows that the three cohorts were generally similar to each other.

Table 6-5: Summary of functional assay results grouped by contributing centre. (n=472)

Functional assay classification	Contributing centre			
	Bournemouth	Leicester	LRF study	Total
Normal	83	121	117	321
p53 over expression	2	1	5	8
Non-responder	7	16	16	39
Nutlin responder	13	32	20	65
p21-failure	9	14	12	35
Unclassified	0	3	1	4
	114	187	171	472

6.6 **Evolution of dysfunction observed in patient samples**

Longitudinal analysis of samples using the functional assay was available for 48 CLL patients who provided two specimens of blood, a month or more apart. The intervals between sampling ranged from 1-44 months. The frequency of intervals is shown in Figure 6-15

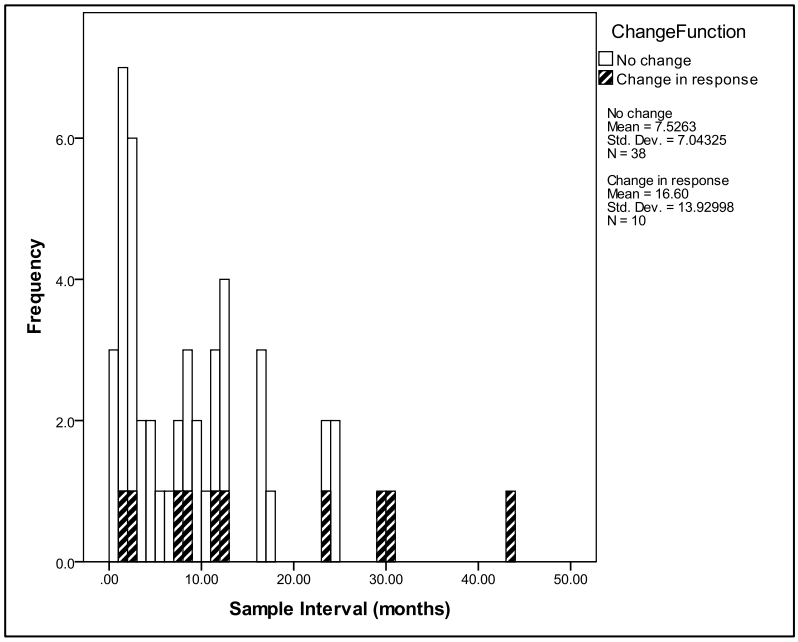

Figure 6-15: The distribution of interval times for 48 CLL patients sampled and tested twice.
The figure highlights the 10 cases which changed response upon the second test.

A total of 38/48 cases (79%) gave concordant assay results at both sampling points. The remaining 10 cases were further investigated to determine whether the changes were a result of changes in the patients tumour clone or if the assay was returning non-reproducible results in 21% of tests. Half of the 10 cases which changed functional classification had displayed a normal response when first sampled and so may represent *de novo* dysfunction due to either acquired defects or then expansion of a dysfunctional sub-clone. Table 6-6 (p168) shows some details for those cases displaying acquired dysfunctional responses. It can be seen that two cases acquired deletion of 17p at some point between sampling

Table 6-6: Details of five CLL cases which appeared to acquire dysfunction between two sampling points.

Sample Number	Assay 1 result	Assay 2 result	Interval (months)	FISH 1	FISH 2	Mutations
1	Normal	Nutlin-responder	2	83% Del(11)q	83% Del(11)q	
2	Normal	Non-resonder	7	Normal	Normal	TP53 Miss-sense
3	Normal	Non-responder	11	46% Del(17)p	60% Del(17)p	TP53 Miss-sense
4	Normal	Non-responder	29	Normal	34% Del(17)p	TP53 2bp deletion
5	Normal	p21-failure	30	Normal	75% Del(17)p	TP53 Miss-sense

The 5 remaining cases gave differing dysfunctional responses to the assay at both time-points tested. Details for these cases are shown in Table 6-7. It can be seen that there were two cases in this group which also acquired an abnormal FISH result after previously testing normal.

Table 6-7: Details of CLL cases which appeared to change dysfunctional category between two sampling points (n=5).

Sample Number	Assay 1 result	Assay 2 result	Interval (months)	FISH 1	FISH 2	Mutations
1	Nutlin-responder	Normal	2	20% 17p	25% 17p	TP53 miss-sense
2	p21-failure	Non-responder	8	45% 17p	68% 17p	TP53 4bp insertion
3	p21-failure	Non-responder	12	Normal	Tetraploidy	TP53 Miss-sense
4	Nutlin-responder	Non-responder	23	Normal	68% 17p	
5	Nutlin-responder	Normal	46	78% 11q	88% 11q	

6.7 **Summary**

The work in this chapter has attempted to address any impact on assay results which arise from the logistical matters of assessing cases referred from other centres. It was initially determined that extremes of temperature or excessive handling may have an impact on results and so a more in depth assessment was made. It was first established that using the light scattering properties of cells determined by flow cytometric analysis to ascertain viability was correlated to more conventional methods. This metric was then used to analyse cell viability in samples from different sources (local and referred) which had been used in the present study. It was found that as a group samples which had been transported from other centres did have attenuated cell viability and this association was significant. Interestingly this significant association was lost for the subgroup with *TP53* abnormalities. In addition to

this the impact on p53 and p21 protein expression was investigated using the functional assay response data form cases with no detected abnormalities of *ATM* or *TP53*. Comparison of the 0-day group results to the 1-day or more group found that both p53 and p21 measurements were significantly different in all culture conditions. Investigating whether this attenuation would result in miss-classifying assay responses seemed to show that a delay of up to 2 days would not introduce sufficient change to result in falsely attributing dysfunction. However, the fact that the viability of samples was affected means that the null hypothesis for this section is accepted: 'Assay results will be affected by prolonged time between venesection of blood sample and storage of PBMCs'.

It has also been shown, by analysing sequential samples from the same individuals, that it is possible for the response obtained using the assay to change over time. It was also shown that this may represent the emergence of underlying genetic abnormalities or expansion of existing ones.

Chapter Seven:

Discussion & Conclusion

7.1 Introduction

This section will be split in to several smaller discussions dealing with the individual results chapters and particular topics that are relevant to the thesis / project as a whole.

7.2 Assay Discussion

The main stated aim of this project was to determine the validity of the functional assay, described herein, as a means to detect abnormalities of two important DNA damage response pathway genes (*TP53* and *ATM*) in primary CLL cells with the additional benefit of discriminating between the two. When the assay was first developed there were solid reasons for this aim. Fluorescent *in-situ* hybridisation (FISH) was and still is the only routine clinical test performed prior to therapy. FISH can detect with high sensitivity and specificity loss of the chromosomal loci containing genes of interest; which in the routine clinical setting often include *TP53* and *ATM*. It has been shown in section 3.4 (p90) that the assay can detect a dysfunctional response in cases which are known to have loss of 17p13.1 (*TP53*) or 11q22.3 (*ATM*). The data displayed in Table 3-6 (p91) shows that the response classification made possible by the addition of nutlin3a did discriminate between loss of either gene in cases which failed to respond to etoposide, fulfilling one of the main aims of this project. It was noticeable however that a large proportion of cases with deletion of 11q22-23 (31/68) did not display a dysfunctional response, or rather the response was not so severely impaired that the sample did not exceed the previously defined cut off values (Best et al. 2008). It is important to note that of 359 cases with a normal FISH result, 82 (23%) were found to have a dysfunctional response to the assay. These 82 cases did not display uniform dysfunction and were found in each of the different categories of dysfunction and it can be seen in Table 3-6 that they account for at least half of the cases in each category. This could be due in part to mutations of *ATM* or *TP53*, although this cannot explain all the cases as mutations of these genes are most commonly associated with deletion of the other allele and it is

unlikely that the cohort contains such a high proportion of cases with mutation in the absence of deletion (Skowronska et al. 2012; Austen et al. 2007; Zenz, Kröber, et al. 2008).

The results in section 3.5, (Table 3-11, p99) make it apparent that the ability of the assay to detect deleterious mutations was markedly different for *ATM* and *TP53* mutants. Mutations of *TP53* were regularly found to cause either high basal expression of the resting CLL cells or were associated with failure of p21 as either a non-responder or a p21-failure phenotype. In this study *ATM* mutations failed to account for cases with a nutlin-responder phenotype which contradicts the findings of previously published papers which have associated *ATM* mutations with failure to induce a DNA damage response (Best et al. 2008; Lin et al. 2012; Navrkalova et al. 2013).

Aside from the unexpected results there are also a number of other factors which require some discussion.

7.3 **Categorisation**

Categorisation of the sample responses using the assay described herein is complicated by taking into account data for two proteins, p53 and p21, which have been exposed to three different culture conditions (one control and two treated). For example one sample, after etoposide treatment, gave a p21-failure / Type-C response however after treatment with etoposide plus nutlin the sample gave a normal response. The question is therefore raised as to whether this case should be considered a p21-failure or a nutlin-responder? Most cases displaying a p21-failure response did so in both culture conditions and most cases classed as nutlin-responders gave a fully dysfunctional response to etoposide alone and a normal response to etoposide plus nutlin. Should the case in question be put in to a new group for cases such as these? If so then it would have been likely that across the whole cohort extra groups would have needed to be generated for a number of cases and given that these were rare instances there would have been no option to statistically analyse these groups. It is for this reason that it was decided to simply evaluate the sample response twice. Once on etoposide alone in order to call broadly normal and abnormal, and secondly a detailed categorisation of dysfunction that is independent. This independence keeps the analysis

simpler as it reduces the possible number of dysfunctional categories. The only exceptions to this rule were the cases with abnormal p53 over expression in the control culture which, as shown in the results section 3.6.1 (p102), is probably disposable for detecting p53 mutation if also measuring p21 expression.

Those few cases which displayed a non-classical response and were difficult to classify could have been retested. The reason for them not being retested was that the study aimed to test each individual case only once as this is closer to how the assay was envisaged to be used.

7.4 TP53 mutation, 17p deletion and non-responders: discussion

The functional assay was able to detect *TP53* abnormalities with considerable success. The observation that there are different dysfunctional phenotypes associated with these defects deserves further investigation to determine whether they are clinically distinct from each other in any way. The work by Lin *et al* (2012) has demonstrated differences in outcomes between their identified Type-A and Type-C cases, which are analogous to the p53-over expression and p21-failure categories, respectively.

Of the 20 cases in results section 3.5 (Table 3-11, p98) which were found to harbour some form of detected *TP53* abnormality, 16 (80%) were assigned to one of the functional categories associated with *TP53* defects. Of the remaining four only one was assigned to the nutlin-responder category. Three were classified as normal. It would be of interest to follow the progress of these cases. In particular the three normally functioning cases are of interest as it has been previously reported that some CLL cases with *TP53* abnormalities follow a benign clinical course (Best et al. 2009).

One important observation that was made was that 4/5 cases harbouring *TP53* mutations in the absence of 17p-deletion were successfully assigned to one of the *TP53*-associated dysfunctional categories. This is highly relevant as mutation screening is still not routinely performed and this identification of

cases with *TP53* mutation in the absence of 17p-deletion demonstrates the ability of the assay to detect high-risk patients who may be missed by conventional screening methods.

The raw data showing the spectrum of *TP53* mutations detected across our cohort was not included in the main results section. It was hoped to individually assess the impact on the DNA damage response of mutations occurring at different 'hotspots' within the *TP53* gene. A breakdown of mutation types including insertions and deletions would have been very interesting but unfortunately this was not directly relevant to the reporting of the assay results or the validation of the assay.

7.5 ATM mutation, 11q deletion and nutlin responders: discussion

The results in Table 3-6 (p91) show that of 68 cases with del11q22-23 as the sole abnormality detected using FISH, 31 (46%) returned a normal functional response to the assay. A similar observation has been made before (Carter et al., 2006). It could be that mutation of the remaining *ATM* allele is required for the nutlin-responder response and that the cases with normal function lacked a mutation on the remaining allele. Indeed *ATM* mutation alone was posited as the driving force behind the Type-2 response when the assay was first developed (Best et al., 2008b) but there is little evidence to support this hypothesis within the current study. Of the confirmed *ATM* mutations detected so far only those which result in a frame shift (presumably leading to a non-sense or truncated protein) can be linked to a dysfunctional response.

One possible explanation for different assay responses in cases with 11q deletion could be differences in the size of the lost region of chromosomal material on 11q22-23. Several other genes are known to reside in this region, including Mre11 and H2AX. Importantly, Mre11 forms part of the MRN complex which has a primary role in the sensing of double stranded DNA breaks and is upstream in the signalling cascade from ATM. It is therefore reasonable to hypothesise that loss of this gene, either in addition to, or

instead of, *ATM* may lead to a similar dysfunctional phenotype as seen in *ATM* dysfunctional cases. This could also be theoretically rescued by nutlin.

Published results from the UK LRF CLL4 trial found reduced survival in patients with bi-allelic ATM abnormalities (Skowronska et al., 2012). The previous work using the etoposide and nutlin assay had associated *ATM* mutations with dysfunctional responses (Best et al., 2008b). This section has shown that the nutlin-responder response is not as clearly linked to ATM abnormalities as was previously thought. In particular, the lack of cases with detected bi-allelic inactivation of *ATM* (mutation and deletion) was surprising. The only case in this restricted analysis with a confirmed biallelic ATM abnormality was categorised with a 'p21 failure' response; this genetic abnormality would have been predicted to give a 'nutlin-responder' categorisation and being the only example of its kind in this restricted analysis it seems to pose a problem. It is important to point out that this case illustrates one of the challenges of using a cut-off based system in combination with a mutli-step classification system. The case in question gave a dysfunctional response when cultured with etoposide only, eliciting no increase in the measured level of p21 protein and only a modest p53 increase (9% over control). The culture with etoposide plus nutlin gave a very strong p53 response (131%) yet p21 protein showed an increase to only 14%. Therefore despite the addition of nutlin eliciting a very strong p53 response this case failed to make the nutlin-responder category based solely on the p21 response being short of the cut-off by just 1%. This highlights that subjectivity as well as objectivity can be important in attempting to categorise functional responses.

Collaborators in Birmingham carried out mutation screening of the ATM gene. This work was performed by them due to their expertise in working with this gene. They have a previously published and peer-reviewed protocol for the screening of this large (68 exon) gene which employs high-performance liquid chromatography (HPLC) (Austen et al., 2008). The results provided to us covered exons 4-65 of the *ATM* gene. Those with an abnormal result were then sequenced to identify the exact sequence change.

Data was returned on 155 of the cases that were sent for testing. The data set however is not complete for all exons across all samples tested. Six exons in

particular appeared to be susceptible to failure. Data was only available for exons 4, 5, 11, 15, 26 and 39 for approximately half of all cases (46%, 50%, 51%, 47%, 46% and 56% respectively). For the 72 cases with results for exons 4 and 26 there was a very high incidence of polymorphism detection, 58/72 (81.6%) and 52/72 (72.2%) respectively. Of the 155 cases sent for analysis only 17 (11%) had results returned for every exon tested. Figure 7-1 shows the number of exons missing across the 155 samples in descending order. Samples for which data was missing on more than 20% of exons were recorded as untested for the purposes of the analyses in results section 3.5 (p98). The rationale for setting a cut point at 20% was simply that lowering it further would result in a drastic reduction in numbers. One case, which was an exception to this rule, had 2 mutations of *ATM* detected even though 27/62 (43.5%) of the exons had not given results. This was recorded as mutated, as further analysis would not alter the result, and entered in to the analysis. Novel sequence changes could not be verified as non-germline.

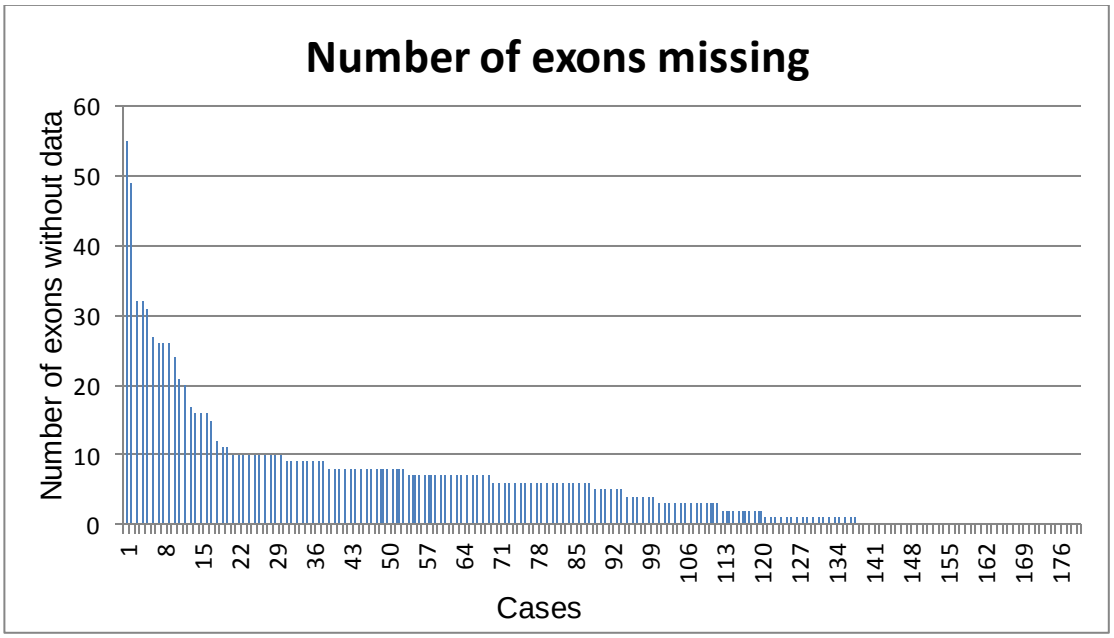

Figure 7-1: Histogram showing the number of exons with missing data across the 155 samples tested.

In general a sequence change was considered to be a mutation if it fulfilled any of the following criteria: previously reported as causative in A-T patients, predicted to affect a splicing site, lead to a premature truncation of the protein

(either through frameshifting or miss-sense introduction of Stop codon), was a short in-frame insertion or deletion, affected a residue conserved between Human and Mouse and/or affected a conserved domain within the protein. Despite the lack of data the incidence of *ATM* mutations in the cases included in section 3.5 (p98) was approximately what would be expected (~10%).

In addition to cases with *ATM* abnormalities and normal function it is also necessary to address those nutlin responding cases which were found to be free from any *ATM* abnormalities. There may be other gene or genes involved in the nutlin-responder response. This may be remote from ATM involving an abnormality somewhere else within the genome or it may be within or close to the 11q22-23 loci. Interesting candidates for the latter hypothesis are the genes for *MRE11* and *H2AFX* which both reside on chromosome 11q and have been recently shown to be often deleted in addition to *ATM* (Ouillette *et al*, 2010). Mutations of *MRE11* have been associated with ataxia telengiectasia-like disorder (Stewart *et al*, 1999). It may therefore be that del11q involves multiple genes in the same region and FISH cannot discriminate between loss that does or does not involve all three genes.

Nutlin responders with no detected *ATM* abnormalities could also possibly be due to over expression of MDM2, which would/could affect the damage response to etoposide and yet it would be overcome by nutlin. The activation of some oncogenes such as SKI, has been shown to increase SUMOlyation of MDM2 and subsequently increase the polyubiquitination of, and therefore degradation of, p53 (Ding et al., 2012). If an MDM2 related mechanism was repressing p53 activation in response to etoposide it could be reasonably assumed that nutlin would interrupt this, resulting in p53 activation and a nutlin-responder response to the assay conditions.

Another interesting observation, made in section 3.4.4 (Figure 3-5, p94), was that the proportion of cells with 11q-deletion was invariably either large (>70%) or small (<30%) with a lack of intermediate clone sizes like those seen for cases with 17p-deletion (Figure 3-4, p93). One explanation for this lack of cases with intermediate clone size is that cases with *ATM* deletion fall into relatively stable groups with either large or small clone sizes and that when or if a secondary event occurs it causes a relatively rapid expansion of the

deleted clone such that patients rarely present at clinic during the expansion event.

7.6 Investigating p21-failure: discussion

Although the findings of Chapter 4 (p106) highlighted the role of *TP53* mutation and deletion of 17p13.1 in the p21-failure response, and suggested one mechanism by which this phenotype can occur, there remain p21-failure cases with no detected abnormality of *TP53* or 17p13 and therefore no obvious means of explaining the response in this way. This does not necessarily rule out a diluted p53/p21 dysfunctional clone emerging within a responding clone as the Non-responder group also contains cases with a fully dysfunctional result yet no detected abnormalities of *TP53*.

One explanation for the discrepancy between the published results obtained using ionising radiation (Johnson et al. 2009) and results reported herein using etoposide is the possibility that the DNA damage responses elicited by these different mechanisms are not identical. The original work developing the etoposide and nutlin assay compared etoposide to IR and found them to be similar in terms of DNA damage induced, as detected by gamma-H2AX phosphorylation (Best et al., 2008b). Other comparisons of p53-dependant protein expression changes in response to ionising radiation or etoposide have shown them to be synonymous and similarly affected by p53 mutation (Jäämaa et al., 2010, Saleh et al., 2011). For example the pro-apoptotic protein BID has been shown to be activated by both IR and etoposide (Maas *et al*, 2011). Comparison of IR, UV and etoposide in a murine cell line has also shown that IR and etoposide provoke similar ATM and p53 dependant responses. These were themselves different to the response induced by UV, which resulted in phosphorylation of p53 protein at serine-389, a modification that neither IR or etoposide produced (Lu et al., 1998). However UV has been shown to differ from ionising radiation with a bias against the transcription of p21 in UV treated cells as opposed to IR treated cell (Bodzak et al., 2008). Post-translational modification has been shown to inhibit p53 transcriptional activity at the *CDKN1A* promoter in HCT116 cells after treatment with gemcitabine or chromium, creating a pro-death phenotype (Hill et al., 2011). However, treatment with IR or doxorubicin resulted in expression of p21 and a

pro-cell cycle arrest phenotype. It was shown that this difference in p53 transcription of the *CDKN1A* gene was achieved through altered phosphorylation of the p53 protein via interaction with DNA-PK_{cs}. These studies would suggest that no difference between IR and etoposide responses should be expected, however the work is all performed on cell lines. There does therefore remain the possibility that altered post-translational modification of p53 may be a factor in the p21-failure / Type-C responses for which no *TP53* gene abnormalities are detected.

Another possible reason for any discrepancy is that the responses are the same but the rates at which they occur are different, resulting in the sample being analysed at a point when the apoptotic targets of p53 are being expressed (late), not the cell cycle regulation targets (early). The difference in the incidence of p21 failure between that reported using the IR functional assay and the etoposide based assay could also be related to the different cut-off values used in the respective assays. The most comprehensive way to address this question would be a sample sharing scheme between two or more centres using the alternative assays.

Another issue that was encountered in section 4.3 (p109) was the different incidences in *CDKN1A* polymorphisms detected in our cohort and the previously published work which identified single nucleotide polymorphisms as the cause of the Type-C response (Johnson et al. 2009). In particular, determining that the two SNPs were linked in our cohort contradicts the original work by Johnson. After determining that the RFLP technique used initially gave unclear results the work was repeated using a much more sensitive and specific methodology, namely genotyping of both SNPs using Taqman™ technology. Pyrosequencing was also used to confirm the codon-31 results in a subset of those cases. Previously published studies also informed us that the finding of linkage between the two SNPs of interest was to be expected (Facher et al. 1997; Konishi et al. 2000; Taghavi et al. 2010). Taken together, our work here and previous studies provided us with the confidence required to suggest that the hypothesis relating *CDKN1A* SNPs to the p21-failure response may require revision.

7.7 **miR-34a Discussion**

The investigation of miR-34a confirmed the finding that basal expression is affected by *TP53* abnormalities in CLL. It was also demonstrated that the measurement of miR-34a could not detect abnormalities involving the *ATM* gene. This is not entirely unsurprising and does suggest that ATM does not play a significant part of miR-34a regulation in the absence of DNA damage. It may have been possible to detect ATM abnormalities if the response of miR-34a to DNA damage was investigated. This however would lead to a number of issues. The cells would need to be treated in a similar fashion to the etoposide and nutlin assay with relative quantification of the micro RNA being taken in each separate culture. It may well be likely that the same results would be seen as are seen with the flow cytometric measurement of p53 and p21. If this was the case then the same result would be achieved except that the analysis would be more costly, take longer to perform and would have been less reliable due to the increased handling of samples and the labile nature of RNA itself.

As a possible target for future work, the cluster of differentiation 44 (CD44) has recently been shown in prostate cancer cells to be directly repressed by miR-34a (Liu et al., 2011). That study also showed that knockdown of mir34a lead to increased expression of CD44. A comparison of leukocytes from healthy individuals and CLL patients has previously shown there to be no significant difference in the expression of CD44 (Belov et al., 2001). CD44 over-expression on CLL cells and its release as a serum marker has previously been shown to associate with advanced disease by both Binet and Rai scales and also the need for chemotherapy (Eisterer et al., 2004). CD44 expression in CLL has not yet been directly linked to *TP53* loss or mutation but the downregulation of miR-34a seen in the *TP53* mutated samples in this result section could lead to the hypothesis that those samples may display over-expression of surface and serum CD44 compared to the TP53 wildtype cases. This could be of interest as a cell surface target that can be used to infer p53 abnormalities could potentially be added to flow cytometry assessments much more easily than intra-cellular staining for protein.

7.8 **Sample validation discussion**

The preliminary work shown in section 6.3, (Figure 6-1, p146), suggested that the ambient conditions blood samples experienced between venesection of the peripheral whole blood and storage of the isolated PBMCs may have some impact on the viability of samples. The most pronounced effect was seen when the ambient temperature was allowed to reach 37^{o}C. Unsurprisingly, the data also show a general reduction in viability of CLL cells after 24 hours in culture. CLL cells experience spontaneous apoptosis *ex-vivo* and so this reduction is most likely a result of this. The data displayed in Table 6-1, again suggest that it may be possible for handling to affect functional assay results. The main problem with this preliminary work is the low numbers tested precludes statistical analysis. In addition, the extra handling of a sample required to set up the different ambient conditions for that experiment could have had an effect on the responses of the samples.

It was decided to analyse the assay data on the cohort for evidence of reduced cell viability or impaired assay responses between local and referral samples. To achieve this, data relating to the light scattering properties of the cells acquired during FACS analysis was used as a surrogate method of estimating the proportion of non-apoptotic, viable cells in the sample. A comparison of the light scatter data to results obtained using the trypan-blue exclusion test of viability was made for 64 samples and the results found a significant correlation between to two methods (Figure 6-2, p149). Establishing that the use of light-scattering properties could be interpreted as a guide to cell viability in section 6.4.2 (p148) facilitated the subsequent analysis in sections 6.4.3-6.4.5 (pp149-154). This was an attempt to make the most of the available flow cytometric data and also to find a method for investigating cell viability retrospectively. It would have been preferable to be able to use a more rigorous method during the actual experimental work, for example staining with Annexin V and propidium iodide can give very detailed information concerning the stage of apoptosis and it is a flow cytometry based technique which would have been ideal for use. However given the numbers of samples to be tested it would have likely led to a considerable cost increase and further complicated the benchwork associated with the assay.

It was decided to analyse the assay data on the cohort for evidence of reduced cell viability or impaired assay responses between local and referral samples. To achieve this, the light scattering properties of the cells during FACS analysis were used as a surrogate method of estimating the proportion of non-apoptotic, live cells in the sample. Firstly this data was compared to results obtained using the trypan-blue exclusion test of viability. Data was generated for 64 samples and the results found a significant correlation between to two methods (Figure 6-2, p149). This allowed for potential effects upon viability and assay response to be assessed retrospectively on a larger number of previously assayed samples. This was also a money saving alternative to retesting those samples which had already been analysed using the assay. In addition to the percentage of live cells, the measured MFI data for p53 and p21 was also analysed for differences between local and referred samples.

Within the samples that had taken less than a day to be processed it was interesting to note that those with *TP53* abnormalities had lower viabilities than those samples with *ATM* abnormalities or those with no abnormalities of either gene (Figure 6-9, p158). This relationship wasn't seen in the samples which had taken a day or more to arrive in Bournemouth. In addition the viabilities of wildtype or *ATM* abnormal cases seem to be reduced in samples with a day or more between venesection and processing, whereas the cases with *TP53* involvement had similar viabilities regardless of the duration of time between venesection and arrival in Bournemouth. A possible explanation for this observation is the involvement of p53 in the cellular response to oxidative stress and hypoxia. Wildtype p53 has a cyto-protective role to play under these conditions and so its loss of action may have a short term disadvantage. Alternatively, the higher lymphocyte count of whole blood samples with *TP53* abnormalities may simply mean that the samples became depleted of oxygen faster than other samples and this led to a more acute short term impact on viability.

Whilst there was a statistically significant effect introduced by transport on both the viability of cells and the responses of p53 and p21 to drug treatment it was demonstrated that this is not likely to be severe enough to cause the

misclassification of normal responding samples as abnormal (Figure 6-13, p164 & Figure 6-14, p165). The question of whether *ex-vivo* analysis of the DNA damage response in primary CLL cells meaningfully relates to the *in-vivo* responses of the same cells is not possible to address. Certainly the role of the micro-environment in tumour cell behaviour cannot be over-estimated in terms of cell activation and proliferation but any effects concerning the acquisition of therapy resistance are not understood. The effects of chemokine inhibitors such as CAL-101 and PC-2375 in flushing CLL cells from lymphoid tissues suggests that in some if not many cases the CLL cells circulating in the peripheral blood may not be completely akin to those residing in lymphatic tissues. This therefore, is a criticism of all *in-vitro* analysis.

The work in the sample validation chapter demonstrates that there is some impact upon functional analysis introduced by transporting blood samples. Testing samples that have spent three or more days in transit is feasible but not recommended and an element of caution would need to be taken. Any results that are close to the established cut-offs would require further analysis.

7.9 Functional assay in a clinical versus research setting

The potential use of functional assays in a clinical setting may be limited. Despite the significant relationships seen between response patterns and cytogenetic or genetic abnormalities, there are sufficient cases with unexpected responses to suggest that there are unknown factors involved.

It had been hoped to analyse treatment and response data for the cohort to determine if the assay was able to predict the response to therapy. Whilst this data was available for a proportion of the cases tested with the assay there were complications which made generating meaningful results difficult.

An analysis of the incidence of previous treatment was made in Table 3-12 and Table 3-13 in section 3.7 (p104) for 121 cases with that data available. It was shown that there was a slight trend for the previously treated group to contain more cases with either a genetic abnormality of *TP53* or a dysfunctional assay response than the treatment naïve group. However the low numbers in many of the groups may have had an effect on statistical analyses.

An analysis of the response to therapy which occurred subsequent to the patient being sampled was not included. Data on subsequent treatment type and response was available for 91 cases; 45 who at the time of sampling were 'treatment naïve' and 46 who had been treated previously. It was however realised that the patients would have been treated by clinicians who would have based treatment decisions on existing FISH results and other clinical data available to them. Therefore it was highly likely that the cases with deletion of 17p or 11q may be skewed towards particular therapy regimens containing antibody therapy such as alemtuzumab or rituximab. In addition to this there were a total of sixteen different therapies or combinations of therapies used and this meant that many groups had very low numbers, again making reliable statistical analysis unlikely. What this problem does highlight is that testing and validating an assay such as that used in this work would be best achieved with the controls on therapy choice and data collection associated with a clinical trial.

One further issue regarding the potential clinical relevance of the assay used in this project is how it relates to the current advances in treatment therapies.

Clinicians are now able to access a greater variety of drugs for patients through clinical trials which do not employ DNA damage to kill tumour cells. In addition to immunotherapies such as rituximab, drugs targeting pro-survival signalling in CLL are showing great promise. A recent multicentre, phase 3 study, randomly assigned 391 patients with relapsed or refractory CLL or SLL to receive either ibrutinib or the anti-CD20 antibody ofatumumab (Byrd et al., 2014b). The analysis of progression-free survival in these two groups showed that ibrutinib had an advantage over the antibody therapy. Median progression-free survival was not reached after a median follow-up of 9.4 months whilst the median progression-free survival for the ofatumumab treated arm was reached at 8.1 months. The sub-group of patients with deletion of 17p13.1 in the ibrutinib arm also did not reach median progression-free survival, compared to a median of 5.8 months for the 17p deleted patients in the ofatumumab arm. However it has to be noted that patients on ibrutinib did eventually progress with approximately a third having progressed after 12 months. In addition to this a reported case of ibrutinib resistance in a patient lead to the characterisation of a novel, selected, functional mutation of the *BTK* gene which disrupts the binding of ibrutinib to the Bruton's tyrosine kinase protein (Cheng et al., 2014). As new pathways are exploited for therapeutic benefits it becomes necessary to find new ways to study them. It is quite appropriate to think that a flow cytometry based assay could be adapted to monitor the efficacy of drugs like ibrutinib. This may be especially warranted as ibrutinib is a daily, oral medication that patients currently stay on for as long as benefits persist.

7.10 Future Direction

Ideally the next stage of development for the assay used in this work would be for it to be performed in tandem with a stage III clinical trial involving any therapy of combination therapy which contains a drug that is reliant upon the ATM/p53 pathway for efficacy. It should also be performed prospectively rather than retrospectively to eliminate any issues of sample viability due to long term storage. This would allow the assay results to be compared with the outcome data when the follow-up period is over. The main issue with this would be that the testing of samples would therefore be performed five or more years before the survival and outcome data is released. Despite that, this would be the most powerful way of answering questions about the different functional categories and their relationship to outcomes, especially for dysfunctional cases with no high risk markers. With increasing ease of access to, and the gradually reducing cost of, next generation sequencing technologies, it may be possible to look for new mutations in CLL cells which affect the ATM/p53 pathway by investigating those cases with dysfunction in the absence of known high risk markers if they are found to have poorer outcomes than normal cases.

Another direction in which this kind of project could be taken would be to investigate adapting the assay to predict treatment responses for the newer classes of drugs which are becoming increasingly more relevant in CLL therapy. This includes inhibitors of proteins in B-cell receptor signalling pathways or apoptosis/ cell survival pathways as well as immunotherapies. This would therefore involve the detection of activation, or inhibition, of the cellular pathways relevant to these new therapies, for example detecting the successful inhibition of Bruton's tyrosine kinase (BTK) mediated BCR-signalling in CLL cells treated by ibrutinib or acalabrutinib. However, detection of p53 abnormalities may remain relevant even to these new treatments as mutant p53 is likely to have an impact on cellular pathways other than just the DNA damage response.

7.11 Conclusion

The stated aims of this project were to (i) determine the value of the etoposide/nutlin3a functional assay for detecting patients with abnormalities of the ATM/p53-dependant DNA damage response which would contra-indicate treatment with alkylating agents or purine analogues; and, (ii) test the ability of the assay to discriminate between ATM and p53 abnormalities as these have differing prognostic impact in CLL.

Broadly, the project fulfilled these aims. It has been determined that the assay does detect *TP53* mutations and deletion of 17p and that the use of nutlin is effective at separating the p53 dysfunctional cases from ATM dysfunctional cases. Despite this many cases with ATM abnormalities were classified as having normal responses to the assay conditions with *ATM* mutations in particular not showing the impaired DNA damage response to etoposide that had been expected. The assay also detected many cases with apparent dysfunction of the DNA damage response for reasons other than involvement of p53 or ATM.

This work has also shown that p21 failure is a characteristic of all the dysfunctional categories described herein. It should be considered that p21 protein expression is a more uniform indicator of a failure of the ATM-p53 pathway than p53 protein expression.

It is likely that the functional assessment of primary CLL cells may serve better as a research tool rather than a clinical test simply because the therapeutic options available for clinicians are rapidly developing. However, until these assays are performed prospectively, as an associated part of a clinical trial, it will be difficult to tell for sure how well the dysfunctional responses relate to patient outcomes. This is particularly true for those cases with no other high risk markers.

Published journal articles and posters

Articles

BEST,O., GARDINER,A., DAVIS,Z., **TRACY,I**., IBBOTSON,R., MAJID,A., DYER,M., OSCIER,D., 2009. A subset of Binet stage A CLL patients with *TP53* abnormalities and mutated IGHV genes have stable disease. *Leukemia*. **(23)** pp212-214 (Currently cited 10 times)

ZENZ,T., VOLLMER,D., TRBUSEK,M., SMARDOVA,J., BENNER,A., SOUSSI,T., HELFERICH,H., HEUBERGER,M., HOTH,P., FUGE,M., DENZEL,T., HABE,S., MALCIKOVA,J., KUGLIK,P., TRUONG,S., PATTEN,N., WU,L., OSCIER,D., IBBOTSON,R., GARDINER,A., **TRACY,I**., LIN,K., PETTITT,A., POSPISLOVA,S., MAYER,J., HALLEK,M., DOHNER,H., STILGENBAUER,S., 2010. *TP53* mutation profile in chronic lymphocytic leukaemia: evidence for a disease specific profile from a comprehensive analysis of 268 mutations. *Leukemia*. **(24)** pp2072-2079

PEPPER,C., MAJID,A., LIN,T., HEWAMANA,S., PRATT,G., WALEWSKA,R., GESK,S., SIEBERT,R., DAVID,Z., **TRACY,I**., GARDINER,A., BRENNAN,P., HILLS,R., DYER,M., OSCIER,D., FEGAN,C., 2010. Defining the prognosis of early stage CLL patients. *British Journal of Haematology.* **(156)** pp499-507

GARDINER,A., PARKER,H., GLIDE,S., MOULD,S., ROBINSON,H., **TRACY,I**.,STANKOVIC,T., OSCIER,D., STREFFORD,J., 2012. A new minimal deleted region at 11q22.3 reveals the importance of interpretation of diminished FISH signals and the choice of probe for ATM deletion screening in chronic lymphocytic leukemia. *Leukemia Research*. **(36)** pp307-310

MALCIKOVA,J., STALIKA,E., DAVIS,Z., PLEVOVA,K., TRBUSEK,M., MANSOURI,L., SCARFO,L., BALIAKAS,P., GARDINER,A., SUTTON,LA., FRANCOVA,HS., AGATHANGELIDIS,A., ANAGNOSTOPOULAS., **TRACY,I**., MAKRIS,A., SMARDOVA,J., GHIA,P., BELESSI,C., GONZALEZ,D., ROSENQUIST,R., OSCIER,D., POSPISILOVA,S., STAMATOPOULOS,K., 2014. The frequency of TP53 gene defects differs between chronic lymphocytic leukemia subgroups harbouring distinct antigen receptors. *British Journal of Haemotology*. **(166)** pp621-625

Oral presentation and poster

Presented at the 13th IwCLL conference, Barcelona. October 2009.

TRACY,I., PARKER,A., BEST,OG., MAJID,A., STANKOVIC,T., DYER,M., OSCIER,D. Type-C p53 pathway dysfunction resulting from the presence of an emerging *TP53* mutated sub-clone in CLL.

Contributions to posters

Presented at the 13th IwCLL conference, Barcelona. October 2009.

GARDINER,A., PARKER,H., GLIDE,S., MOULD,S., **TRACY,I**.,ROBINSON,H., STANKOVIC,T., STREFFORD,J., OSCIER,D. Screening for ATM by FISH: size matters.

MAJID,A., WALEWSKA,R., **TRACY,I**., GESK,S., HARDER,L., SIEBERT,R., KENNEDY,D., OSCIER,D., WAGNER,S., DYER,M. Clinical outcome in patients with *TP53* dysfunction- a subgroup with good clinical prognosis.

PEPPER,C., MAJID,A., LIN,S., HEWAMANA,S., PRATT,G., WALEWSKA,R., GESK,S., SIEBERT,R., DAVIS,Z., **TRACY,I**., GARDINER,A., BRENNAN,P., DYER,M., OSCIER,D., FEGAN,C., Concordant IGVH gene mutation status and CD38 expression offers the most reliable prognostic information for stage A CLL patients.

References

ALDERBORN, A., KRISTOFFERSON, A. & HAMMERLING, U. 2000. Determination of single-nucleotide polymorphisms by real-time pyrophosphate DNA sequencing. *Genome Res,* 10**,** 1249-58.

ASSLABER, D., PINON, J. D., SEYFRIED, I., DESCH, P., STOCHER, M., TINHOFER, I., EGLE, A., MERKEL, O. & GREIL, R. 2010. microRNA-34a expression correlates with MDM2 SNP309 polymorphism and treatment-free survival in chronic lymphocytic leukemia. *Blood,* 115**,** 4191-7.

AUSTEN, B., BARONE, G., REIMAN, A., BYRD, P. J., BAKER, C., STARCZYNSKI, J., NOBBS, M. C., MURPHY, R. P., ENRIGHT, H., CHAILA, E., QUINN, J., STANKOVIC, T., PRATT, G. & TAYLOR, A. M. R. 2008. Pathogenic ATM mutations occur rarely in a subset of multiple myeloma patients. *British Journal of Haematology,* 142**,** 925-933.

AUSTEN, B., SKOWRONSKA, A., BAKER, C., POWELL, J. E., GARDINER, A., OSCIER, D., MAJID, A., DYER, M., SIEBERT, R., TAYLOR, A. M., MOSS, P. A. & STANKOVIC, T. 2007. Mutation status of the residual ATM allele is an important determinant of the cellular response to chemotherapy and survival in patients with chronic lymphocytic leukemia containing an 11q deletion. *J Clin Oncol,* 25**,** 5448-57.

BARAKAT, K., MANE, J., FRIESEN, D. & TUSZYNSKI, J. 2010. Ensemble-based virtual screening reveals dual-inhibitors for the p53-MDM2/MDMX interactions. *J Mol Graph Model,* 28**,** 555-68.

BARTEL, D. P. 2004. MicroRNAs: Genomics, Biogenesis, Mechanism, and Function. *Cell,* 116**,** 281-297.

BARTEL, D. P. 2009. MicroRNAs: target recognition and regulatory functions. *Cell,* 136**,** 215-33.

BEIJNEN, J. H. 1994. p53 selected as molecule of the year 1993. *Pharmacy World and Science,* 16**,** 1-1.

BELOV, L., DE LA VEGA, O., DOS REMEDIOS, C. G., MULLIGAN, S. P. & CHRISTOPHERSON, R. I. 2001. Immunophenotyping of Leukemias Using a Cluster of Differentiation Antibody Microarray. *Cancer Research,* 61**,** 4483-4489.

BENE, M. C., NEBE, T., BETTELHEIM, P., BULDINI, B., BUMBEA, H., KERN, W., LACOMBE, F., LEMEZ, P., MARINOV, I., MATUTES, E., MAYNADIE, M., OELSCHLAGEL, U., ORFAO, A., SCHABATH, R., SOLENTHALER, M., TSCHURTSCHENTHALER, G., VLADAREANU, A. M., ZINI, G., FAURE, G. C. & PORWIT, A. 2011. Immunophenotyping of acute leukemia and lymphoproliferative disorders: a consensus proposal of the European LeukemiaNet Work Package 10. *Leukemia,* 25**,** 567-574.

BEST, O. G., GARDINER, A. C., DAVIS, Z. A., TRACY, I., IBBOTSON, R. E., MAJID, A., DYER, M. J. S. & OSCIER, D. G. 2008a. A subset of Binet stage A CLL patients with TP53 abnormalities and mutated IGHV genes have stable disease. *Leukemia,* 23**,** 212-214.

BEST, O. G., GARDINER, A. C., MAJID, A., WALEWSKA, R., AUSTEN, B., SKOWRONSKA, A., IBBOTSON, R., STANKOVIC, T., DYER, M. J. S. & OSCIER, D. G. 2008b. A novel functional assay using etoposide plus

nutlin-3a detects and distinguishes between ATM and TP53 mutations in CLL. *Leukemia,* 22**,** 1456-1459.

BIENZ, B., ZAKUT-HOURI, R., GIVOL, D. & OREN, M. 1984. Analysis of the gene coding for the murine cellular tumour antigen p53. *EMBO J,* 3**,** 2179-83.

BINET, J. L., AUQUIER, A., DIGHIERO, G., CHASTANG, C., PIGUET, H., GOASGUEN, J., VAUGIER, G., POTRON, G., COLONA, P., OBERLING, F., THOMAS, M., TCHERNIA, G., JACQUILLAT, C., BOIVIN, P., LESTY, C., DUAULT, M. T., MONCONDUIT, M., BELABBES, S. & GREMY, F. 1981. A new prognostic classification of chronic lymphocytic leukemia derived from a multivariate survival analysis. *Cancer,* 48**,** 198-206.

BLAGOSKLONNY, M. V. 2000. p53 from complexity to simplicity: mutant p53 stabilization, gain-of-function, and dominant-negative effect. *FASEB J,* 14**,** 1901-7.

BODZAK, E., BLOUGH, M. D., LEE, P. W. K. & HILL, R. 2008. p53 binding to the p21 promoter is dependent on the nature of DNA damage. *Cell Cycle,* 7**,** 2535-2543.

BOELENS, J., PHILIPPE, J. & OFFNER, F. 2007. B-CLL cells from lymph nodes express higher ZAP-70 levels than B-CLL cells from peripheral blood. *Leuk Res,* 31**,** 719-20.

BROSH, R. & ROTTER, V. 2009. When mutants gain new powers: news from the mutant p53 field. *Nat Rev Cancer,* 9**,** 701-13.

BULIAN, P., SHANAFELT, T. D., FEGAN, C., ZUCCHETTO, A., CRO, L., NUCKEL, H., BALDINI, L., KURTOVA, A. V., FERRAJOLI, A., BURGER, J. A., GAIDANO, G., DEL POETA, G., PEPPER, C., ROSSI, D. & GATTEI, V. 2014. CD49d is the strongest flow cytometry-based predictor of overall survival in chronic lymphocytic leukemia. *J Clin Oncol,* 32**,** 897-904.

BYRD, J. C., BROWN, J. R., O'BRIEN, S., BARRIENTOS, J. C., KAY, N. E., REDDY, N. M., COUTRE, S., TAM, C. S., MULLIGAN, S. P., JAEGER, U., DEVEREUX, S., BARR, P. M., FURMAN, R. R., KIPPS, T. J., CYMBALISTA, F., POCOCK, C., THORNTON, P., CALIGARIS-CAPPIO, F., ROBAK, T., DELGADO, J., SCHUSTER, S. J., MONTILLO, M., SCHUH, A., DE VOS, S., GILL, D., BLOOR, A., DEARDEN, C., MORENO, C., JONES, J. J., CHU, A. D., FARDIS, M., MCGREIVY, J., CLOW, F., JAMES, D. F. & HILLMEN, P. 2014a. Ibrutinib versus Ofatumumab in Previously Treated Chronic Lymphoid Leukemia. *New England Journal of Medicine,* 371**,** 213-223.

BYRD, J. C., BROWN, J. R., O'BRIEN, S., BARRIENTOS, J. C., KAY, N. E., REDDY, N. M., COUTRE, S., TAM, C. S., MULLIGAN, S. P., JAEGER, U., DEVEREUX, S., BARR, P. M., FURMAN, R. R., KIPPS, T. J., CYMBALISTA, F., POCOCK, C., THORNTON, P., CALIGARIS-CAPPIO, F., ROBAK, T., DELGADO, J., SCHUSTER, S. J., MONTILLO, M., SCHUH, A., DE VOS, S., GILL, D., BLOOR, A., DEARDEN, C., MORENO, C., JONES, J. J., CHU, A. D., FARDIS, M., MCGREIVY, J., CLOW, F., JAMES, D. F., HILLMEN, P. & INVESTIGATORS, R. 2014b. Ibrutinib versus ofatumumab in previously treated chronic lymphoid leukemia. *N Engl J Med,* 371**,** 213-23.

CAI, Z., CHEHAB, N. H. & PAVLETICH, N. P. 2009. Structure and activation mechanism of the CHK2 DNA damage checkpoint kinase. *Mol Cell,* 35**,** 818-29.

CALABRETTA, B., KACZMAREK, L., SELLERI, L., TORELLI, G., MING, P. M., MING, S. C. & MERCER, W. E. 1986. Growth-dependent expression of human Mr 53,000 tumor antigen messenger RNA in normal and neoplastic cells. *Cancer Res,* 46**,** 5738-42.

CARTER, A., LIN, K., SHERRINGTON, P. D., ATHERTON, M., PEARSON, K., DOUGLAS, A., BURFORD, A., BRITO-BABAPULLE, V., MATUTES, E., CATOVSKY, D. & PETTITT, A. R. 2006. Imperfect correlation between p53 dysfunction and deletion of TP53 and ATM in chronic lymphocytic leukaemia. *Leukemia,* 20**,** 737-40.

CARTER, A., LIN, K., SHERRINGTON, P. D. & PETTITT, A. R. 2004a. Detection of p53 dysfunction by flow cytometry in chronic lymphocytic leukaemia. *British Journal of Haematology,* 127**,** 425-428.

CARTER, A., LIN, K., SHERRINGTON, P. D. & PETTITT, A. R. 2004b. Detection of p53 dysfunction by flow cytometry in chronic lymphocytic leukaemia. *Br J Haematol,* 127**,** 425-8.

CARTER, S. & VOUSDEN, K. H. 2009. Modifications of p53: competing for the lysines. *Curr Opin Genet Dev,* 19**,** 18-24.

CHAN, A. C., IWASHIMA, M., TURCK, C. W. & WEISS, A. 1992. ZAP-70: a 70 kd protein-tyrosine kinase that associates with the TCR zeta chain. *Cell,* 71**,** 649-62.

CHANG, H., JIANG, A. M. & QI, C. X. 2010. Aberrant nuclear p53 expression predicts hemizygous 17p (TP53) deletion in chronic lymphocytic leukemia. *Am J Clin Pathol,* 133**,** 70-4.

CHANG, H., YEUNG, J., QI, C. & XU, W. 2007. Aberrant nuclear p53 protein expression detected by immunohistochemistry is associated with hemizygous P53 deletion and poor survival for multiple myeloma. *Br J Haematol,* 138**,** 324-9.

CHEN, L., WIDHOPF, G., HUYNH, L., RASSENTI, L., RAI, K. R., WEISS, A. & KIPPS, T. J. 2002. Expression of ZAP-70 is associated with increased B-cell receptor signaling in chronic lymphocytic leukemia. *Blood,* 100**,** 4609-14.

CHENG, S., GUO, A., LU, P., MA, J., COLEMAN, M. & WANG, Y. L. 2014. Functional characterization of BTK mutation that confers ibrutinib resistance: exploration of alternative kinase inhibitors. *Leukemia*.

CHO, Y., GORINA, S., JEFFREY, P. D. & PAVLETICH, N. P. 1994. Crystal structure of a p53 tumor suppressor-DNA complex: understanding tumorigenic mutations. *Science,* 265**,** 346-55.

COIFFIER, B., LEPRETRE, S., PEDERSEN, L. M., GADEBERG, O., FREDRIKSEN, H., VAN OERS, M. H., WOOLDRIDGE, J., KLOCZKO, J., HOLOWIECKI, J., HELLMANN, A., WALEWSKI, J., FLENSBURG, M., PETERSEN, J. & ROBAK, T. 2008. Safety and efficacy of ofatumumab, a fully human monoclonal anti-CD20 antibody, in patients with relapsed or refractory B-cell chronic lymphocytic leukemia: a phase 1-2 study. *Blood,* 111**,** 1094-100.

COLOMER, A., ERILL, N., VERDU, M., ROMAN, R., VIDAL, A., CORDON-CARDO, C. & PUIG, X. 2003. Lack of p53 nuclear immunostaining is

not indicative of absence of TP53 gene mutations in colorectal adenocarcinomas. *Appl Immunohistochem Mol Morphol,* 11**,** 130-7.

CORCORAN, M., PARKER, A., ORCHARD, J., DAVIS, Z., WIRTZ, M., SCHMITZ, O. J. & OSCIER, D. 2005. ZAP-70 methylation status is associated with ZAP-70 expression status in chronic lymphocytic leukemia. *Haematologica,* 90**,** 1078-88.

CRAWFORD, L. V., PIM, D. C., GURNEY, E. G., GOODFELLOW, P. & TAYLOR-PAPADIMITRIOU, J. 1981. Detection of a common feature in several human tumor cell lines--a 53,000-dalton protein. *Proc Natl Acad Sci U S A,* 78**,** 41-5.

CRESPO, M., BOSCH, F., VILLAMOR, N., BELLOSILLO, B., COLOMER, D., ROZMAN, M., MARCE, S., LOPEZ-GUILLERMO, A., CAMPO, E. & MONTSERRAT, E. 2003. ZAP-70 expression as a surrogate for immunoglobulin-variable-region mutations in chronic lymphocytic leukemia. *N Engl J Med,* 348**,** 1764-75.

CRO, L., FERRARIO, A., LIONETTI, M., BERTONI, F., ZUCAL, N. N., NOBILI, L., FABRIS, S., TODOERTI, K., CORTELEZZI, A., GUFFANTI, A., GOLDANIGA, M., MARCHESELLI, L., NERI, A., LAMBERTENGHI-DELILIERS, G. & BALDINI, L. 2010. The clinical and biological features of a series of immunophenotypic variant of B-CLL. *Eur J Haematol,* 85**,** 120-9.

CROWTHER-SWANEPOEL, D., MANSOURI, M., ENJUANES, A., VEGA, A., SMEDBY, K. E., RUIZ-PONTE, C., JURLANDER, J., JULIUSSON, G., MONTSERRAT, E., CATOVSKY, D., CAMPO, E., CARRACEDO, A., ROSENQUIST, R. & HOULSTON, R. S. 2010. Verification that common variation at 2q37.1, 6p25.3, 11q24.1, 15q23, and 19q13.32 influences chronic lymphocytic leukaemia risk. *British Journal of Haematology,* 150**,** 473-479.

CULLEN, B. R. 2011. Viruses and microRNAs: RISCy interactions with serious consequences. *Genes Dev,* 25**,** 1881-94.

DAL-BO, M., BERTONI, F., FORCONI, F., ZUCCHETTO, A., BOMBEN, R., MARASCA, R., DEAGLIO, S., LAURENTI, L., EFREMOV, D. G., GAIDANO, G., DEL POETA, G. & GATTEI, V. 2009. Intrinsic and extrinsic factors influencing the clinical course of B-cell chronic lymphocytic leukemia: prognostic markers with pathogenetic relevance. *J Transl Med,* 7**,** 76.

DAMLE, R. N., WASIL, T., FAIS, F., GHIOTTO, F., VALETTO, A., ALLEN, S. L., BUCHBINDER, A., BUDMAN, D., DITTMAR, K., KOLITZ, J., LICHTMAN, S. M., SCHULMAN, P., VINCIGUERRA, V. P., RAI, K. R., FERRARINI, M. & CHIORAZZI, N. 1999. Ig V gene mutation status and CD38 expression as novel prognostic indicators in chronic lymphocytic leukemia. *Blood,* 94**,** 1840-7.

DE JAGER, M., VAN NOORT, J., VAN GENT, D. C., DEKKER, C., KANAAR, R. & WYMAN, C. 2001. Human Rad50/Mre11 is a flexible complex that can tether DNA ends. *Mol Cell,* 8**,** 1129-35.

DE OLIVEIRA, F. M., BRANDAO, R. A., LEITE-CUEVA, S. D., DE PAULA CARETA, F., SIMOES, B. P., REGO, E. M. & FALCAO, R. P. 2010. Tetrasomy 8 in a patient with chronic lymphocytic leukemia. *Cancer Genet Cytogenet,* 198**,** 166-9.

DE VIRON, E., KNOOPS, L., CONNEROTTE, T., SMAL, C., MICHAUX, L., SAUSSOY, P., VANNUFFEL, P., BEERT, E., VEKEMANS, M. C., HERMANS, C., BONTEMPS, F. & VAN DEN NESTE, E. 2009. Impaired up-regulation of polo-like kinase 2 in B-cell chronic lymphocytic leukaemia lymphocytes resistant to fludarabine and 2-chlorodeoxyadenosine: a potential marker of defective damage response. *Br J Haematol,* 147**,** 641-52.

DEAGLIO, S., AYDIN, S., GRAND, M. M., VAISITTI, T., BERGUI, L., D'ARENA, G., CHIORINO, G. & MALAVASI, F. 2010. CD38/CD31 interactions activate genetic pathways leading to proliferation and migration in chronic lymphocytic leukemia cells. *Mol Med,* 16**,** 87-91.

DELEO, A. B., JAY, G., APPELLA, E., DUBOIS, G. C., LAW, L. W. & OLD, L. J. 1979. Detection of a transformation-related antigen in chemically induced sarcomas and other transformed cells of the mouse. *Proc Natl Acad Sci U S A,* 76**,** 2420-4.

DEWSON, G. & KLUCK, R. M. 2009. Mechanisms by which Bak and Bax permeabilise mitochondria during apoptosis. *Journal of Cell Science,* 122**,** 2801-2808.

DI AGOSTINO, S., STRANO, S., EMILIOZZI, V., ZERBINI, V., MOTTOLESE, M., SACCHI, A., BLANDINO, G. & PIAGGIO, G. 2006. Gain of function of mutant p53: The mutant p53/NF-Y protein complex reveals an aberrant transcriptional mechanism of cell cycle regulation. *Cancer cell,* 10**,** 191-202.

DING, B., SUN, Y. & HUANG, J. 2012. Overexpression of SKI oncoprotein leads to p53 degradation through regulation of MDM2 protein sumoylation. *J Biol Chem,* 287**,** 14621-30.

DOHNER, H., STILGENBAUER, S., DOHNER, K., BENTZ, M. & LICHTER, P. 1999. Chromosome aberrations in B-cell chronic lymphocytic leukemia: reassessment based on molecular cytogenetic analysis. *J Mol Med (Berl),* 77**,** 266-81.

DOHNER, H., STILGENBAUER, S., FISCHER, K., BENTZ, M. & LICHTER, P. 1997a. Cytogenetic and molecular cytogenetic analysis of B cell chronic lymphocytic leukemia: specific chromosome aberrations identify prognostic subgroups of patients and point to loci of candidate genes. *Leukemia,* 11 Suppl 2**,** S19-24.

DOHNER, H., STILGENBAUER, S., JAMES, M. R., BENNER, A., WEILGUNI, T., BENTZ, M., FISCHER, K., HUNSTEIN, W. & LICHTER, P. 1997b. 11q deletions identify a new subset of B-cell chronic lymphocytic leukemia characterized by extensive nodal involvement and inferior prognosis. *Blood,* 89**,** 2516-22.

DUROT, E., PATEY, M., LUQUET, I., GAILLARD, B., KOLB, B. & DELMER, A. 2012. An aggressive B-cell lymphoma with rearrangements of MYC and CCND1 genes: a rare subtype of double-hit lymphoma. *Leuk Lymphoma*.

DZIKIEWICZ-KRAWCZYK, A. 2008. The importance of making ends meet: mutations in genes and altered expression of proteins of the MRN complex and cancer. *Mutat Res,* 659**,** 262-73.

EISTERER, W., BECHTER, O., SÖDERBERG, O., NILSSON, K., TEROL, M., GREIL, R., THALER, J., HEROLD, M., FINKE, L., GÜNTHERT, U., MONTSERRAT, E. & STAUDER, R. 2004. Elevated levels of soluble

CD44 are associated with advanced disease and in vitro proliferation of neoplastic lymphocytes in B-cell chronic lymphocytic leukaemia. *Leukemia research,* 28**,** 1043-1051.

ERSTER, S., MIHARA, M., KIM, R. H., PETRENKO, O. & MOLL, U. M. 2004. In vivo mitochondrial p53 translocation triggers a rapid first wave of cell death in response to DNA damage that can precede p53 target gene activation. *Mol Cell Biol,* 24**,** 6728-41.

FERRAJOLI, A., LEE, B. N., SCHLETTE, E. J., O'BRIEN, S. M., GAO, H., WEN, S., WIERDA, W. G., ESTROV, Z., FADERL, S., COHEN, E. N., LI, C., REUBEN, J. M. & KEATING, M. J. 2008. Lenalidomide induces complete and partial remissions in patients with relapsed and refractory chronic lymphocytic leukemia. *Blood,* 111**,** 5291-7.

FONSECA, S. B., PEREIRA, M. P., MOURTADA, R., GRONDA, M., HORTON, K. L., HURREN, R., MINDEN, M. D., SCHIMMER, A. D. & KELLEY, S. O. 2011. Rerouting chlorambucil to mitochondria combats drug deactivation and resistance in cancer cells. *Chem Biol,* 18**,** 445-53.

GOHLER, T., REIMANN, M., CHERNY, D., WALTER, K., WARNECKE, G., KIM, E. & DEPPERT, W. 2002. Specific interaction of p53 with target binding sites is determined by DNA conformation and is regulated by the C-terminal domain. *J Biol Chem,* 277**,** 41192-203.

GOLDIN, L. R., BJORKHOLM, M., KRISTINSSON, S. Y., TURESSON, I. & LANDGREN, O. 2009. Elevated risk of chronic lymphocytic leukemia and other indolent non-Hodgkin's lymphomas among relatives of patients with chronic lymphocytic leukemia. *Haematologica,* 94**,** 647-53.

GONZALEZ, D., MARTINEZ, P., WADE, R., HOCKLEY, S., OSCIER, D., MATUTES, E., DEARDEN, C. E., RICHARDS, S. M., CATOVSKY, D. & MORGAN, G. J. 2011. Mutational Status of the TP53 Gene As a Predictor of Response and Survival in Patients With Chronic Lymphocytic Leukemia: Results From the LRF CLL4 Trial. *Journal of Clinical Oncology,* 29**,** 2223-2229.

HALLEK, M. 2013a. Chronic lymphocytic leukemia: 2013 update on diagnosis, risk stratification and treatment. *Am J Hematol*.

HALLEK, M. 2013b. Chronic lymphocytic leukemia: 2013 update on diagnosis, risk stratification and treatment. *Am J Hematol,* 88**,** 803-16.

HALLEK, M., CHESON, B. D., CATOVSKY, D., CALIGARIS-CAPPIO, F., DIGHIERO, G., DÖHNER, H., HILLMEN, P., KEATING, M. J., MONTSERRAT, E., RAI, K. R. & KIPPS, T. J. 2008. Guidelines for the diagnosis and treatment of chronic lymphocytic leukemia: a report from the International Workshop on Chronic Lymphocytic Leukemia updating the National Cancer Institute–Working Group 1996 guidelines. *Blood,* 111**,** 5446-5456.

HAMBLIN, T. J., DAVIS, Z., GARDINER, A., OSCIER, D. G. & STEVENSON, F. K. 1999. Unmutated Ig V(H) genes are associated with a more aggressive form of chronic lymphocytic leukemia. *Blood,* 94**,** 1848-54.

HAMBLIN, T. J., ORCHARD, J. A., IBBOTSON, R. E., DAVIS, Z., THOMAS, P. W., STEVENSON, F. K. & OSCIER, D. G. 2002. CD38 expression and immunoglobulin variable region mutations are independent prognostic variables in chronic lymphocytic leukemia, but CD38

expression may vary during the course of the disease. *Blood,* 99**,** 1023-9.

HASSANEIN, N. M., PERKINSON, K. R., ALCANCIA, F., GOODMAN, B. K., WEINBERG, J. B. & LAGOO, A. S. 2010. A single tube, four-color flow cytometry assay for evaluation of ZAP-70 and CD38 expression in chronic lymphocytic leukemia. *Am J Clin Pathol,* 133**,** 708-17.

HE, L., HE, X., LOWE, S. W. & HANNON, G. J. 2007. microRNAs join the p53 network--another piece in the tumour-suppression puzzle. *Nat Rev Cancer,* 7**,** 819-22.

HE, Y. & WANG, Z. J. 2012. Let-7 microRNAs and opioid tolerance. *Frontiers in Genetics,* 3.

HILL, R., MADUREIRA, P. A., WAISMAN, D. M. & LEE, P. W. 2011. DNA-PKCS binding to p53 on the p21WAF1/CIP1 promoter blocks transcription resulting in cell death. *Oncotarget,* 2**,** 1094-108.

HINDS, P., FINLAY, C. & LEVINE, A. J. 1989. Mutation is required to activate the p53 gene for cooperation with the ras oncogene and transformation. *J Virol,* 63**,** 739-46.

HIRAO, A., KONG, Y. Y., MATSUOKA, S., WAKEHAM, A., RULAND, J., YOSHIDA, H., LIU, D., ELLEDGE, S. J. & MAK, T. W. 2000. DNA damage-induced activation of p53 by the checkpoint kinase Chk2. *Science,* 287**,** 1824-7.

HUTVAGNER, G., MCLACHLAN, J., PASQUINELLI, A. E., BALINT, E., TUSCHL, T. & ZAMORE, P. D. 2001. A cellular function for the RNA-interference enzyme Dicer in the maturation of the let-7 small temporal RNA. *Science,* 293**,** 834-8.

JÄÄMAA, S., AF HÄLLSTRÖM, T. M., SANKILA, A., RANTANEN, V., KOISTINEN, H., STENMAN, U.-H., ZHANG, Z., YANG, Z., DE MARZO, A. M., TAARI, K., RUUTU, M., ANDERSSON, L. C. & LAIHO, M. 2010. DNA Damage Recognition via Activated ATM and p53 Pathway in Nonproliferating Human Prostate Tissue. *Cancer Research,* 70**,** 8630-8641.

JIA, S., ZHAO, L., TANG, W. & LUO, Y. 2012. The gain of function of p53 mutant p53S in promoting tumorigenesis by cross-talking with H-RasV12. *Int J Biol Sci,* 8**,** 596-605.

JOHNSON, G. G., SHERRINGTON, P. D., CARTER, A., LIN, K., LILOGLOU, T., FIELD, J. K. & PETTITT, A. R. 2009. A Novel Type of p53 Pathway Dysfunction in Chronic Lymphocytic Leukemia Resulting from Two Interacting Single Nucleotide Polymorphisms within the p21 Gene. *Cancer Research,* 69**,** 5210-5217.

JORDAN, J. J., MENENDEZ, D., INGA, A., NOUREDDINE, M., BELL, D. A. & RESNICK, M. A. 2008. Noncanonical DNA motifs as transactivation targets by wild type and mutant p53. *PLoS Genet,* 4**,** e1000104.

JULIUSSON, G., OSCIER, D. G., FITCHETT, M., ROSS, F. M., STOCKDILL, G., MACKIE, M. J., PARKER, A. C., CASTOLDI, G. L., GUNEO, A., KNUUTILA, S., ELONEN, E. & GAHRTON, G. 1990. Prognostic subgroups in B-cell chronic lymphocytic leukemia defined by specific chromosomal abnormalities. *N Engl J Med,* 323**,** 720-4.

KHOSRAVI, R., MAYA, R., GOTTLIEB, T., OREN, M., SHILOH, Y. & SHKEDY, D. 1999. Rapid ATM-dependent phosphorylation of MDM2

precedes p53 accumulation in response to DNA damage. *Proc Natl Acad Sci U S A,* 96**,** 14973-7.

KOJIMA, K., KONOPLEVA, M., MCQUEEN, T., O'BRIEN, S., PLUNKETT, W. & ANDREEFF, M. 2006. Mdm2 inhibitor Nutlin-3a induces p53-mediated apoptosis by transcription-dependent and transcription-independent mechanisms and may overcome Atm-mediated resistance to fludarabine in chronic lymphocytic leukemia. *Blood,* 108**,** 993-1000.

LANDGREN, O., GOLDIN, L. R., KRISTINSSON, S. Y., HELGADOTTIR, E. A., SAMUELSSON, J. & BJORKHOLM, M. 2008. Increased risks of polycythemia vera, essential thrombocythemia, and myelofibrosis among 24,577 first-degree relatives of 11,039 patients with myeloproliferative neoplasms in Sweden. *Blood,* 112**,** 2199-204.

LEE, R. C., FEINBAUM, R. L. & AMBROS, V. 1993. The C. elegans heterochronic gene lin-4 encodes small RNAs with antisense complementarity to lin-14. *Cell,* 75**,** 843-854.

LEE, Y., AHN, C., HAN, J., CHOI, H., KIM, J., YIM, J., LEE, J., PROVOST, P., RADMARK, O., KIM, S. & KIM, V. N. 2003. The nuclear RNase III Drosha initiates microRNA processing. *Nature,* 425**,** 415-419.

LI, X., KHANNA, A., LI, N. & WANG, E. 2011. Circulatory miR34a as an RNAbased, noninvasive biomarker for brain aging. *Aging (Albany NY),* 3**,** 985-1002.

LIN, K., ADAMSON, J., JOHNSON, G. G., CARTER, A., OATES, M., WADE, R., RICHARDS, S., GONZALEZ, D., MATUTES, E., DEARDEN, C., OSCIER, D. G., CATOVSKY, D. & PETTITT, A. R. 2012. Functional analysis of the ATM-p53-p21 pathway in the LRF CLL4 trial: blockade at the level of p21 is associated with short response duration. *Clin Cancer Res,* 18**,** 4191-200.

LISBY, M., BARLOW, J. H., BURGESS, R. C. & ROTHSTEIN, R. 2004. Choreography of the DNA damage response: spatiotemporal relationships among checkpoint and repair proteins. *Cell,* 118**,** 699-713.

LIU, C., KELNAR, K., LIU, B., CHEN, X., CALHOUN-DAVIS, T., LI, H., PATRAWALA, L., YAN, H., JETER, C., HONORIO, S., WIGGINS, J. F., BADER, A. G., FAGIN, R., BROWN, D. & TANG, D. G. 2011. The microRNA miR-34a inhibits prostate cancer stem cells and metastasis by directly repressing CD44. *Nat Med,* 17**,** 211-5.

LIU, L., SCOLNICK, D. M., TRIEVEL, R. C., ZHANG, H. B., MARMORSTEIN, R., HALAZONETIS, T. D. & BERGER, S. L. 1999. p53 sites acetylated in vitro by PCAF and p300 are acetylated in vivo in response to DNA damage. *Mol Cell Biol,* 19**,** 1202-9.

LIVAK, K. J. 1999. Allelic discrimination using fluorogenic probes and the 5' nuclease assay. *Genet Anal,* 14**,** 143-9.

LU, H., TAYA, Y., IKEDA, M. & LEVINE, A. J. 1998. Ultraviolet radiation, but not γ radiation or etoposide-induced DNA damage, results in the phosphorylation of the murine p53 protein at serine-389. *Proceedings of the National Academy of Sciences,* 95**,** 6399-6402.

MACKUS, W. J., KATER, A. P., GRUMMELS, A., EVERS, L. M., HOOIJBRINK, B., KRAMER, M. H., CASTRO, J. E., KIPPS, T. J., VAN LIER, R. A., VAN OERS, M. H. & ELDERING, E. 2005. Chronic

lymphocytic leukemia cells display p53-dependent drug-induced Puma upregulation. *Leukemia,* 19**,** 427-34.

MAINOU-FOWLER, T., DIGNUM, H. M., PROCTOR, S. J. & SUMMERFIELD, G. P. 2004. The prognostic value of CD38 expression and its quantification in B cell chronic lymphocytic leukemia (B-CLL). *Leuk Lymphoma,* 45**,** 455-62.

MALCIKOVA, J., SMARDOVA, J., ROCNOVA, L., TICHY, B., KUGLIK, P., VRANOVA, V., CEJKOVA, S., SVITAKOVA, M., SKUHROVA FRANCOVA, H., BRYCHTOVA, Y., DOUBEK, M., BREJCHA, M., KLABUSAY, M., MAYER, J., POSPISILOVA, S. & TRBUSEK, M. 2009. Monoallelic and biallelic inactivation of TP53 gene in chronic lymphocytic leukemia: selection, impact on survival, and response to DNA damage. *Blood,* 114**,** 5307-14.

MARCHENKO, N. D., WOLFF, S., ERSTER, S., BECKER, K. & MOLL, U. M. 2007. Monoubiquitylation promotes mitochondrial p53 translocation. *EMBO J,* 26**,** 923-34.

MATHEU, A., MARAVER, A. & SERRANO, M. 2008. The Arf/p53 pathway in cancer and aging. *Cancer Res,* 68**,** 6031-4.

MERCER, W. E., AVIGNOLO, C. & BASERGA, R. 1984. Role of the p53 protein in cell proliferation as studied by microinjection of monoclonal antibodies. *Mol Cell Biol,* 4**,** 276-81.

MERKEL, O., ASSLABER, D., PINON, J. D., EGLE, A. & GREIL, R. 2010. Interdependent regulation of p53 and miR-34a in chronic lymphocytic leukemia. *Cell Cycle,* 9**,** 2764-8.

MONNI, O. & KNUUTILA, S. 2001. 11q deletions in hematological malignancies. *Leuk Lymphoma,* 40**,** 259-66.

MONTSERRAT, E., GOMIS, F., VALLESPI, T., RIOS, A., ROMERO, A., SOLER, J., ALCALA, A., MOREY, M., FERRAN, C., DIAZ-MEDIAVILLA, J. & ET AL. 1991. Presenting features and prognosis of chronic lymphocytic leukemia in younger adults. *Blood,* 78**,** 1545-51.

MORABITO, F., MANGIOLA, M., OLIVA, B., STELITANO, C., CALLEA, V., DEAGLIO, S., IACOPINO, P., BRUGIATELLI, M. & MALAVASI, F. 2001. Peripheral blood CD38 expression predicts survival in B-cell chronic lymphocytic leukemia. *Leuk Res,* 25**,** 927-32.

MOREAU, E. J., MATUTES, E., A'HERN, R. P., MORILLA, A. M., MORILLA, R. M., OWUSU-ANKOMAH, K. A., SEON, B. K. & CATOVSKY, D. 1997. Improvement of the chronic lymphocytic leukemia scoring system with the monoclonal antibody SN8 (CD79b). *Am J Clin Pathol,* 108**,** 378-82.

MRAZ, M., POSPISILOVA, S., MALINOVA, K., SLAPAK, I. & MAYER, J. 2009. MicroRNAs in chronic lymphocytic leukemia pathogenesis and disease subtypes. *Leuk Lymphoma,* 50**,** 506-9.

MUDHASANI, R., ZHU, Z., HUTVAGNER, G., EISCHEN, C. M., LYLE, S., HALL, L. L., LAWRENCE, J. B., IMBALZANO, A. N. & JONES, S. N. 2008. Loss of miRNA biogenesis induces p19Arf-p53 signaling and senescence in primary cells. *J Cell Biol,* 181**,** 1055-63.

OLDE LOOHUIS, N. F., KOS, A., MARTENS, G. J., VAN BOKHOVEN, H., NADIF KASRI, N. & ASCHRAFI, A. 2012. MicroRNA networks direct neuronal development and plasticity. *Cell Mol Life Sci,* 69**,** 89-102.

OSCIER, D., DEARDEN, C., EREN, E., FEGAN, C., FOLLOWS, G., HILLMEN, P., ILLIDGE, T., MATUTES, E., MILLIGAN, D. W., PETTITT, A., SCHUH, A., WIMPERIS, J. & BRITISH COMMITTEE FOR STANDARDS IN, H. 2012. Guidelines on the diagnosis, investigation and management of chronic lymphocytic leukaemia. *Br J Haematol,* 159**,** 541-64.

OSCIER, D., WADE, R., DAVIS, Z., MORILLA, A., BEST, G., RICHARDS, S., ELSE, M., MATUTES, E. & CATOVSKY, D. 2010. Prognostic factors identified three risk groups in the LRF CLL4 trial, independent of treatment allocation. *Haematologica,* 95**,** 1705-1712.

OUILLETTE, P., ERBA, H., KUJAWSKI, L., KAMINSKI, M., SHEDDEN, K. & MALEK, S. N. 2008. Integrated genomic profiling of chronic lymphocytic leukemia identifies subtypes of deletion 13q14. *Cancer Res,* 68**,** 1012-21.

PATTON, J. T., MAYO, L. D., SINGHI, A. D., GUDKOV, A. V., STARK, G. R. & JACKSON, M. W. 2006. Levels of HdmX expression dictate the sensitivity of normal and transformed cells to Nutlin-3. *Cancer Res,* 66**,** 3169-76.

PAULL, T. T. & GELLERT, M. 1999. Nbs1 potentiates ATP-driven DNA unwinding and endonuclease cleavage by the Mre11/Rad50 complex. *Genes Dev,* 13**,** 1276-88.

PENNICA, D., GOEDDEL, D. V., HAYFLICK, J. S., REICH, N. C., ANDERSON, C. W. & LEVINE, A. J. 1984. The amino acid sequence of murine p53 determined from a c-DNA clone. *Virology,* 134**,** 477-82.

PETRINI, J. H. & STRACKER, T. H. 2003. The cellular response to DNA double-strand breaks: defining the sensors and mediators. *Trends Cell Biol,* 13**,** 458-62.

PETTITT, A. R., SHERRINGTON, P. D., STEWART, G., CAWLEY, J. C., TAYLOR, A. M. R. & STANKOVIC, T. 2001. p53 dysfunction in B-cell chronic lymphocytic leukemia: inactivation of ATM as an alternative toTP53 mutation. *Blood,* 98**,** 814-822.

PINKEL, D., SEGRAVES, R., SUDAR, D., CLARK, S., POOLE, I., KOWBEL, D., COLLINS, C., KUO, W. L., CHEN, C., ZHAI, Y., DAIRKEE, S. H., LJUNG, B. M., GRAY, J. W. & ALBERTSON, D. G. 1998. High resolution analysis of DNA copy number variation using comparative genomic hybridization to microarrays. *Nat Genet,* 20**,** 207-11.

POZZO, F., DAL BO, M., PERAGINE, N., BOMBEN, R., ZUCCHETTO, A., ROSSI, F., DEGAN, M., ROSSI, D., CHIARENZA, A., GROSSI, A., DI RAIMONDO, F., ZAJA, F., POZZATO, G., SECCHIERO, P., GAIDANO, G., DEL POETA, G., ZAULI, G., FO, A. R., GUARINI, A. & GATTEI, V. 2013. Detection of TP53 dysfunction in chronic lymphocytic leukemia by an in vitro functional assay based on TP53 activation by the non-genotoxic drug Nutlin-3: a proposal for clinical application. *J Hematol Oncol,* 6**,** 83.

RAI, K. R., SAWITSKY, A., CRONKITE, E. P., CHANANA, A. D., LEVY, R. N. & PASTERNACK, B. S. 1975. Clinical staging of chronic lymphocytic leukemia. *Blood,* 46**,** 219-34.

REINHART, B. J., SLACK, F. J., BASSON, M., PASQUINELLI, A. E., BETTINGER, J. C., ROUGVIE, A. E., HORVITZ, H. R. & RUVKUN, G.

2000. The 21-nucleotide let-7 RNA regulates developmental timing in Caenorhabditis elegans. *Nature,* 403**,** 901-906.

RONAGHI, M., KARAMOHAMED, S., PETTERSSON, B., UHLEN, M. & NYREN, P. 1996. Real-time DNA sequencing using detection of pyrophosphate release. *Anal Biochem,* 242**,** 84-9.

ROSSI, D., CERRI, M., DEAMBROGI, C., SOZZI, E., CRESTA, S., RASI, S., DE PAOLI, L., SPINA, V., GATTEI, V., CAPELLO, D., FORCONI, F., LAURIA, F. & GAIDANO, G. 2009. The prognostic value of TP53 mutations in chronic lymphocytic leukemia is independent of Del17p13: implications for overall survival and chemorefractoriness. *Clin Cancer Res,* 15**,** 995-1004.

SADDLER, C., OUILLETTE, P., KUJAWSKI, L., SHANGARY, S., TALPAZ, M., KAMINSKI, M., ERBA, H., SHEDDEN, K., WANG, S. & MALEK, S. N. 2008. Comprehensive biomarker and genomic analysis identifies p53 status as the major determinant of response to MDM2 inhibitors in chronic lymphocytic leukemia. *Blood,* 111**,** 1584-93.

SALEH, A. D., SAVAGE, J. E., CAO, L., SOULE, B. P., LY, D., DEGRAFF, W., HARRIS, C. C., MITCHELL, J. B. & SIMONE, N. L. 2011. Cellular Stress Induced Alterations in MicroRNA let-7a and let-7b Expression Are Dependent on p53. *PLoS ONE,* 6**,** e24429.

SANCHEZ, O., ESCOBAR, J. I. & YUNIS, J. J. 1973. A simple G-banding technique. *Lancet,* 2**,** 269.

SANDBERG, A. A. 1981. Chromosomes as markers in human cancer. *Int Adv Surg Oncol,* 4**,** 311-36.

SANGER, F., NICKLEN, S. & COULSON, A. R. 1977. DNA sequencing with chain-terminating inhibitors. *Proc Natl Acad Sci U S A,* 74**,** 5463-7.

SARTOR, G. C., ST. LAURENT, G. & WAHLESTEDT, C. 2012. The emerging role of non-coding RNAs in drug addiction. *Frontiers in Genetics,* 3.

SCHOUTEN, J. P., MCELGUNN, C. J., WAAIJER, R., ZWIJNENBURG, D., DIEPVENS, F. & PALS, G. 2002. Relative quantification of 40 nucleic acid sequences by multiplex ligation-dependent probe amplification. *Nucleic Acids Res,* 30**,** e57.

SECCHIERO, P., BARBAROTTO, E., TIRIBELLI, M., ZERBINATI, C., DI IASIO, M. G., GONELLI, A., CAVAZZINI, F., CAMPIONI, D., FANIN, R., CUNEO, A. & ZAULI, G. 2006. Functional integrity of the p53-mediated apoptotic pathway induced by the nongenotoxic agent nutlin-3 in B-cell chronic lymphocytic leukemia (B-CLL). *Blood,* 107**,** 4122-9.

SELLICK, G. S., WEBB, E. L., ALLINSON, R., MATUTES, E., DYER, M. J., JONSSON, V., LANGERAK, A. W., MAURO, F. R., FULLER, S., WILEY, J., LYTTELTON, M., CALLEA, V., YUILLE, M., CATOVSKY, D. & HOULSTON, R. S. 2005. A high-density SNP genomewide linkage scan for chronic lymphocytic leukemia-susceptibility loci. *Am J Hum Genet,* 77**,** 420-9.

SHOHAT, O., GREENBERG, M., REISMAN, D., OREN, M. & ROTTER, V. 1987. Inhibition of cell growth mediated by plasmids encoding p53 anti-sense. *Oncogene,* 1**,** 277-83.

SHVARTS, A., STEEGENGA, W. T., RITECO, N., VAN LAAR, T., DEKKER, P., BAZUINE, M., VAN HAM, R. C., VAN DER HOUVEN VAN OORDT, W., HATEBOER, G., VAN DER EB, A. J. & JOCHEMSEN, A. G. 1996.

MDMX: a novel p53-binding protein with some functional properties of MDM2. *EMBO J,* 15**,** 5349-57.

SINHA, S., MALONIA, S. K., MITTAL, S. P., MATHAI, J., PAL, J. K. & CHATTOPADHYAY, S. 2012. Chromatin remodelling protein SMAR1 inhibits p53 dependent transactivation by regulating acetyl transferase p300. *Int J Biochem Cell Biol,* 44**,** 46-52.

SKOWRONSKA, A., PARKER, A., AHMED, G., OLDREIVE, C., DAVIS, Z., RICHARDS, S., DYER, M., MATUTES, E., GONZALEZ, D., TAYLOR, A. M., MOSS, P., THOMAS, P., OSCIER, D. & STANKOVIC, T. 2012. Biallelic ATM inactivation significantly reduces survival in patients treated on the United Kingdom Leukemia Research Fund Chronic Lymphocytic Leukemia 4 trial. *J Clin Oncol,* 30**,** 4524-32.

SOUSSI, T., RUBIO-NEVADO, J. M. & ISHIOKA, C. 2006. MUT-TP53: a versatile matrix for TP53 mutation verification and publication. *Hum Mutat,* 27**,** 1151-4.

STANKOVIC, T., BYRD, P. J., COOPER, P. R., MCCONVILLE, C. M., MUNROE, D. J., RILEY, J. H., WATTS, G. D., AMBROSE, H., MCGUIRE, G., SMITH, A. D., SUTCLIFFE, A., MILLS, T. & TAYLOR, A. M. 1997. Construction of a transcription map around the gene for ataxia telangiectasia: identification of at least four novel genes. *Genomics,* 40**,** 267-76.

STANKOVIC, T., HUBANK, M., CRONIN, D., STEWART, G. S., FLETCHER, D., BIGNELL, C. R., ALVI, A. J., AUSTEN, B., WESTON, V. J., FEGAN, C., BYRD, P. J., MOSS, P. A. & TAYLOR, A. M. 2004. Microarray analysis reveals that TP53- and ATM-mutant B-CLLs share a defect in activating proapoptotic responses after DNA damage but are distinguished by major differences in activating prosurvival responses. *Blood,* 103**,** 291-300.

STANKOVIC, T., KIDD, A. M., SUTCLIFFE, A., MCGUIRE, G. M., ROBINSON, P., WEBER, P., BEDENHAM, T., BRADWELL, A. R., EASTON, D. F., LENNOX, G. G., HAITES, N., BYRD, P. J. & TAYLOR, A. M. 1998. ATM mutations and phenotypes in ataxia-telangiectasia families in the British Isles: expression of mutant ATM and the risk of leukemia, lymphoma, and breast cancer. *Am J Hum Genet,* 62**,** 334-45.

STANKOVIC, T., STEWART, G. S., BYRD, P., FEGAN, C., MOSS, P. A. & TAYLOR, A. M. 2002. ATM mutations in sporadic lymphoid tumours. *Leuk Lymphoma,* 43**,** 1563-71.

STANKOVIC, T., WEBER, P., STEWART, G., BEDENHAM, T., MURRAY, J., BYRD, P. J., MOSS, P. A. & TAYLOR, A. M. 1999. Inactivation of ataxia telangiectasia mutated gene in B-cell chronic lymphocytic leukaemia. *Lancet,* 353**,** 26-9.

STEELE, A. J., PRENTICE, A. G., HOFFBRAND, A. V., YOGASHANGARY, B. C., HART, S. M., NACHEVA, E. P., HOWARD-REEVES, J. D., DUKE, V. M., KOTTARIDIS, P. D., CWYNARSKI, K., VASSILEV, L. T. & WICKREMASINGHE, R. G. 2008. p53-mediated apoptosis of CLL cells: evidence for a transcription-independent mechanism. *Blood,* 112**,** 3827-34.

SUZUKI, H. I., YAMAGATA, K., SUGIMOTO, K., IWAMOTO, T., KATO, S. & MIYAZONO, K. 2009. Modulation of microRNA processing by p53. *Nature,* 460**,** 529-33.

TAM, C. S., SHANAFELT, T. D., WIERDA, W. G., ABRUZZO, L. V., VAN DYKE, D. L., O'BRIEN, S., FERRAJOLI, A., LERNER, S. A., LYNN, A., KAY, N. E. & KEATING, M. J. 2009. De novo deletion 17p13.1 chronic lymphocytic leukemia shows significant clinical heterogeneity: the M. D. Anderson and Mayo Clinic experience. *Blood,* 114**,** 957-64.

TERZIAN, T., SUH, Y. A., IWAKUMA, T., POST, S. M., NEUMANN, M., LANG, G. A., VAN PELT, C. S. & LOZANO, G. 2008. The inherent instability of mutant p53 is alleviated by Mdm2 or p16INK4a loss. *Genes Dev,* 22**,** 1337-44.

TOBIN, G., THUNBERG, U., JOHNSON, A., THORN, I., SODERBERG, O., HULTDIN, M., BOTLING, J., ENBLAD, G., SALLSTROM, J., SUNDSTROM, C., ROOS, G. & ROSENQUIST, R. 2002. Somatically mutated Ig V(H)3-21 genes characterize a new subset of chronic lymphocytic leukemia. *Blood,* 99**,** 2262-4.

TYYBAKINOJA, A., VILPO, J. & KNUUTILA, S. 2007. High-resolution oligonucleotide array-CGH pinpoints genes involved in cryptic losses in chronic lymphocytic leukemia. *Cytogenet Genome Res,* 118**,** 8-12.

VAN DELFT, J., GAJ, S., LIENHARD, M., ALBRECHT, M., KIRPIY, A., BRAUERS, K., CLAESSEN, S., LIZARRAGA, D., LEHRACH, H., HERWIG, R. & KLEINJANS, J. 2012. RNA-seq provides new insights in the transcriptome responses induced by the carcinogen benzo[a]pyrene. *Toxicol Sci*.

VARLEY, J. M., EVANS, D. G. & BIRCH, J. M. 1997. Li-Fraumeni syndrome--a molecular and clinical review. *Br J Cancer,* 76**,** 1-14.

VASEVA, A. V. & MOLL, U. M. 2009. The mitochondrial p53 pathway. *Biochim Biophys Acta,* 1787**,** 414-20.

WANG, Z., GERSTEIN, M. & SNYDER, M. 2009. RNA-Seq: a revolutionary tool for transcriptomics. *Nat Rev Genet,* 10**,** 57-63.

WEI, C. L., WU, Q., VEGA, V. B., CHIU, K. P., NG, P., ZHANG, T., SHAHAB, A., YONG, H. C., FU, Y., WENG, Z., LIU, J., ZHAO, X. D., CHEW, J. L., LEE, Y. L., KUZNETSOV, V. A., SUNG, W. K., MILLER, L. D., LIM, B., LIU, E. T., YU, Q., NG, H. H. & RUAN, Y. 2006. A global map of p53 transcription-factor binding sites in the human genome. *Cell,* 124**,** 207-19.

WEINBERG, R. L., VEPRINTSEV, D. B., BYCROFT, M. & FERSHT, A. R. 2005. Comparative binding of p53 to its promoter and DNA recognition elements. *J Mol Biol,* 348**,** 589-96.

WIESTNER, A., ROSENWALD, A., BARRY, T. S., WRIGHT, G., DAVIS, R. E., HENRICKSON, S. E., ZHAO, H., IBBOTSON, R. E., ORCHARD, J. A., DAVIS, Z., STETLER-STEVENSON, M., RAFFELD, M., ARTHUR, D. C., MARTI, G. E., WILSON, W. H., HAMBLIN, T. J., OSCIER, D. G. & STAUDT, L. M. 2003. ZAP-70 expression identifies a chronic lymphocytic leukemia subtype with unmutated immunoglobulin genes, inferior clinical outcome, and distinct gene expression profile. *Blood,* 101**,** 4944-51.

WILLANDER, K., UNGERBACK, J., KARLSSON, K., FREDRIKSON, M., SODERKVIST, P. & LINDERHOLM, M. 2010. MDM2 SNP309 promoter polymorphism, an independent prognostic factor in chronic lymphocytic leukemia. *Eur J Haematol,* 85**,** 251-6.

WILLMORE, E., ELLIOTT, S. L., MAINOU-FOWLER, T., SUMMERFIELD, G. P., JACKSON, G. H., O'NEILL, F., LOWE, C., CARTER, A., HARRIS, R., PETTITT, A. R., CANO-SOUMILLAC, C., GRIFFIN, R. J., COWELL, I. G., AUSTIN, C. A. & DURKACZ, B. W. 2008. DNA-dependent protein kinase is a therapeutic target and an indicator of poor prognosis in B-cell chronic lymphocytic leukemia. *Clin Cancer Res,* 14**,** 3984-92.

WONG, T. S., RAJAGOPALAN, S., TOWNSLEY, F. M., FREUND, S. M., PETROVICH, M., LOAKES, D. & FERSHT, A. R. 2009. Physical and functional interactions between human mitochondrial single-stranded DNA-binding protein and tumour suppressor p53. *Nucleic Acids Res,* 37**,** 568-81.

YI, R., QIN, Y., MACARA, I. G. & CULLEN, B. R. 2003. Exportin-5 mediates the nuclear export of pre-microRNAs and short hairpin RNAs. *Genes Dev,* 17**,** 3011-6.

YUNIS, J. J. & SANCHEZ, O. 1975. The G-banded prophase chromosomes of man. *Humangenetik,* 27**,** 167-72.

ZENZ, T., HABE, S., DENZEL, T., MOHR, J., WINKLER, D., BUHLER, A., SARNO, A., GRONER, S., MERTENS, D., BUSCH, R., HALLEK, M., DOHNER, H. & STILGENBAUER, S. 2009. Detailed analysis of p53 pathway defects in fludarabine-refractory chronic lymphocytic leukemia (CLL): dissecting the contribution of 17p deletion, TP53 mutation, p53-p21 dysfunction, and miR34a in a prospective clinical trial. *Blood,* 114**,** 2589-97.

ZENZ, T., HABE, S., DENZEL, T., WINKLER, D., DOHNER, H. & STILGENBAUER, S. 2008a. How little is too much? p53 inactivation: from laboratory cut-off to biological basis of chemotherapy resistance. *Leukemia,* 22**,** 2257-8.

ZENZ, T., KRÖBER, A., SCHERER, K., HÄBE, S., BÜHLER, A., BENNER, A., DENZEL, T., WINKLER, D., EDELMANN, J., SCHWÄNEN, C., DÖHNER, H. & STILGENBAUER, S. 2008b. Monoallelic TP53 inactivation is associated with poor prognosis in chronic lymphocytic leukemia: results from a detailed genetic characterization with long-term follow-up. *Blood,* 112**,** 3322-3329.

ZENZ, T., MERTENS, D., KUPPERS, R., DOHNER, H. & STILGENBAUER, S. 2010. From pathogenesis to treatment of chronic lymphocytic leukaemia. *Nat Rev Cancer,* 10**,** 37-50.

ZENZ, T. & STILGENBAUER, S. 2009. Therapy with the FCR regimen does not overcome chronic lymphocytic leukemia biology: aberrant p53 expression predicts response and survival. *Leuk Lymphoma,* 50**,** 1559-61.

Appendices

10.1 Appendix I: Research participant information sheet

The following 3 pages are a copy of the 'Research Participant Information sheet', Version 2, 26/04/06.

Research Participant Information Sheet

STUDY TITLE

Identification and characterisation of prognostic factors in chronic B cell lymphoproliferative disorders.

WHAT IS THE PURPOSE OF THE STUDY AND WHY I HAVE BEEN CHOSEN?

Blood normally contains a variety of white cells which defend us against infection. One type of white cell, called a B lymphocyte, produce antibodies which recognise and help to destroy bacteria.

A group of diseases called the chronic B cell lymphoproliferative disorders are characterised by an over-production of B lymphocytes. The numbers of B lymphocytes in the blood and bone marrow are frequently increased and sometimes there is enlargement of lymph glands and/or the spleen.
The commonest of these disorders is chronic lymphocytic leukaemia. Other rarer conditions include splenic marginal zone lymphoma, mantle cell lymphoma and prolymphocytic leukaemia.

These disorders are often picked up by chance on a routine blood test performed for another reason, such as before surgery. Many patients never require treatment. In other patients, the diseases progress slowly and eventually need treating, while in a minority, treatment is required soon after diagnosis. Currently these conditions are incurable but they respond well to the many types of treatment that are now available.

The Haematology Department at the Royal Bournemouth Hospital has an international reputation for research carried out on the B cell chronic lymphoproliferative disorders over the past 20 years. We have developed blood tests which help to distinguish between those patients likely to have stable disease and those whose disease will progress and require treatment. The tests are also helpful in choosing the right treatment for each patient.
We should like to continue our research to try and discover the cause of these diseases and to develop simple, more reliable and inexpensive tests that can be used in laboratories worldwide to help predict the course of these diseases and the likely response to treatment.

We would like to offer the opportunity to take part in this research project to all patients with a chronic lymphoproliferative disorder who have been referred to the Haematology Department at the Royal Bournemouth Hospital.

DO I HAVE TO TAKE PART?

Taking part in research is entirely voluntary. If you do decide to take part you will be asked to sign a consent form. If you decide to take part and then change your mind you are free to withdraw at any time without giving a reason. Samples that have been stored in our laboratory would either be thrown away or returned to you in accordance with your wishes. A decision to withdraw from the study at any time or not to take part at all will not affect the standard of the care you receive.

WHAT WILL HAPPEN TO ME IF I TAKE PART?

Most of the research studies will be performed on residual cells (from blood, bone marrow or occasionally lymph node or spleen) that have been taken as part of your routine clinical care. Occasionally requests may be made for an additional 20ml blood sample purely for research purposes. Most of the tests will be performed in the Haematology Department at Bournemouth but anonymised samples may also be sent to other specialist laboratories that are working with us on the same diseases. We are also asking for your consent to store any unused samples for future ethically approved studies into the chronic B cell lymphoproliferative disorders. If you do not wish this to happen you can state this on the consent form.

WHAT ARE THE RISKS/BENEFITS OF TAKING PART?

There are no risks to taking part in this study apart from the mild discomfort of having blood taken. Since many of our patients are followed up for more than ten years it is possible but not guaranteed that the results of our research may be helpful to you. We hope this research will also help patients in the future.

WILL MY TAKING PART IN THIS STUDY BE KEPT CONFIDENTIAL?

All the information which is collected about you during the course of the research will be kept strictly confidential. Any information about you would only be accessed by the doctor or their support team involved in your normal clinical care.

WHAT WILL HAPPEN TO THE RESULTS OF THE RESEARCH STUDY?

We anticipate that these studies will provide new information and that the results will be presented at scientific meetings and published in scientific journals. To date our department has published over 150 papers on B cell chronic lymphoproliferative disorders in major scientific journals.

WHO IS ORGANISING AND FUNDING THE RESEARCH?

The chief investigator is Dr D G Oscier at the Royal Bournemouth Hospital. The research is currently funded by the Leukaemia Research Fund, Tenovus (a Cardiff-based charity supporting research into chronic lymphoproliferative disorders and cancer) and the Bournemouth Leukaemia Fund.

WHO HAS REVIEWED THE STUDY?

The study has been reviewed scientifically by the Leukaemia Research Fund and Tenovus, and ethically by the Somerset Research Ethics Committee.

CONTACT FOR FURTHER INFORMATION

Dr D G Oscier
Consultant Haematologist
Royal Bournemouth Hospital
Castle Lane East
Bournemouth
Dorset BH7 7DW

Telephone 01202 704790

FAX 01202 300248

Email david.oscier@rbch.nhs.uk

10.2 Appendix II: Patient consent form

The following 2 pages are a copy of the standardised consent template used, Version 2, 26/04/06.

*STANDARDISED **CONSENT** TEMPLATE FOR STUDIES USING Human Biological Samples*

CONSENT FORM (staged)

Thank you for reading the information about our research project. If you would like to take part, please read and sign this form.

Title of project: Identification and characterisation of prognostic factors in chronic B cell lymphoproliferative disorders
Name of researcher: Dr D G Oscier.
Contact details for research team: 01202 704790

***PART A**: Consent for the current study*
(Samples to be destroyed on study completion unless part B completed)

PLEASE **INITIAL** THE BOXES IF YOU AGREE WITH EACH SECTION:

1. I have read the information sheet dated 26/04/06, version 2 for the above study and have been given a copy to keep. I have been able to ask questions about the study and I understand why the research is being done and any risks involved. ☐

2. I agree to give a sample of (blood/ tissue/ other as appropriate) for research in this project.
I understand how the sample will be collected, that giving a sample for this research is voluntary and that I am free to withdraw my approval for use of the sample at any time without my medical treatment or legal rights being affected. ☐

3. I give permission for someone from the research team to look at my medical records to get information. I understand that the information will be kept confidential. ☐

4. I understand that my Doctor and I may be informed if any of the results of tests done as part of the research are important for my health. However, I also understand that the research may not directly benefit my health. ☐

5. I understand that I will not benefit financially if this research leads to the development of a new treatment or test. ☐

6. I know how to contact the research team if I need to. ☐

_____ _____ _____
Name of patient Date
Signature

_____ _____ _____
Name of person taking consent Date
Signature

Samples for storage and use in possible future studies

PART B *Linked or linked anonymised samples:*

7. I give permission for my sample and the information gathered about me to be stored by Dr D.G. Oscier at the Royal Bournemouth Hospital for possible use in future projects, as described in the information sheet. I understand that some of these projects may be carried out by other researchers, including researchers working for commercial companies. I understand that **future studies will be reviewed and approved by a Research Ethics Committee prior to my sample being used, and that I can alter these decisions at any stage by letting the research team know.**

a) I give permission for the sample to be used for research about chronic lymphoproliferative disease.

b) I give permission for the sample to be used for other unrelated research studies the precise nature of which will depend upon future scientific advances.

8. I want / do not want (*delete as applicable)* to be told the results of any future test which may have health implications for me.

9. I give permission for sections of my medical notes to be looked at by responsible individuals where it is relevant to such future study. I expect that my medical notes will be treated confidentially at all times.

_____ _____
_____
Name of patient Date
Signature

_____ _____
_____
Name of person taking consent Date
Signature

10.3 Appendix III: Antibodies

ANTIBODY	Use	CLONE	SUPPLIER	CODE
Beta actin rabbit Pab	WB		Abcam, UK	Ab8227-50
Beta actin-HRP mouse Mab	WB		Abcam, UK	Ab20272-10
CD2-RPE mouse Mab	FC	MT910	DAKO, Denmark	R080701
CD5-FITC mouse Mab	FC	DK23	DAKO, Denmark	F079501
CD5-APC mouse Mab	FC	DK23	DAKO, Denmark	C7242
CD7-PE mouse Mab	FC	MT701	BD biosciences, UK	332774
CD19-RPE/CY5 mouse Mab	FC	C706601	DAKO, Denmark	C706601
CD38-PE mouse Mab	FC	HB7	BD biosciences, UK	345806
CD49d-PE mouse Mab	FC	--	BD biosciences, UK	340296
Goat anti-mouse secondary-FITC	FC		BD biosciences, UK	349031
IgG1 isotype control AlexaFluor-488 mouse Mab	FC		Caltag, US	MG120
IgG2a isotype control	FC		DAKO, Denmark	094301
Kappa-APC rabbit Pab	FC		DAKO, Denmark	C0222
Lambda-PE rabbit Pab	FC		DAKO, Denmark	R0437
p53 (Ab-6) mouse Mab	FC	D0-1	Calbiochem, UK	OP43
p21 (Ab-1) mouse Mab	FC	EA10	Calbiochem, UK	OP64
p53 mouse Mab	WB	D0-1	SantaCruz, US	SC126
p21 mouse Mab	WB	--	Zymed, US	33-7000
p53 mouse Mab	WB	D0-11	Serotec, UK	MCA1704
Zap-70 AlexaFluor-488 mouse Mab	FC		Caltag, US	MHZAP702(

10.1 Appendix IV: Reagents and materials list

Item	Supplier	Code
Agarose LE analytical grade	Promega, ES	V3125
Ammonium chloride $NH_4Cl_{(S)}$ 500g	Sigma Aldrich, UK	A9434
BigDye® Terminator v3.1 cycle sequencing kit	Applied Biosystems, UK	4336917
BigDye® Terminator v3.1 buffer	Applied Biosystems, UK	4336697
DMSO (DiMethyl Sulphoxide)	Sigma Aldrich, UK	D8418
Dulbeccos Modified Eagle Medium 500ml	Sigma Aldrich, UK	D6546
Elkay 2ml cryovials	Simport, Canada	T311-3
Etoposide™ [25mM] 400µl	Trevigen Inc, USA	4886-400-01
Fast-Read 102® cell counting slides	Immune Sytems Ltd, UK	BVS100
FBS (foetal Bovine Serum)	BioSera, UK	51900
GelRed™ Nucleic Acid Gel Stain, 10,000X 500µl	Biotium, USA	41003
Glycerol, ≥99% 500ml	Sigma Aldrich, UK	G-5516
Heparin 1000u/ml ampoules	CP Pharmaceuticals, UK	PL04543/0221
Hi-DI™ Formamide	Applied Biosystems, UK	4311320
Histopaque®-1077 500ml	Sigma Aldrich, UK	10771
Immobilon™ PVDF membrane	Millipore, UK	IPVH00010
L-glutamine 200mM 100ml	Sigma Aldrich, UK	G7513
NuPage® MES-SDS Running buffer (20x)	Invitrogen, UK	NP0002
NuPage® transfer buffer (20x)	Invitrogen, UK	NP0006-1
Nutlin3a 1mg	Calbiochem, UK	444143
Paraformaldehyde	BDH lab supplies, UK	294474L
Phosphate buffered saline solution (PBS) 500ml pH7.4	Invitrogen, UK	10010
Pierce Supersignal® Chemiluminescent substrate	ThermoScientific, USA	
Propidium Iodide solution 10ml	Sigma Aldrich, UK	P4864
RNAlater® solution 250ml	Ambion, UK	AM7024
RPMI 1640 media + HEPES 500ml Gibco®	Invitrogen, UK	42401
SeeBlue® Plus2 Prestained standard	Invitrogen, UK	LC5925
Sodium Acetate buffer solution	Sigma Aldrich, UK	S-7899
Sodium Azide	Sigma Aldrich, UK	S2002
Sureclean 25ml	Bioline, UK	37046
TAE (Tris-Acetate/EDTA) buffer (50x)	Alpha Laboratories, UK	EL0077
Titanium™ *taq* PCR kit	Clontech, USA	639210
TrackIt™ Cyan/Orange loading buffer	Invitrogen, UK	10482-028
Trizma®-base	Sigma Aldrich, UK	T1503
Trypan Blue solution 100ml (0.4%)	Sigma Aldrich, UK	T8154
Tween-20	BDH lab supplies, UK	66368
Water-bath treatment	Sigma Aldrich, UK	55525

10.2 Appendix V: Primers

Code	Sequence 5′ → 3′	Target	Fragment size
5/6 UB	CTC TGT CTC CTT CCT CTT CCT ACA	*TP53* exons 5 & 6	462bp
5/6D	AGG GCC ACT GAC AAC CAC CCT TA		
7/8 UB	CCT CAT CTT GGG CCT GTG TTA TCT	*TP53* exons 7,8 & 9	820bp
789D	CTT TCC ACT TGA TAA GAG GTC CC		
P21GCOD31F	GTC AGA ACC GGC TGG GGA TG	*CDKN1A* exon 2	272bp
P21GCOD31R	CTC CTC CCA ACT CAT CCC GG		
P21GUTRF	AGT TCT TCC TGT TCT CAG CAG	*CDKN1A* 3′UTR	327bp
P21GUTRR	CCA GGG TAT GTA CAT GAG GAG		
Cod31PyroFBio	CTC TTC GGC CCA GTG GAC A	*CDKN1A* exon 2	81bp
Cod31PyroSeq	AGC GCA TCA CAG TCG		
Cod31PyroRev	CTC ACG GGC CTC CTG GAT		

Type C p53 Pathway Dysfunction Resulting From The Presence Of An Emerging TP53 Mutated Subclone In CLL

Ian Tracy(1), Anton Parker(2), Giles Best(3), Aneela Majid(4), Tanya Stankovic(5), Martin Dyer(4), David Oscier(2)

1)University of Bournemouth, Bournemouth, UK. 2)Royal Bournemouth Hospital, Bournemouth, UK. 3)CLL Research Consortium, Northern Blood Research Centre, Kolling Institute, Royal North Shore Hospital, Australia. 4)Medical Research Council Toxicology Unit, Leicester University, Leicester, United Kingdom. 5)CRUK Institute for Cancer Studies, University of Birmingham, Edgbaston, Birmingham, UK.

Background

Mutation and or loss of *TP*53 are known adverse prognostic markers in CLL, frequently associated with aggressive and chemo-refractory disease. Increased expression of p53 and its downstream target p21 are essential for effective response to DNA damage.

Functional assays have been developed to test CLL cells for their in-vitro response to DNA damage using either ionising radiation [1] or radio-mimetic drugs [2] Levels of p53 and p21 before and after DNA damage are used to assign samples to one of four functional categories (figure 1).

Johnson *et al* [3] recently reported an association between type C response and the genotype of single nucleotide polymorphisms (SNP) at codon 31 and in the 3'UTR of the p21 gene.

Control cells	Treated cells		
P53 baseline			
High or Low	P53 increase	P21 increase	Functional category
1 Low	Yes	Yes	Normal
2 High	Yes or No	Yes or No	Type A
3 Low	No	No	Type B
4 Low	Yes	No	Type C

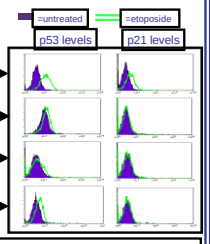

Figure 1: Typical response patterns derived from flow cytometric analysis of CLL cells for levels of P53 and P21 after 24hours incubation with or without 50µM etoposide. 1) Normal response. Low baseline level of p53 in control cells and both p53 and p21 increase in response to etoposide. 2) Type A response, elevated baseline level of p53 in control cells 3) Type B response, Both p53 and p21 fail to increase by >20% and >15% respectively. 4) Type C response, p21 fails to increase by >15% despite normal p53 response.

Functional Analysis

Functional analysis of 513 unselected local and referral CLL cases using the radio-mimetic drug, Etoposide and FACS analysis of p53 and p21 expression showed 16 type A, 118 type B, 25 type C and 354 normal response cases using cutoffs defined in [2].

P21 genotypes and type C dysfunction

Genotyping of the p21 codon 31 and 3'UTR SNPs in all 25 type C cases plus enlarged cohorts comprising 6 type A, 32 type B, and 117 normal response cases by TaqMan genotyping (ABI) assays showed no significant association between either genotype and the type C response (Table 1).

In addition all cases were observed to fall into one of only two diplotypes, being either heterozygous or homozygous at both SNPs, precluding direct association of our data with that of Johnson et al who suggest the type C response is associated with heterozygosity at codon 31 and homozygosity at 3'UTR.

Incidence of p53 abnormalities and type C dysfunction.

Genotyping of samples was carried out as previously described. Mutation detection was achieved through a combination of mutational screening by DHPLC and direct sequencing in a total of 135 cases. Loss of chromosomal locus 17p was detected by fluorescent in situ hybridisation in 31/173 cases. Associations between tp53 mutation status, chromosomal loss and the type C functional response were calculated using Fisher's exact test, all p values are two-tailed.

A highly significant association was seen between the type C response and both *TP*53 mutation and loss of 17p when compared to normal cases. This association was lost when comparing type C cases to either type A or B.

Table 1: A) Distribution of SNP diplotypes, *TP*53 mutation and chromosome 17p loss within series. Codon 31 SNP (rs1801270) Ser/Ser or Ser/Arg occurs with 3'UTR SNP (rs1059234) C/C or C/T respectively. *TP*53 mutations detected by DHPLC and direct sequencing. Chromosome 17p13.1 loss detected by fluorescent in situ hybridisation (Vysis LSI TP53).
B) Associations between the type C phenotype and *TP*53 mutation or 17p13.1 loss compared to each functional category. All tested using Fishers exact test, significance is two-tailed.

A

Functional category	SNP diplotypes Ser/Ser + C/C	Ser/Arg+C/T	TP53 mutation	17p loss
Normal (n=117)	104	13	1/88	6/114
Type A (n=6)	2	4	5/6	3/6
Type B (n=32)	27	5	7/20	10/30
Type C (n=25)	23	2	8/21	12/23

B

Association of TP53	mutation	17p loss
Type C vs Normal	p<0.0001	p<0.0001
Type C vs Type A	p=0.0760	p=1
Type C vs Type B	p=1	p=0.2606

Original sample	Function	TP53 mutation	17p loss
10039	Normal	yes	17p +/+
4080-2006	Type 3	yes	17p +/-45%
2355-2005	Type 3	unknown	17p +/+

Repeat sample	Function	TP53 mutation	17p loss	Intervening time	Intervening treatment
10099	Type 3	yes	17p +/+	7 months	Flud / Cyc
4080-2007	Type 1	yes	17p +/- 68%	7 months	No
2355-2006	Type 1 L.Node	unknown	tetra + 17pdel	13 months	R-CHOP

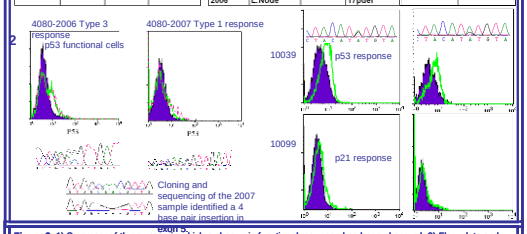

Figure 2: 1) Summary of three cases in which a change in functional response has been observed. 2) Flow plots and electropherograms of mutations showing the changes over time in two patients.

Observed evolution of dysfunction

In longitudinal analysis of 49 samples, 4 cases were observed to change functional category. Figure 2 Shows information and assay plots from a selection of these cases. Changes in response were accompanied by either an increasing clone size as evidenced by FISH or direct sequencing, or karyotypic evolution and/or intervening treatment.

Patient 4080: A 4 base pair deletion in exon 5 of *TP*53 was detectable at both time points. FISH analysis showed a modest increase in clone size over a 7 month period.

Sample 10039: Normal function when first tested and no loss of 17p observed. Post Fludarabine sample (10099) showed type C function. Direct sequencing detected a missense mutation in exon 7 of this sample which was then found to be present at lower levels in the original sample.

Replicating the effect of an emerging p53 abnormal clone.

We hypothesised that the presence of a type B, *TP*53 mutated, sub-clone would dilute the measured response of normal CLL cells so that p21 fell below its cutoff before p53 fell below its cutoff.

CLL cells from normal function cases were mixed with CLL cells from type B cases with known *TP*53 abnormalities. Paired samples were chosen with respect to their surface immunoglobulin light chain restriction so that cells of different origin could be distinguished from one another. Manipulation of the proportion of lambda versus kappa cells facilitated approximation of various clone sizes (Figure 3). Using type B cells it was possible to achieve a type C result. This was not possible when using type A cells.

Sample	SNP genotype	17p FISH	TP53 mutation	Function	Sig light chain
47	Hetero	+/+	no	Normal	Kappa
4080	Hetero	+/- 68%	4bp insert exon 5	Type B	Lambda
32	Homo	+/+	no	Normal	Kappa
89	Homo	+/- 28%	Missense Codon 237	Type B	lambda

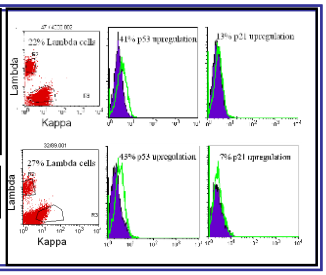

Figure 3: Examples of two mixing experiments. The table above shows data on the chosen samples. The images to the right show the final plots after manipulating the percentages of cells for analysis. TOP: Samples 47 and 4080; BOTTOM: Samples 32 and 89

Conclusion

This study describes an association between the previously described type C response and the presence of *TP*53 loss or mutation.

Further detailed follow up will be required to establish the clinical significance in these patients

There remains a number of cases for which the cause of the type C dysfunction remains to be explained. Longitudinal analysis of these cases coupled with clinical information will elucidate the true prognostic relevance of this functional category and whether it should be stratified further.

[1] CARTER,A., LIN,K., SHERRINGTON,P., PETTITT,A., 2004. Detection of p53 dysfunction by flow cytometry in chronic lymphocytic leukaemia. *British Journal of haematology*. **(127)** pp425-428.
[2] BEST,G., GARDINER,A., MAJID,A., WALEWSKA,R., AUSTEN,B., SKOWRONSKA,A., IBBOTSON,R., STANKOVIC,T., DYER,M., OSCIER,D., 2008. A novel functional assay detects and distinguishes between ATM and TP53 mutations in CLL. *Leukemia*. **(22)** pp1456-1459
[3] JOHNSON,G., SHERRINGTON,P., CARTER,A., LIN,K., LILOGLOU,T., FIELD,J., PETTITT,A., 2004. A novel type of p53 pathway dysfunction in chronic lymphocytic leukemia resulting from two interacting single nucleotide polymorphisms within the p21 gene

10.4 Appendix VII: Poster for IwCLL conference, Houston, Texas. 2011

FUNCTIONAL CATEGORISATION OF CLL-TUMOUR CELL p53/p21 RESPONSES TO ETOPOSIDE AND NUTLIN3A EXPOSURE CORRELATES WITH BI-ALLELIC *ATM* LESIONS AND MONO- AND BI-ALLELIC *TP53* LESIONS

Ian Tracy (1) Giles Best (2) Anne Gardiner (1) Gulshanara Ahmed (3) Jade Forster (1) Adrian Copplestone (4) Guy Pratt (5) Feargal McNicholl (6) Tanya Stankovic (3) David Oscier (1) Anton Parker

(1) Royal Bournemouth Hospital, Bournemouth. UK (2) Royal North Shore Hospital, Sydney. Australia. (3) School of Cancer Sciences, Birmingham University. Birmingham, UK. (4) Derriford Hospital. Plymouth, UK.
(5) Birmingham Heartlands Hospital. (6) Altnagelvin Hospital, Londonderry. Ireland.

Introduction

- Both mono and bi-allelic *TP53* abnormalities are associated with a poor response to standard therapy in CLL [1].
- Analysis of the UK CLL4 trial (ASH, 2011)[2] shows an increasingly poor outcome for patients with either mono-allelic *ATM* mutation, del(11q) and wildtype (wt) *ATM*, or bi-allelic inactivation of *ATM*.
- As mutational analysis, especially for *ATM*, is not widely available, a surrogate assay sensitive to *TP53* and *ATM* loss and mutation has potential clinical value
- p53-pathway functional assays measure up regulation of p53 and downstream targets such as p21 in response to *in-vitro* DNA damage.
- The small-molecule MDM2-antagonist, Nutlin3a, activates the p53 pathway in a p53-dependant manner [3].
- Preliminary data utilising Nutlin3a, in combination with the radio-mimetic drug, Etoposide, suggest that the assay is more sensitive to *TP53* or *ATM* mutations than loss.

Aim

- To validate the ability of the Etoposide / Nutlin3a assay to detect, and discriminate between, cases harbouring *TP53* and *ATM* structural abnormalities.

Materials and Methods

- Peripheral blood mono-nuclear cells (PBMNCs) from 136 CLL patients collected prior to initial or subsequent therapy.

All samples were tested using:

- Etoposide / Nutlin3a functional assay
- FISH to detect loss of 11q or 17p loci
- Mutation screening of entire *ATM* coding region (62 exons and flanking introns)
- Combination of mutation screening and/or direct sequencing of exons 2-10 of *TP53*

Materials and Methods

The functional assay was performed as described in Best *et al* (2008) [4].

•Patient PBMNCs cultured for 24hrs in RPMI-1640 (10% foetal calf serum + 2mM L-Glutamine) at a density of $5x10^6$ cells/ml in each of three wells:

1. Control culture
2. Etoposide (50uM) culture
3. Etoposide (50uM) + Nutlin3a (5uM) culture

•Intracellular levels of p53 and p21 proteins were measured by flow cytometry and the median fluorescence intensity (MFI) was used for calculations.

•Previously defined cut-offs for 'normal' p53 and p21 protein responses to treatment were 30% and 15% above the control MFI values respectively.

•Samples were classified as normal if p53 and p21 levels responded to both treatment cultures.

•Samples which failed to respond to Etoposide were then categorised on their response to Etoposide plus Nutlin3a.

•The system for assigning functional category, based on ability to increase protein levels, is shown below.

Table 1: Cases were categorised on their responses to both treatment cultures. In addition to the pre-existing categories a small number of samples responded with 'other' abnormal patterns of response.

	Etoposide		Etoposide + nutlin3a	
	p53	p21	p53	p21
NORMAL	Y	Y	Y	Y
CATEGORY-1	N	N	N	N
CATEGORY-2	N	N	Y	Y
CATEGORY-3	Y	N	Y	N
Other Abnormal	Y	N	Y	Y
	Y	N	N	N
	N	N	Y	N

Results

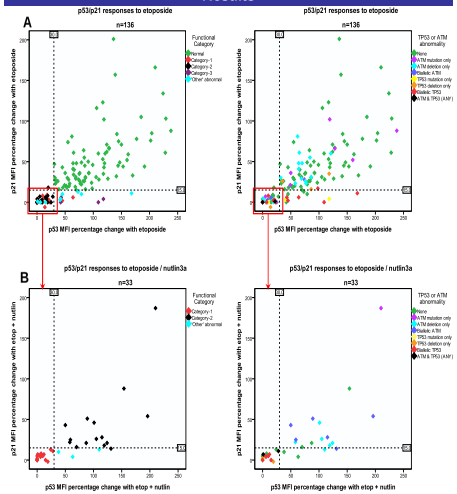

Figure 1: Categorisation of p53/p21 responses. The p53/p21 response to Etoposide alone for this study cohort is shown in panel A (n=136). Panel B shows the effect of Etoposide plus Nutlin3a on those samples which failed to respond to Etoposide alone (n=33). Panels on the left are labelled by category, panels on the right are labelled by abnormality.

Table 2: Distribution of genetic findings within functional categories. a) 5 cases with del(11)q plus mutation, 1 case with bi-allelic mutation. b) 12 cases with del(17)p plus mutation, 1 case with bi-allelic mutation.

TP53 / *ATM* abnormality	Functional Category					
	Normal	Cat-1	Cat-2	Cat-3	Other abnormal	Total
None	66	4	3	1	5	**79**
ATM mutation only	7	0	1	0	0	**8**
ATM deletion only	13	0	5	0	2	**20**
Biallelic *ATM* lesion[a]	0	0	6	0	0	**6**
TP53 deletion only	3	2	0	0	0	**5**
TP53 mutation only	0	1	0	1	1	**3**
Biallelic *TP53* lesion[b]	2	8	0	2	1	**13**
ATM & *TP53* lesion	0	2	0	0	0	**2**
Total	**91**	**17**	**15**	**4**	**9**	**136**

Observations

•The main observations that have been made as a result of this work are:

•Of 136 cases 91, 17, 15, 4 and 9 were classified as Normal, Cat-1, Cat-2, Cat-3 and 'other' respectively (Table 2).

•*TP53* and/or *ATM* abnormalities were detected in 42% of samples (57/136). Samples were classified into genotypic groups (Table 2).

•25 of 91 Normal function cases harboured *ATM* or *TP53* abnormalities; 20 of which were mono-allelic *ATM* abnormalities.

•13 of 17 Category-1 cases harboured abnormalities of *TP53*.

•3 of 4 Category-3 cases harboured *TP53* abnormalities.

•No Category-1 or Category-3 cases harboured *ATM* abnormalities.

•4 of 9 'Other' abnormal function cases harboured *ATM* or *TP53* abnormalities.

•12 of 15 Category-2 cases harboured *ATM* abnormalities.

•No Category-2 cases harboured *TP53* abnormalities.

•All 6 cases with bi-allelic *ATM* inactivation were categorised as Category-2, including the one case with bi-allelic *ATM* mutation.

•14 of 16 cases with a *TP53* mutation were categorised as having abnormal function, including all 3 cases with mono-allelic mutation and the single case with bi-allelic mutation.

•Two cases showed abnormalities of both *ATM* and *TP53*; both displayed Category-1 dysfunction. One had low level (12%) del(11q) and 65% del(17)p detected using FISH. The second had a frame-shifting mutation of *ATM* accompanied by both 47% del(17)p and a miss-sense mutation of *TP53*.

Discussion

•The majority of cases with structural abnormalities of *TP53* show some form of dysfunctional response to the assay irrespective of whether the abnormalities are mono or bi-allelic.

•The Etoposide / Nutlin3a assay is more sensitive to bi-allelic, rather than mono-allelic, abnormalities of *ATM*, with the majority of mono-allelic del(11)q cases reaching the previously defined cut-offs in response to Etoposide alone.

•All cases with bi-allelic *ATM* inactivation were identified as category-2 by the assay.

•Etoposide + Nutlin3a did not up-regulate p53 or p21 in any cases with mutant *TP53* that had failed to respond to Etoposide alone.

•*TP53* abnormalities are associated with both the Category-1 and -3 responses, both of which are typified by a failure to increase p21 levels.

•The detection of high baseline levels of p53 in control cultures is not required to determine dysfunction of p53.

Conclusion

The use of the p53 activating drug, Nutlin3a, in addition to DNA damaging drugs, successfully discriminates between cases with DNA damage pathway failure due to *TP53* abnormalities or *ATM* abnormalities, in particular bi-allelic *ATM* abnormalities. This was not achievable with previous methodologies that rely solely on DNA damaging agents alone.

References

[1] Zenz, T., et al., *Monoallelic TP53 inactivation is associated with poor prognosis in chronic lymphocytic leukaemia: Results from a detailed genetic characterisation with long-term follow up.* Blood, 2008. **112** (8):p. 3322-9

[2] ASH 2011. Publication No:467. *Biallelic ATM inactivation significantly reduces survival in Chronic Lymphocytic Leukaemia patients treated with alkylating agent/purine analogue therapy: results from the UKCLL4 trial.*

[3] Kojima, K., et al., *Mdm2 inhibitor Nutlin-3a induces p53-mediated apoptosis by transcription-dependent and transcription-independent mechanisms and may overcome Atm-mediated resistance to fludarabine in chronic lymphocytic leukaemia.* Blood, 2006. **108**(3): p. 993-1000

[4] Best, G. G., et al., *A novel functional assay using etoposide plus nutlin-3a detects and distinguishes between ATM and TP53 mutations in CLL.* Leukaemia, 2008. **22**(7): p. 1456-1459.